

INVESTIGATION OF LOW TEMPERATURE CRACKING IN  
ASPHALT CONCRETE PAVEMENT

A THESIS SUBMITTED TO  
THE GRADUATE SCHOOL OF NATURAL AND APPLIED  
SCIENCES OF  
THE MIDDLE EAST TECHNICAL UNIVERSITY

BY

ADNAN QADIR

IN PARTIAL FULFILLMENT OF THE REQUIREMENTS  
FOR  
THE DEGREE OF DOCTOR OF PHILOSOPHY  
IN  
CIVIL ENGINEERING

NOVEMBER 2010

Approval of the Thesis:

**INVESTIGATION OF LOW TEMPERATURE CRACKING IN  
ASPHALT CONCRETE PAVEMENT**

Submitted by **ADNAN QADIR** in partial fulfillment of the requirements for the degree of **Doctor of Philosophy in Civil Engineering Department, Middle East Technical University** by,

Prof. Dr. Canan Özgen

Dean, Graduate School of **Natural and Applied Sciences** \_\_\_\_\_

Prof. Dr. Güney Özcebe

Head of Department, **Civil Engineering** \_\_\_\_\_

Assoc. Prof. Dr. Murat Güler

Supervisor, **Civil Engineering Dept., METU** \_\_\_\_\_

**Examining Committee Members:**

Prof. Dr. Ayhan İnal

Civil Engineering Dept., METU \_\_\_\_\_

Assoc. Prof. Dr. Murat Güler

Civil Engineering Dept., METU \_\_\_\_\_

Assoc. Prof. Dr. İsmail Özgür Yaman

Civil Engineering Dept., METU \_\_\_\_\_

Dr. Soner Osman Acar

Civil Engineering Dept., METU \_\_\_\_\_

Assist. Prof. Dr. Hikmet Bayırtepe

Civil Engineering Dept., Gazi University \_\_\_\_\_

**November 5, 2010**

**I hereby declare that all information in this document has been obtained and presented in accordance with academic rules and ethical conduct. I also declare that, as required by these rules and conduct, I have fully cited and referenced all material and results that are not original to this work.**

Name, Last Name: Adnan Qadir

Signature :

## **ABSTRACT**

# **INVESTIGATION OF LOW TEMPERATURE CRACKING IN ASPHALT CONCRETE PAVEMENT**

Qadir, Adnan

Ph.D., Department of Civil Engineering

Supervisor: Assoc. Prof. Dr. Murat Guler

November 2010, 235 pages

In this study, low temperature cracking of asphalt concrete is investigated based on a laboratory experimental program including the design variables of aggregate type, gradation, asphalt content, binder grading, binder modification, and the experimental variables of cooling rate, and specimen size. The design of experiment is proposed according to the fractional factorial design principles to reduce the required number of test specimens. Mix designs are performed according to the Superpave mix design guidelines using materials obtained from the Turkish General Directorate of Highways. In the course of this study, a test setup for thermal stress restrained specimen test for asphalt concrete is developed and used successfully to test a number of asphalt concrete beam specimens. The same setup is also used for measuring the glass transition temperatures to obtain various thermo-volumetric properties of mixtures. Statistical methods are used to identify the effect of experimental variables on fracture strength, fracture temperature and other dependent variables obtained from the testing program. Statistical models are also developed to predict the fracture strength, fracture temperature and other thermo-volumetric properties of mixtures. Results of analyses show that aggregate type, binder modification, and asphalt content significantly affect both the fracture strength and fracture temperature of asphalt concrete. While the glass transition temperature is affected by only aggregate type, coefficients

of contraction before and after the glass transition temperature are not influenced by any of the experimental variables. The results of this study provide an important basis to prevent low temperature cracking in asphalt concrete pavements.

**Keywords:** Low Temperature Cracking, Fracture Strength, Fracture Temperature, Thermal Stress Restrained Specimen Test, Glass Transition Temperature

## ÖZ

# ASFALT BETON KAPLAMALARDA DÜŞÜK SICAKLIK ÇATLAĞININ İNCELENMESİ

Qadir, Adnan

Doktora, İnşaat Mühendisliği Bölümü

Tez Yöneticisi: Doç. Dr. Murat Güler

Kasım 2010, 235

Bu çalışmada asfalt betonunda oluşan düşük sıcaklık çatlakları, tasarım parametreleri olarak agrega cinsi, gradasyon, bitüm oranı, bitüm derecesi, bitüm modifikasyonu ve deneysel değişkenler olarak da soğutma hızı ve numune boyutu dikkate alınarak irdelenmektedir. Deney tasarımı, gerekli numune sayısının azaltılması için kesirli faktöriyel tasarım yöntemi olarak önerilmektedir. Karışım tasarımları Superpave karışım tasarım şartnamelerine uygun olarak Karayolları Genel Müdürlüğünden elde edilen malzemeler ile yapılmaktadır. Bu çalışma kapsamında, sıcaklık gerilmeleri sınırlandırılmış numune test cihazı geliştirilmekte ve birçok prizmatik asfalt beton numunesinin deneylerinde başarıyla kullanılmaktadır. Aynı deney düzeneği kullanılarak karışımların çeşitli termo-hacimsel özelliklerinin elde edilmesi için camsı geçiş sıcaklık deneyleri de yapılmaktadır. İstatistiksel yöntemler kullanılarak deney değişkenlerinin çatlama dayanımı, çatlama sıcaklığı ve diğer bağımlı değişkenler üzerindeki etkileri belirlenmektedir. Çatlama dayanımı, çatlama sıcaklığı ve diğer termo-hacimsel özelliklerin tahmini için istatistiksel modeller kurulmaktadır. Analiz sonuçları agrega cinsinin, bitüm modifikasyonun ve bitüm oranının asfalt betonu çatlama dayanımı ve çatlama sıcaklığı üzerinde ciddi etkisi olduğunu göstermektedir. Camsı geçiş sıcaklığının yalnızca agrega cinsinden etkileniyor olmasına rağmen, camsı geçiş sıcaklığından önce ve sonraki büzülme katsayıları hiçbir deneysel değişkenlerden etkilenmemektedir. Bu çalışmanın

sonuları, asfalt beton yollarda oluřan dřük sıcaklık atlaklarının nlemesi iin nemli bir zemin saėlamaktadır.

**Anahtar kelimeler:** Dřük Sıcaklık atlaėı, atlama Dayanımı, atlama Sıcaklıėı, Sıcaklık Gerilmeleri Sınırlandırılmıř Numune Deneyi, Camsı Geiř Sıcaklıėı

*To Any, Afra and Asra*

## ACKNOWLEDGEMENTS

The writing of this dissertation would not have been realized without the able support, patience and guidance of the following people and organizations. I owe deepest gratitude to them.

Associate Professor, Dr. Murat Güler for his guidance, advice, criticism and insight throughout the research.

Assistant Prof. Dr. Hikmet Bayırtepe, committee member, for his valuable time in reviewing and giving constructive suggestions for analyzing the data.

Dr. Tanvir Wasti, retired Professor and Associate Professor Dr. Ismail Özgür Yaman for their able suggestions, moral support and guidance during the study.

Professor Dr. Ayhan İnal and Dr Murat Gündüz, for providing me the encouragement and confidence during my study.

Mr. Okan Demirel in helping me in the machine software and Mr. Ahmet Sağlam, laboratory technician for providing me the able assistance all through the research period and helping hand in the gigantic laboratory task required for this research.

Turkish General Directorate of Highways (TGDH) pavement division director for their asphalt laboratory staff, giving man and infrastructural support in this research.

Scientific and Technological Research Council of Turkey (TÜBİTAK) for financial support of this study ( Project Number 105M193).

NED University of Engineering and Technology, Karachi, Pakistan for keeping faith in my abilities and awarding full financial support during my stay in Turkey. Gratitude specially to Engineer Abul Kalam, Vice Chancellor ; Dr. S.F.A Rafeeqi, Pro Vice Chancellor and Dr.S.H.Lodi, Dean Civil Engineering and Architecture..

My wife Any, without whom this effort would not have been worth enough. Your love, support and constant patience have taught me sacrifice, discipline and compromise.

My daughters Afra and Asra, who spent many years with their mother and my in-laws to allow me to focus. I am deeply sorry for the time we spent apart.

Last but not least to all those people whose name are not mentioned here, but are remembered in my heart, for their moral and ethical support in achieving me this endeavor. *“One person seeking glory doesn’t accomplish much. Success is the result of people pulling together to meet common goals”* (John Maxwell).

## TABLE OF CONTENTS

ABSTRACT .....	iv
ÖZ .....	vi
ACKNOWLEDGEMENTS .....	ix
TABLE OF CONTENTS .....	xi
LIST OF TABLES .....	xiv
LIST OF FIGURES .....	xviii
LIST OF ABBREVIATIONS USED .....	xx
CHAPTERS	
1. INTRODUCTION .....	1
1.1. Background .....	1
1.2. Research Objective .....	3
1.3. Scope .....	3
1.4. Outline of Research .....	4
2. LITERATURE REVIEW .....	5
2.1. Introduction .....	5
2.2. Low temperature cracking .....	5
2.3. Factors affecting low temperature cracking .....	10
2.3.1. Climate .....	10
2.3.2. Component material properties .....	13
2.3.3. Asphalt mixture properties .....	21
2.4. Test methods to evaluate thermal properties of asphalt concrete .....	27
2.4.1. Fracture mechanics test .....	27
2.4.2. Thermal Stress Restrained Specimen Test (TSRST) .....	27
2.4.3. Indirect tension creep test .....	28
2.5. Models for low temperature cracking .....	29
2.5.1. Empirical models .....	29

2.5.2.	Mechanistic models.....	30
3.	METHODOLOGY.....	31
3.1.	Introduction .....	31
3.2.	Machine manufacture .....	31
3.2.1.	Design and fabrication .....	31
3.2.2.	Programming .....	39
3.2.3.	The system control.....	42
3.2.4.	Temperature calibration for the extension bars .....	43
3.3.	Sample preparation.....	45
3.3.1.	Design of experiment.....	46
3.3.2.	Materials selected for research .....	50
3.3.3.	Superpave mix design for the selected mixtures .....	52
3.3.4.	Sample preparation for TSRST testing.....	54
3.4.	Laboratory tests applied on the mixtures.....	59
3.4.1.	TSRST testing of specimens.....	59
4.	RESULT ANALYSIS OF TESTS .....	68
4.1.	Introduction .....	68
4.2.	Analysis of variance tests (ANOVA) for research outcomes.....	68
4.2.1.	Analysis of variance tests (ANOVA) for TSRST results .....	68
4.2.2.	Analysis of variance tests (ANOVA) for glass transition temperature measurements .....	84
4.3.	Principal component (PC) analysis .....	88
4.3.1.	Principal component analysis for fracture stress data.....	88
4.3.2.	Principal component analysis for glass transition data.....	97
4.4.	Cluster analysis.....	99
4.4.1.	ANOVA for fracture data of clusters.....	100
4.4.2.	Statistical analysis of glass transition data from cluster analysis	104
4.5.	Discriminant analysis .....	106
4.5.1.	ANOVA for glass transition of clusters from discriminant analysis .....	106
4.6.	Regression analysis .....	108

4.6.1.	Stepwise regression.....	109
4.6.2.	Standard regression.....	111
4.7.	Statistical modeling .....	117
4.7.1.	Statistical model for fracture strength.....	117
4.7.2.	Statistical model for fracture temperature .....	119
4.7.3.	Statistical model for glass transition temperature.....	121
4.8.	Parametric study of statistical models .....	123
5.	CONCLUSIONS AND RECOMMENDATIONS .....	129
5.1.	Introduction .....	129
5.2.	Conclusions .....	129
5.3.	Recommendations for future work .....	132
	REFERENCES.....	133
APPENDICES		
	A-FRACTURE PLOTS.....	141
	B-GLASS TRANSITION PLOTS .....	157
	C-MATLAB CODES .....	166
	C1- For fracture analysis .....	166
	C2- For ANOVA of fracture data.....	187
	C3- For ANOVA of glass transition temperature data.....	188
	D- ANOVA TABLES .....	189
	E- CLUSTERS DETAILS FROM FRACTURE TEST.....	199
	F- CLUSTERS DETAILS FROM GLASS TEST .....	207
	G- PREDICTED VALUES FROM STATISTICAL MODELS .....	212
	H- SOFTWARE MANUALS .....	221
	CURRICULUM VITAE .....	234

## LIST OF TABLES

### TABLES

Table 2.1- Typical stiffness values for asphalt binder at loading times.....	16
Table 2.2- Values of glass transition temperatures and thermal coefficients measured by Wada and Hirose, (1960).....	19
Table 2.3- Glass transition temperatures and coefficients of contraction reported by different authors for asphalt concrete .....	25
Table 3.1- Thermal paramaters measured from the calibration process .....	45
Table 3.2- Detail of variables used in the design .....	47
Table 3.3- Standard matrix available for fractional factorial design of $2^{5-2}$ .....	48
Table 3.4- Design matrix for 2 level 3 factor design .....	48
Table 3.5- Design matrix as a result of fractional factorial design $2^{5-2} \times 3^2$ .....	49
Table 3.6- Properties of aggregates.....	50
Table 3.7- Properties of asphalt .....	50
Table 3.8- Estimation of quantity of materials for samples .....	51
Table 3.9- Design parameters for Superpave mix (AASHTO T 312) .....	53
Table 3.10- Summary of calculated AC content.....	54
Table 3.11- Summary of sample prepared for TSRST and glass test measurement.....	57
Table 3.12- Detail of specimen tested at $-20^{\circ}\text{C/h}$ .....	60
Table 3.13- Detail of specimen tested at $-10^{\circ}\text{C/h}$ .....	61
Table 3.14- Detail of specimen tested at $-5^{\circ}\text{C/h}$ .....	62
Table 3.15- Detail of samples tested for glass transition temperature .....	65
Table 4.1 - Descriptive statistics of fracture strength .....	69
Table 4.2- ANOVA analysis for fracture strength.....	70
Table 4.3- Fracture strength values for experimental variables.....	71
Table 4.4- ANOVA analysis for fracture temperature.....	75
Table 4.5- Fracture temperature values for experimental variables.....	75
Table 4.6- ANOVA analysis of relaxation stress.....	77
Table 4.7- Relaxation stress values for experimental variables.....	78
Table 4.8- ANOVA analysis for transition temperature .....	79

Table 4.9- Transition temperature values for experimental variables.....	79
Table 4.10- Analysis of variance for $\Delta S/\Delta T$ .....	80
Table 4.11- Slope( $\Delta S/\Delta T$ ) constant values for experimental variables .....	81
Table 4.12 - Correlation of air voids with various response variables.....	83
Table 4.13- ANOVA for tensile load eccentricity .....	83
Table 4.14- Probability values calculated from ANOVA .....	84
Table 4.15- Statistics for the glass transition temperature measurement.....	85
Table 4.16- Probability values calculated from ANOVA .....	86
Table 4.17- Statistical parameters for thermal coefficients in the case of gradation type .....	87
Table 4.18 - Statistical parameters for thermal coefficients in the case of asphalt type .....	87
Table 4.19- Statistical parameters for thermal coefficients in the case of asphalt con- tent .....	88
Table 4.20- Coefficients of principle components for fracture strength.....	89
Table 4.21- Eigen values for principal component analysis .....	89
Table 4.22- Clusters from principal components analysis .....	91
Table 4.23- Response of the fracture strength against experimental variable .....	92
Table 4.24- Response of fracture temperature against experimental variable .....	93
Table 4.25- Relaxation stress response to experimental variables.....	93
Table 4.26- Transition temperature response to experimental variables .....	94
Table 4.27- Effect of experimental variables on slope constant .....	95
Table 4.28- Air voids probability results for experimental variables .....	96
Table 4.29- Effect of eccentricity on experimental variables .....	96
Table 4.30- Principal components of glass transition temperature .....	97
Table 4.31- Cluster of glass transition temperature from PC using similarity.....	97
Table 4.32- ANOVA for glass transition temperature for clusters from PC .....	98
Table 4.33- Probability values for thermal coefficients.....	99
Table 4.34- Cluster from fracture and glass transition measurements.....	99
Table 4.35- Response of fracture strength against experimental variables.....	100
Table 4.36- Response of fracture temperature against experimental variables .....	101

Table 4.37- Relaxation stress response to experimental variables.....	102
Table 4.38- Transition temperature response in clusters .....	102
Table 4.39- Effect of variables on $\Delta S / \Delta T$ of the mix .....	103
Table 4.40- Air voids probability results for variable in the clusters.....	104
Table 4.41- Eccentricity as a response for the clusters .....	104
Table 4.42- Probability values for glass transition response for clusters.....	105
Table 4.43- Probability values for thermal coefficients.....	105
Table 4.44- Probability values for glass transition temperature response for clusters .....	107
Table 4.45- Probability values for thermal coefficients.....	107
Table 4.46- Variable codes used in regression analyses .....	108
Table 4.47- Typical output of stepwise regression analysis .....	109
Table 4.48- Output of stepwise regression analysis for fracture strength and glass transition temperature .....	111
Table 4.49- Comparison of regression coefficients for fracture strength .....	112
Table 4.50- Coefficients of regression for fracture temperature in cluster group..	114
Table 4.51- Comparison for glass transition temperatures .....	116
Table 4.52- Statistical parameters for fracture strength models .....	118
Table 4.53- Statistical parameters for fracture temperature.....	120
Table 4.54- Statistical parameters for glass transition temperature .....	123
Table D1- For fracture strength response.....	189
Table D2- For fracture temperature response .....	190
Table D3- For response of relaxation stress.....	191
Table D4- Response of transition temperature.....	192
Table D5- For response of slope ( $\Delta S/\Delta T$ ) .....	193
Table D6- For response of air voids.....	194
Table D7- For response of eccentricity .....	195
Table D8- For response of glass transition temperatures.....	196
Table D9- For response of thermal coefficients before glass transition temperature, $\alpha_h$ .....	197

Table D10- For response of thermal coefficients after glass transition temperature, $\alpha_g$ .....	198
Table E1- Cluster (15 samples).....	199
Table E2- Cluster (30 samples).....	199
Table E3- Cluster from PC covariance (44 samples).....	200
Table E4- Cluster from PC covariance (40 samples).....	202
Table E5- Cluster from PC correlation (50 samples).....	203
Table E6- Cluster from PC correlation (44 samples).....	204
Table E7- Cluster from PC correlation (11 samples).....	206
Table F1- Glass transition temperature cluster (10 samples).....	207
Table F2- Glass transition temperature cluster (13 samples).....	207
Table F3- Glass transition temperature cluster from PC covariance (10 samples)	208
Table F4- Glass transition temperature cluster from PC covariance (13 samples)	208
Table F5- Glass transition temperature cluster from PC correlation (10 samples)	208
Table F6- Glass transition temperature cluster from PC correlation (13 samples)	209
Table F7- Glass transition temperature cluster from discriminant analysis (10 samples).....	209
Table F8- Glass transition temperature cluster from discriminant analysis (12 samples).....	210
Table F9- Glass transition temperature cluster from discriminant analysis (14 samples).....	210
Table G1- Material combinations for parametric studies .....	212

## LIST OF FIGURES

### FIGURES

Figure 2.1- Phenomena of low temperature cracking in AC pavements .....	5
Figure 2.2- A view of low temperature cracking on an AC pavement section .....	6
Figure 2.3- Cross section of AC pavement showing low temperature cracks at uniform intervals.....	7
Figure 2.4- Thermal stress gradients .....	7
Figure 2.5- An example of a low temperature cracking in AC pavements .....	8
Figure 2.6- Range of temperatures corresponding to low temperature cracking and thermal fatigue cracking .....	9
Figure 2.7- Stiffness behavior of asphalt binder .....	16
Figure 2.8- Estimating stiffness of asphalt binder using Van der Poel, (1954) nomograph .....	17
Figure 2.9- Glass transition temperature of asphalt .....	20
Figure 2.10- Typical transition behavior of asphalt binder with temperature.....	20
Figure 2.11- Classical representation of asphalt mixture.....	22
Figure 2.12- Prediction of mix stiffness by Bonnaure et al., (1977) method.....	23
Figure 2.13- An AC specimen preparation before IDT .....	29
Figure 3.1- Flow diagram for research methodology.....	32
Figure 3.2- Details of the structural steel frame for TSRST test device .....	34
Figure 3.3- FEM analysis of TSRST device .....	34
Figure 3.4- Main components of the TSRST device .....	35
Figure 3.5- Liquid nitrogen supply arrangements.....	36
Figure 3.6- Displacement and temperature sensor arrangement .....	37
Figure 3.7- Nozzle system placed in the device.....	38
Figure 3.8- Auxiliary apparatus used in the preparation.....	38
Figure 3.9- Platform where the specimens are mounted and glued .....	39
Figure 3.10- Interaction diagram between software and test device.....	40
Figure 3.11- A view of control panel for user interface program showing control knobs, indicators and various graphs .....	41

Figure 3.12- A view of the calibration process .....	45
Figure 3.13- Flow diagram of the experimental design .....	47
Figure 3.14- Selected gradation for the project.....	51
Figure 3.15- Mix design samples according to the Superpave method .....	52
Figure 3.16- Sample specimen preparation during and after compaction .....	55
Figure 3.17- Specimen section for cutting .....	56
Figure 3.18- Specimens cut to required dimensions .....	57
Figure 3.19- Centring of sample by gluing the ring and fixing to the projection ....	58
Figure 3.20- Beam specimen in the process of gluing to the loading platens.....	59
Figure 3.21- A view of fracture specimen and user software interface at failure ....	63
Figure 3.22- Details of the fracture stress versus temperature curve obtained from the fracture test .....	64
Figure 3.23- A plot of Equation 3.1 for glass transition temperature measurement	67
Figure 4.1- Perpendicularity of principal component for fracture data .....	90
Figure 4.2- Line of equality plot for fracture strength .....	119
Figure 4.3- Line of equality plot for fracture temperature.....	121
Figure 4.4- Line of equality plot for glass transition temperature .....	122
Figure 4.5- Identification code for sample combination for parametric .....	123
Figure 4.6- Fracture strength for samples not tested.....	126
Figure 4.7- Fracture temperature for samples not tested.....	127
Figure 4.8- Glass transition temperature for samples not tested.....	128
Figure A1- Fracture plot of small sample tested at $-5^{\circ}\text{C/h}$ .....	141
Figure A2- Fracture plot of tall sample tested at $-5^{\circ}\text{C/h}$ .....	144
Figure A3- Fracture plot of small sample tested at $-10^{\circ}\text{C/h}$ .....	147
Figure A4- Fracture plot of tall sample tested at $-10^{\circ}\text{C/h}$ .....	149
Figure A5- Fracture plot of small sample tested at $-20^{\circ}\text{C/h}$ .....	152
Figure A6- Fracture plot of tall sample tested at $-20^{\circ}\text{C/h}$ .....	154
Figure B1- Glass transition temperature plots .....	157
Figure H1- Manual for fracture test .....	221
Figure H2- Manual for glass transition temperature test .....	227

## LIST OF ABBREVIATIONS USED

<b>AASHTO:</b>	American Association of State Highway and Transportation Officials
<b>AC:</b>	Asphalt Cement
<b>acc %:</b>	Asphalt cement content
<b>acgr:</b>	AC type
<b>aggr:</b>	Aggregate
<b>ANOVA:</b>	Analysis of Variance
<b>ASTM:</b>	American Society of Testing and Materials
<b>AV:</b>	Air Voids
<b><math>\alpha_g</math> :</b>	thermal coefficients after glass transition temperature
<b><math>\alpha_h</math> :</b>	thermal coefficients before glass transition temperature
<b>B:</b>	Basalt Aggregate
<b>BBR:</b>	Bending Beam Rheometer
<b>BC:</b>	Basalt Coarse Graded Mix
<b>BF:</b>	Basalt Fine Graded Mix
<b>C:</b>	Coarse Gradation
<b>cool:</b>	Cooling rate
<b>DSR:</b>	Dynamic Shear Rheometer
<b>DTT:</b>	Direct Tension Test
<b>ESAL:</b>	Equivalent Single Axle Load
<b>F:</b>	Fine Gradation
<b>FHWA:</b>	Federal Highway Administration
<b>FS:</b>	Fracture Strength
<b>FT:</b>	Fracture Temperature
<b>grde:</b>	Gradation
<b>GTT:</b>	Glass Transition Temperature
<b>HMA:</b>	Hot Mix Asphalt
<b>ITT:</b>	Indirect Tension Test
<b>L:</b>	Limestone Aggregate
<b>LC:</b>	Limestone Coarse Graded Mix
<b>LCPC:</b>	Laboratoire Central des Ponts et Chaussees)
<b>LF:</b>	Basalt Fine Graded Mix
<b>LVDT:</b>	Linear Variable Displacement Transducers
<b>M:</b>	Specimen size 200 mm
<b>N.B.</b>	nota bene (Note well)
<b>NCHRP:</b>	National Cooperative Highway Research Program
<b>N.E.D:</b>	Nadirshah Edulji Dinshaw

<b>O:</b>	Optimum AC content at 4% Air Voids
<b>Prob:</b>	Probability value
<b>OM:</b>	O-0.5%
<b>OP:</b>	O+0.5%
<b>PG:</b>	Performance Grade
<b>PMB:</b>	Polymer Modified Bitumen
<b>RS:</b>	Relaxation Strength
<b>RTD:</b>	Resistance Temperature Detectors
<b>R<sup>2</sup>:</b>	Coefficient of determination
<b>S:</b>	SBS Modification
<b>sd:</b>	Standard deviation
<b>size:</b>	Specimen size
<b>SBS:</b>	Styrene Butadiene Styrene
<b>SEM:</b>	Scanning Electron Microscope
<b>SHRP:</b>	Strategic Highway Research Program
<b>Superpave:</b>	SUperior PERforming Asphalt PAVEMENTs
<b>T:</b>	Specimen size, 30 cm
<b>TGDH:</b>	Turkish General Directorate of Highways
<b>TSRST:</b>	Thermal Stress Restrained Specimen Tests
<b>TT:</b>	Transition Temperature
<b>TUBITAK:</b>	Scientific and Technological Research Council of Turkey
<b>Z:</b>	Neat or non modified Asphalt

# CHAPTER 1

## INTRODUCTION

### 1.1. Background

According to the Turkish General Directorate of Highways, more than 80% of the entire road network is made from the mixture of asphalt-aggregate materials, 17% of which is reported as asphalt concrete. Among the major form of distresses commonly seen in Turkish highways is the low temperature cracking. These cracks are caused mainly due to the heavy volume of traffic load and because of exposure of these roads due to various environmental effects. Turkey exhibits continental climate especially in the Eastern Anatolia, in which air temperature usually falls below  $-13^{\circ}\text{C}$  during winter times. Hence, failures in asphalt pavements related to low temperature cracking are among the most important type of distresses within these regions. Moreover, during the autumn and early spring times, repeated variation of daily air temperature contributes to low temperature cracking. It should be noted that the problem of low temperature cracking is not limited to Turkey only or to a specific continent, over the years it has drawn attention of many researchers around the world especially in the United States and Canada. There are a number of researches conducted within these countries to understand the behavior of asphalt concrete under low temperature conditions.

Low temperature cracking is essentially a transverse crack occurring due to shrinkage of pavement surface course by either the variation of daily air temperature or reduction to an extreme minimum temperature. Asphalt concrete exhibits behavior like any other materials which contract upon cooling and expand upon heating. During a significant reduction in the air temperature, since the pavement is restraint to contraction because of the friction at the bottom of the surface, large tensile stresses are developed and cause eventual fracture of the surface layer.

The stress magnitude reached just before fracture is known as fracture strength. Cracking in the surface course can occur even after one cycle, which causes low temperature cracking, or sometimes after the repeated changes of air temperature, causing thermal fatigue cracking.

The thermal fatigue cracking of asphalt concrete is dependent upon the largest and the smallest strain rate as proved by various studies. Visually, the thermal fatigue cracking develops in the form of block cracking as compared to low temperature cracks, which are, in general, one dimensional.

Low temperature cracks form usually with a crack opening of around 2.5-3.5 mm. Because these cracks must be sealed by special sealant materials, they cause increased cost for road maintenance and repair operations and the expense of the economic resources allocated for the construction of new highways. If a proper repair is not done timely, the water will enter to the sub-layers and cause serious structural problems. The seepage of water can cause structural problems either by weakening of the structural layers as they experience erosion under moving traffic loads or by significant volume changes during the freeze-thaw cycles in the spring season. All these distresses cause deterioration of the surface course which influences the riding quality and safety, and shortening of the service life and as a result of loss in the structural capacity of pavements.

Previous studies indicate that low temperature cracking in asphalt concrete is affected by material selection process, effect of mix properties, i.e., aggregate , gradation, AC types, polymer modification, air void content, and the test parameters, namely, size of specimen, air void content, and cooling rate. Even though a number of researches have been conducted to study effect of these factors, there is, however, no a well-developed test method and agreement among the outcomes of different researches. This is due to the fact that researchers used different configurations for testing thermal properties and the complexity of asphalt concrete properties. Hence, the need to investigate asphalt concrete behavior under low temperatures is still up to

date using well established testing procedures. The motivation for this study is, thus, to research mix properties and testing parameters using an improved testing procedure, verify outcomes of previous findings and investigate thermal behavior of asphalt concrete fabricated using local materials.

## **1.2. Research Objective**

The objectives of the proposed research can be summarized as follows:

- (1) Design and set up a test configuration that can allow conducting Thermal Stress Restrained Specimen Testing (TSRST) of asphalt concrete beam specimens at an accuracy level consistent with the previous studies.
- (2) Identify important mix design and testing parameters for low temperature cracking of asphalt concrete using statistical tools.

Based on the outcomes of this research, it is aimed that mix properties and testing parameters that are important for low temperature cracking performance of asphalt concrete will be identified using a well set-up testing procedure. It is assumed that the outcomes of this research will help practitioners to understand the fracture mechanism of asphalt concrete, develop guidelines for the selection of proper materials and mix design parameters, which, in turn, reduce the potential for low temperature cracking of asphalt pavements.

## **1.3. Scope**

The study for this research was conducted in three phases:

- (1) Development of a test device and methods for TSRST testing of asphalt concrete specimens,
- (2) Developing an experimental design for the testing program and performing TSRST tests for asphalt concrete beam specimens prepared in the laboratory conditions,
- (3) Analysis of test results and identification of significant design and testing parameters based on statistical analyses.

A modified version of TSRST equipment will be developed to accurately measure the fracture stress and fracture temperature of the asphalt concrete samples, simulating the field conditions. An experimental design will be conducted to include the number of asphalt concrete samples required fabricated according to the state of the art Superpave mix design method. Analysis variance (ANOVA) and cluster analysis will be performed to identify the material parameters important for the low temperature cracking of asphalt concrete.

#### **1.4. Outline of Research**

An extensive literature review of the previous research efforts for low temperature cracking of asphalt concrete is presented in Chapter 2. The review includes a summary of research outcomes on effect of mix properties, climatic factors, test set-up used to measure fracture strength, and some modeling efforts to address low temperature cracking performance of asphalt concrete pavements.

In Chapter 3, a statistical design of experiment accommodating all testing variables is proposed. Also included in this chapter are the details on the development of a TSRST test frame, development of a user interface program for TSRST device and testing procedures used to measure fracture strength of asphalt concrete samples.

Chapter 4 is dedicated to the statistical analysis of findings obtained from both TSRST and glass transition tests. In this section, significant mix design variables needed to address the low temperature cracking are identified and incorporated in various statistical models.

Chapter 5 summarizes the outcomes of this study, presents recommendations for future work.

Various graphical results for fracture strength and glass transition tests are given in the appendices. Matlab<sup>®</sup> codes, ANOVA tables, cluster tables, and a software tutorial for TSRST testing, related to the research are also included in these sections.

## CHAPTER 2

### LITERATURE REVIEW

#### 2.1. Introduction

This chapter describes the concept and the mechanism for low temperature cracking on asphalt concrete (AC) pavements. The factors responsible for low temperature cracking constitute the major part of discussion being presented here, which are supported by findings of various studies investigating low temperature cracking phenomenon in asphalt concrete pavements. Also included here are the tests needed to determine the low temperature cracking and the available models that can be used to predict thermal cracking.

#### 2.2. Low temperature cracking

Low temperature cracking is one of the main distress types in asphalt concrete pavements occurring perpendicular to the roadway axis (Figure 2.1).

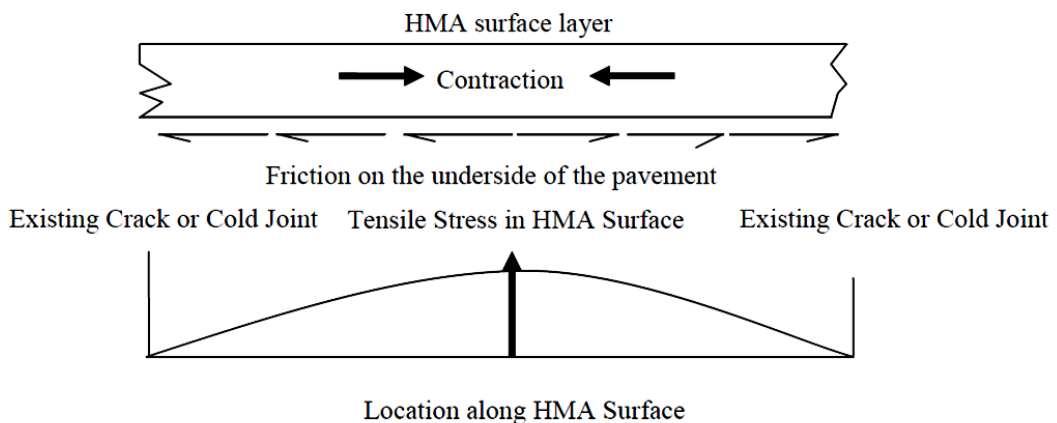


**Figure 2.1- Phenomena of low temperature cracking in AC pavements  
(FHWA courses, 1998)**

Low temperature cracking results from significant reductions in daily air temperature especially during winter session. As the temperature falls below zero degrees, it causes shrinkage in the surface course producing eventually large contractive forces as depicted in Figure 2.2.



**Figure 2.2- A view of low temperature cracking on an AC pavement section (Transport Pooled Fund Study 776, 2007)**

Since the surface course is restraint to free contraction because of bonding with the base course, large tensile stresses are developed and cause eventual fracture of the surface layer (Figure 2.2). The fracture may occur even after one cycle or after a number of cycles of temperature changes. The maximum stress level reached before fracture occurring in the surface course is known as the fracture strength of asphalt concrete.

Low temperature cracks are usually developed at uniform spacing because of the phenomenon as shown in Figure 2.1. If the thermal stresses reach to the strength level during each temperature drop cycle, the pavement will continue to fracture at certain intervals (Figure 2.3) until the spacing remained between the fractured parts will not allow a stress level that is no longer larger than the strength of the surface layer.

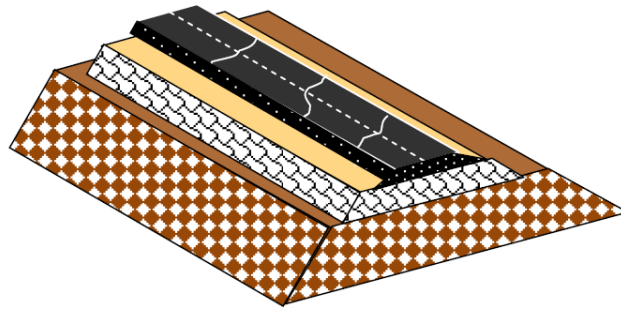


**Figure 2.3- Cross section of AC pavement showing low temperature cracks at uniform intervals**

According to the results of heat transfer analysis performed by Haas et al., 1987, the thermal stress becomes highest at the surface of upper layer and then gradually decreases with depth in a parabolic form. This behavior is due to the presence of temperature gradient that exists between air and the pavement foundation. The lowest temperature occurring on the surface (Figure 2.4) obviously results in the largest thermal stress in the surface course hence produces greater potential for low temperature cracking.

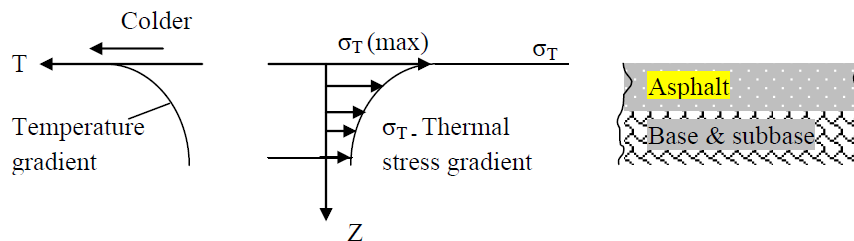


**Figure 2.4- Thermal stress gradients (Haas et al., 1987)**

Figure 2.5 is an illustration of low temperature cracking having 2.5 -3.5 mm crack opening. These cracks often have to be sealed by coatings resulting in high maintenance costs and expense of the economic resources allocated for the construction of new routes. If these repairs are not achieved in time, it will allow seepage of water through the cracks and eventually reach to the pavement foundation, which causes serious structural problems. Another form of damage that is driven by low temperature cracking is the spalling and the disintegration of crack edges by the effect of volume expansion of freezing water within the crack region. All these detrimental effects shorten the service life of AC pavements as a result of loss in the structural capacity of pavements. Low temperature cracks lower the riding quality of pavements and, if not repaired, can result in safety issues endangering lives and property.



**Figure 2.5- An example of a low temperature cracking in AC pavements**

**(Centria, 2009)**

The problem of low temperature cracking is not limited to one country or continent. Over the years it has drawn attention of many researchers around the world. Researchers found a number of factors that can contribute to low temperature cracking due to temperature variations.

Thermal fatigue cracking is another form of low temperature cracking resulting from variations in daily air temperatures. The repetition of such cycles causes thermal fatigue cracking in AC pavements. Vinson et al. (1989) presented in Figure 2.6. is a very good representation of the defining limits for thermal fatigue cracking and low temperature cracking.

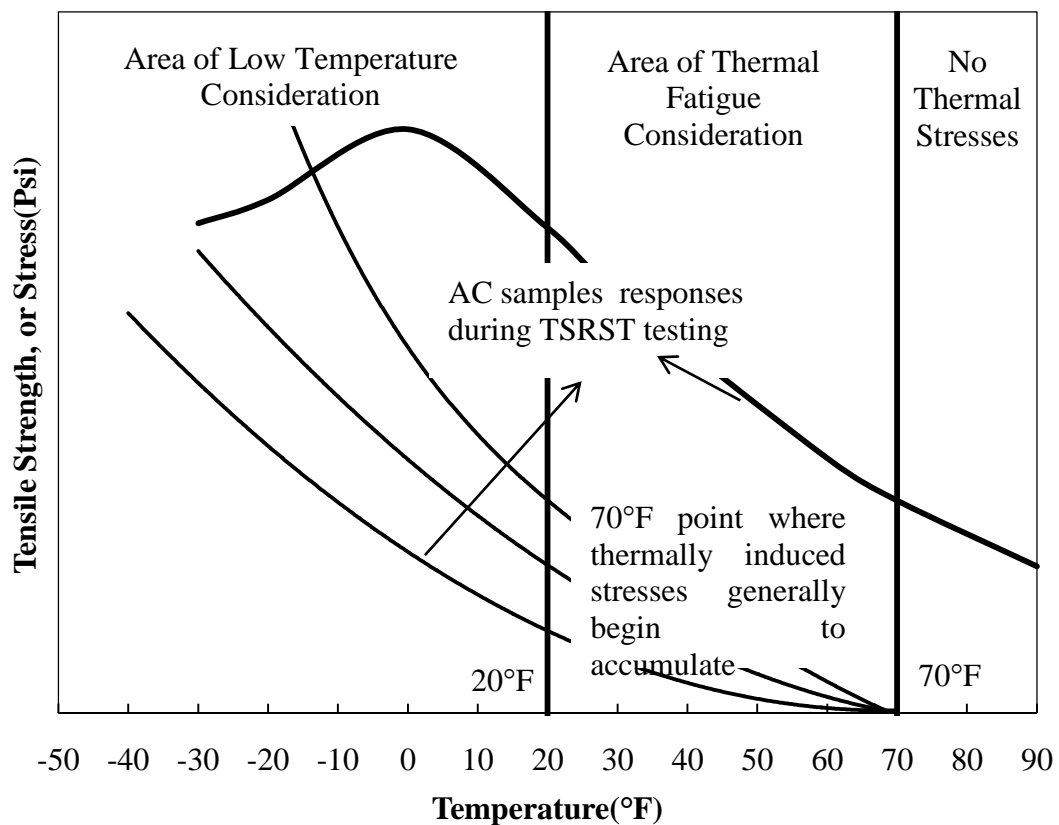


**Figure 2.6- Range of temperatures corresponding to low temperature cracking and thermal fatigue cracking (Vinson et al., 1989)**

Figure 2.6 shows that most of the thermal fatigue cracking of asphalt concrete specimens subject to TSRST testing occurs between temperatures 6.5 to 21°C (20-70°F) while the region in which air temperature is lower than 6.5°C is regarded for low temperature cracking. Thermal fatigue cracking of asphalt concrete is generally dependent upon the largest and the smallest strain rates developed at cold temperatures.

### **2.3. Factors affecting low temperature cracking**

Haas et al., (1987) categorized six main factors affecting low temperature cracking including climate, asphalt binder properties, asphalt mix, design and construction of pavements, age of pavement, and weathering effect of traffic. Their results indicated that there is a strong interaction between climatic effect, pavement layer thicknesses, and pavement aging and binder properties. In a report submitted to the Federal Highway Administration(FHWA) authorities for the Strategic Highway Research Program (SHRP) by Vinson et al., (1989), the effect of climate, material and pavement characteristics were defined as the broad reasons for low temperature cracking. In the following sections, each factor that is reported in various studies is discussed in terms of its role for low temperature cracking.

#### **2.3.1. Climate**

Low temperature cracking is a common distress type for countries subjected to severe cold temperatures during winter seasons. Thermal fatigue cracking is, on the other hand, the main distress type for especially desert regions where the difference between day and night temperatures is very high. The parameters related to thermal cracking in the context of climate are the pavement surface temperature and the average cooling rate in pavement structure. These parameters contribute to the aging of AC pavements and influences upon the fracture resistance of surface course. Given the influential effect of climate, a detailed discussion of these parameters is necessary in terms of their effects on low temperature cracking of AC, which are presented in the following sections.

### **a) Temperature**

Temperature is the primary reason for low temperature cracking in areas subjected to extreme cold climates during winter season, and in regions where the range of maximum and minimum air temperatures is very large especially during autumn and spring season. Under cold temperatures, pavements experience significant volume changes by shrinkage and excessive aging of binder, which elevates the potential for cracking by increasing the binder stiffness. A study conducted by Kliewer, (1996) concluded that increase in aging effect of binder is due to increase in the maximum temperature on pavement surface, which, in turn, increases the potential for low temperature cracking. SHRP program introduced the performance based grading system which takes the low temperature performance of binders into account based on a series of laboratory testing. For instance, a PG 64-32 grading means that the binder can tolerate up to 64°C of average seven-day-maximum pavement design temperature and -32°C minimum pavement design temperature without experiencing any plastic deformations under hot temperatures, and low temperature cracking under cold temperatures. It must be emphasized that these critical temperatures define in-field air temperatures rather than pavement temperatures for which a conversion procedure is applied in the relevant design standards. In general, the pavement surface temperature is 10-15°C warmer than the air temperature as identified using a standard conversion procedure.

The effect of temperature on low temperature cracking was investigated in a number of recent studies. The research conducted by Vinson et al., (1996) pointed out that the frequency of cracking increases once the temperature of pavement falls below the glass temperature of the binder for long time durations. Shah, (2004) investigated the field maps obtained as a result of distressed survey on six test sections constructed with different PG graded binders. She found that binders graded according to the PG grading system provide more resistance to low temperature cracking compared to the binders graded based on other systems. Nam and Bahia, (2005) also reported that the binder glass temperature does not truly defines low temperature cracking behavior of asphalt concrete, in fact, there is a need for specifying and measuring the

glass temperature of the mix. In a research conducted in Transport pooled study 776, (2007) by the Minnesota Department of Highway, it was found that the range of glass temperatures measured for various mixtures depends on both the type of mix and binder, and that these temperatures are, in general, nearer to the fracture temperature of the tested mixtures.

#### **b) Cooling rate**

It is generally assumed that the cooling rate of AC pavements is around 1°C per hour in the field at which the pavement experiences a slow relaxation of thermal stresses, and eventually falls beyond the viscoelastic region in which low temperature cracking potential becomes higher. However, behavior of an AC specimen at this cooling rate is difficult to simulate in laboratory conditions as it requires significant amount of time to run a test and obtain the results. Hence, researchers generally test AC specimens at a relatively higher cooling rate to overcome these difficulties. Effect of cooling rate on mix behavior was also investigated in several studies. Jung and Vinson, (1994) observed that higher cooling rate causes early occurrence of cracks since the glass transition temperature is reached earlier during testing. Shen and Kirkener, (2001) found the cooling rate as one of the contributing factors for thermal stresses that cause cracking based on their semi analytical model used to calculate the time of occurrence of cracks in flexible pavements. Conversely, in Transport pooled study 776, (2007) conducted by the Minnesota Department of Highway, researchers could not find any correlation between the cooling rate and the fracture strength of AC specimens.

#### **c) Pavement aging**

Aging is defined as the stiffening of asphalt binder over time by oxidation and other chemical transformations in binder structure, which take place under varying environmental conditions (Papagianakis and Masad, 2007). The performance of AC pavements is greatly influenced by the age hardening of asphalt binder. The pavement aging is directly related to the binder aging, and it is a function of temperature and time of service. Aging in binder is believed to influence the failure strain, failure

stress and the stiffness of the mix material. It is a well-known fact that older pavements tend to develop thermal cracking earlier than do the new AC surface courses. Effect of aging was investigated based on a number of studies conducted on either binder or asphalt mix materials in recent studies. Jung and Vinson, (1994) reported that binder aging is one of the significant factors influencing the low temperature cracking of AC pavements. Mouillet, (2004) conducted bending beam rheometer (BBR) tests on two base binders and the same binders modified with varying contents of polymer modifiers. Each binder was also subjected to rolling thin film oven (RTFO) test and pressure aging vessel (PAV) test to simulate the binder aging during construction and service conditions. Test results indicated that the aging process yield increased binder stiffness and elevated temperature level to meet the required stiffness criterion. Kliewer et al., (1996) tested AC slab and cylindrical specimens that were aged at 50°C and 85°C for 100 days. TSRSTs were then conducted to measure the fracture stress and the fracture temperature for each mixes. They concluded that the SHRP long term aging process adequately reflects the field aging conditions for AC pavements. The authors also reported that the presence of high content of non-polar components in an asphalt binder may be one of the reasons for the thermal cracking. Similarly, Sebaaly et al., (2002), and Lee, (2009) conducted detailed field evaluations of asphalt mixtures for aging effect and founded that there exists a strong correlation between aging of pavement and thermal cracking.

### **2.3.2. Component material properties**

The word material refers to aggregate and binder used in the construction of AC pavements; it also refers to the size, shape and texture of aggregates and the stiffness of binder in particular. The climatic condition described cannot be controlled by the engineer; however what he can do is to select the materials that is best suited to the given climatic condition and that can sustain their chemical and physical properties over a long period of time.

### **a) Aggregate**

Major portion of hot mix asphalt is composed of aggregates. In the past, it was the misconception that the low temperature cracking is mostly associated with asphalt, but it has been shown by many researchers that the selection of a suitable aggregate cannot be ignored. People involved in the pavement research area now believes that the quality of aggregate used in an asphalt mix plays a more important role for crack formation than do the binder characteristics and aging only. Vinson and Jung, (1994) investigated the impact of aggregate in TSRST testing of mixtures and reported that the fracture temperature, although sensitive to binder type, is influenced by type of aggregate. In a similar study by Stuart and Youtchef, (2002), a total of 11 mixtures prepared with different types of aggregate including black granite, limestone, granite and granite treated with hydrated lime were tested to observe the effect of aggregate on low temperature cracking of AC specimens. Their experimental results showed that the change of aggregate does not significantly contribute to low temperature cracking response of asphalt concrete samples. Contrary to this study, the results of Transport pooled study 776, (2006) showed that that aggregate is a statistically significant factor affecting the fracture strength of AC pavements. Similar findings were also reported by Xinjun et al., (2010). Based on a comprehensive laboratory testing program, Drüschner, (2004) came to a conclusion that not only aggregate properties but also its adhesion properties play important role for the low temperature cracking performance of asphalt mixtures. Tan et al., (2008) investigated the effect of aggregate gradation on low temperature cracking resistance of asphalt mixtures based on statistical analyses. They concluded that there is a positive correlation between the degree of aggregate interlock and the low temperature performance of asphalt concrete mixes.

Although the influence of aggregate on low temperature cracking is well established, however, influence of the maximum aggregate size and gradation is not well documented in the literature, and there are also some conflicting studies as described.

## **b) Asphalt binder**

The selection of a suitable binder is absolutely necessary for construction of long lasting pavements in cold regions. Investigations have revealed that binder rheological properties to handle temperature are the most important factors for controlling the low temperature cracking of AC pavements. The behavior of binder largely depends on its stiffness, glass transition temperature, alteration, and intrinsic mechanistic behavior. Sufficient literature is available discussing the role of asphalt binders in thermal cracking, and it was believed for quite some time that it is the only factor that dictates low temperature cracking performance. The paragraphs to follow are an attempt to describe these properties in detail.

## **c) Asphalt cement stiffness**

The stiffness is the resistance of an elastic body to deformation by an applied force. It is a material property commonly evaluated by dividing the force with the corresponding displacement. The study of stiffness is necessary for evaluating the response of AC pavements. Furthermore, the stiffness of asphalt binder is important in determining the behavior of mix in extreme temperature and loading conditions. Characteristics of binder stiffness are given in the literature as follows:

- Stiffness is independent of time for very short duration of loading, and it approaches the modulus of elasticity,  $E$ .
- Material at long loading durations behaves purely viscous as the stiffness decreases at a uniform rate,
- Visco-elastic behavior is observed at intermediate loading times, The stiffness characteristic of binder can be well understood by Figure 2.7.

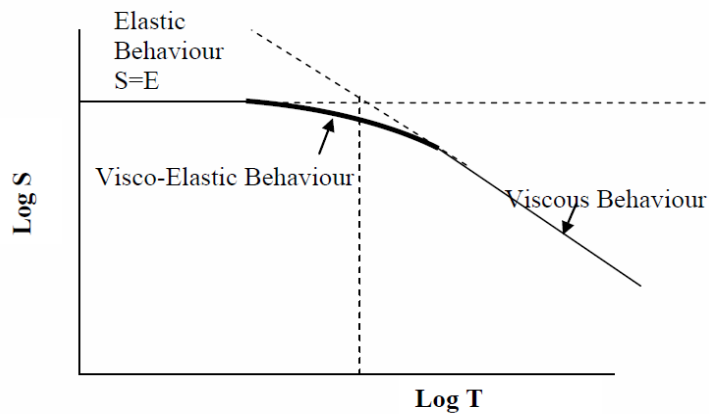


**Figure 2.7- Stiffness behavior of asphalt binder (Roberts et al., 1996)**

Since asphalt is a viscoelastic material its stiffness is defined by the ratio of stress to strain as a function of time and temperature (Vinson et al., 1989). The stiffness of asphalt depends upon the state of stress, temperature, moisture, and strain rate and damage conditions. Roberts et al., (1996) emphasized that the stiffness of asphalt concrete is primarily dependent upon the stiffness of asphalt cement and for low temperature cracking a low stiffness binder is desired. The author provided references of many researchers specifying the limiting stiffness value of binder as 275 Kg/cm<sup>2</sup> at a minimum pavement temperature of -230° C and 20,000 seconds loading time.

Another reference available from the literature by Roberts et al., (1996) is the St. Anne Test Road in Canada, where many researchers defined the critical value of stiffness according to various loading times, some of which are illustrated in Table 2.1.

**Table 2.1- Typical stiffness values for asphalt binder at loading times (Roberts et al., 1996)**

Stiffness (N/m <sup>2</sup> )	Loading time (seconds)
1 x 10 <sup>9</sup>	1800
5 x 10 <sup>8</sup>	3000
2 x 10 <sup>8</sup>	7200
1.4 x 10 <sup>8</sup>	10000

The methods to determine stiffness of asphalt can be broadly classified into two categories (a) Indirect Method, and (b) Direct method.

In the indirect method, the values of stiffness are estimated by nomographs developed by Van der Poel, (1954). This nomograph (Figure 2.8 ) extrapolates the stiffness value based on the penetration grade of asphalt cement at different temperatures, operating temperature and time of loading.

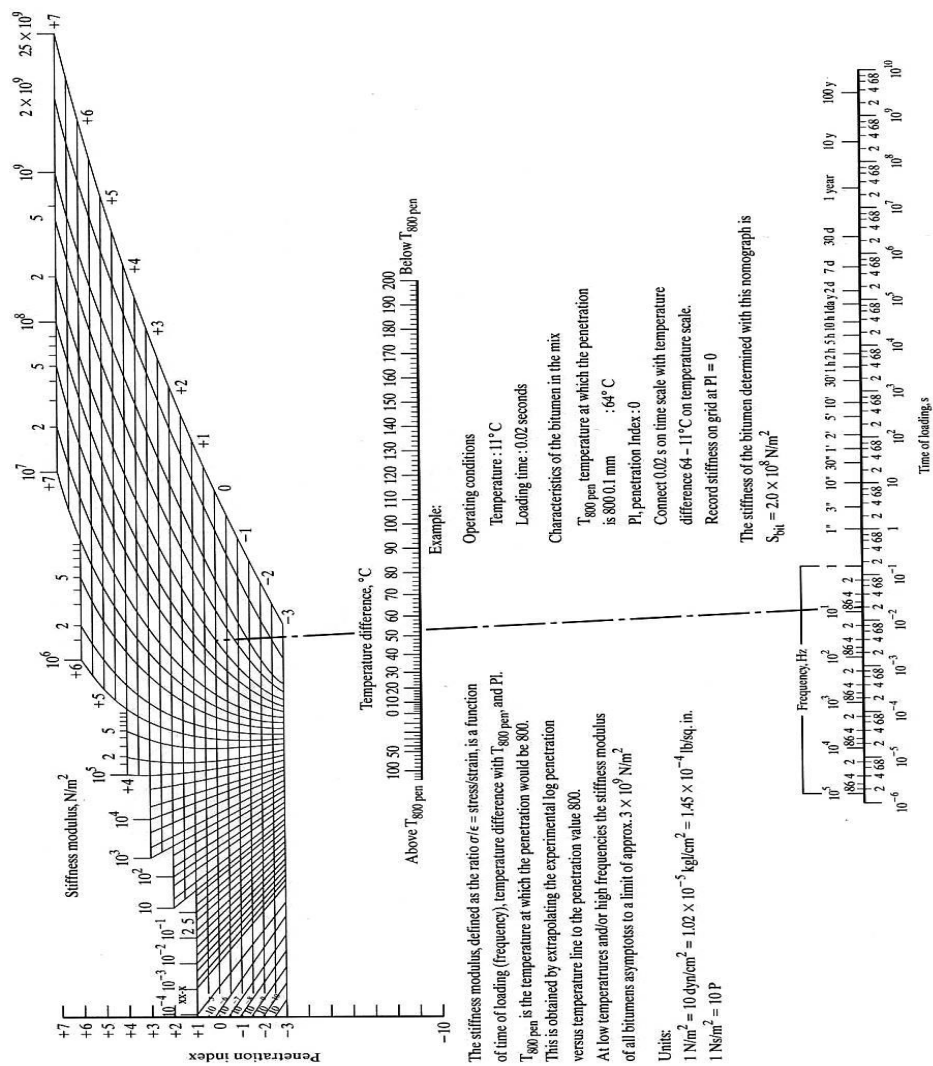


Figure 2.8- Estimating stiffness of asphalt binder using Van der Poel, (1954) nomograph

Improvements in measuring the binder rheological properties has now made the direct methods very common, and prompted researchers to measure stiffness directly instead of estimating using nomographs. This method includes creep testing, relaxation testing or constant rate of strain testing in either tension or compression mode based on indirect tensile test and bending beam rheometer test procedures (Robert et al., 1996).

The creep is measured by the dynamic shear rheometer (DSR) device and the test method can allow measuring the presence of elastic response in a binder and the change in elastic response at different stress levels, as outlined in the ASTM D7405-08 standard.

In the BBR test, the binder stiffness and an m-value are evaluated. The m-value is actually the slope of the log creep stiffness versus log time curve at any time (t). The Superpave specifies the m value be greater than or equal to 0.300 when measured at 60 seconds. The maximum value for stiffness is specified as 300MPa.

Another test called direct tension test (DTT) is being used to measure the stiffness of asphalt binder. Normally, this test is preferred if the binder stiffness exceeds 300 MPa in the BBR test, especially for polymer modified binders. A dog bone specimen of binder is prepared and stretched from it ends until it breaks. The strain is then calculated in terms of the percent elongation along the specimen length. The Superpave specifications require the strain rate be at least 1%. Sebaaly et al., (2002) investigated the applicability of the tests specified by SHRP for characterizing the low temperature response of binders and mixtures used in the construction of highways in Nevada,USA. Based on their research outcomes, they concluded that either DTT or BBR test can well characterize the response of binder to low temperature cracking. From the literature as presented, it is understood that the stiffness of asphalt binder is the key factor for the performance of AC pavements at cold temperature conditions. It is generally suggested that a low stiffness binder should be preferred to resist low temperature cracking.

#### d) Asphalt cement thermal properties

Another important property of asphalt binder for low temperature cracking is the glass transition temperature. The glass transition of a binder defines the temperature level at which the binder rheological properties move from viscoelastic to elastic medium. Wada and Hirose, (1960) measured the thermal coefficient of nine asphalt binders before and after glass transition temperature having varying percent of asphaltenes using a pyrex glass dilatometer. They found that the glass transition temperatures range from 2 to -37 °C and the thermal coefficients below the glass transition are between  $3.7 \times 10^{-4}$  to  $3.4 \times 10^{-4}/^{\circ}\text{C}$ . They attributed the difference in the measure properties to the existence of varying percent of asphaltenes in the binders. These results are presented in Table 2.2.

**Table 2.2- Values of glass transition temperatures and thermal coefficients measured by Wada and Hirose, (1960)**

Sample	Asphaltenes Wt %	Density (20 °C) g/cc	Glass Transition Temperature (°C)	Thermal Expansion Coefficient ( $10^{-4}/^{\circ}\text{C}$ )		
A	100.0	1.079	none	-	-	-
B	75.0	1.053	none	-	-	-
C	61.9	1.039	2.0	5.8	3.7	2.1
D	58.6	1.034	0.0	6.0	3.8	2.2
E	57.1	1.030	-2.0	6.3	4.0	2.3
F	52.5	1.027	-6.5	6.6	3.9	2.7
G	50.8	1.026	-7.5	6.8	3.9	2.9
H	28.6	1.014	-22.5	6.9	3.7	3.2
I	0.0	1.004	-37.5	7.6	3.4	4.2

Breen and Stephens, (1967) describes the glass transition behavior of asphalt as a second order transition behind the melting point. They believe that a glass transition occurs when a change of volume rate with respect to temperature enters a discontinuous phase. This phenomenon is illustrated in Figure 2.9.

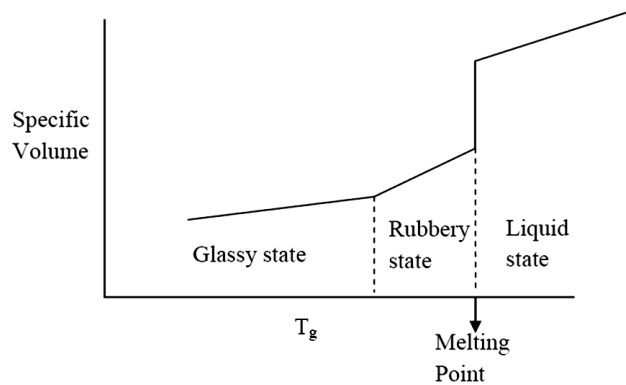


**Figure 2.9- Glass transition temperature of asphalt (Breen and Stephens, 1967)**

Schmidt and Santucci, (1966) also measured the glass transition point of asphalt binder and found that there is a particular change of slope in the volume change versus temperature plot, which indicates an abrupt change in the thermal coefficients, once the glass transition temperature is reached as depicted in Figure 2.10.

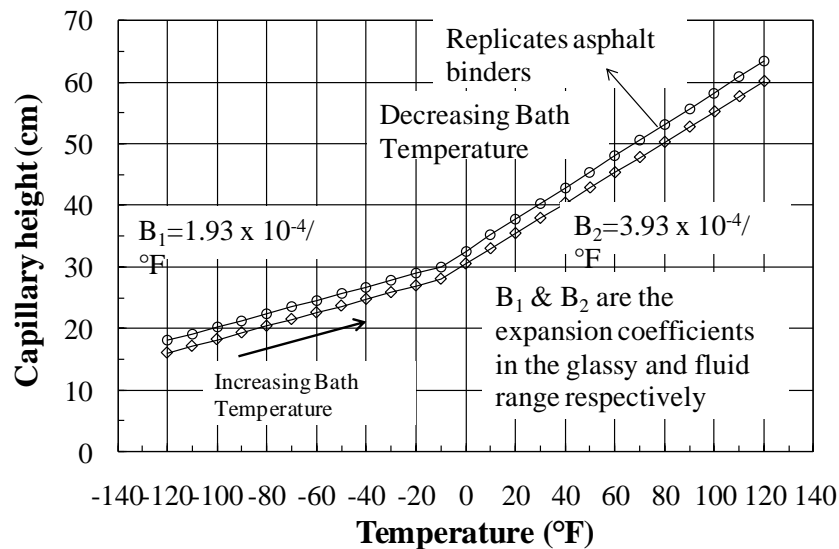


**Figure 2.10- Typical transition behavior of asphalt binder with temperature (Schmidt and Santucci, 1966)**

### **e) Asphalt cement modification**

All asphalt binders and mixtures may not require modification. It is only required when some specific purpose is needed and where a locally available binder cannot fulfill the requirement such as to obtain a less stiff binder for service conditions at low temperatures. The modification of binder can be achieved in various ways, but the most common method in the highway industry is using crumb rubber, mineral filler and polymers. Polymer modifiers are of two kinds, elastomers and plastomers. Elastomeric modifiers can stretch and elastically recover their shape while plastomers impart high strength to resist heavy load, but crack when subjected to higher strains. Two common elastomers are used in the highway industry: one is styrene-butadiene-styrene (SBS) and the other is styrene-butadiene-rubber (SBR).

There are also a number of studies exist investigating the effect of modification on low temperature cracking. Isacson and Zeng, (1996) studied the effect of modification for mixes prepared at different gradations and found positive contribution of binder modification to low temperature cracking resistance of asphalt concrete. Similar findings were also reported by Youtchef and Stuart, (2002) based on the TRRST testing of AC specimens. Shah, (2004), however, found that the binder modification used in the state highways increased the frequency of low temperature cracking. Ho and Zonzotto, (2005) used modified and unmodified binders to investigate low temperature performance based on secant modulus and fracture energy concept. Their results indicated that the modified binders used in the testing program provide superior performance than do the unmodified binders. In terms of the performance of modified binders at low temperatures, similar findings were also reported in Transport pooled study 776, (2007), and study by Nam and Bahia, (2009).

### **2.3.3. Asphalt mixture properties**

After discussing the individual components of asphalt mixtures, it necessary to discuss the properties of mixture itself. The hot mix asphalt is a heterogeneous material having asphalt, aggregate and air voids (Figure 2.11).

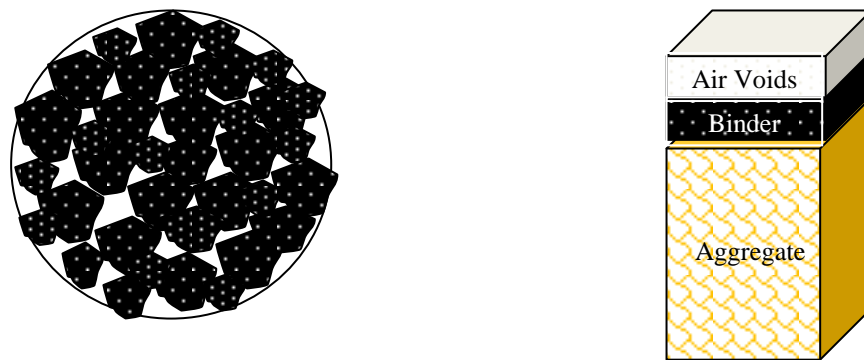


**Figure 2.11- Classical representation of asphalt mixture**

The percentage of each of this component has great influence in resisting the distresses caused due to either environmental effects or traffic loading.

On one side, it is the type of binder and the presence of volatile or polymer component in the form of modification, which can make a durable pavement surface. While, on the other end, it is the aggregate and its gradation along with its shape, mineralogical composition, texture and surface area that are largely responsible to produce a desirable asphalt concrete. In the following sections, characteristics of asphalt mixture in terms of low temperature cracking are discussed in detail.

**a) Stiffness of asphalt mixture**

The stiffness of a mix is an important property of asphalt concrete that determines the potential of surviving in extreme conditions of loading and temperature. It is believed that mixture having shear stiffness  $|G^*|$ , above 250 MPa measured at 40°C with 10 Hz frequency is adequate enough to provide long lasting pavements (Pellinen and Xiao, 2006 ).

There is a strong correlation between the asphalt concrete mix stiffness and fracture strength against low temperature cracking; it is believed that mixes with high stiffness value can resist low temperature cracking well as compared to mixes with low

stiffness. However, a little or no research outcome is available regarding the contribution of aggregate in imparting or improving the stiffness of the mix.

To achieve a successful design of asphalt concrete for low temperature conditions, the measurement of the mix stiffness is necessary for predicting the thermal response of AC pavements. There are also various ways of determining the stiffness of a mix either by estimation or direct measurement method. One conventional, although empirical, way to measure the mix stiffness is to use the nomograph developed by Bonnaure et al., (1977) as shown in Figure 2.12.

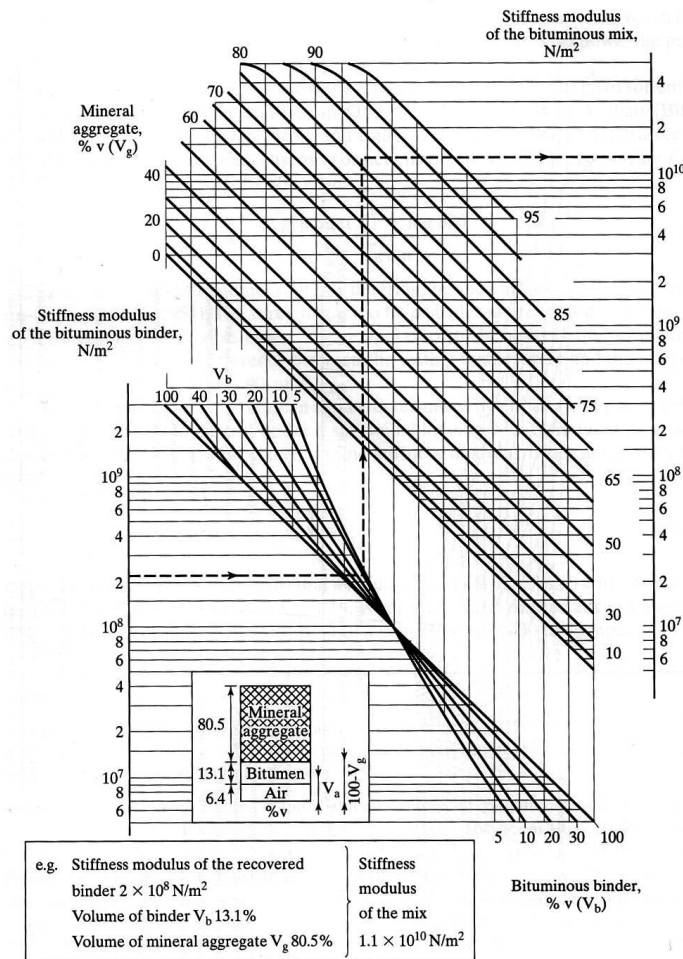


**Figure 2.12- Prediction of mix stiffness by Bonnaure et al., (1977) method**

The nomograph takes the stiffness modulus of binder, the volume of binder in the mix and the air voids in mineral aggregate as an input, and returns the stiffness of the mix by extrapolation.

Test protocols have also been developed to determine the stiffness of mix directly in the laboratory either for a cored sample from the field or specimen made in the laboratory. The types of tests that have been used nowadays include the indirect tension creep test, the dynamic modulus test, and the shear dynamic modulus test.

#### **b) Quantity of binder in a mix and air void content**

Changes in asphalt cement content, within a reasonable range about the optimum, do not have a significant influence on the low temperature cracking performance of AC pavements. Vinson et al., (1989) concluded that the increase in AC content lowers the stiffness of asphalt concrete mixtures.

The air void content is another variable that should be taken into consideration while evaluating the mix performance for low temperature cracking. Shah, (2004) found that the constructed test sections at 4% and 7% voids did not show large variations in the frequency of thermal cracks. Similar results were also published by Xinjun et al., (2010) and in the Transport pooled study 776, (2007).

#### **c) Thermal properties of asphalt mixture**

Thermo-volumetric properties of asphalt concrete are the coefficient of contraction and the glass transition temperature. These properties are required to be measured to evaluate the mix performance under low service temperatures. The behavior of asphalt mixtures that are subjected to extreme low temperatures shows a bilinear curve for volume change versus temperature relationship. At the glass transition temperature, the slope changes abruptly and the value of coefficient of contraction is lower than the value measured before.

The history of measuring the glass transition temperature is not long, and in the last decade scientist found various successful laboratory methods to measure it. Table 2.3 shows various glass transition temperatures and the coefficients of thermal contraction values reported in the literature.

**Table 2.3- Glass transition temperatures and coefficients of contraction reported by different authors for asphalt concrete**

Researchers	Range of $T_g$ (°C)	Range of $\alpha_l$ ( $\times 10^{-4}$ )	Range of $\alpha_g$ ( $\times 10^{-4}$ )
Wada and Hirose,1960	+2 to -37.5	5.8-7.6	3.4-4.0
Schmidt and Santucci,1966	+5.9 to -36.4	5.6-6.2	2.7-3.3
Jongepier and Kuilman,1970	N.A.	N.A.	2.7-3.6
Bahia and Anderson,1993	-4.1 to -28.2	5.9-6.8	3.3-3.6
Nam, 2005	-17.2 to -54.7	5.2-7.3	2.3-4.9
Nam and Bahia, 2005	-24.5 to -45.4	5.8-5.87	2.9-3.6
Transport pool study 776,2007	-20 to -43.6	4.44-5.83	1.25-3.50

Where

$T_g$  = glass transition temperature;

$\alpha_l$  = thermal expansion coefficient for  $T > T_g$ ; and

$\alpha_g$  = thermal expansion coefficient for  $T < T_g$

Conventionally, the researchers in the past used to estimate the thermal properties of asphalt concrete from the thermal properties of binder and aggregate. Jones et al. (1968) suggested such an empirical equation to estimate the mix thermal properties from the properties of binder and aggregate in Equation (2.1).

$$\alpha_{mix} = \frac{VMA * \alpha_{AC} + V_{agg} * \alpha_{agg}}{3 * V_{total}} \quad (2.1)$$

Where

$\alpha_{mix}$  = the linear coefficient of thermal contraction of asphalt mixture (1/°C)

$\alpha_{AC}$  = the volumetric coefficient of thermal contraction of asphalt binder in the solid state (1/°C). An average value of  $3.45 \times 10^{-4}$  (1/°C) was used.

$\alpha_{agg}$  = the volumetric coefficient of thermal contraction of aggregate (1/°C)

VMA= the percent volume of voids in mineral aggregate (air voids + volume of effective asphalt)

$V_{agg}$  = the percent volume of aggregate in the mixture

$V_{total}$  = is the total volume, 100 percent

Bahia and Anderson (1993) proposed Equation (2.2) for fitting a five a parameter curve to the change of volume versus temperature data.

$$v = C_v + \alpha_g (T - T_g) + R(\alpha_l - \alpha_g) \ln \left[ 1 + \exp \left( \frac{T - T_g}{R} \right) \right] \quad (2.2)$$

Where

$v$  = specific volume at temperature  $T$ ;

$C_v$  = volume at a given temperature;

$T_g$  = glass transition temperature;

$R$  = constant defining the curvature;

$\alpha_l$  = thermal expansion coefficient for  $T > T_g$  ; and

$\alpha_g$  = thermal expansion coefficient for  $T < T_g$

Nam, (2005) used a simple dilatometer to measure the glass transition temperature of varying asphalt binders. The test setup included a special compression chamber equipped with two linear variable displacement transducers to measure the amount of contraction of asphalt binder sample. The volume change measurement was then converted into volumetric strain as a function of temperature. The bilinear curve was fitted to Equation (2.2) by applying non-linear regression methods to calculate the glass transition temperature and the coefficients of thermal contractions. Results of his tests showed that the glass temperature is highly dependent upon the type of

aggregate and the modification used. The author also pointed out that the glass transition temperature alone cannot be a good indicator to estimate the potential of a mix for low temperature cracking.

#### **2.4. Test methods to evaluate thermal properties of asphalt concrete**

Over the years, researchers have used different tests to evaluate the fracture resistance of asphalt concrete pavements at varying degree of success. The indirect tensile test, fracture mechanics tests, fixed frame restraining cooling test and the TSRST are among those that are being used for testing low temperature performance asphalt concrete. However, it is believed that among the tests conducted, the TSRST best describes the fracture resistance of asphalt concrete (Vinson and Jung, 1994; Marras-teanu, 2004; Dongré et al., 2007). These tests are being discussed in detail in the following sections.

##### **2.4.1. Fracture mechanics test**

This test measures the energy required to mechanically break a loaded AC specimen, which is related to the low temperature cracking performance of the specimen. There are three ways of conducting this test: disk shaped compaction test, semi circular bending test and bending beam test. A predetermined notch is made in the centre of the sample to define the failure location. The load produced for measuring the fracture allows for the determination of stress and strain from which the fracture toughness and the fracture energy are calculated.

##### **2.4.2. Thermal Stress Restrained Specimen Test (TSRST)**

TSRST test was first introduced by Vinson et al., (1989) to measure the fracture strength of asphalt mixtures. Over the years, it has been modified by many researchers (Nam and Bahia, 2005) to measure thermal stress at a higher rate with same time and liquid nitrogen consumption. In the present setup, a rectangular AC specimen is prepared with loading platens glued using an epoxy at their bases and allowed for curing for approximately 12 hours. The specimen is then mounted on the testing device and the linear variable displacement transducers are attached to the platens to

measure the thermal shortening of the specimen. Resistance temperature detectors (RTDs) are placed to all four faces of the specimen to measure the temperature change during the cooling operation. In the test setup used in this study, one of the RTDs is also attached to the extension bars to account for the temperature effect on the periphery of the device. The specimen is then subjected to a constantly decreasing cooling rate by the cooling system. As the temperature decreases, the specimen length is forced to remain constant by the actuator of the testing device so that the thermal stress is built up in the specimen until fracture. As the testing proceeds, the temperature and the stress level at which the fracture takes place is then recorded to finalize the testing process.

There are, however, various shortcomings associated with the TSRST. Vinson and Jung, (1994) pointed out that small eccentricities produced during specimen preparation process induce bending stress, which introduces variability in the test results. Epps, (1998) commented on the high pricing of the chamber coolant (liquid nitrogen). Wargo, (2008) pointed out that time spent for sample preparation for TSRST is a long process to make this test uneconomical for a routine mixture test.

### **2.4.3. Indirect tension creep test**

This test is conducted at two different modes for asphalt concrete specimens: one is the measurement of creep and failure strain performed by keeping the stress constant, called as indirect tensile creep test, and the other is the measurement of strength by applying a constant rate of deformation, also known as indirect tensile strength test. In both types of this test, a 100 mm diameter and 50 mm thick AC specimen is subjected to compressive diametrical loading at three different temperature, depending upon the specifications for instance if the specification is 25°C, then -20°C, -30°C are selected and temperature of -10°C or -40°C should then be selected to complete the third required temperature. The loading is applied by vertical movement of loading strips placed on the specimen at a rate of 12.5 mm/min. One of the advantages of this test is the measurement of poisson ratio that is important in the mechanistic design of pavement thickness.

The measured creep compliance is converted into relaxation modulus thus a very important parameter in defining the constitutive relation for asphalt concrete mixtures. These tests are the current standards of AASHTO for determining the fracture resistance of asphalt concrete at low temperatures. Figure 2.13 illustrates an AC specimen prepared for the IDT testing.

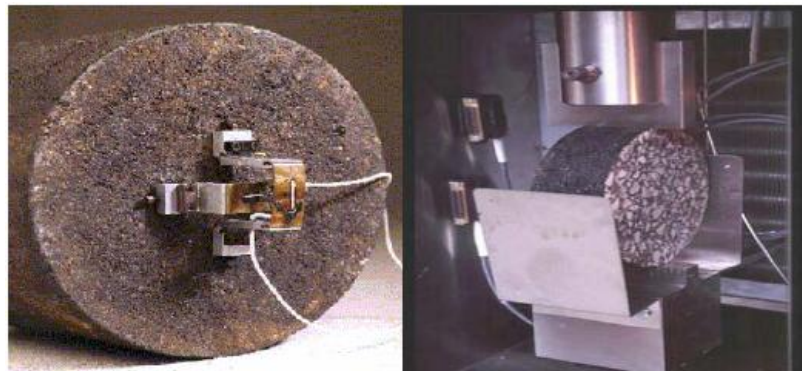


**Figure 2.13- An AC specimen preparation before IDT  
(North Central Superpave Centre)**

## **2.5. Models for low temperature cracking**

The models available for predicting thermal cracking can be categorized into two areas:

### **2.5.1. Empirical models**

These models are also known as statistical models described in terms of regression coefficients, and their values are derived as a result of thorough analysis using ANOVA. Empirical models are highly dependent upon the set of experiment variables and generally not valid for other set of data.

In the literature, most of the empirical models are related to the field measurement of cracks that are correlated with the experimental data. Since the scope of this study is

limited to laboratory investigation only, it seems inappropriate to discuss these models here.

### **2.5.2. Mechanistic models**

Mechanistic models describe the relation between the properties measured from laboratory experiments and field performance of the mixture. Some of these methods are COLD MODEL (Finn et al., 1986), University of Florida model (Ruth et al., 1982), and Texas A&M Model (Lytton et al., 1983). The latest model is thermal cracking model (TC model) and viscoelastoplastic continuum damage (VEPCD) model.

#### **a) Thermal cracking model**

This model is presently available in the AASHTO 2002 Mechanistic Empirical design guide to predict thermal cracking in AC pavements. The mechanistic-empirical model predicts the amount of thermal cracking versus time based upon mixture creep, strength, and thermal contraction properties, along with climatic inputs and information related to the overall pavement structure. The present TC Model, however, utilizes mixture tensile strength at a single test temperature of  $-10^{\circ}\text{C}$ , and then develops fracture parameters by taking this value as an estimate of the undamaged tensile strength of the mixture, along with a slope parameter from the master compliance curve (m-value). This model lacks the inclusion of mixture aging with time; also a more concise fracture test measurement such as from TSRST is needed.

#### **b) Viscoelastoplastic Continuum Damage (VEPCD) model**

This model was developed under NCHRP 9-19 project by Chehab et al., (2005). The model characterizes the viscoelastic and viscoplastic response of asphalt concrete in addition to micro-cracking and has the capability to accurately characterize the tensile behavior of asphalt concrete under thermally induced loading. It also measures the strain at fracture during TSRST testing. This model has been tested on a limited number of samples and does not consider variables such as aggregate gradation and type that can significantly affect the fracture strength of asphalt concrete.

## **CHAPTER 3**

### **METHODOLOGY**

#### **3.1. Introduction**

This chapter describes the methodology adopted in this research. The main contents presented in this chapter includes design, fabrication, programming and calibration of TSRST device, experimental design of samples, determining the number of samples required, estimation of quantities of materials, sample mixing, compaction and sizing. Discussion also includes modification of apparatus and preparation of sample for testing along with the details of configuration of samples tested under various testing conditions. The research methodology is summarized in Figure 3.1.

#### **3.2. Machine manufacture**

Although TSRST has long been in practice by the researchers around the world, no consensus has been, however, reached on the specification of a standard testing machine. Researchers from different institutions are still coming with their own design of test setup and procedures to perform this test. This would mean that there may not be one manufacturer around the world who may have the capability to produce the machine on regular basis, or this can be put in this word that a TSRST machine designed is not patented yet. Therefore, fabrication and design of a test device is another task that needs to be performed in this study.

##### **3.2.1. Design and fabrication**

The first task in this research is to manufacture a TSRST machine that can be used to measure the fracture strength and the fracture temperature of AC beam specimens under controlled loading and deformation states.

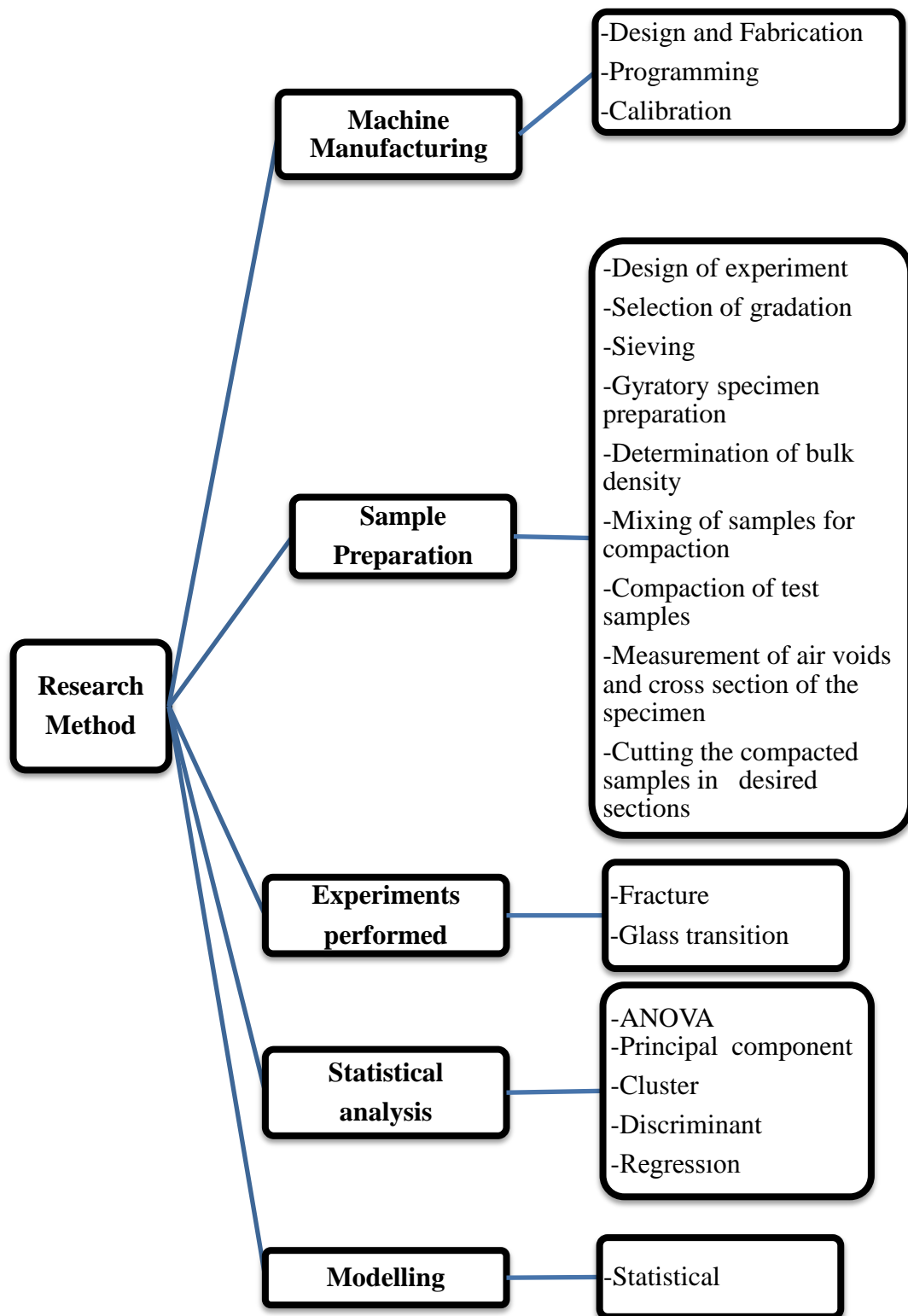


**Figure 3.1- Flow diagram for research methodology**

The TSRST machine comprises of four key components that include refrigerating compartment, servo motor for applying loading, compressor unit, and liquid nitrogen tank.

The test device has a servo-controlled loading capacity of 50 kN. A data acquisition system is attached with a personal computer for operating the device, controlling the units, and for collecting the test data.

The device can control the axial load and displacement through a mechanical actuator driven by a servo motor. The temperature is also controlled through the user interface program at a selected cooling rate. The test is conducted until the fracture of specimen to determine the fracture strength and the corresponding temperature.

The design of the device was inspired from the Arand's (1987) TSRST device for testing thermal properties of asphalt concrete. The design consists of two layers; outside layer is made from structural steel frame, and the inner layer from a special foam material for insulation purpose.

As it can be seen from Figure 3.2, 65 mm thick steel plates on the top and bottom of the frame are welded to two 20 mm thick steel sheets to build the structural frame. An insulation material with a thickness of 170 mm was used to cover the structural frame which helps maintain the temperature at a target level during testing. An actuator assembly having 50 kN capacity has been installed on the frame to test specimens at a maximum of 30 kN loading.

To justify the stiffness of the structural frame relative to the stiffness of specimens to be tested, the maximum deflection in the frame that can be reached during testing was calculated by the finite element modeling of the frame. The vertical deflection contour plot drawn for the steel frame is shown in Figure 3.3.

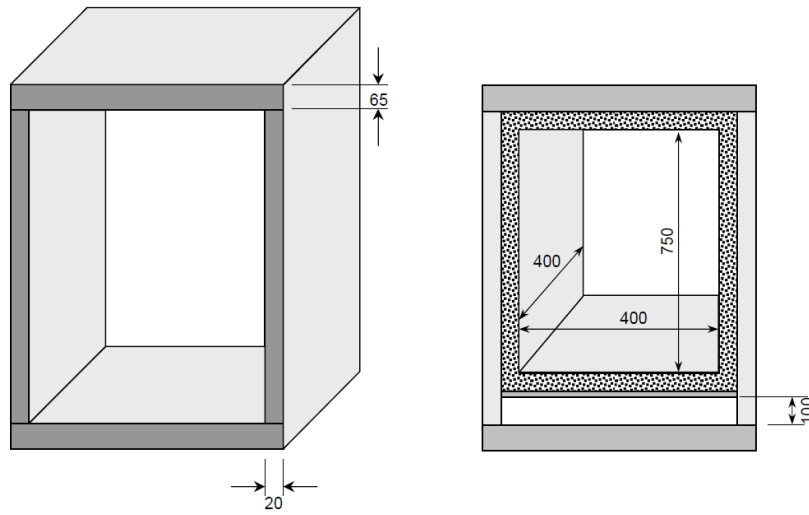


**Figure 3.2- Details of the structural steel frame for TSRST test device**

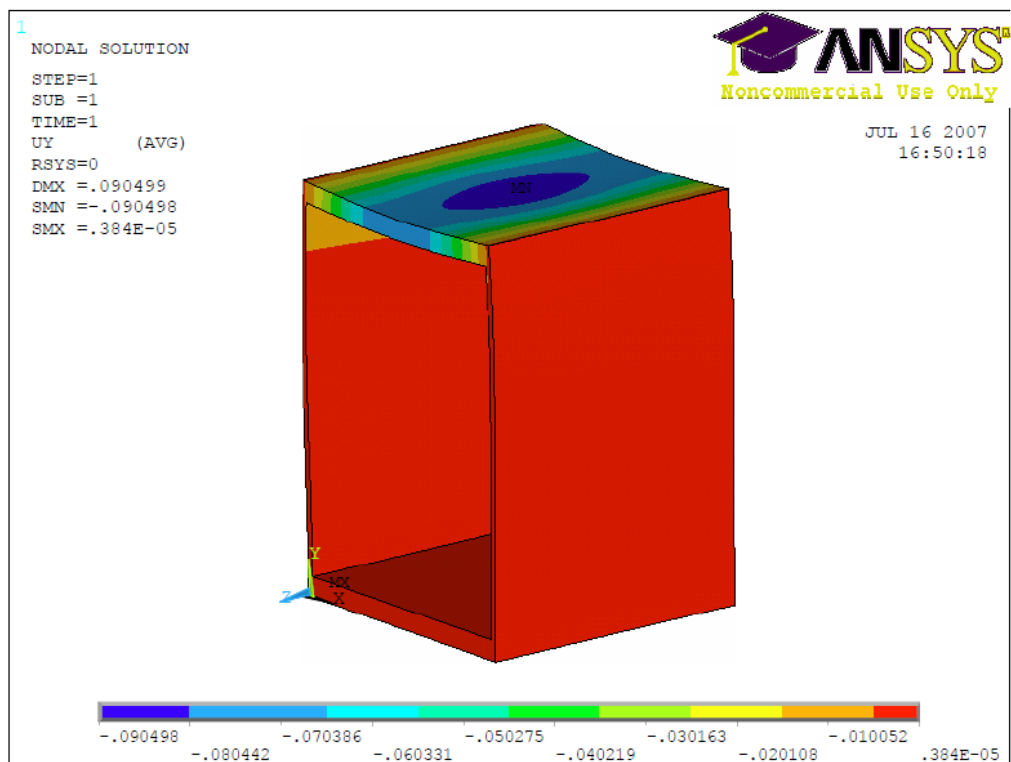


**Figure 3.3- FEM analysis of TSRST device**

It can be observed that the maximum deflection can reach up to 90 micron when the actuator is loaded to 30 kN, which is the limiting value for the installed load cell. The calculated deflection is considered to be minimal, and it is assumed that the test results may not be affected by non-linearity due to significant geometrical distortion of the frame. It should be noted that any effect of deflection of the frame on the displacement control unit will be compensated by the servo-controlled loading system. Hence, the design of the test device assures not only the stiffness requirement but also the elimination of the effect of geometrical distortions on test readings. Figure 3.4 illustrates the main components of the TSRST device.

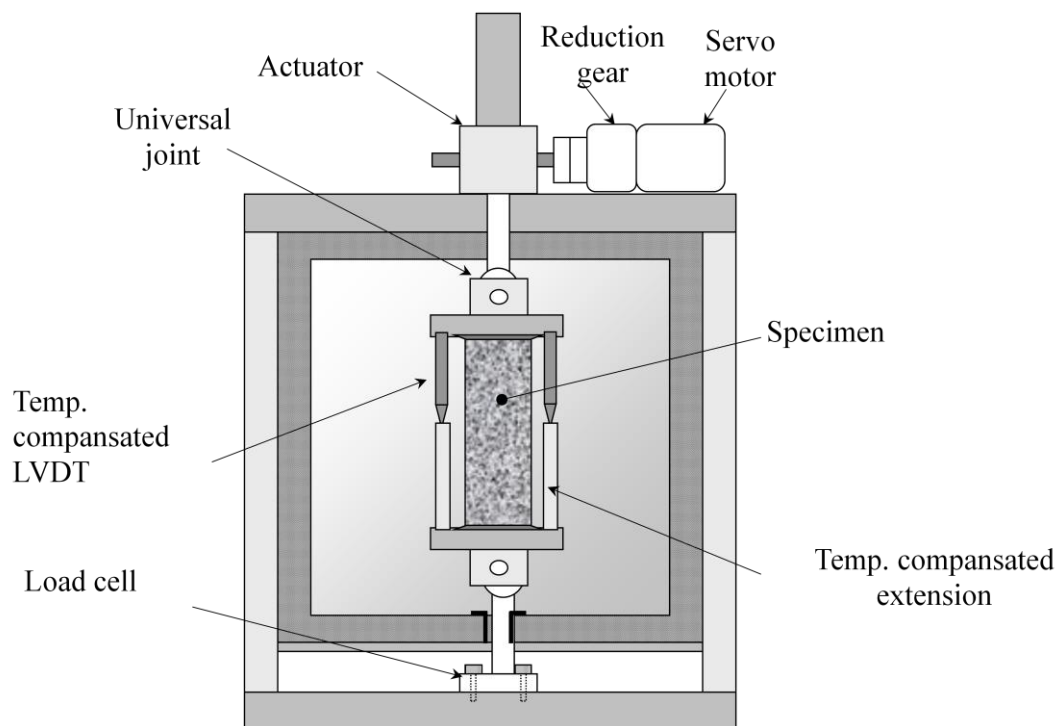


**Figure 3.4- Main components of the TSRST device**

The device is controlled by a personal computer and operates in response to changes in electrical signals from the two LVDT's located on opposite sides of the specimen. The LVDT's are attached to the top platen and the extension rods are attached to the bottom platen. When the LVDT's measure a reduction in specimen length due to cooling, the servo motor pulls the specimen back to its original length. At this moment, a tensile stress is induced in the specimen because it is restrained from free contraction. The load cell installed to the bottom of the device is used to measure the stress level, which is then correlated with the measured temperature and time.

The temperature control system consists of a liquid nitrogen tank, environmental chamber, compressor, a temperature controller and a resistance temperature device. The cooling process is performed by vaporizing compressed liquid nitrogen into the environmental chamber through a solenoid valve (Figure 3.5).

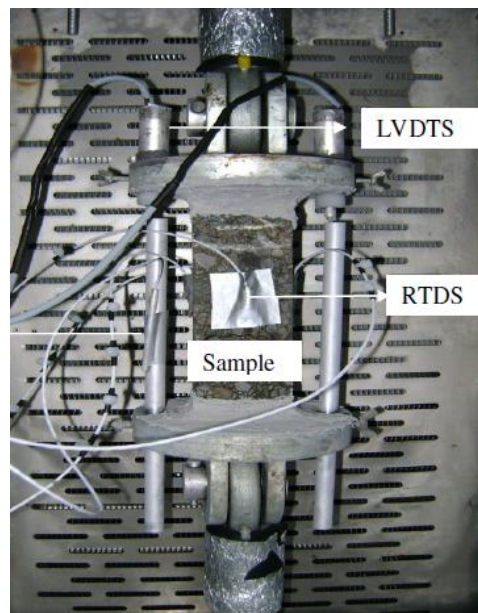


**Figure 3.5- Liquid nitrogen supply arrangements**

The cool air is circulated with a fan so that the temperature distribution is uniform within the environmental chamber. The resistance temperature device connected to the data acquisition monitors the temperature in the environmental chamber and regulates the amount of liquid nitrogen required to reach or maintain a specified tem-

perature. Four RTDs (Figure 3.6) are attached to all specimen surfaces to monitor the temperature.

A special arrangement was made to transfer the liquid nitrogen into the chamber. For this purpose, four nozzles were fabricated from aluminum material and installed inside the chamber so that the liquid nitrogen can be sprayed uniformly during testing. Rear panel of the device has been fitted with two turbo-fans to achieve the air circulation.



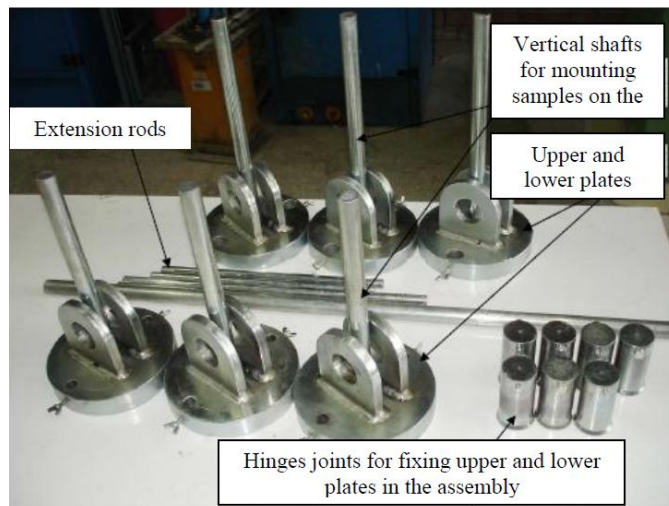
**Figure 3.6- Displacement and temperature sensor arrangement**

Figure 3.7 illustrates the nozzle system used in the device. In the test equipment, liquid nitrogen supply provides a very important contribution to the cooling system. Even though testing at  $-5^{\circ}\text{C}/\text{h}$  does not need liquid nitrogen experiments performed at a cooling rate of  $-20^{\circ}\text{C}/\text{h}$  and for the glass transition temperature measurements require such arrangements to make economical use of liquid nitrogen.



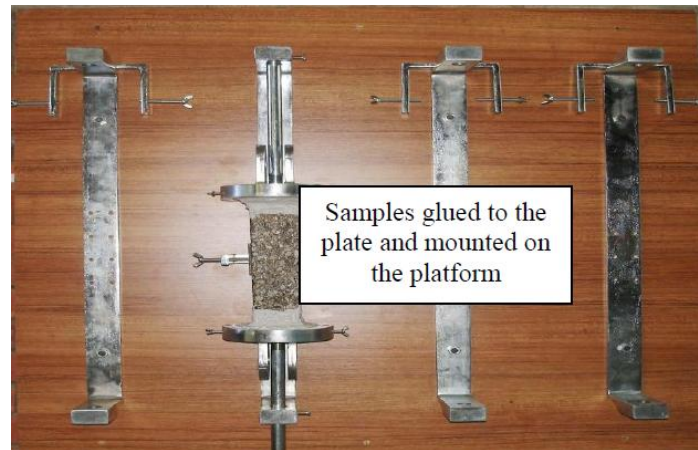
**Figure 3.7- Nozzle system placed in the device**

Figure 3.8 illustrates the auxiliary parts used for preparing test specimen and mounting it to the test device.



**Figure 3.8- Auxiliary apparatus used in the preparation**

Figure 3.9 is also shown in this section to illustrate the platform consisting of four stainless steel channel sections. Each flange of the channel has a hole with a tightening knob to hold the vertical mounting shaft and hence keeping the specimen vertical.



**Figure 3.9- Platform where the specimens are mounted and glued**

The channels are also provided with “u”-shaped holders to hold the sample in upright position. The platform has the capacity to accommodate four specimens at one time.

### **3.2.2. Programming**

The data acquisition system consists of transducer signal conditioners, a data acquisition card, and a personal computer. All electrical signals from the load cell, two LVDTs, and four resistance temperature devices (RTD) are processed through this system and stored in the computer for analysis (Figure 3.9). Another task performed in this research was to write user interface software for controlling the test and achieving the data acquisition during testing. The software was written in the graphical programming language (G language) called LabVIEW®. It is a high level language that enables quick development of test, measurement, and control applications.

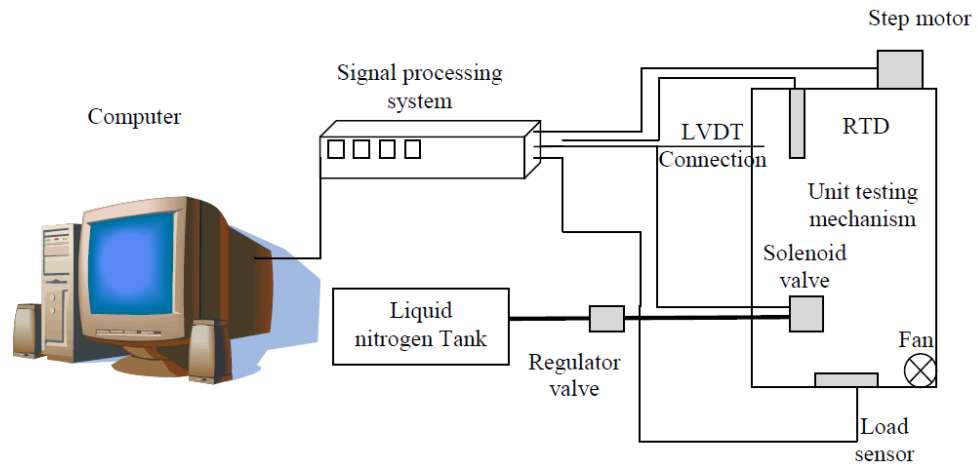


**Figure 3.10- Interaction diagram between software and test device**

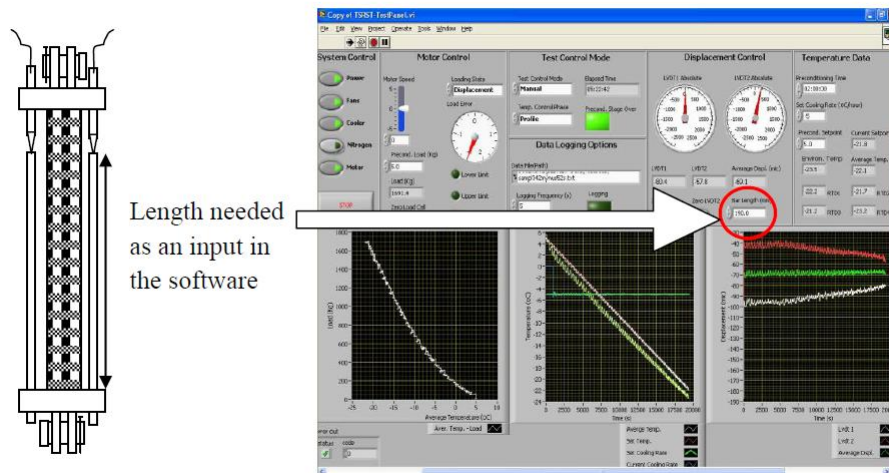
Regardless of the user experience, engineers and scientists can rapidly and cost-effectively develop simple solutions through this programming language for measurement, hardware control, and data analysis, for standalone applications and distributed systems.

Figure 3.11 gives a snapshot of the user interface program developed for the TSRST test device. A complete operational sequence of this software is given in the appendix section of this thesis. However, a brief introduction of the program is being discussed here. The test device operates in two different modes determined by the purpose of measurement:

- Measurement of fracture strength and fracture temperature
- Measurement of glass transition temperature

These two types of measurement can be achieved by using the same program at slightly different modes. The conditioning mode is, however, the same for both modes of measurement. The Displacement-Profile mode is run for the measurement of fracture strength and fracture temperature, which mainly controls the LVDT readings to maintain the specimen's initial length. In this mode, the measured load versus

temperature is recorded to calculate the fracture strength and the fracture temperature.



**Figure 3.11- A view of control panel for user interface program showing control knobs, indicators and various graphs**

For the measurement of glass transition temperature, the device is operated in the Load-Profile mode thereby measuring the contraction in the specimen subjected to only a 5 N loading while the temperature is cooled down at a certain rate. In this mode, the reduction in the specimen length versus temperature is recorded to calculate the volumetric strain from which the glass transition temperature can be obtained. The software window is divided into two major sections: the input section having radio buttons while the output section has graphical plots area. The input section is further divided into five sections namely system control, motor control, test control mode, and displacement control and temperature control. The output section contains plots obtained during testing of the specimen. These plots include average temperature versus load, time versus temperature, and time versus displacement data.

### **3.2.3. The system control**

The system control contains the power switch along with fans, cooler, liquid nitrogen supply and motor on and off mode. Most of the buttons are required to be switched on during the test except for the liquid nitrogen button that is only needed for specific test condition such as testing at  $-20^{\circ}\text{C/h}$  or during glass transition temperature measurement.

#### **a) The motor control**

The motor control state facilitates accurate control of the specimen length when experienced contraction under continuously reduced temperature. This state is crucial to accurately measure the fracture strength and the fracture temperature on the displacement mode. It is also important to accurately determine the volumetric strain data from which the glass transition temperature is obtained in the loading mode. The basic function of the motor is to rotate the actuator in a way that the specimen's initial length remains constant throughout the test while in the displacement mode. In the loading mode, however, a preloading (5 N) is kept constant to accurately measure the glass transition temperature. The accuracy of displacement and load control is displayed using a dialed gage indicator in the user interface program.

#### **b) The test control**

The test control section of the software gives the option to user either to run the machine on manual or automatic mode and to select the time lag during the test. This section also use input from the user about the running mode of the device either at preconditioning or profile mode (if the automatic mode is selected the machine automatically switches to the profile mode once the preset preconditioning time is reached). A blinking control button warns the operator once the precondition period is over. A field is also provided for saving the output data to a specified folder which requires the input of the file path by the operator. The indicator positioned next to the file path blinks every time the data is recorded in a text file. The frequency of data recording is also input within this section. The default value is set to 5 seconds meaning that a total of 12 recordings take place in one minute.

### **c) The displacement control**

This section contains steps for entering the averaged initial length of the extension bars and setting the LVDT readings to zero before starting off the test. The software calculates the amount of shortening of the extension bars and subtracts from the amount of shortening measured by the LVDTs. This is necessary because the reduction in the length of the extension bars gives positive readings to the LVDTs as opposed to the negative readings from the test specimen. Setting the initial LVDT readings to zero is optional, but not a required step. It is only necessary to monitor the precision of the displacement control on the user interface when the fracture strength experiment is in progress.

### **d) The temperature control**

This control phase requires inputs for preconditioning temperature and time period before starting a new test and the cooling rate to be applied in the displacement mode testing. The preconditioning temperature is applied for the time duration entered in hour format. After the completion of this phase, the software proceeds either automatically or manually to the testing mode. The cooling rate is used to cool down the specimen by allowing the entrance of liquid nitrogen through the solenoid valve at a specified rate based on the readings from four RTDs attached to the specimen side surfaces. The temperature measured on the specimen surface, on the extension bars, the set cooling rate, and the achieved cooling rate are all shown on the same plot on the user interface program.

### **3.2.4. Temperature calibration for the extension bars**

As described earlier about the development of the test device, few other tasks were completed to make device ready for testing and measurement according to the test procedures. In the general setup of the test device, the strains or deformations in the test specimen are measured through LVDTs that are mounted across the extension bars. As discussed in the previous section, as the environment temperature is reduced the extension bars also shrink around 490-540 microns and produce an opposite ef-

fect on the displacement readings. This problem obviously causes erroneous reading on the actual dimensional change in the test specimen during testing. One purpose of the temperature calibration process is to remedy this problem so that the amount of change in the specimen length is accurately detected and then transferred to the load control system to generate the correct thermal stress within the specimen. The other source of error that is produced is due to the difference in the coefficient of thermal conductivity for asphalt concrete and the steel extension bars. Asphalt cement has a thermal conductivity of 0.92 W/m K, while the stainless steel around 0.50. This would suggest that the asphalt sample will require approximately twice the thermal energy loss to cause shrinkage that of stainless steel. In other words, the thermal contraction of the stainless steel happens twice as faster as compare to the asphalt sample under the same degree of temperature reduction. Hence, by thermally calibrating the extension bars, this problem can also be overcome to produce more accurate readings from the LVDTs. To calibrate the extension bars, two bars with different lengths, 30 cm and 40 cm, were tied with each other and then placed into the environmental chamber. One of the LVDTs was connected to the longest bar while its tip comes across with the shortest one as shown in Figure 3.10. RTDs were attached to each bar to measure the temperature while cooling down the chamber. This calibration arrangement was repeated for two different sets and tested side by side as shown in Figure 3.10. The temperature was reduced at a rate of 2°C per minute up to -60°C. During the test, the temperature and the LVDT readings were recorded in a file for data analysis. The thermal coefficients for the extension bars were then calculated based on the recorded temperature and the displacement data from the LVDTs. The average calculated coefficient of linear contraction for the stainless steel bars were determined nearly identical for each set as  $2.75 \times 10^{-6} / ^\circ\text{C}$ . The amount of displacement for the steel bars was measured to be 490 microns for the smaller bar and 540 microns for the larger bar. Table 3.1 summarizes the input and output values obtained during the calibration process.

**Table 3.1- Thermal paramaters measured from the calibration process**

<b>Description</b>	<b>1</b>	<b>2</b>
Approx. length of steel bars, L(mm)	400	300
Gage length of LVDT attached (mm)	99.91	98.90
Change of temperature, $\Delta T$ ( $^{\circ}\text{C}$ )	70	70
Change in length , ( $\alpha L\Delta T$ ) (micron)	540	490
Calculated value of alpha, $\alpha$ ( $1/^{\circ}\text{C}$ )	$2.64 \times 10^{-6}$	$2.88 \times 10^{-6}$

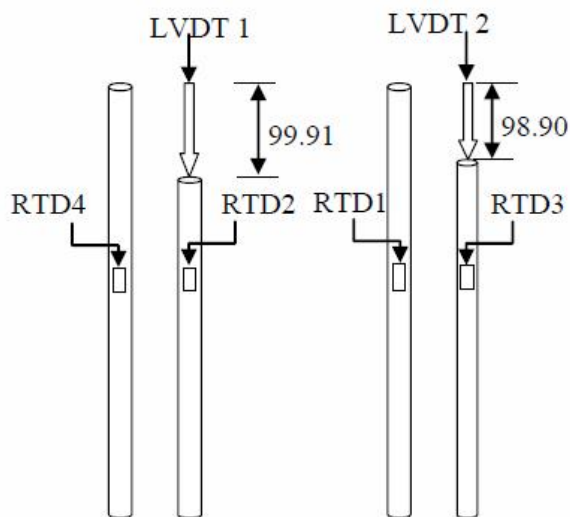


**Figure 3.12- A view of the calibration process**

### 3.3. Sample preparation

The task of sample preparation involved a number of steps including setting up design of experiment, selection of mix design and test variables such as sieving, mixing and compaction, preparing mixtures for slab specimens, compaction, obtaining beam specimens from compacted slabs and measuring mix volumetrics for beam specimens. Each step of the experiment is discussed in detail in the following sections.

### 3.3.1. Design of experiment

Literature review showed that previous researchers investigated different variables affecting the response of asphalt paving mixtures against fracture resistance at low temperatures. No researcher tried to combine these variable parameters in one study. In light of this, it was considered necessary to study the effects of all parameters, i.e., asphalt type, polymer modified asphalt, aggregate type and gradation, optimum asphalt content, sample size and cooling rate, on low temperature cracking of HMA. Therefore, to accommodate these seven variables, a complete experimental program was needed to determine the total number of samples required for the tests. Flow diagram of the experimental design is shown in Figure 3.11. The diagram shows two levels of aggregates, basalt and limestone, each of the aggregate are then sieved for two types of gradation as Type 1 and Type 2 which is not shown for limestone in the diagram. Each of the gradations were mixed with two types of asphalts, 50-70 and 71-100, and each of the asphalt type was modified with SBS in one group and remained unaltered (neat) in the other group. Each of the modified and neat mixes was then mixed with three different asphalt contents namely, optimum, optimum+0.5% and optimum-0.5%. Each of the mix thus obtained was tested at three different cooling rates. Due to symmetry in procedures only one quarter of the detail is shown in Figure 3.13.

In this study, a fractional factorial design of  $2^{5-2} \times 3^2$  was selected avoiding full factorial design which would have required a large number of samples that are difficult to manage. A fractional factorial design is defined as an approach in which a class of design is studied using many variables in a relatively limited number of tests. The design variable in this study contained two different asphalt grades, two types of gradation, two types of asphalt binder with SBS modifier and with no modifier, two specimen dimensions, three asphalt contents (optimum, optimum  $\pm$  0.5) at three temperature cooling rates.

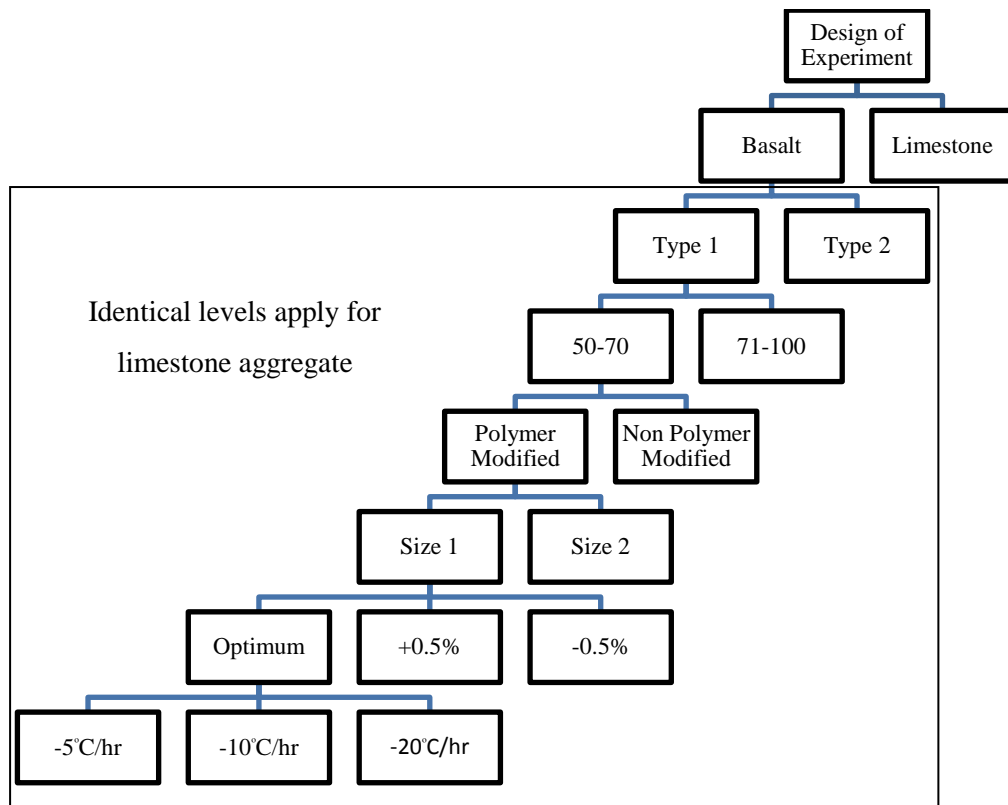


**Figure 3.13- Flow diagram of the experimental design**

Confounding was done between specimen size and aggregate type and also between specimen size and asphalt type. Hence, a simple mathematical calculation from a fractional factorial design resulted in 16 material configurations and a total of 72 specimens. Table 3.2 illustrates these variables with their codes.

**Table 3.2- Details of variables used in the design**

S.no	Name of variable	Alphabet	Level	Symbols	Coded
1	Aggregate type	X1	2	L,B	+1,-1
2	Gradation	X2	2	C, F	+1,-1
3	Specimen length	X3	2	M, T	+1,-1
4	Polymer modification	X4	2	S,Z	+1,-1
5	AC type	X5	2	57,71	+1,-1
6	AC content	X6	3	OP,O, OM	+1, 0,-1
7	Cooling rate	X7	3	-20,-10, -5	+1, 0,-1

Table 3.3 shows typical design matrix needed for the fractional factorial design at 2 levels having 5 variables confounded with two variables while Table 3.4 indicates the matrix of 3 factors having two levels. Secondary data presented in Table 3.5 was then generated from Table 3.3 and 3.4 and identifies the sample to be tested by this experimental design.

**Table 3.3- Standard matrix available for fractional factorial design of  $2^{5-2}$**   
(NIST-Engineering statistics handbook)

<b>Design Matrix for a <math>2^{5-2}</math> Fractional Factorial</b>					
<b>Seq.</b>	<b>X1</b>	<b>X2</b>	<b>X3</b>	<b>X4 = X1X2</b>	<b>X5 = X1X3</b>
1	-1	-1	-1	+1	+1
2	+1	-1	-1	-1	-1
3	-1	+1	-1	-1	+1
4	+1	+1	-1	+1	-1
5	-1	-1	+1	+1	-1
6	+1	-1	+1	-1	+1
7	-1	+1	+1	-1	-1
8	+1	+1	+1	+1	+1

**Table 3.4- Design matrix for 2 level 3 factor design**

<b>Design matrix for <math>3^2</math></b>		
<b>Sequence</b>	<b>X6</b>	<b>X7</b>
1	-1	-1
2	-1	0
3	-1	+1
4	0	-1
5	0	0
6	0	+1
7	+1	-1
8	+1	0
9	+1	+1

**Table 3.5- Design matrix as a result of fractional factorial design  $2^{5-2} \times 3^2$**

Seq.	X1	X2	X3	X4	X5	X6	X7	Seq.	X1	X2	X3	X4	X5	X6	X7
1	-1	-1	-1	1	1	-1	-1	37	-1	-1	1	1	-1	0	0
2	1	-1	-1	-1	-1	-1	-1	38	1	-1	1	-1	1	0	0
3	-1	1	-1	-1	1	-1	-1	39	-1	1	1	-1	-1	0	0
4	1	1	-1	1	-1	-1	-1	40	1	1	1	1	1	0	0
5	-1	-1	1	1	-1	-1	-1	41	-1	-1	-1	1	1	0	1
6	1	-1	1	-1	1	-1	-1	42	1	-1	-1	-1	-1	0	1
7	-1	1	1	-1	-1	-1	-1	43	-1	1	-1	-1	1	0	1
8	1	1	1	1	1	-1	-1	44	1	1	-1	1	-1	0	1
9	-1	-1	-1	1	1	-1	0	45	-1	-1	1	1	-1	0	1
10	1	-1	-1	-1	-1	-1	0	46	1	-1	1	-1	1	0	1
11	-1	1	-1	-1	1	-1	0	47	-1	1	1	-1	-1	0	1
12	1	1	-1	1	-1	-1	0	48	1	1	1	1	1	0	1
13	-1	-1	1	1	-1	-1	0	49	-1	-1	-1	1	1	1	-1
14	1	-1	1	-1	1	-1	0	50	1	-1	-1	-1	-1	1	-1
15	-1	1	1	-1	-1	-1	0	51	-1	1	-1	-1	1	1	-1
16	1	1	1	1	1	-1	0	52	1	1	-1	1	-1	1	-1
17	-1	-1	-1	1	1	-1	1	53	-1	-1	1	1	-1	1	-1
18	1	-1	-1	-1	-1	-1	1	54	1	-1	1	-1	1	1	-1
19	-1	1	-1	-1	1	-1	1	55	-1	1	1	-1	-1	1	-1
20	1	1	-1	1	-1	-1	1	56	1	1	1	1	1	1	-1
21	-1	-1	1	1	-1	-1	1	57	-1	-1	-1	1	1	1	0
22	1	-1	1	-1	1	-1	1	58	1	-1	-1	-1	-1	1	0
23	-1	1	1	-1	-1	-1	1	59	-1	1	-1	-1	1	1	0
24	1	1	1	1	1	-1	1	60	1	1	-1	1	-1	1	0
25	-1	-1	-1	1	1	0	-1	61	-1	-1	1	1	-1	1	0
26	1	-1	-1	-1	-1	0	-1	62	1	-1	1	-1	1	1	0
27	-1	1	-1	-1	1	0	-1	63	-1	1	1	-1	-1	1	0
28	1	1	-1	1	-1	0	-1	64	1	1	1	1	1	1	1
29	-1	-1	1	1	-1	0	-1	65	-1	-1	-1	1	1	1	1
30	1	-1	1	-1	1	0	-1	66	1	-1	-1	-1	-1	1	1
31	-1	1	1	-1	-1	0	-1	67	-1	1	-1	-1	1	1	1
32	1	1	1	1	1	0	-1	68	1	1	-1	1	-1	1	1
33	-1	-1	-1	1	1	0	0	69	-1	-1	1	1	-1	1	1

**Table 3.5 (continued)**

34	1	-1	-1	-1	-1	0	0	70	1	-1	1	-1	1	1	1
35	-1	1	-1	-1	1	0	0	71	-1	1	1	-1	-1	1	1
36	1	1	-1	1	-1	0	0	72	1	1	1	1	1	1	1

**3.3.2. Materials selected for research**

Limestone and basalt aggregates were selected to fulfill the design requirements. The materials were collected from the asphalt plant located in the suburbs of Ankara. The neat and modified binder used in this study, were provided by the Turkish General Directorate of Highways (TGDH). The basic properties of materials used in the study are summarized in the Table 3.6 and 3.7.

**Table 3.6- Properties of aggregates**

Properties measured	Aggregates	
	Limestone	Basalt
Specific gravity	2.75	2.93
Average absorption, %	1.45	1.00
LA abrasion value, %	28	15

**Table 3.7- Properties of asphalt**

Properties measured	Asphalt	
	50-70	71-100
Penetration(0.1 mm)	54	73
Specific gravity	1.025	1.034

The grading requirement of this study was selected by following TGDH specification book (2006). The wearing course is specified in two types namely Type 1 and Type 2 therefore, coarse gradation was selected as Type 1 and fine gradation was selected as Type 2. This was done to take the extreme values of gradations required for road construction in Turkey. Figure 3.14 represents the selected gradations plotted on a 0.45 gradation chart.

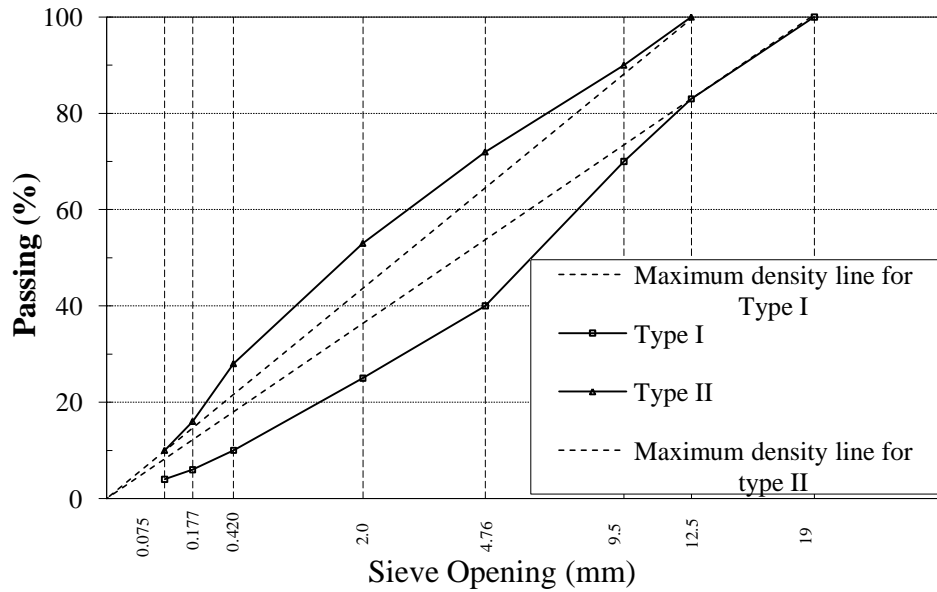


**Figure 3.14- Selected gradation for the project**

After selecting the mix gradations and estimating the number of samples, they were subjected to sieve analysis for separation of aggregates according to various size fractions. Some of the required samples were unavailable, therefore they were crushed to into smaller size using a jaw crusher. Table 3.8 shows the total quantity of materials required for the project, preparation of cylindrical specimen for Superpave mix design, theoretical maximum specific gravity tests and preparation of slab specimens for TSRST tests.

**Table 3.8- Estimation of quantity of materials for test samples**

Sieve size (mm)	TSRST	Superpave mix design	Theoretical specific gravity	Required (Kg)
12.50	134.4	12.8	2.0	149.2
10.00	102.8	9.8	1.4	114.0
4.76	463.4	65.6	6.6	535.6
2.00	272.2	40.4	4.0	316.6
0.42	320.6	49.6	4.6	374.8
0.18	128.6	21.4	1.8	151.8
0.075	64.2	10.8	0.8	75.8
Pan	112.4	18.4	1.6	132.4
Total (kg)				1850.4

### **3.3.3. Superpave mix design for the selected mixtures**

Preparation of test samples at the optimum asphalt contents was one of the factors that were emphasized in this study. Selection of the optimum asphalt contents was achieved based on the Superpave method of mix design. Superpave is a term used for Superior Performing Pavements and replaced the conventional Marshal mix design method for the selection of aggregates and binder proportion. Although Superpave mix design can be used for the selection of asphalt binder grade, aggregate gradation, and asphalt content, the method was used only for the selection of optimum asphalt contents for the test mixes due to the gradation requirements of TGDH.

#### **a) Mix design for the for the determination of optimum asphalt contents**

Three samples for each combination were prepared and tested for the optimum asphalt content and two replicates were prepared after finding the asphalt contents according to the Superpave mix design procedures, which requires 4% air voids at the optimum asphalt content. A total of 96 cylindrical specimens were prepared. A picture of the design samples is shown in Figure 3.15.



**Figure 3.15- Mix design samples according to the Superpave method**

Since a gyratory compactor was not available locally, the test mixes were first prepared and packed in paper bags and taken to the TGDH for compaction. The samples

were put in the oven for three hours to achieve short term aging and then compacted using the Servopack gyratory compactor according to required number of gyrations for  $10^6$  ESAL traffic. Table 3.9 presents the details of the Superpave mix design standards used in this study.

**Table 3.9- Design parameters used for Superpave mix design (AASHTO T 312)**

<b>Design parameters</b>	<b>Selected parameters values</b>
Number of Gyration ( $N_{des}$ )	100
Cumulative traffic assumed	3-10 Million
Mixing Temperature	165°C
Compaction Temperature	145°C
Air void content selected for design	4 %

The compacted cylindrical specimens were then brought back to the Middle East Technical University (METU) transportation laboratory. In order to find the optimum asphalt contents at target air voids, the values of bulk specific gravities and theoretical maximum specific gravities are required. The values of the specimen bulk specific gravities (AASHTO T 166) and theoretical maximum density (AASHTO T 209) were measured by applying the standard methods.

The optimum asphalt content for each mix configuration was then calculated. Three samples were further made to confirm the required optimum content. After the value of the optimum asphalt content, voids filled with asphalt (VFA), voids in mineral aggregates (VMA), and the weight required for each combination of mixes were calculated and are summarized in Table 3.10. An tolerance limit of  $\pm 0.5$  percent in air voids was assumed to compensate for the variability in the design air voids contents. Some deviations from the target air voids, VFA and VMA can be allowed according to the relevant AASHTO standards. A total of 16 different mix designs were prepared at the optimum asphalt contents. The values of bulk specific gravity determined from the design samples were then used to calculate the total required amount of materials needed to prepare slab specimens of 50 x 18 x 10 cm. Table 3.10 summarizes the value of optimum asphalt contents, air voids, VMA, VFA, bulk specific gravity and the weight of materials required for each slab samples.

**Table 3.10- Summary of calculated asphalt contents**

S.N O	Ag- gre- gate	Asphalt	Modifi- cation	Grad- ation	Optimum AC %	Air Vo- ids %	Weight required (Kg)
1	B	57	Z	F	5.0	4.0	20.90
2	B	57	Z	C	4.4	4.0	20.93
3	B	57	S	F	5.2	4.0	20.21
4	B	57	S	C	4.8	3.6	20.71
5	B	71	Z	F	5.3	4.0	20.63
6	B	71	Z	C	4.5	3.9	20.35
7	B	71	S	F	5.4	4.0	20.87
8	B	71	S	C	5.0	3.9	21.07
9	L	57	Z	C	4.5	3.9	22.41
10	L	57	Z	F	5.3	4.0	22.14
11	L	57	S	C	5.0	4.0	22.14
12	L	57	S	F	5.5	4.0	22.09
13	L	71	Z	C	4.8	4.0	21.80
14	L	71	Z	F	5.4	4.0	22.46
15	L	71	S	C	5.5	4.0	21.92
16	L	71	S	F	5.1	3.9	22.50
AASHTO 2001Criteria				12.5 mm (Maximum size of aggregate)			
VMA (%)				14			
VFA (%)				65-75			
Symbol used: Aggregate Type: L-limestone, B-Basalt; Gradation: C- Coarse, F-Fine; Size; Modification: Z-No Modification, S-SBS Modification; Asphalt type: 57-50 70, 71- 71 100;VMA-Voids in mineral aggregate; VFA-Voids filled with asphalt							

### 3.3.4. Sample preparation for TSRST testing

Since TSRST requires beam specimens, first slab specimens that were 50 x 18 x 10 cm in size were prepared and then beam specimens were obtained from the slab specimens by cutting them into appropriate sizes as specified in the design of experiment. The details of this procedure is explained in the following sections.

#### a) Preparation of slab specimens

To prepare the slab specimens, around 22-23 kg of asphalt and aggregate materials were mixed to prepare a total of 72 slab samples. Each mix sample was divided into four batches because of the limiting capacity of the available mixer. Because a slab compactor is not available locally, it was planned to prepare the mixes in the METU

Transportation laboratory and then compact them in the TGDH laboratory using the French (LCPC) slab compacter. Before compaction, the mix samples were subjected to short term aging for three hours in an oven. Figure 3.16 illustrates the prepared samples during and after the compaction process.



**Figure 3.16- Slab sample preparation during and after compaction**

**b) Preparation of beam specimens**

After compaction, the slab specimens were cut into sections of 50 x 65 x 200 mm and 50x 65 x 300 mm. A uniform cross section of 65 x 50 mm was chosen to keep the length to width aspect ratio between 4 and 6. This value is selected to eliminate the effect of aspect ratio on the response variables of testing experimental design based on the findings of Vinson et al. (1989) who suggested that the effect of aspect ratio would not be statistically significant for test results if the aspect ratio is maintained constant.

The prepared samples were then cut to the required dimensions using a saw diamond machine. Also uniform code numbers were assigned to each sample after cutting not only to recall material configuration of sample in terms of aggregate type, asphalt grade, polymer treatment, and percentage asphalt added but also to identify its location of section in a given specimen (Figure 3.17).

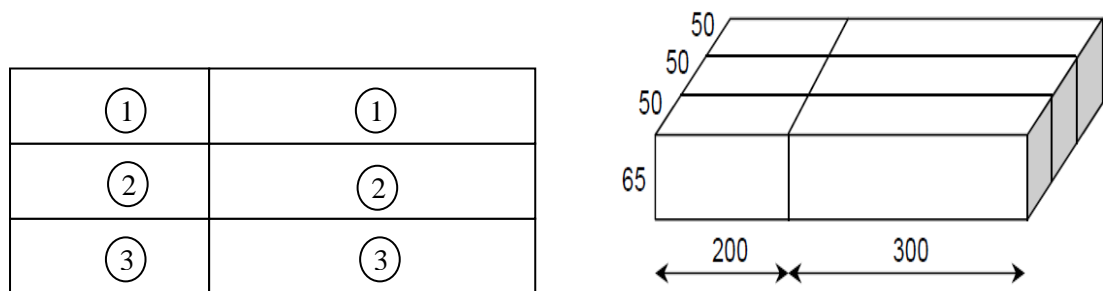


**Figure 3.17- Specimen section for cutting**

For example, the digit 1 or 3 indicates that the specimen was cut from the side of the slab sample while the number 2 indicates that it was cut from the center. The main idea behind this marking is to differentiate between specimens that were cut either from sides or in the middle due to the fact that the middle of the slab sample is compacted usually more than the side sections. This may mean that the specimens taken from the sides have less air voids than those in the center. During the cutting operation, the cutting saw was cooled down with water to achieve a smooth cutting surface and prevent overheating of the beam specimen. In order to avoid the discontinuities on the surface of the beam specimens, the slab specimens were cut from both sides. The bulk specific gravity of each specimen was then measured after the required dimensions have been achieved. Figure 3.18 shows a picture taken after sizing and bulk measurements. Table 3.11 summarises the sample prepared in this thesis.



**Figure 3.18- Specimens cut to required dimensions**

**Table 3.11- Summary of specimens prepared for TSRST and glass transition tests**

S.no	Variables	Explanations	
1.	Aggregate Type	Limestone(L) and Basalt(B)	
2.	Asphalt Type	Penetration grade 50-70 and 71-100	
3.	Gradation	Coarse(C) and Fine(F)	
4.	AC content	Optimum, Optimum+0.5, Optimum-0.5,	
5.	Compaction Machine	Superpave Gyrotory	LCPC
6.	Specifications	AASHTO T 312	AASHTO TP 63
7.	Shape of specimen	Cylindrical	Prismatic
8.	Sample size	10cm dia.; 115cm height	50 x 18 x 10 cm
9.	Samples prepared	96	72

### c) Sample preparation for TSRST testing

A new technique of specimen preparation is adopted in this research. Before mounting the specimen to the loading platens, a set of circular ring having 15 mm outside diameter is first glued on both sides to the center of the cross section of the specimen as shown in the Figure 3.19. This ring is then seated on the projection coming out from the loading plate; hence ensuring easily centering of test specimens.



**Figure 3.19- Centring of test specimen by gluing the ring and fixing to the projection**

The prismatic asphalt specimen was then glued to the plate using a solid high-strength epoxy with thickener. The epoxy Sikadur®-31, according to the manufacturer, can sustain the tensile strength of 40-60 MPa for asphalt and concrete surface in 24 hours while its adhesion strength to steel is 14-16 MPa. Given the typical tensile resistance of asphalt concrete which is around 5.0 - 5.5 MPa, the strength of the epoxy used is quite sufficient.

The specimens were glued first to the bottom platen making the gluing epoxy smeared all around the specimen. This ensures enough adhesion surfaces available for the specimen to be fixed with the platen. The amount of epoxy used for sticking the specimens to the loading platens were kept less for the glass transition temperature tests since no tensile load is applied to the specimen during testing. A picture of the specimen gluing operation to the loading platens are shown in Figure 3.20.

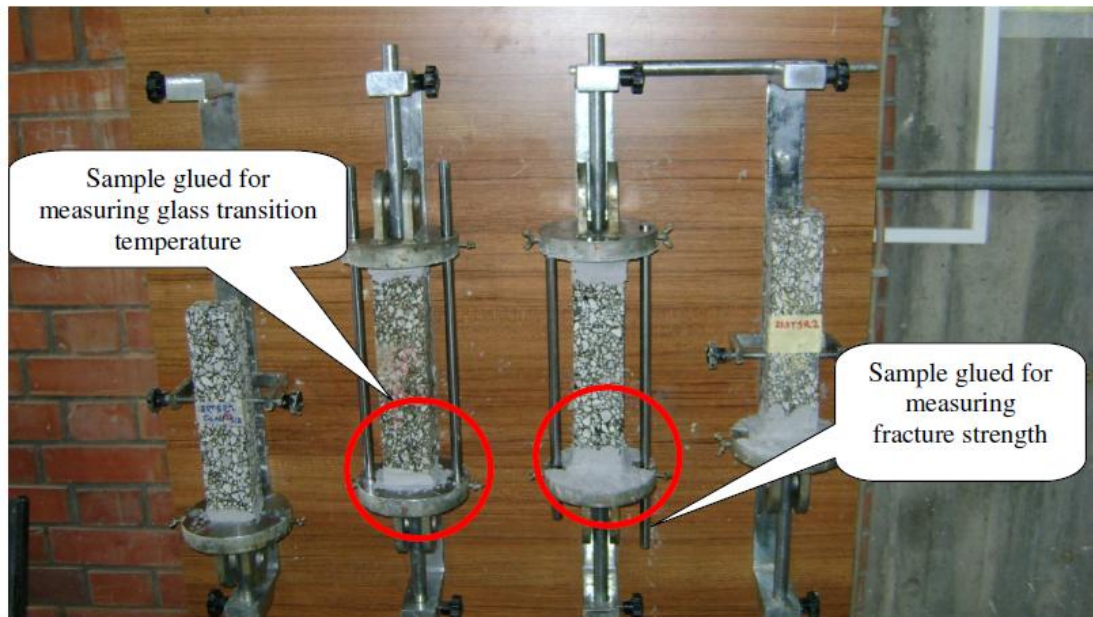


**Figure 3.20- Beam specimens in the process of gluing to the loading platens**

### **3.4. Laboratory testing of beam specimens**

In this research, two different sets of experiments were conducted: one for the measurement of fracture strength, and one for the measurement of glass transition temperature. These tests are briefly described in the relevant sections below.

#### **3.4.1. TSRST testing of specimens**

From the fractional factorial design, it was known that 144 specimens would have to be tested for fracture strength using two replicates. Another requirement for the study was to measure the glass transition temperature of the mixes. However, because of the time and cost constraints, the number of specimens to be tested for glass transition temperature was limited to 36.

##### **a) Testing for fracture strength**

From the design of experiment matrix, the following listed specimens are selected to be tested at various cooling rates for fracture strength and fracture temperature. Table 3.12 thru 3.14 presents the details of the specimens tested.

**Table 3.12- Details of specimens tested at -20°C/h**

S. No.	Aggregate type	Gradation	Specimen length	Polymer modification	AC type	AC content
1	L	C	T	Z	57	O
2	L	C	T	Z	57	OP
3	L	F	T	Z	57	OM
4	L	C	T	S	57	O
5	L	F	T	S	57	OP
6	L	F	T	S	57	OM
7	B	F	T	Z	71	O
8	B	F	T	Z	71	OP
9	B	F	T	Z	71	OM
10	B	C	T	S	71	O
11	B	C	T	S	71	OP
12	B	C	T	S	71	OM
13	L	C	M	Z	71	O
14	L	C	M	Z	71	OP
15	L	C	M	Z	71	OM
16	L	C	M	S	71	OP
17	L	F	M	S	71	O
18	L	F	M	S	71	OM
19	B	F	M	Z	57	O
20	B	F	M	Z	57	OP
21	B	F	M	Z	57	OM
22	B	C	M	S	57	O
23	B	C	M	S	57	OP
24	B	C	M	S	57	OM

Symbol used: Aggregate Type: L Limestone, B Basalt; Gradation: C Coarse, F Fine; Specimen length: T Tall, M Small; Polymer modification: Z-no Modification ,S-SBS Modification; AC type: 57-50 70, 71- 71 100;AC content: O-optimum, OP optimum plus, OM optimum minus.

**Table 3.13 - Details of specimens tested at -10°C/h**

S. No.	Aggregate type	Gradation	Specimen length	Polymer modification	AC type	AC content
1	L	F	T	Z	57	OP
2	L	C	T	S	57	O
3	L	F	T	S	57	OM
4	L	C	T	Z	71	OP
5	L	F	T	Z	71	OM
6	L	C	T	S	71	OP
7	B	C	T	Z	57	OP
8	B	F	T	Z	57	O
9	B	C	T	S	57	OM
10	B	C	T	Z	71	OP
11	B	F	T	S	71	OM
12	B	F	T	S	71	O
13	L	C	M	Z	57	OP
14	L	C	M	Z	57	OM
15	L	F	M	Z	57	O
16	L	C	M	S	71	OP
17	L	F	M	S	71	O
18	L	F	M	S	71	OM
19	B	C	M	Z	57	O
20	B	F	M	S	57	OP
21	B	F	M	S	57	OM
22	B	F	M	Z	71	OM
23	B	C	M	Z	71	O
24	B	C	M	S	71	OP

Symbol used: Aggregate Type: L-limestone, B-Basalt; Gradation: C- Coarse, F-Fine; Specimen length: T-Tall, M-Small; Polymer modification: Z-no Modification, S-SBS Modification; AC type: 57-50 70, 71- 71 100; AC content: O-optimum, OP- optimum plus, OM-optimum minus.

**Table 3.14- Details of specimens tested at -5°C/h**

S. No.	Aggregate type	Gradation	Specimen length	Polymer modification	AC type	AC content
1	L	C	T	Z	57	OM
2	L	F	T	S	57	OP
3	L	C	T	Z	71	O
4	L	F	T	Z	71	O
5	L	C	T	S	71	OM
6	L	F	T	S	57	OP
7	B	C	T	Z	57	OP
8	B	F	T	S	57	O
9	B	F	T	S	57	OM
10	B	C	T	Z	71	O
11	B	C	T	Z	71	OP
12	B	F	T	S	71	OM
13	L	C	M	Z	57	O
14	L	C	M	Z	57	OP
15	L	F	M	S	57	OM
16	L	C	M	Z	71	OM
17	L	F	M	S	71	O
18	L	F	M	S	71	OP
19	B	C	M	Z	57	O
20	B	F	M	Z	57	OP
21	B	C	M	S	57	OM
22	B	F	M	S	71	O
23	B	C	M	S	71	OM
24	B	F	M	S	71	OP

Symbol used: Aggregate Type: L-limestone, B-Basalt; Gradation: C- Coarse, F- Fine; Specimen length: T-Tall, M-Small; Polymer modification: Z-no Modification, S-SBS Modification; AC type: 57-50 70, 71- 71 100; AC content: O-optimum, OP- optimum plus, OM-optimum minus.

The specimens for the fracture strength test were first mounted in the machine and the LVDTs and RTDS were fixed at their relevant places. All the RTD sensors used are platinum-plated PT-100 Class-A, and can measure temperature at 0.385 ohm /°C precision level. The machine was then turned to the fracture mode and all the required entries are fed into to the user software. The specimen was first allowed to be conditioned at 5°C for three hours. The user software is programmed in a way that it has an auto mode at which once the specimen completes its preconditioning stage,

the automatic mode switches on the fracture mode and after the fracture takes place the machine stops automatically. A tutorial for the user software is attached in Appendix H. The data are recorded for every 5 seconds and the file is saved as a text file. A typical window obtained after the fracture of specimen is shown in Figure 3.21.

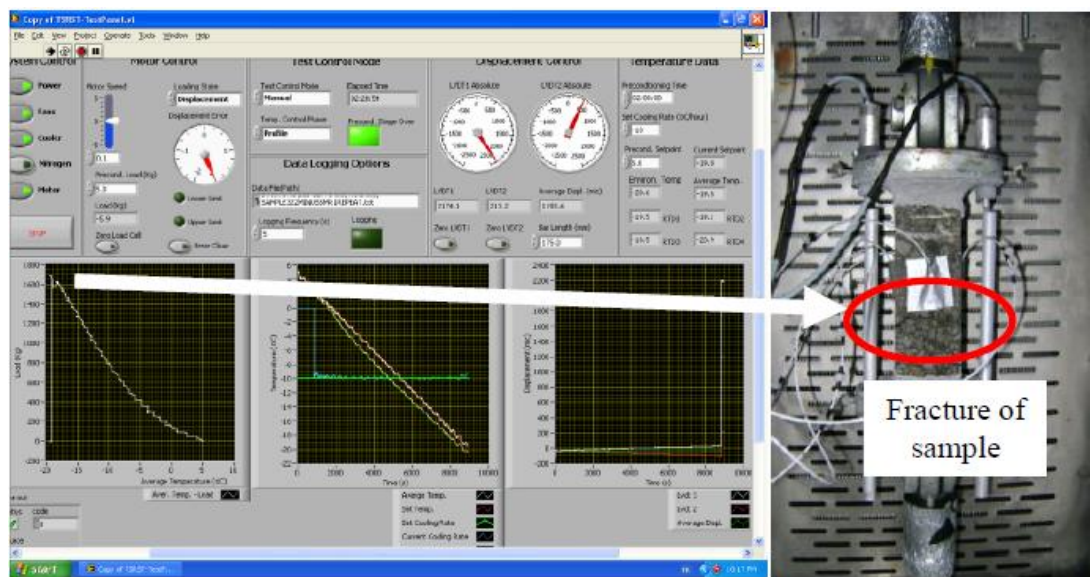


**Figure 3.21- A view of fractured specimen and user software interface at failure**

From Figure 3.21, it can be seen that there are graphs showing the temperature versus load relation, the rate of temperature change along with the temperature of the test specimen and temperature of the environment. In the window also there is a graph showing the displacement of LVDT against the decrease of temperature at the given cooling rate till it fractures, a typical relation of stress versus time is also shown in the control panel of the user program. A fractured specimen is also illustrated in the picture on the right with its corresponding test graphs on the left. In this stage, a total of 144 specimens were tested for fracture strength.

As can be seen, the software can calculate the load applied, , however, the analysis requires different parameters to be calculated like fracture stress, relaxation stress and transition temperature as well as the eccentricity occurring during testing. A Matlab® code was written for analyzing the data obtained from the test. The output of the code is presented in the form of a graph as illustrated in Figure 3.22.

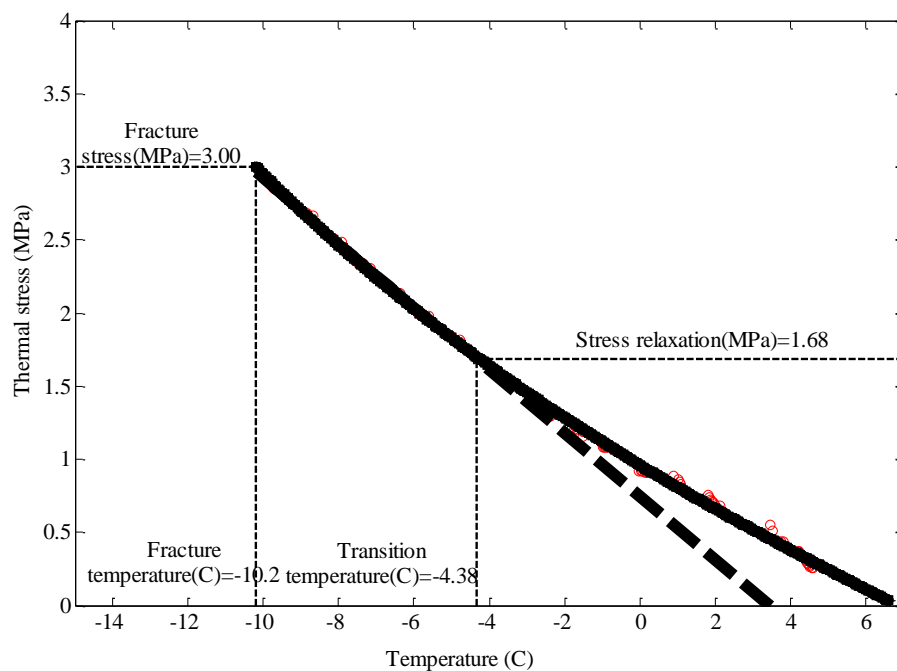


**Figure 3.22- Details of the fracture stress versus temperature curve obtained from the fracture test**

### **b) Testing of specimens for glass transition temperature**

The test methodology, the variables and the responses measured by this method were slightly different from the fracture strength test as discussed in the previous section. Two independent variables that are not included in this stage were the specimen size and the rate of cooling. The specimen length was selected as 30 cm, and a constant rate of cooling of 1°C/min was selected for all the 36 test specimens.

Glass transition temperature is defined as the temperature at which the viscoelastic zone is separated from the elastic region. The asphalt behaviour before the glass temperature is viscoelastic and changes to nearly linear behaviour once it is near the glass transition temperature. At the glass temperature, the slope of the volumetric strain-temperature curve changes abruptly and the value of the coefficient of contraction is lower than the value before it. Table 3.15 below gives the details of the specimens tested for the glass transition temperature.

**Table 3.15- Details of specimens tested for glass transition temperature**

S.No	Aggregate type	Gradation	Polymer modification	AC type	AC content
1.	L	C	Z	57	O
2.	L	C	Z	57	OP
3.	L	F	Z	57	O
4.	L	F	Z	57	OP
5.	L	F	Z	57	OM
6.	L	C	S	57	O
7.	L	C	Z	71	OP
8.	L	C	S	57	OM
9.	L	F	S	57	O
10.	L	F	S	57	OP
11.	L	F	S	57	OM
12.	L	C	Z	71	OM
13.	L	F	Z	71	OM
14.	L	F	Z	71	O
15.	L	F	S	71	OP
16.	L	C	S	71	O
17.	L	C	S	71	OM
18.	L	C	S	71	OP
19.	B	C	Z	57	OM
20.	B	F	Z	57	OP
21.	B	F	Z	57	O
22.	B	F	Z	57	OM
23.	B	C	S	57	O
24.	B	C	S	57	OP
25.	B	F	S	57	OP
26.	B	C	Z	71	O
27.	B	C	Z	71	OP

**Table 3.16 (continued)**

28.	B	F	S	71	O
29.	B	F	Z	71	O
30.	B	F	Z	71	OP
31.	B	C	S	57	OM
32.	B	C	S	71	O
33.	B	C	S	71	OM
34.	B	C	S	71	OP
35.	B	F	S	71	OM
36.	B	F	Z	71	OM

Symbol used: Aggregate Type: L-limestone, B-Basalt; Gradation: C- Coarse, F-Fine; Modification: Z-no Modification ,S-SBS Modification; AC type: 57-50 70, 71-71 100;AC content: O-optimum, OP –Optimum Plus.

In this test, test specimens were first conditioned in the machine at the room temperature, and then allowed to contract at a rate of  $-60^{\circ}\text{C}/\text{h}$  till the average temperature reaches around  $-70^{\circ}\text{C}$ . The contraction thus recorded is converted into strain and the thermal conductivity before and after the glass transition is determined by applying Bahia's and Anderson equation, (1993). Bahia and Anderson, (1993) proposed the following relation for fitting a five a parameter curve to the change of volumetric data against temperature.

$$v = C_v + \alpha_g (T - T_g) + R(\alpha_l - \alpha_g) \ln \left[ 1 + \exp \left( \frac{T - T_g}{R} \right) \right] \quad (3.1)$$

where  $v$  = specific volume in ml/g at temperature  $T$ ;  $C_v$  = specific volume at initial temperature ;  $T_g$  = glass transition temperature;  $R$  = constant defining curvature;  $\alpha_g$  = thermal expansion coefficient for  $T < T_g$ ; and  $\alpha_l$  = thermal expansion coefficient for  $T > T_g$

Once the data are obtained, the least squares method was applied to fit the model parameters and values of the thermal coefficients and the glass transition temperature were estimated. In this study, the method of least squares technique was applied by Microsoft Excel® add-ins package solver functions. Figure 3.23 gives a typical

graphical representation of Equation 3.1. The graphical plots for all the 36 specimens are given in Appendix B.

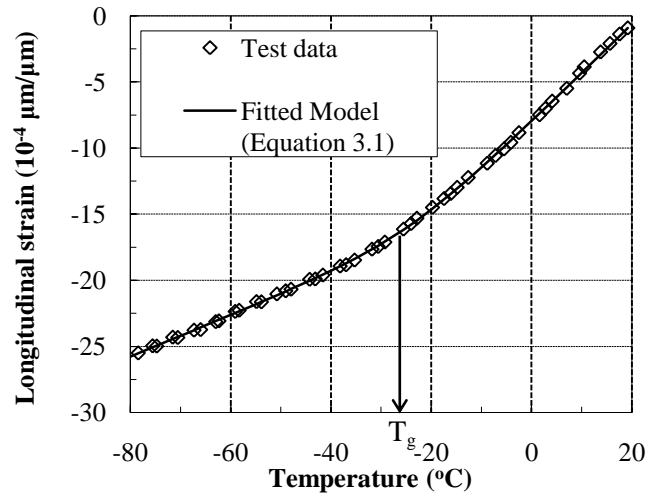


**Figure 3.23- A plot of Equation 3.1 for glass transition temperature measurement**

## CHAPTER 4

### RESULT ANALYSIS OF TESTS

#### 4.1. Introduction

This chapter presents discussions on the statistical analysis of the test results obtained from 144 TSRST tests and 36 glass transition temperature tests. The results were analyzed by adopting ANOVA technique and applying advanced statistical analysis methodologies including principal component analyses, cluster analyses, discriminant analyses, and stepwise and regular regression analyses.

The chapter concentrates on the relationships between input variables and the output variables. The results of analyses are presented with relevant references for comparison with the current research outcomes. Parametric studies are also provided to explain the effect of design variables on the output variables evaluated in this study. The chapter ends with conclusions based on these analyses.

#### 4.2. Analysis of variance tests (ANOVA) for research outcomes

The output data contain results from two major categories of experiments: TSRST results for fracture strength and fracture temperature, and glass transition temperature measurements. Both of these measurements differ in terms of the input and output variables. In this section, results of data analysis are presented separately based on the analysis of variance tests (ANOVA) for both categories

##### 4.2.1. Analysis of variance tests (ANOVA) for TSRST results

According to the experimental program, a total of 144 prismatic beam specimens were tested in TSRST to obtain various thermal properties. Results obtained from the TSRST of AC specimens involve a number of dependent and independent variables. In the ANOVA analyses, the experimental design variables as discussed in Chapter

3, were treated as independent variables while the measured outcomes, i.e., fracture strength, fracture temperature, transition temperature, stress relaxation, and the slope of thermal stress-temperature ( $\Delta S/\Delta T$ ) relation were taken as dependent variables. Besides, the load eccentricity and air voids of the specimens were also considered to be dependent variables in the analyses.

In the following sections, the influence of each of the input variables on the output variables will be discussed separately based on the ANOVA of the research outcomes.

### **a) Results of analysis for fracture strength**

The fracture strength of asphalt concrete is defined as the maximum stress level that can be reached under continuously decreasing temperature. In this research, the thermal stress built up in the field when the environment temperature decreases is simulated in the laboratory by the TSRST device under controlled loading and temperature. One of the important outcomes of TSRST is the fracture strength which was measured for 144 test specimens in the study. The results indicate that the average strength value of the tested specimens is around 3.18 MPa with a standard deviation of 1.16 MPa (Table 4.1). In addition, the maximum strength value reached is 5.77 MPa for specimens fabricated with limestone aggregate and the minimum strength found is 0.70 MPa for those specimens prepared with basalt aggregate.

**Table 4.1- Descriptive statistics of fracture strength**

<b>Statistical parameter</b>	<b>Value</b>
Mean	3.18
Standard deviation	1.16
Maximum strength	5.77
Minimum strength	0.70

Apart from the descriptive analysis, ANOVA was also applied to determine the influencing factors on the fracture strength of the specimens tested. The Table 4.2

summarizes probability values obtained from ANOVA for each experimental variable.

**Table 4.2- ANOVA analysis for fracture strength**

<b>Source</b>	<b>Probability</b>
Aggregate type	0.000
Gradation	0.061
Specimen length	0.071
Polymer modification	0.019
AC type	0.222
AC content	0.000
Cooling rate	0.078

It can be observed that the ANOVA analysis of the data singles out the design variable of aggregate type as the most dominant factor having probability nearly equal to zero for a confidence interval of 5% ( $p < 0.05$ ), in response to fracture strength. This statistical significance of aggregate is in complete agreement with the conclusions of a similar study on factors responsible for low temperature cracking conducted by Xinju et al., (2010).

The average value of fracture strength for aggregate type indicates that the highest fracture strength is obtained for limestone aggregate. The finding of this study is in agreement with the results of several researchers (Vinson and Jung, 1994; Stuart and Youtchef, 2001) as they found similar behavior when aggregates from two different sources were compared for low temperature cracking potential. The quantitative values obtained from descriptive statistics are summarized in Table 4.3.

The mean value of fracture strength for the basalt aggregate mixes obtained during the tests is nearly 75% of the average fracture strength of limestone aggregate mixes. It is believed that the lower fracture strength of specimens prepared with the basalt aggregate is due to the low absorption capacity of aggregate as reported in a similar study by Drüschner et al., (2004).

**Table 4.3- Fracture strength values for experimental variables**

Design Parameters	Levels	Symbol	Average	Standard deviation	Median
			MPa	MPa	MPa
Aggregate type	Limestone	L	3.816	0.910	3.915
	Basalt	B	2.867	1.203	2.735
Gradation	Coarse	C	3.498	1.106	3.565
	Fine	F	3.186	1.208	3.335
AC type	50-70	57	3.346	1.108	3.380
	71-100	71	3.348	1.227	3.540
Polymer modification	SBS	S	3.337	1.234	3.715
	Neat (Zero)	Z	3.346	1.100	3.330
Specimen length	200 (Small)	M	3.362	1.177	3.565
	300 (Tall)	T	3.321	1.160	3.375
AC content	Optimum	O	3.688	0.913	3.755
	Optimum-0.5%	OM	2.859	1.191	2.840
	Optimum+0.5%	OP	3.478	1.223	3.770
Cooling rate	-20 C/h	-20	3.601	1.093	3.835
	-10 C/h	-10	3.404	1.187	3.565
	-5 C/h	-5	3.021	1.160	2.960

Another reason might be the difference between the two aggregates in terms of surface texture and aggregate shape that all affect the bonding strength of binder (Nam and Bahia, 2005). Similar observations on the effect of aggregate type were also made by Jung and Vinson, (1994). Limestone has proven to be a better material not only for low temperature cracking but also for creep performance (Qudais and Shweily, 2007). It is anticipated that the limestone aggregate also influences the oxidative nature of binder and holds its oxygen thereby making the binder less aged and consequently reduces the low temperature potential threat to asphalt concrete (Vinson et al., 1989). On the basis of the discussion presented here, it can be concluded that the type of aggregate is a governing factor in determining the low temperature properties of hot mix asphalt paving mixtures, and this is also in agreement with the findings of the final report presented to the Minnesota Department of Highways by Transport pool study 776, (2007).

The size and proportion of aggregate, also known as gradation, is a very important and influential characteristic in determining the performance of paving mixture. Two types of gradation were chosen in this study; both of them were on the extreme ends of the specifications as described in the Turkish General Directory of Highways Manual (TGDH, 2006) categorized as coarse and fine, respectively. The gradation is not known to have an effect on the low temperature cracking potential of asphalt paving mixture in the existing literature (Vinson et al., 1989). The results obtained in this study using both gradations are inconclusive and not significant according to 5% confidence interval. Thus, the p-value of 0.061 shown in Table 4.3 indicates that gradation has no strong effect upon the fracture strength of the mixes tested in this study. From the data summary in Table 4.3, it is found that the average value of fracture strength for coarse gradation is 3.498 MPa. When such a relation is evaluated for mixes made with the fine gradation, the results indicate that the mean value of fracture strength is 3.186 MPa, which is 91% of the mixes prepared with the coarse gradation. Although on a normal scale the average value of fracture strength for the coarse gradation seems to be meaningful, the results for both gradations are very close. However, the higher average strength for the coarse gradation do indicate its advantage of using in asphalt concrete to take care of rutting distress (Fakhri and Mahmoud, 2006; Williams, 2006).

Asphalt binder is the most dominant contributor of providing durable pavements. It is believed by many scientists that softer binder provides more resistance to low temperature cracking as compare to stiffer binder (Robert et al., 1996). In this study, the type of asphalt seems to have reasonable impact on the strength of specimens in terms of temperature cracking performance and the significance of using a soft grade asphalt is verified by the research outcomes. From Table 4.3, it can be observed that the average strength values for 71-100 asphalt is higher than those for 50-70 grade asphalt, which proves the results of a study conducted by Jung and Vinson, (1994).

In this research, asphalt was modified using a SBS modifier and 72 samples were mixed and then tested for fracture strength and other dependant variables. The mod-

ification does not seem to have any positive contribution to the fracture resistance of asphalt concrete. On the contrary, it is observed that the neat or unmodified asphalt yields more resistance to low temperature cracking than does the modified asphalt. This finding is surprising and in contradiction to the findings of other researchers (Zeng and Issacson, 1998; Sebaaly et al., 2002; and Stuart and Youtcheff, 2001). However, Dongre, (2007) has pointed out that the TSRST results are affected by the stiffness of the base binder, which may be the reason for these results. On the other hand, the results validate the findings of research conducted by Shah, (2004) where she found the frequency of low temperature cracking on test pavements made with modified binders to be higher than those with unmodified binders. The mean values obtained for both types of AC types are quite close to each other (Table 4.3), confirming the results of ANOVA analysis. The response of the modified mixes may also be due to the amount of polymer added to the base asphalt, which may not be adequate to change the performance grade of the bitumen used, since it is reported that the amount of polymer used correlates directly with its low temperature cracking performance (King et al., 1993; Zhao et al., 2009).

The results in the ANOVA table do not show any individual significance for the specimen lengths used as another experimental variable. The specimen length does not seem to have an influence on the fracture response of hot mix asphalt concrete probably for the reason that the area of cross section is important rather than the specimen length in calculating the fracture stresses. This result is also consistent with the finding of Vinson and Jung, (1994), who concluded that the size of specimen does not alter the fracture strength of asphalt concrete. The results in Table 4.3 prove this fact by showing that the median values for both lengths (smaller and taller) are close to each other. The same statement can also be made for the mean strength values by again noting that the mean fracture strength obtained for the taller specimens is 96% of that obtained for the smaller specimens. Hence, it is clearly seen that the change of length does not, indeed, have any influence on the fracture strength of the test specimens.

Measuring the fracture strength in the laboratory at various cooling rates is still a controversial issue. In this study, the impact of cooling rate could not be proven as significant for the fracture strength as evident from the probability value of 0.078. Table 4.3 illustrates that the average fracture strength corresponding to the cooling rate of  $-10^{\circ}\text{C}/\text{h}$  falls in between  $-5^{\circ}\text{C}/\text{h}$  and at  $-20^{\circ}\text{C}/\text{h}$ . It should be reminded that the cooling rate of  $-10^{\circ}\text{C}/\text{h}$  is considered by Jung and Vinson, (1994) as the most representative cooling rate that can be used for testing of fracture strength. Therefore, the marginal differences between the average strength values prove that conducting TSRST experiment at a faster cooling rate may not over or under estimate the expected value of fracture strength.

The results of analyses show that the change in asphalt content within  $\pm 0.5\%$  relative to the optimum has a profound effect on the fracture strength. The results of ANOVA in Table 4.3 indicate that the highest strength can be obtained at the optimum asphalt content with the average strength of 3.688 MPa. The presented result for the effect of asphalt content is consistent with the finding of Vinson et al., (1989) who reported that small changes in asphalt content may increase the coefficient of thermal contraction and lower the strength of asphalt concrete.

#### **b) Results of analysis for fracture temperature**

In this study, the fracture temperature was considered as another dependent variable to evaluate for the low temperature cracking performance of the AC specimens. The results of ANOVA analysis for the experimental variables are shown in Table 4.4.

It can be observed that only three variables, i.e., aggregate type, polymer modification, and AC content, seem to be significant for fracture temperature at 5% confidence level. The aggregate type is a significant factor with a probability of nearly zero as seen in Table 4.4.

**Table 4.4- ANOVA analysis for fracture temperature**

Source	Probability
Aggregate type	0.000
Gradation	0.325
Specimen length	0.527
Polymer modification	0.000
AC type	0.140
AC content	0.000
Cooling rate	0.179

Limestone aggregate has an average fracture temperature of -14.173 °C while it is -13.191 °C for basalt aggregate as seen in Table 4.5. Hence, the lower average fracture temperature obtained from limestone aggregate highlights its contribution to the low temperature cracking resistance of the specimens.

**Table 4.5- Fracture temperature values for experimental variables**

Design Parameters	Levels	Symbol	Average	Standard deviation	Median
			°C	°C	°C
Aggregate type	Limestone	L	-14.173	6.420	-16.260
	Basalt	B	-13.191	5.887	-14.770
Gradation	Coarse	C	-13.868	5.893	-15.650
	Fine	F	-13.495	6.448	-15.500
AC type	50-70	57	-13.428	5.680	-15.550
	71-100	71	-13.936	6.632	-15.650
Polymer Modification	SBS	S	-13.140	6.515	-15.650
	Neat(Zero)	Z	-14.224	5.773	-15.450
Specimen length	200(Small)	M	-13.348	6.463	-15.600
	300(Tall)	T	-14.016	5.863	-15.550
AC content	Optimum	O	-15.495	4.319	-16.175
	Optimum-0.5	OM	-12.491	6.354	-13.875
	Optimum+0.5	OP	-13.06	7.15	-15.950
Cooling rate	-20° C/hr	-20	-13.639	6.826	-15.850
	-10° C/hr	-10	-14.484	5.301	-16.000
	-5° C/hr	-5	-12.923	6.279	-14.500

Another significant factor for fracture temperature is the polymer modification used in the test mixes. The results of ANOVA analysis show a probability value of nearly zero, as in the case of aggregate type, for polymer modification as seen in Table 4.5. The average fracture temperatures for this variable are  $-13.140^{\circ}\text{C}$  for the SBS modified binder and  $-14.224^{\circ}\text{C}$  for the neat binder used in the fabrication of test mixes. The meaning of this behavior is that mix prepared with the neat binder will experience fracture at a lower temperature than with the SBS modified binder in the same service conditions. With respect to specimen length, the results of analyses show that the short specimens have on average higher fracture temperature as compared to the tall specimens. This behavior may result from the fact that tall specimens need more time to reach the thermal equilibrium, and by that time the thermal stress may have already reach its ultimate value. Even though this result is in accordance with the findings reported by by Vinson and Jung, (1994), the ANOVA results indicate that this variable is not important for fracture temperature as implied by the probability value of 0.527 in Table 4.4. The ANOVA analysis summarized in Table 4.4 shows that asphalt content is also a significant factor for fracture temperature given the corresponding probability values of nearly zero. It can be seen from Table 4.4 that the lowest fracture temperature is obtained for the optimum asphalt content, and the next lowest temperature corresponds to the optimum+0.5% content. This clearly indicates that the highest resistance, hence the lowest fracture temperature, is obtained for the optimum asphalt content. However, asphalt content less than optimum provides higher fracture temperature or less resistance due to insufficient binding between aggregates. The explanation for this mechanism is identical to the case of fracture strength as given in the above section.

The result of ANOVA analysis for cooling rate does not show any significance as observed from (Table 4.4. This result is also in agreement with the findings of Vinson et al., (1989) and Nam and Bahia, (2005). Even though there is a difference in the mean fracture temperatures for the cooling rates used, it is not, however, a statistically significant factor as proved with the calculated probability of 0.179 in Table 4.4.

### c) Results of analysis for relaxation stress

Relaxation stress is defined as the point after which the stress-temperature relationship becomes nearly linear in the TSRTS testing. The relaxation stress defines a point for the nearness of fracture failure of the specimen. In this study the relaxation stress from the data was calculated with the help of a code written in Matlab<sup>®</sup>. The ANOVA analysis of relaxation stress is being summarized in Table 4.6. The aggregate type again shows to have significant impact on the relaxation strength of the mixes tested. The average values of relaxation stress obtained in the study are summarized in Table 4.7. It can be observed that the average relaxation stress of the mixes made with limestone aggregate is lower than that of mixes made with basalt aggregate. The difference in the values is attributed to the fact that limestone mixes react earlier to the change in temperature as compared to the mixes with basalt aggregate. This behavior can be as a result of the difference in the thermal behavior of two aggregates. A similar statement can also be made for the other significant factors, i.e., mix gradation and AC content, as given in Table 4.6.

**Table 4.6- ANOVA analysis of relaxation stress**

Source	Probability
Aggregate Type	0.000
Gradation	0.031
Specimen length	0.960
Polymer modification	0.294
AC type	0.642
AC content	0.000
Cooling rate	0.608

ANOVA analysis of relaxation stress that mix gradation is also a statistically significant factor with a probability of 0.031. The average relaxation stress the coarse gradation seems to be higher than for the fine gradation indicating that the coarse gradation yields an early start of the linear trend between the relaxation stress and temperature. AC content is also a statistically significant factor with a probability value of nearly zero as seen in Table 4.6. In terms of the average stress found, the optimum asphalt content gives the highest relaxation stress followed by the optimum+0.5%

and optimum-0.5% asphalt contents. The meaning of relaxation stress in terms of mix performance in low temperature cracking, however, not elaborated in the literature, and therefore, no comparison is possible with the results of this study.

**Table 4.7- Relaxation stress values for experimental variables**

Design Parameters	Levels	Symbol	Average	Standard deviation	Median
			MPa	MPa	MPa
Aggregate Type	Limestone	L	1.389	0.887	1.325
	Basalt	B	2.095	0.747	2.035
Gradation	Coarse	C	1.912	0.862	1.895
	Fine	F	1.572	0.892	1.645
Asphalt type	50-70	57	1.804	0.925	1.795
	71-100	71	1.681	0.856	1.865
Polymer modification	SBS	S	1.705	0.984	1.855
	Neat(Zero)	Z	1.780	0.797	1.840
Sample length	200(Small)	M	1.706	0.970	1.865
	300(Tall)	T	1.778	0.809	1.840
AC content	Optimum	O	1.966	0.813	1.915
	Optimum-0.5	OM	1.481	0.808	1.535
	Optimum+0.5	OP	1.780	0.989	1.890
Cooling rate	-20 C/hr	-20	1.937	0.832	1.950
	-10 C/hr	-10	1.772	0.914	1.855
	-5 C/hr	-5	1.518	0.891	1.510

#### **d) Results of analysis for transition temperature**

The temperature corresponding to relaxation stress is called as transition temperature in a stress versus temperature relationship. In order to determine the transition temperatures for the test specimens, a special Matlab<sup>®</sup> code was written to analyze the data and to locate the point of transition. The results of ANOVA analysis for transition temperature as a dependent variable is given in Table 4.8.

**Table 4.8- ANOVA analysis for transition temperature**

Source	Probability
Aggregate type	0.001
Gradation	0.254
Specimen length	0.644
Polymer modification	0.079
AC type	0.453
AC content	0.004
Cooling rate	0.742

It can be observed that aggregate type and AC content are the only experimental variables that are significant for transition temperature. The aggregate type has a probability value of 0.001 meaning that it is significant at 5% confidence level. As already discussed in the previous sections about the effect of aggregate type, the transition temperature is also affected by the aggregate used in the fabrication of mixes. The mean value of transition temperature for limestone is lower than for basalt aggregate as seen in Table 4.9. This can be expected since a similar trend for aggregate type is also observed for the relaxation stress. Another significant factor for transition temperature is the AC content of the test mixtures having a probability of 0.004. The mean value calculated for the optimum asphalt content is lowest as in the case of relaxation stress. The order of mean temperatures for the other AC contents is also the same as for the relaxation stress. Because the effect of transition temperature in terms of mix performance is not studied comprehensively, discussion on the comparison of research outcomes with previous studies will not be given here.

**Table 4.9- Transition temperature values for experimental variables**

Design Parameters	Levels	Symbol	Average	Standard deviation	Median
			°C	°C	°C
Aggregate type	Limestone	L	-8.134	5.159	-9.040
	Basalt	B	-6.085	4.858	-5.310
Gradation	Coarse	C	-7.783	5.280	-8.360
	Fine	F	-6.436	4.852	-7.105
AC type	50-70	57	-7.462	5.041	-7.950
	71-100	71	-6.578	5.165	-7.105

**Table 4.9 (continued)**

Polymer modification	SBS	S	-6.919	5.275	-6.905
	Neat(Zero)	Z	-7.300	4.944	-8.060
Specimen length	200(Small)	M	-6.682	5.058	-7.305
	300(Tall)	T	-7.538	5.137	-7.950
AC content	Optimum	O	-7.905	5.005	-9.020
	Optimum-0.5	OM	-6.048	5.001	-5.510
	Optimum+0.5	OP	-7.375	5.210	-7.650
Cooling rate	-20°C/hr	-20	-7.894	5.296	-8.800
	-10°C/hr	-10	-6.480	4.919	-6.870
	-5°C/hr	-5	-6.956	5.076	-7.170

**e) Results of analysis for slope ( $\Delta S/\Delta T$ )**

Slope constant is defined as the ratio of thermal stress to temperature, which essentially gives the unit change of thermal stress per unit change of temperature. The reason for considering this ratio as another dependent variable is that it was used in previous studies as a parameter to differentiate between varying mixtures in terms of their performance on low temperature cracking. The ANOVA values obtained for  $\Delta S/\Delta T$  as response variable have been summarized in Table 4.10.

**Table 4.10- Analysis of variance for  $\Delta S/\Delta T$** 

Source	Probability
Aggregate type	0.002
Gradation	0.234
Specimen length	0.304
Polymer modification	0.087
AC type	0.431
AC content	0.005
Cooling rate	0.208

The ANOVA table shows that the significant factor is the aggregate type as presented in Table 4.10. From Table 4.11, it is evident the median value for the rate of change in the tensile stress per unit drop in the environment temperature is -0.237 for specimens prepared with limestone and -0.193 for specimens with basalt aggregate. These findings confirm that specimens with limestone aggregate can sustain their strength at lower temperatures than do specimens with basalt aggregate. The re-

sponse to temperature change also seems to be faster for specimens of limestone aggregate as indicated by the average rate of changes in the slope constant. Looking at Table 4.10, the slope value for coarse gradation is lower than fine gradation meaning that it can sustain more fracture strength as compared to fine gradation mix.

**Table 4.11- Slope( $\Delta S/\Delta T$ ) constant values for experimental variables**

Design Parameters	Levels	Symbol	Average	Standard deviation	Median
Aggregate type	Limestone	L	-0.237	0.678	-0.249
	Basalt	B	-0.193	0.082	-0.181
Gradation	Coarse	C	-0.229	0.079	-0.251
	Fine	F	-0.201	0.075	-0.208
AC type	50-70	57	-0.219	0.078	-0.224
	71-100	71	-0.211	0.078	-0.234
Polymer modification	SBS	S	-0.206	0.077	-0.218
	Neat(Zero)	Z	-0.224	0.079	-0.239
Specimen length	200(Small)	M	-0.219	0.078	-0.223
	300(Tall)	T	-0.211	0.078	-0.236
AC content	Optimum	O	-0.235	0.066	-0.240
	Optimum-0.5	OM	-0.185	0.086	-0.191
	Optimum+0.5	OP	-0.225	0.074	-0.250
Cooling rate	-20 C/hr	-20	-0.237	0.068	-0.254
	-10 C/hr	-10	-0.215	0.083	-0.231
	-5 C/hr	-5	-0.194	0.078	-0.201

The asphalt type has no effect on the slope value as can be referred from Table 4.10. The use of polymer modification also fail to produce any significant effect on the slope constant as highlighted by the probability value of 0.087 in Table 4.11. The impact of sample length is also insignificant for the slope given the calculated probability value in Table 4.10. Table 4.10 shows that varying asphalt contents also affect the slope constant. The ANOVA analysis to compare significance of using different cooling rate is again proven to be insignificant (Table 4.10). The average slope value

for the cooling rate of  $-10^{\circ}\text{C/h}$  is higher as compared to the other cooling rates used in this study.

#### **f) Air voids as a dependent variable**

Ever since the evolution of flexible pavement, percent air void is agreed to be one of the most crucial parameters. Air void is the most important design criteria as addressed in all of the job-mix formulae whether the design method is performed according to Hveem, Marshall or the state of the art method, the Superpave volumetric mix design procedure. The optimum air void is needed to allow for suitable traffic compaction under traffic for the pavement, on the other hand, the presence of more voids will accelerate the rate of aging of pavement, consequently making it more susceptible to thermal cracking. Moreover, the excess air void results in interconnecting voids that can allow water to penetrate and form ice lenses in freezing temperature, thus increasing the chance of low temperature cracking. One of the parameters in the experimental design of this study is the various air void contents;  $\pm 0.5\%$  and the optimum asphalt content that can produce 4% air voids.

The impact of air voids on the measured parameters of thermal performance of test mixtures is prominent from all the responses measured. In general, higher values are obtained for low air void specimens, i.e., at Optimum+0.5, while lower values are obtained from Optimum-0.5AC. These results are consistent with the outcomes of Transport pooled study 776, (2007) according to which thermal strength is lower for 7% air void as compared to 4% voids. Table 4.12 shows the value of correlation of air voids with each of the response variables studied in this thesis. All the values are consistent showing moderate to high correlation indicating that low air void content increases fracture strength, and relaxation stress, however, decreases fracture temperature, transition temperature and slope constant.

**Table 4.12- Correlation of air voids with various response variables**

<b>S.no</b>	<b>Response variable</b>	<b>Correlation values</b>	<b>R sq values</b>
1	Fracture strength	-0.793	0.646
2	Relaxation stress	-0.617	0.438
3	Fracture temperature	0.475	0.226
4	Transition temperature	0.415	0.17
5	Slope constant	0.602	0.464

**g) Eccentricity**

One of the disadvantages associated with the TSRST test was identified as eccentricity of tensile loading (Vinson and Jung, 1994; Velásquez et al., 2009) causing sample to fail in bending rather than in tension during the test. In this study, eccentricity was calculated from the difference of the linear variable differential transformer (LVDT) readings one minute before the failure of the specimen. A Matlab® code was written for this purpose to calculate the eccentricity of the tensile loading. The maximum eccentricity obtained in the study was 261 microns while the minimum value was 2 microns. The ANOVA analysis in Table 4.13 shows no significant effect of eccentricity for any of the response variables.

**Table 4.13- ANOVA for tensile load eccentricity**

<b>Source</b>	<b>Probability</b>
Aggregate type	0.170
Gradation	0.663
Specimen length	0.589
Polymer modification	0.283
AC type	0.088
AC content	0.873
Cooling rate	0.043

A closer look at the test data suggests that the average median eccentricity obtained ranges between 40-50 microns. This, in turn, shows the effectiveness of the technique used to control the eccentricity in the TSRST set up.

#### 4.2.2. Analysis of variance tests (ANOVA) for glass transition temperature measurements

This section presents a discussion on the results of tests conducted for measuring the glass transition of 36 TSRST specimens. The results were analyzed using ANOVA and listed in tables. This section is further divided into the following two subsections:

- Glass transition temperature
- Thermal coefficients before and after glass transition temperature

##### a) Glass transition temperature of the test specimens

Table 4.14 presents the summary of ANOVA results obtained from the glass transition temperature measurements. Table 4.15 shows that the glass transition temperatures range between  $-25^{\circ}\text{C}$  to  $-27^{\circ}\text{C}$ . The maximum median value is found for more than optimum asphalt content while the least median value was found for specimens fabricated with asphalt 50-70.

**Table 4.14- Probability values calculated from ANOVA**

Source	Probability
Aggregate type	0.036
Gradation	0.957
Polymer modification	0.339
AC type	0.535
AC content	0.517

The effect of aggregate type was found to be significant on glass transition temperature results (Table 4.14). The results are not surprising since the aggregates are known to impart their own interaction in the mix. The average glass transition temperature for limestone mixes was found to be  $-25.11^{\circ}\text{C}$  as compared to that of basalt mixes  $-27.13^{\circ}\text{C}$ .

**Table 4.15- Statistics for glass transition temperature measurements**

Design Parameters	Levels	Symbol	Average	Standard deviation	Median
			°C	°C	°C
Aggregate type	Limestone	L	-25.11	4.94	-24.63
	Basalt	B	-27.13	5.23	-26.80
Gradation	Coarse	C	-26.14	4.85	-25.90
	Fine	F	-26.10	5.51	-26.02
AC type	50-70	57	-25.16	5.56	-23.72
	71-100	71	-27.07	4.59	-27.19
Polymer modification	SBS	S	-25.24	4.92	-25.73
	Neat(Zero)	Z	-26.99	5.30	-26.19
AC content	Optimum	O	-25.70	5.06	-26.02
	Optimum-0.5	OM	-25.12	5.53	-24.85
	Optimum+0.5	OP	-27.53	4.86	-27.81

The gradation of the mix was not found to be significant factor influencing the glass transition temperature. It can also be judged from the corresponding probability value as shown in Table 4.14. The median values presented in Table 4.15 show that the difference in the values is only 0.12°C which is not noticeable.

The polymer modified mixes when tested for glass transition temperature give no significant result. The average value of the mixes with polymer modification was -1.75°C higher than the mixes with neat binders (Table 4.15). These results do not conform to similar studies on modified mixes (Nam and Bahia, 2005; Transport pool study 776, 2007).

The asphalt type statistically appears to be insignificant in determining the glass transition temperature. The results acquired for specimens with 50-70 asphalt grade have an average value of -25.16°C. The average difference in the mean glass temperature between two types of asphalt was found to be -1.91°C in Table 4.14. The variability of the asphalt content for glass transition temperature measurement was insignificant according to the ANOVA analysis. The median values acquired for mixes with more asphalt contents are higher than those of mixes with less asphalt content. The differ-

ence in the average values for the two extreme asphalt contents was found to be - 2.41°C as shown in Table 4.15.

**b) Thermal coefficients before and after glass transition temperature**

The thermal coefficients are important parameters in determining the glass transition behavior of asphalt concrete. ANOVA analysis of the results obtained for thermal coefficients are presented in Table 4.16.

**Table 4.16- Probability values calculated from ANOVA**

Source	Coefficient after glass transition	Coefficient before glass transition
Aggregate type	0.200	0.218
Gradation	0.533	0.711
Polymer modification	0.455	0.830
AC type	0.455	0.439
AC content	0.745	0.660

Apparently, no significant effect of aggregate type was observed from the analysis. The coefficients of linear contraction for limestone mixes both before and after the glass transition temperature are lower than the corresponding coefficients for basalt aggregate mixes.

The gradation affects appear to be also insignificant which is in accordance with the findings of Nam and Bahia, (2009). A comparison of the calculated values suggests that the fine gradation mixes show less contraction than do the coarse gradation mixes. This can be explained by the presence of low air void spaces which leads to reduced conductivity and hence less contraction of the specimens. Various statistical parameters computed for these coefficients are given for gradation in Table 4.17.

**Table 4.17- Statistical parameters for thermal coefficients in the case of gradation type**

Gradation	Measured Coefficient	Average	Standard deviation	Median
		$\times 10^{-6}$	$\times 10^{-6}$	$\times 10^{-6}$
Coarse	after transition	13.9	14.4	12.3
	before transition	40.5	15.7	39.2
Fine	after transition	12.3	4.7	12.0
	before transition	38.4	6.5	37.7

The ANOVA analysis for asphalt type seems to be insignificant showing more than 5% probability. Researches also contend that although the binder behavior is important in determining the thermo volumetric properties of asphalt paving mixtures, sometimes interaction of gradation and source of aggregate make the binder less active (Nam and Bahia, 2005). However, the acquired values affirm the trend of less stiffer binder performing better than a stiffer binder. These values are summarized in Table 4.18.

**Table 4.18- Statistical parameters for thermal coefficients in the case of asphalt type**

AC type	Measured Coefficient	Average	Standard Deviation	Median
		$\times 10^{-6}$	$\times 10^{-6}$	$\times 10^{-6}$
50-70	after transition	11.0	4.9	11.3
	before transition	40.5	15.7	39.2
71-100	after transition	15.2	14.0	14.6
	before transition	39.6	15.5	36.9

Although varying asphalt contents produce different values of glass transition temperatures and the coefficient of contraction before and after the glass transition temperature, they fail to prove any statistically significant difference. Table 4.19 shows

also various statistical parameters calculated from the thermal coefficients for varying asphalt contents.

**Table 4.19- Statistical parameters for thermal coefficients in the case of asphalt content**

Asphalt Content	Measured Coefficient	Average	Standard Deviation	Median
		$\times 10^{-6}$	$\times 10^{-6}$	$\times 10^{-6}$
Optimum	after transition	13.8	5.83	15.8
	before transition	3.71	4.89	37.7
Optimum Minus	after transition	10.0	5.56	10.2
	before transition	38.3	6.25	38.8
Optimum plus	after transition	15.4	16.5	11.7
	before transition	42.9	19.1	39.0

### 4.3. Principal component (PC) analysis

Principal component analysis is one of the advanced statistical analysis tools that is used to identify the homogenous groups within the data and helps in developing mathematical models. These principal components help in determining new variables from the existing data and minimize the proportion of total variances between the variables. Since two types of experiments were conducted in this study, the principal component analysis is also discussed here accordingly.

#### 4.3.1. Principal component analysis for fracture strength data

The principal component analyses performed on 144 samples for fracture stress data resulted in the correlation and covariance coefficients as presented in Table 4.20. The new variables were calculated as a linear combination of these coefficients and the designed variables of the study by using the following relation (equation 4.1).

$$PC_n = a_1 * FS + a_2 * FT + a_3 * RS + a_4 * TT + a_5 * \Delta S / \Delta T + a_6 * AV + a_7 * Ecc. \quad (4.1)$$

where  $a_1, \dots, a_7$  are coefficients summarized in Table 4.21; FS= Fracture stress; FT= Fracture temperature; RS= Relaxation stress; TT= Transition temperature;  $\Delta S / \Delta T$ = Slope; AV=Air voids; Ecc=Eccentricity; and PCn=Principal components 1, 2 or 3 as required. The calculated values of principal components from Equation 4.1 are presented in Table 4.20.

**Table 4.20- Coefficients of for principle components for fracture strength**

Coef fi- cient	Correlations			Covariance		
	PC1	PC2	PC3	PC1	PC2	PC3
a <sub>1</sub>	-0.46058	0.071236	-0.18041	0.004177	0.168493	-0.20174
a <sub>2</sub>	0.380342	0.149685	-0.3779	-0.00533	-0.50085	0.106751
a <sub>3</sub>	-0.43327	-0.15024	0.108446	0.001068	0.139946	-0.02817
a <sub>4</sub>	0.388707	0.267471	-0.51586	-0.00418	-0.77367	-0.4707
a <sub>5</sub>	0.387422	-0.11502	0.431538	-0.00028	-0.01112	0.014982
a <sub>6</sub>	0.077609	-0.90773	-0.40105	-0.99991	0.01025	-0.00876
a <sub>7</sub>	0.385065	-0.20301	0.446881	-0.0109	-0.31998	0.85162

The findings of analysis of the fracture data for principal components using Minitab 14<sup>®</sup>, as presented in Table 4.21 show that:

- One PC is enough to get 98% confidence.
- If we use two PCs, the confidence becomes 99.5%. 3 PCs must be use to get 99.8% confidence.

**Table 4.21- Eigen values for principal component analysis**

Eigen value	1920.1	28.5	6.2	3.7	0.3	0.1
Proportion	0.98	0.015	0.003	0.002	0	0
Cumulative	0.98	0.995	0.998	1	1	1

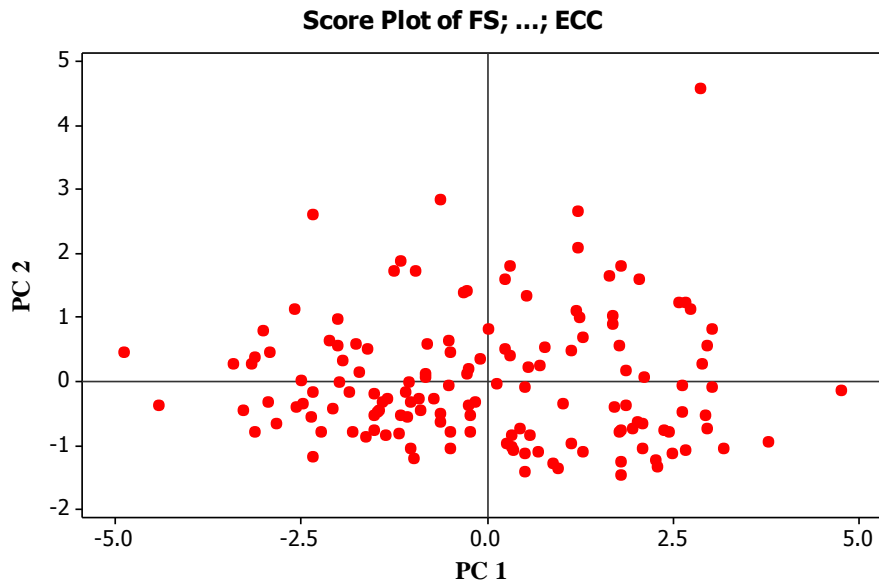


**Figure 4.1- Perpendicularity of principal components for fracture strength data**

Figure 4.1 shows the perpendicularity of principal components indicating their independence from each other.

**a) Clusters from the principal component analysis**

This section discusses the ANOVA analysis of the cluster groups generated through principal component analysis of the data. This discussion is essential to address the unexpected number of clusters emerging out of this analysis. These clusters resulted from the principal component analysis of the covariance's and correlations. The number of members in each cluster groups varies. A significant number of the cluster groups unexpectedly contain single member, thus becoming insignificant further deliberation. It may be due to the error in sample preparation, experimentation or non homogeneous asphalt concrete specimens. Therefore, only those cluster groups

having more than ten members, with 98 % similarity level, are selected here for further discussion. The existence of five such cluster groups is evident from Table 4.22.

**Table 4.22- Clusters from principal components analysis**

	Cluster from PC using			
	Correlation		Covariance	
	No of observation each level			
Similarity Level	97	98	97	98
Total Clusters	<b>10</b>	<b>32</b>	<b>9</b>	<b>23</b>
Cluster 1	120	44	134	50
Cluster 2	12	40	2	41
Cluster 3	4	8	2	11
Cluster 4	2	7		7
Cluster 5		4		6
Cluster 6		3		3
Cluster 7		3		3
Cluster 8		3		3
<b>No. of obs. =2</b>	1	8	2	5
<b>No. of obs. =1</b>	<b>6</b>	<b>16</b>	<b>5</b>	<b>10</b>

The ANOVA analysis of these five clusters is summarized in Table 4.23-4.28 with individual dependant variables. The discussion is mainly focused on comparison of the findings acquired from different cluster groups with that of the original unclustered data of 144 samples.

**i) Comparison of clusters for the fracture strength**

The fracture response of ANOVA presented in Table 4.23 helps to formulate following inferences:

- It shows that the aggregate type has statistically significant values for majority of the clusters.
- The gradation of the mixes used in this study is not significant except in the cluster having 50 data points.

- The specimen length, modification, cooling rate and the asphalt type do not have any influence on the fracture strength of specimen, as indicated by high probability values of most of the clusters summarized in Table 4.23.
- The asphalt content has overall significant values for three clusters while other clusters did not show any significant values of probability.

**Table 4.23- Response of the fracture strength against variable**

Variables	Cluster group from					
	Original data	Principal components				
		Covariance			Correlation	
	144	44	40	50	41	11
Aggregate type	0.000	0.014	0.000	0.000	0.001	0.909
Gradation	0.061	0.395	0.000	0.005	0.184	0.524
Specimen length	0.071	0.553	0.899	0.489	0.963	0.956
Polymer modification	0.019	0.460	0.898	0.565	0.288	0.487
AC type	0.222	0.101	0.320	0.359	0.107	0.547
AC Content	0.000	0.743	0.031	0.016	0.342	0.442
Cooling rate	0.078	0.282	0.643	0.494	0.758	0.951

#### ii) Comparison of clusters for the fracture temperature

The fracture temperature values as response to the variables for different clusters, presented in Table 4.24, helps to draw the following conclusions:

- The probability values of all the clusters resulted in a significant effect of aggregate type on fracture temperature of the specimens tested except cluster having 11 observations.
- The values of probability are insignificant for specimen size, gradation, cooling rate and asphalt type of the mixes used in the study.
- There is a significant effect of non-modified mixes on fracture temperature in half of the clusters (i.e. three clusters) studied here, while such an effect is not evident for the rest of clusters.
- Asphalt contents reflect high influence on the fracture temperature of mixes in originally unclustered observations but such phenomenon was not ob-

served in the clusters produced through the principal component analysis in Table 4.24.

**Table 4.24- Response of fracture temperature against experimental variables**

Variables	Cluster group from					
	Original data	Principal components				
		Covariance			Correlation	
	144	44	40	50	41	11
Aggregate type	0.000	0.004	0.003	0.000	0.001	0.182
Gradation	0.340	0.789	0.018	0.052	0.861	0.056
Specimen length	0.602	0.980	0.911	0.429	0.834	0.049
Polymer modification	0.003	0.295	0.004	0.002	0.152	0.116
AC type	0.263	0.366	0.006	0.006	0.507	0.035
AC content	0.000	0.372	0.482	0.400	0.134	0.074
Cooling rate	0.283	0.390	0.338	0.443	0.470	0.042

### iii) Comparison of clusters for relaxation stress

The different response of relaxation stresses in various clusters as summarized in Table 4.25 shows the following observations:

- Aggregate type is again found to be significant in majority of the clusters analyzed by ANOVA.
- The effect of gradation and no-modification is significant in only two clusters, while the other groups do not show any such trend.
- The ANOVA analysis assigns insignificant probability values for specimen size, asphalt type, asphalt contents and cooling rate for all the clusters (Table 4.25).

**Table 4.25- Relaxation stress response to experimental variables**

Variables	Cluster group from					
	Original data	Principal components				
		Covariance			Correlation	
	144	44	40	50	41	11
Aggregate type	0.000	0.035	0.000	0.000	0.012	0.532
Gradation	0.002	0.266	0.005	0.023	0.171	0.620
Specimen length	0.647	0.538	0.564	0.476	0.901	0.784

**Table 4.25 (continued)**

Polymer modification	0.033	0.476	0.092	0.158	0.223	0.815
AC type	0.566	0.817	0.156	0.552	0.793	0.295
AC content	0.000	0.829	0.251	0.255	0.625	0.905
Cooling rate	0.241	0.490	0.125	0.144	0.705	0.690

**iv) Comparison of clusters for the transition temperature**

The responses in respect to transition temperatures in various clusters, as summarized in Table 4.26, identify the following interpretations:

- The aggregate type proved to be an influential variable in determining the transition temperature of mixes in the majority of clusters.
- The gradation effect has shown its influence marginally in two clusters only.
- The influence of specimen size, asphalt type and cooling rate again proved to be insignificant.
- The effect of asphalt modification and asphalt content is evident in majority of the clusters, while it is insignificant in the cluster having 11 observations.

**Table 4.26- Transition temperature response to experimental variables**

Variables	Cluster group from					
	Original data	Principal components				
		Covariance		Correlation		
	144	44	40	50	41	11
Aggregate type	0.000	0.082	0.057	0.017	0.022	0.567
Gradation	0.054	0.645	0.085	0.125	0.302	0.661
Specimen length	0.950	0.690	0.909	0.646	0.945	0.893
Polymer modification	0.000	0.080	0.003	0.001	0.017	0.786
AC type	0.731	0.324	0.033	0.069	0.400	0.404
AC content	0.002	0.534	0.181	0.117	0.285	0.853
Cooling rate	0.816	0.648	0.907	0.556	0.594	0.672

**v) Comparison of clusters for  $\Delta S/\Delta T$**

The responses in respect to  $\Delta S/\Delta T$  in various clusters, as summarized in Table 4.27, show the following trends:

- It shows significant effects of aggregate type, gradation and asphalt content on the mixes in the original data, but not in most of the clusters.
- The specimen size, asphalt type and modification have higher probability values to illustrate that there is no influence of these variables.

**Table 4.27- Effect of experimental variables on slope constant**

Variables	Cluster group from					
	Original data	Principal components				
		Covariance		Correlation		
	144	44	40	50	41	11
Aggregate type	0.000	0.272	0.148	0.063	0.025	0.713
Gradation	0.015	0.297	0.038	0.041	0.104	0.550
Specimen length	0.253	0.326	0.541	0.641	0.844	0.489
Polymer modification	0.665	0.162	0.403	0.709	0.101	0.388
AC type	0.688	0.034	0.781	0.675	0.026	0.239
AC content	0.000	0.424	0.277	0.138	0.375	0.420
Cooling rate	0.588	0.646	0.825	0.755	0.792	0.964

**vi) Comparison of clusters for air voids**

The responses in respect to air voids in various clusters, as summarized in Table 4.28, gives rise to the following patterns:

- The air voids is greatly influenced by aggregate type, gradation, asphalt type, and asphalt content, as expected.
- The specimen size and cooling rate do not show any influence on air voids.

**Table 4.28- Air voids probability results for experimental variables**

Variables	Cluster group from					
	Original data	Principal components				
		Covariance		Correlation		
	144	44	40	50	41	11
Aggregate type	0.000	0.000	0.000	0.000	0.000	0.686
Gradation	0.006	0.001	0.002	0.001	0.002	0.729
Specimen length	0.813	0.369	0.628	0.710	0.251	0.687
Polymer modification	0.104	0.292	0.078	0.088	0.279	0.468
AC type	0.005	0.032	0.005	0.001	0.006	0.930
AC content	0.000	0.015	0.004	0.001	0.022	0.537
Cooling rate	0.539	0.088	0.671	0.339	0.028	0.896

**vii) Comparison of clusters for eccentricity in clusters**

The responses in respect to eccentricity in various clusters, as summarized in Table 4.29, do not show any influential response of eccentricity against any variables. It again shows the control achieved in avoiding the eccentricity effect during testing of the mixes in this particular study.

**Table 4.29- Effect of eccentricity on experimental variables**

Variables	Cluster group from					
	Original data	Principal components				
		Covariance		Correlation		
	144	44	40	50	41	11
Aggregate type	0.357	0.541	0.031	0.212	0.559	0.799
Gradation	0.351	0.101	0.186	0.312	0.047	0.982
Specimen length	0.849	0.905	0.516	0.705	0.669	0.887
Polymer modification	0.673	0.280	0.240	0.347	0.138	0.994
AC type	0.572	0.651	0.142	0.295	0.876	0.908
AC content	0.910	0.518	0.716	0.837	0.529	0.712
Cooling rate	0.152	0.913	0.158	0.265	0.936	0.596

### 4.3.2. Principal component analysis for glass transition temperature

The principal component analysis of the experimental data finds that only two principal factors are needed to explain glass transition data having eigen values more than 1. These values are illustrated in the Table 4.30.

**Table 4.30- Principal components of glass transition temperature**

Variables	FS	FT	RS	TT	$\Delta s/\Delta T$	Eccentricity	Air void
Eigen value	4.202	1.032	0.75	0.44	0.36	0.149	0.060
Proportion	0.600	0.147	0.11	0.06	0.05	0.021	0.009
Cumulative	0.600	0.748	0.86	0.92	0.97	0.991	1.000
PC1	-0.004	0.005	-0.001	0.004	0	1	0.011
PC2	-0.168	0.501	-0.14	0.774	0.011	-0.01	0.32
PC3	0.202	-0.107	0.028	0.471	-0.015	0.009	-0.852
PC4	-0.01	0.85	0.13	-0.395	-0.005	0.001	-0.323
PC5	-0.789	-0.077	-0.536	-0.113	0.061	0	-0.259

#### a) Statistical analysis of glass transition data from principal component

As used for fracture data, the same type of analysis is performed here for glass transition data obtained in this research. The similarity level for analysis here is 95%, in order to accommodate clusters having more than 10 observations. Table 4.31 presents summary of clusters using the principal component analysis.

**Table 4.31- Cluster of glass transition from PC using similarity**

	Cluster from PC using correlation			Cluster from PC using covariance		
	Similarity Level			Similarity Level		
	95	97	98	95	97	98
<b>Similarity Level</b>	<b>95</b>	<b>97</b>	<b>98</b>	<b>95</b>	<b>97</b>	<b>98</b>
Total Clusters	7	13	17	7	13	17
Cluster 1	13	6	5	13	6	5
Cluster 2	10	5	5	10	5	5
Cluster 3	4	5	4	4	5	4
Cluster 4	3	4	4	3	4	4
Cluster 5	3	3	3	3	3	3
Cluster 6	2	3	3	2	3	3

**Table 4.31 (continued)**

Cluster 7		2	2		2	2
Cluster 8		2			2	
Cluster 9		2			2	
Observation =1	1	4	10	1	4	10

**i) Discussion on ANOVA for glass transition from PC clusters**

The ANOVA analyses summarized in Table 4.32 provides the following inferences:

- The effect of aggregate type cannot be calculated in clusters having 10 observations because of the presence of single aggregate type which make the ANOVA not applicable.
- Only modification seems to have an effect on the glass transition temperature of the mixes. This finding is different from that of the original unclustered data, (i.e., comprises of 36 observations).
- The gradation, asphalt type, and asphalt content appear to be insignificant.

**Table 4.32- ANOVA for glass transition response for clusters from PC**

Variables	Cluster group from				
	Original data	Principal components			
		Covariance		Correlation	
36	13	10	13	10	
Aggregate type	0.036	0.729	-	0.729	-
Gradation	0.957	0.978	0.705	0.978	0.705
Polymer modification	0.339	0.823	0.008	0.823	0.008
AC type	0.535	0.828	0.231	0.828	0.231
AC content	0.517	0.437	0.489	0.437	0.489

**ii) Discussion on ANOVA for thermal coefficients from PC clusters**

From the ANOVA analyses summarized in Table 4.33, none of the variables is found to have influence on the glass transition coefficients. The effect of aggregate

type cannot be calculated in clusters having 10 observations because of the presence of single aggregate type which make the ANOVA not applicable.

**Table 4.33- Probability values for thermal coefficients**

Variables	Cluster group from				
	Original data	Principal components			
		Covariance		Correlation	
Coefficients after glass transition temperature					
	36	13	10	13	10
Aggregate type	0.200	0.584	-	0.584	-
Gradation	0.533	0.315	0.394	0.315	0.394
Polymer modification	0.455	0.906	0.499	0.906	0.499
AC type	0.455	0.457	0.331	0.457	0.331
AC content	0.745	0.276	0.785	0.276	0.785
Variables	Coefficients before glass transition temperature				
Aggregate type	0.218	0.673	-	0.673	-
Gradation	0.711	0.997	0.202	0.997	0.202
Polymer modification	0.830	0.866	0.713	0.866	0.713
AC type	0.439	0.915	0.467	0.915	0.467
AC content	0.660	0.796	0.663	0.796	0.663

#### 4.4. Cluster analysis

This section presents cluster analysis carried out by using the values of variables directly. These clusters are different from the ones derived by using principal components as discussed in previous section of this chapter. The number of these clusters with their respective number of observations are presented in Table 4.34, according to different similarity levels.

**Table 4.34- Cluster from fracture and glass transition measurements**

	Fracture Data		Glass Data		
	97	98	95	97	98
Total Clusters	<b>11</b>	<b>53</b>	<b>8</b>	<b>17</b>	<b>19</b>
Cluster 1	120	30	13	5	5
Cluster 2	12	15	10	5	5
Cluster 3		9	4	4	4

**Table 4.34 (continued)**

Cluster 4		7	3	4	3
Cluster 5		5		3	3
Cluster 6		5		3	
Cluster 7		5			
Cluster 8		5			
Cluster 9		3			
Cluster 10		3			
Cluster 11		3			
Cluster 12		3			
<b>No. of obs. =2</b>	<b>3</b>	<b>10</b>	<b>2</b>	<b>1</b>	<b>2</b>
<b>No. of obs. =1</b>	<b>6</b>	<b>31</b>	<b>2</b>	<b>10</b>	<b>12</b>

#### 4.4.1. ANOVA for fracture data of clusters

The analysis of fracture data is further divided into the seven independent variable responses and will be discussed accordingly in the following subsections. Similar to the case of principle component clusters, only those clusters having more than 10 sample observations along with 98% similarity level were chosen for further analysis.

##### a) ANOVA for fracture strength

The fracture responses of ANOVA, as presented in Table 4.35, provide the following inferences:

- The aggregate type has significant effect for the majority of the clusters.
- The specimen size, modification, asphalt type, asphalt content and cooling rate were found to have no influence on the fracture strength of specimen, as indicated by high probability values in smaller group of clusters.

**Table 4.35- Response of fracture strength against experimental variable**

<b>Variables</b>	<b>Original data</b>	<b>Cluster at 98% SL</b>	
<b>No. of samples</b>	<b>144</b>	<b>30</b>	<b>15</b>
Aggregate type	0.000	0.032	0.654
Gradation	0.061	0.496	0.351
Specimen length	0.071	0.957	0.841

**Table 4.35 (continued)**

Polymer modification	0.019	0.798	0.849
AC type	0.222	0.071	0.947
AC content	0.000	0.602	0.694
Cooling rate	0.078	0.825	0.299

**b) Comparison of clusters for fracture temperature**

The values of fracture temperature as response to the variables for different clusters, as presented in Table 4.36, give the following conclusions:

- The probability value of all clusters results in a significant effect of aggregate type on fracture temperature of the specimens except cluster having 15 observations.
- The values of probability are insignificant for all other variables except aggregate type.

**Table 4.36- Response of fracture temperature against experimental variables**

<b>Variables</b>	<b>Original data</b>	<b>Cluster at 98% SL</b>	
<b>No. of samples</b>	<b>144</b>	<b>30</b>	<b>15</b>
Aggregate type	0.000	0.030	0.354
Gradation	0.340	0.879	0.633
Specimen length	0.602	0.532	0.877
Polymer modification	0.003	0.688	0.190
AC type	0.263	0.539	0.056
AC content	0.000	0.534	0.543
Cooling rate	0.283	0.329	0.034

**c) Comparison of clusters for relaxation stress**

The different responses of relaxation stresses to variables in different clusters, as summarized in Table 4.37, resulted in findings as given below:

- Aggregate type again appears to be significant in clusters having more than 30 observations analyzed.

- The relaxation stress as a response variable gives insignificant probability values for gradation, specimen size, modification, asphalt type, asphalt contents and cooling rate for smaller clusters.

**Table 4.37- Relaxation stress response to experimental variables**

Variables	Original data	Cluster at 98% SL	
		144	30
Aggregate type	0.000	0.019	0.598
Gradation	0.002	0.371	0.334
Specimen length	0.647	0.936	0.762
Polymer modification	0.033	0.203	0.588
AC type	0.566	0.217	0.561
AC content	0.000	0.306	0.809
Cooling rate	0.241	0.487	0.321

**d) Comparison of clusters for transition temperature**

The responses of transition temperature in different clusters, as summarized in Table 4.38, provide the following findings:

- Aggregate type and asphalt content appear to be significant in originally unclustered data.
- The effect of modification is evident in the cluster having greater than 30 observations, while the group with 15 observations showed insignificant probability values.
- The transitions temperature as a response variable gives insignificant probability values for gradation, specimen, asphalt type, and cooling rate for all the clusters.

**Table 4.38- Transition temperature response in clusters**

Variables	Original data	Cluster at 98% SL	
		144	30
Aggregate type	0.000	0.124	0.740
Gradation	0.054	0.738	0.481
Specimen length	0.950	0.650	0.896

**Table 4.38 (continued)**

Polymer modification	0.000	0.050	0.436
AC type	0.731	0.246	0.493
AC content	0.002	0.442	0.645
Cooling rate	0.816	0.446	0.650

**e) Comparison of clusters for slope ( $\Delta S / \Delta T$ )**

The responses of slope in different clusters, as summarized in Table 4.39, provide the following inferences:

- Aggregate type, gradation, and asphalt content appear to be significant in originally unclustered data.
- The slope as a response variable gives insignificant probability values for modification, specimen size, asphalt type, and cooling rate for all the clusters.

**Table 4.39- Effect of variables on  $\Delta S / \Delta T$  of the mix**

Variables	Original data	Cluster at 98% SL	
		30	15
<b>No. of samples</b>	<b>144</b>	<b>30</b>	<b>15</b>
Aggregate type	0.000	0.148	0.880
Gradation	0.015	0.373	0.210
Specimen length	0.253	0.707	0.945
Polymer modification	0.665	0.217	0.954
AC type	0.688	0.014	0.392
AC content	0.000	0.490	0.206
Cooling rate	0.588	0.473	0.504

**f) Comparison of clusters for air voids**

The responses of air void in different clusters, as summarized in Table 4.40, provide the following conclusions:

- Aggregate type, gradation and asphalt type appear to be significant in clusters having more than 30 observations analyzed.
- The modification, specimen size and cooling rate in all the clusters are found to be insignificant.

- Asphalt content appears to be significant in the originally unclustered data.

**Table 4.40- Air voids probability results for variable in the clusters**

Variables	Original data	Cluster at 98% SL	
		30	15
<b>No. of samples</b>	<b>144</b>	<b>30</b>	<b>15</b>
Aggregate type	0.000	0.000	0.735
Gradation	0.006	0.007	0.563
Specimen length	0.813	0.105	0.317
Polymer modification	0.104	0.052	0.748
AC type	0.005	0.005	0.092
AC content	0.000	0.312	0.172
Cooling rate	0.539	0.059	0.832

**g) Comparison of clusters for eccentricity**

The responses in respect to eccentricity in various clusters, as summarized in Table 4.41, do not show any influence against any variables.

**Table 4.41- Eccentricity as a response for the clusters**

Variables	Original data	Cluster at 98% SL	
		30	15
<b>No. of samples</b>	<b>144</b>	<b>30</b>	<b>15</b>
Aggregate type	0.357	0.525	0.072
Gradation	0.351	0.091	0.130
Specimen length	0.849	0.768	0.090
Polymer modification	0.673	0.070	0.082
AC type	0.572	0.430	0.423
AC content	0.910	0.152	0.075
Cooling rate	0.152	0.583	0.335

**4.4.2. Statistical analysis of glass transition temperature from cluster analysis**

As used for the fracture data, the same type of analysis is performed here for the glass transition data obtained in this research. The similarity level for analysis here is 95%, in order to accommodate clusters having more than 10 observations. Table 4.34 presents a summary of clusters using the principal component analysis.

**a) Discussion on ANOVA for glass transition temperatures from clusters**

The ANOVA analyses summarized in Table 4.42 provides the following inferences:

- Aggregate type do not seem to have an effect on the glass transition temperature of the mixes. This finding is different from that of the original unclustered data, i.e., comprising of 36 observations.
- The modification, gradation, asphalt type, and asphalt content were found to have no influence on the glass transition temperature of the specimens as indicated by high probability values.

**Table 4.42- Probability values for glass transition response for clusters**

<b>Variables</b>	<b>Original data</b>	<b>Cluster at 95% SL</b>	
<b>No. of samples</b>	<b>36</b>	<b>13</b>	<b>10</b>
Aggregate type	0.036	0.453	0.569
Gradation	0.957	0.575	0.100
Polymer modification	0.339	0.488	0.080
AC type	0.535	0.542	0.098
AC content	0.517	0.564	0.147

**b) Discussion on ANOVA for thermal coefficients from clusters only**

The ANOVA analyses presented in Table 4.43 show that none of the variables is found to have influence on the glass transition coefficients.

**Table 4.43- Probability values for thermal transition coefficients**

<b>Variables</b>	<b>Original data</b>	<b>Cluster at 95% SL</b>	
	<b>Coefficients after glass transition temperature</b>		
<b>No. of samples</b>	<b>36</b>	<b>13</b>	<b>10</b>
Aggregate type	0.200	0.358	0.557
Gradation	0.533	0.513	0.691
Polymer modification	0.455	0.761	0.820
AC type	0.455	0.892	0.924
AC content	0.745	0.881	0.659

**Table 4.43 (continued)**

<b>Variables</b>	<b>Coefficients before glass transition temperature</b>		
Aggregate type	0.218	0.500	0.972
Gradation	0.711	0.378	0.591
Polymer modification	0.830	0.108	0.436
AC type	0.439	0.328	0.541
AC content	0.660	0.497	0.574

#### **4.5. Discriminant analysis**

Discriminant analysis is another technique related to the advanced statistical analysis tool and help to classify observations into two or more groups. In this study, the discriminant analysis resulted in 53 clusters for the fracture strength data and 3 clusters for the glass transition temperature data. The detailed ANOVA analysis was not performed for fracture strength because only two of the clusters have more than 10 observations which were also identical to the clusters (see clusters 1 and 2 in Table 4.34) already discussed in the previous section of this chapter. However, only ANOVA analysis for the glass transition temperature data is presented here.

##### **4.5.1. ANOVA for glass transition temperature of clusters from discriminant analysis**

As used for all the previous clusters, the same type of analysis is performed here for clusters from the discriminant analysis of the data obtained in this research.

##### **a) For glass transition temperature**

The ANOVA analyses summarized in Table 4.44 provides the following inferences:

- Aggregate type do not seem to have an effect on the glass transition temperature of the mixes. This finding is different from that of the original unclustered data, i.e., comprising of 36 observations.
- Only the asphalt type and asphalt content seem to have an effect on the glass transition temperature of the mixes in only one cluster. This finding is also different from that of the original unclustered data for 36 observations.

- The gradation and modification were found to have no influence on the glass transition temperature of the specimens as indicated by high probability values.

**Table 4.44- Probability values for glass transition temperature response for clusters**

Variables	Original data	Clusters for discriminant analysis		
		10	12	14
<b>No. of obs.</b>	<b>36</b>			
Aggregate type	0.036	0.573	0.877	0.605
Gradation	0.957	0.409	0.973	0.363
Polymer modification	0.339	0.547	0.993	0.786
AC type	0.535	0.846	0.053	0.428
AC content	0.517	0.968	0.019	0.204

**b) For thermal coefficients from clusters only**

The ANOVA analyses presented in Table 4.45 show that none of the variables is found to have influence on the thermal coefficients.

**Table 4.45- Probability values for thermal coefficients**

Variables	Original data	Clusters for discriminant analysis		
	Coefficients after glass transition temperature			
<b>No. of samples</b>	<b>36</b>	<b>10</b>	<b>12</b>	<b>14</b>
Aggregate type	0.200	0.899	0.358	0.186
Gradation	0.533	0.935	0.369	0.276
Polymer modification	0.455	0.569	0.711	0.683
AC type	0.455	0.857	0.436	0.622
AC content	0.745	0.757	0.333	0.473
Variables	Coefficients before glass transition temperature			
Aggregate type	0.218	0.373	0.430	0.653
Gradation	0.711	0.465	0.369	0.926
Polymer modification	0.830	0.979	0.761	0.215
AC type	0.439	0.769	0.540	0.611
AC content	0.660	0.769	0.388	0.763

#### 4.6. Regression analysis

All the clusters identified and discussed in Sections 4.5, 4.6 and 4.7 were then further analyzed for regression to find out the effective factors present either directly or indirectly in determining the response in respect to fracture strength, fracture temperature and glass transition temperature. Minitab 14® was used to perform the stepwise regressions.

In these analyses, multiplications and divisions of variables used in this study are also added as different independent variables to generate mathematical or statistical relationships. Since this procedure was found to be successful, other mathematical forms of the independent variables are not required to further study the interaction of factors between the variables.

The variables were coded in terms of (-1, 1) for two level factors and (-1, 1e-06, +1) for three level factors. It is to be noted here that for three levels factors, second level is defined by 1e-06 which can be assumed to be zero, but mathematically not. This value is taken for the new variables that were derived by dividing the existing variables to form new variables and which could have remained statistically undefined otherwise. Table 4.44 gives the list of coded variables used for performing the regression analysis by Minitab 14®.

**Table 4.46- Variable codes used in regression analyses**

S.no	Name of variable	Level	Uncoded	Coded
1	Aggregate type	2	L,B	+1,-1
2	Gradation	2	C, F	+1,-1
3	Specimen length	2	M, T	+1,-1
4	Polymer modification	2	S,Z	+1,-1
5	AC type	2	57,71	+1,-1
6	AC content	3	OP,O, OM	+1, E-06,-1
7	Cooling rate	3	-20,-10, -5	+1, E-06,-1

The regression step is further divided into two levels:

- Stepwise regression
- Standard regression

#### 4.6.1. Stepwise regression

In stepwise regression, all variables are studied at the same time either adding the most correlated to the least one by one or omitting the variables that are least significant. Alternatively, in each step, all the significant variables can be added or dropped based on the alpha values and a new regression equation is formed by calculating additional parameters for each case. The process is continued up to completion of this process. During this study, default alpha value of 15% was used to add or drop the variables.

The generated statistical models are evaluated according to their adjusted coefficients of determination ( $R^2$ -adjusted) and standard deviations (sd) of the models. As an optimum, models with minimum number of variables were used considering greater  $R^2$ -adjusted values and smaller sd values of the model.

A typical output of stepwise regression analysis for the selected clusters is shown in Table 4.47.

**Table 4.47- Typical output of stepwise regression analysis**

	Selected equations					
Variables	3	4	5	6	7	8
Constant	-17.02	-16.69	-16.72	-16.53	-16.83	-16.9
cool	2.37	2.81	2.56	2.25	2.24	1.96
T-Value	4.5	7.97	7.63	6.92	8.94	8.36
P-Value	0.001	0	0	0	0	0
aggr*modi	1.51	1.86	1.75	1.61	1.53	1.6
T-Value	3.47	6.38	6.73	6.89	8.32	10.76
P-Value	0.005	0	0	0	0	0

**Table 4.47 (continued)**

aggr*acgr	1.14	1.29	1.13	1.14	0.94	0.64
T-Value	2.68	4.7	4.46	5.25	5.09	3.21
P-Value	0.022	0.001	0.002	0.001	0.001	0.018
acgr*acc%		1.42	1.44	1.32	1.2	1.1
T-Value		4.12	4.77	4.94	5.67	6.38
P-Value		0.002	0.001	0.001	0.001	0.001
grde*acgr			-0.51	-0.7	-0.68	-0.72
T-Value			-1.99	-2.94	-3.71	-4.91
P-Value			0.077	0.019	0.008	0.003
size				-0.54	-0.74	-0.98
T-Value				-2.05	-3.37	-4.82
P-Value				0.074	0.012	0.003
size/acc%					0	0
T-Value					2.54	3.93
P-Value					0.039	0.008
size*modi						-0.48
T-Value						-2.28
P-Value						0.063
<b>sd</b>	<b>1.560</b>	<b>0.998</b>	<b>0.877</b>	<b>0.753</b>	<b>0.580</b>	<b>0.459</b>
<b>R-Sq</b>	<b>71.42</b>	<b>89.39</b>	<b>92.64</b>	<b>95.18</b>	<b>97.49</b>	<b>98.65</b>
<b>R-Sq(adj)</b>	<b>63.62</b>	<b>85.15</b>	<b>88.55</b>	<b>91.56</b>	<b>94.98</b>	<b>96.86</b>

Symbols used:

aggr\*grde; aggr\*size; aggr\*modi; aggr\*acgr; aggr\*acc; aggr\*cool; grde\*size; grde\*modi; grde\*acgr; grde\*acc%; grde\*cool;size\*modi; size\*acgr; size\*acc%; size\*cool;modi\*acgr; modi\*acc%; modi\*cool; acgr\*acc%; acgr\*cool; acc%\*cool  
aggr/grde; aggr/size; aggr/modi; aggr/acgr; aggr/acc%; aggr/cool;grde/size; grde/modi; grde/acgr; grde/acc%; grde/cool;size/modi; size/acgr; size/acc%; size/cool; modi/acgr; modi/acc%; modi/cool; acgr/acc%; acgr/cool; acc%/cool.

The stepwise regression analysis for the given data was performed using different variables on different clusters obtained at various similarity levels. The clusters giving maximum  $R^2$  values were selected as the final clusters for fitting the model. Table 4.48 illustrates the summary of the stepwise regression results for various groups for fracture strength and glass transition temperature data.

**Table 4.48- Output of stepwise regression analysis for fracture strength and glass transition temperature**

Description of cluster	No. of observations	Number of regression equations generated	
		FS	FT
<b>Fracture strength data</b>			
Cluster only	15	9	9
Cluster only	30	9	6
Cluster from PC Correlation	11	9	9
Cluster from PC Correlation	50	9	10
Cluster from PC Correlation	41	9	9
Cluster from PC Covariance	40	13	8
Cluster from PC Covariance	44	9	7
<b>Glass transition temperature data</b>		GT	
Cluster only	13	3	
Cluster only	10	8	
Cluster from PC Correlation	13	2	
Cluster from PC Correlation	10	1	
Cluster from discriminant analysis	10	5	
Cluster from discriminant analysis	12	8	
Cluster from discriminant analysis	14	4	

#### 4.6.2. Standard regression

As discussed before, a full regression model was developed for each of the clusters identified earlier. The coefficients for each of the variables are presented in Tables 4.49 - 4.50 for assessing the effectiveness of each of the variable identified.

##### a) Regression coefficients for fracture strength

The coefficients calculated through the regression analysis on the given clusters in order to evaluate fracture strength of the mixes are presented in Table 4.49.

**Table 4.49- Comparison of regression coefficients for fracture strength**

	Cluster		Principal components				
			Covariance		Correlation		
Cluster no	1	2	3	4	5	6	7
Variables	30	15	44	40	50	41	11
constant	3.1	3.79	2.93	3.33	3.3	2.87	2.69
aggr	0.238		0.65	0.627	0.729	0.683	
grde		0.328		0.536	0.408		
modi	-0.179						
acgr	-0.648		-0.158				0.0215
acc%							1.02
cool			0.229			0.281	
aggr*grde	-0.623		-0.746			-0.739	
aggr*size	0.128	0.183		0.218	0.197		
aggr*modi							0.0884
aggr*cool		-0.61	0.345		-0.28	0.598	
grde*acc%		-0.404		-0.381	-0.457		
grde*cool		-0.325	0.378			0.49	-0.246
size*modi				0.345			
size*acgr			0.35			0.552	-0.348
size*acc%	-0.523						
size*cool							-0.515
modi*acgr			-0.521	-0.332	-0.258	-0.562	
modi*acc%	0.486				-0.202		0.498
modi*cool	0.494	-0.208		0.265			
acgr*acc%						0.205	
acgr*cool							0.0698
acc%*cool		0.184		0.42	0.386		
aggr/acc%							-1e-06
aggr/cool			-1e-06	-1e-07			
<b>sd</b>	<b>0.472</b>	<b>0.131</b>	<b>0.579</b>	<b>0.450</b>	<b>0.626</b>	<b>0.5444</b>	<b>0.0083</b>
<b>R-Sq,%</b>	<b>84.3</b>	<b>98.4</b>	<b>79.2</b>	<b>87.8</b>	<b>75.9</b>	<b>83.7</b>	<b>100</b>
R-Sq(adj),%	<b>78.4</b>	<b>96.8</b>	<b>73.7</b>	<b>84.1</b>	<b>71.1</b>	<b>79.0</b>	<b>100</b>

The coefficients summarized in Table 4.49 present different effect of various variables on fractured strength in the following manner:

- Aggregate type is independently effective in all the clusters consisting more than 15 observations. Their combination with other variables also has considerable impacts upon the fracture strength of the mixes.
- Gradation is independently significant in 3 clusters. They also affect the fracture strength of the mixes in other clusters when combined with the other variables.
- Binder modification is independently effective in only one cluster, i.e., cluster 1). In the other 4 clusters, i.e., clusters 1, 2, 4, and 7, its influence on fracture strength results from a combination with the other variables.
- The asphalt grade is independently significant in 3 clusters. In all other clusters, except clusters 1 and 2, its influence on the fracture strength results from a combination with the other variables.
- The asphalt content is independently significant in only one cluster. It also influences the fracture strength of the mixes in 5 clusters when in combination with other variables.
- Specimen size does not, however, seem to be independently significant for the fracture strength of the mixes but appears to be important in 5 clusters when combined with the other 4 independent variables.
- Cooling rate is independently significant in two clusters. When combined with other variables, it also influences the fracture strength of the mixes.

#### **b) Regression Analysis for fracture temperature data**

The coefficients summarized in Table 4.50 present different impact of various variables on fractured temperature in the following manner:

- The aggregate type is independently significant in 4 clusters consisting more than 40 observations. Their combination with the other variables also have considerable impacts upon the fracture temperature of the mixes in all clusters.
- Gradation is independently significant in two clusters. They also affect the fracture temperature of mixes in other 5 clusters when combined with the other variables.

- Binder modification is independently significant in two clusters, i.e., clusters 4 and 5). In all the other 4 clusters, i.e., clusters 2, 4, 5 and 7, its influence on fracture temperature results from a combination with the other variables.
- Asphalt grade is independently significant in two clusters. It also influences fracture temperature in all clusters through interaction with the other variables.
- Asphalt content is independently significant in only one cluster. It also influences the fracture temperature of the mixes in 5 clusters in combination with the other variables.
- Specimen size is independently significant for fracture temperature of the mixes in one cluster. It also appears to be influential on fracture temperature in all the clusters through interaction with the other variables.
- Cooling rate is independently significant in two clusters, When combined with other variables, it also influences the fracture strength of the mixes in all clusters except cluster 2.

**Table 4.50- Coefficients of regression for fracture temperature in cluster group**

	Cluster		Principal components				
	1	2	Covariance		Correlation		
			3	4	5	6	7
Cluster no	30	15	44	40	50	41	11
constant	-14.3	-16.7	-15.8	-15.4	-15.6	-14.7	-14.9
aggr			-1.02	-1.91	-1.35	-1.36	
grde				-1.04	-0.745		
size		-0.837					
modi				1.21	1.23		
acgr				1.33	-0.813		
acc%							-2.27
cool		2.25		0.768			
aggr*grde	1.7		0.939			0.901	
aggr*size				0.683	-0.668		

**Table 4.50 (continued)**

aggr*modi		1.65					0.0987
aggr*acgr		0.789					0.551
aggr*cool				0.819	0.996		2.23
grde*size	-0.902					-0.667	
grde*modi							
grde*acgr		-0.58					
grde*acc%					0.747		
grde*cool	-1.02		-1.02			-0.956	
size*modi		-0.324			-0.836		-0.867
size*acgr			-1			-1.32	
size*acc%							
size*cool			-0.988			-0.954	
modi*acgr				1.09	0.539		
modi*cool							1.55
acgr*acc%	1.53	1.2					
acgr*cool							-0.181
acc%*cool			-1.05		-1.49	-0.91	
<b>sd</b>	<b>1.530</b>	<b>0.263</b>	<b>2.090</b>	<b>2.110</b>	<b>2.029</b>	<b>1.800</b>	<b>0.007</b>
<b>R-Sq</b>	<b>70.9</b>	<b>99.6</b>	<b>56.2</b>	<b>64.0</b>	<b>70.6</b>	<b>74.7</b>	<b>100</b>
<b>R-Sq(adj)</b>	<b>63.3</b>	<b>99</b>	<b>47.7</b>	<b>54.7</b>	<b>63.1</b>	<b>67.4</b>	<b>100</b>

**c) Regression analysis for glass transition temperature data**

The coefficients summarized in Table 4.51 present different impact of various variables on the glass transition temperature in the following manner:

- Aggregate types is influential in only one of the cluster . When combined with the other variables it also has considerable impacts upon the glass transition temperature of the mixes in 5 other clusters.
- Gradation has no influence in combination with the other variables in two clusters (6G and 7G) , however, appears to be influential for the glass transition temperature of the mixes.
- Binder modification is independently influential in 4 clusters, i.e., clusters 1G, 2G, 4G and 5G. In 5other clusters, i.e., clusters 1G, 3G, 5G, 6G and

7G, its influence on glass transition temperature results from a combination with the other variables.

- Asphalt grade is independently influential in two clusters . Its influence on glass transition temperature results from a combination with the other variables in 6more clusters.
- Asphalt content is independently influential in 3 clusters. It also influences the glass transition temperature of the mixes in 5 more clusters when in combination with other variables.

**Table 4.51- Comparison for glass transition temperatures**

Cluster no	Cluster		Principal components		Discriminant analysis		
	1G	2G	3G	4G	5G	6G	7G
<b>Variables</b>	<b>13</b>	<b>10</b>	<b>13</b>	<b>10</b>	<b>14</b>	<b>12</b>	<b>10</b>
constant	-21.00	-26.00	-24.90	-25.50	-20.70	-26.50	-33.40
aggr							0.78
modi	0.55	-0.55		5.15	0.47		
acgr		0.58				0.59	
acc%		-0.140	-3.49			-0.70	
aggr*grde							0.74
aggr*modi						-0.08	
aggr*acc%	-1.06	0.47			-1.19	0.29	-1.60
grde*acc%						0.24	
modi*acgr	-0.57		2.31		-0.84		-0.45
modi*acc%					0.55	0.68	
modi*cool							
acgr*acc%		0.28					
aggr/acc%							-1e-07
grde/acc%						-1e-07	
acgr/acc%		0.00				-1e-07	
<b>Sd</b>	<b>0.83</b>	<b>0.05</b>	<b>3.84</b>	<b>2.97</b>	<b>0.86</b>	<b>0.07</b>	<b>0.25</b>
<b>R-Sq</b>	<b>66.9</b>	<b>99.9</b>	<b>51.3</b>	<b>75.9</b>	<b>77.4</b>	<b>99.9</b>	<b>98.9</b>
<b>R-Sq(adj)</b>	<b>55.9</b>	<b>99.80</b>	<b>41.5</b>	<b>72.9</b>	<b>67.4</b>	<b>99.7</b>	<b>97.5</b>

#### 4.7. Statistical modeling

Statistical models were obtained by evaluating the clusters already discussed in Sections 4.5-4.7. These models are in the form of separate regressed equations for fracture strength, fracture temperature and glass transition temperature. The selection criteria for finding these models is a two-step process: the presence of the highest number of clusters from one particular group, i.e., clusters from PC correlations for fracture strength data and clusters from the discriminant analysis for glass transition temperature data, and evaluation of the sensitivity by the performance of the standard regression parameters in terms of standard deviations, coefficient of determination ( $R^2$ ) values and R-square adjusted values. Hence, for each category, three most acceptable equations were selected with their corresponding clusters (see equation 4.3-4.11). These models are presented in the following sections in terms of fracture strength, fracture temperature and glass transition measurement.

##### 4.7.1. Statistical model for fracture strength

From the regression coefficients presented in Table 4.49, clusters 5-7 derived from the principal component analysis represents the best combination of variables along with adequate statistical parameters. The statistical model thus derived for the prediction of fracture strength is being presented in the form of Equations 4.3 thru 4.5.

$$\begin{aligned} FS = & 3.30 + 0.729 \text{ aggr} - 0.258 \text{ modi*acgr} - 0.457 \text{ grde*acc\%} + 0.408 \\ & \text{grde} + 0.386 \text{ acc\%*cool} - 0.280 \text{ aggr*cool} + 0.197 \text{ aggr*size} - \\ & 0.202 \text{ modi*acc\%} \end{aligned} \quad (4.3)$$

$$\begin{aligned} FS = & 2.87 + 0.683 \text{ aggr} - 0.739 \text{ aggr*grde} - 0.562 \text{ modi*acgr} + 0.552 \\ & \text{size*acgr} + 0.490 \text{ grde*cool} + 0.598 \text{ aggr*cool} + 0.281 \text{ cool} + 0.205 \\ & \text{acgr*acc\%} - 0.000001 \text{ aggr/cool} \end{aligned} \quad (4.4)$$

$$\begin{aligned} FS = & 2.69 + 0.498 \text{ modi*acc\%} + 1.02 \text{ acc\%} - 0.000002 \text{ aggr/acc\%} - 0.515 \\ & \text{size*cool} - 0.348 \text{ size*acgr} - 0.246 \text{ grde*cool} + 0.0884 \text{ aggr*modi} + \\ & 0.0689 \text{ acgr*cool} + 0.0215 \text{ acgr} \end{aligned} \quad (4.5)$$

where

FS= fracture strength of mix in MPa; aggr:aggregate type; grde; gradation; size:Specimen size; acgr:asphalt type; modi:modification; acc %:asphalt cement content; and cool: cooling rate.

The equations explain that aggregate type, gradation, and asphalt type either independently or in combination are important for determining the fracture strength of asphalt concrete mixes. The equations offer a neat presentation of the existence of all the variables studied here for essential factors determining the low temperature cracking potential of asphalt concrete mixes. Figure 4.2, presents the line of equality plot between the predicted and the original values. Table 4.52 summarizes the statistical parameters associated with these models.

**Table 4.52- Statistical parameters for fracture strength models**

<b>Cluster</b>	<b>sd</b>	<b>R<sup>2</sup></b>	<b>R<sup>2</sup>adj</b>	<b>Equation</b>
5	0.626	76	72	4.3
6	0.544	84	79	4.4
7	0.008	100	100	4.5

Since all three models are plotted in one figure, it can be observed that cluster 5 has more deviation as compared to the other cluster plotted, which is understandable because of its higher standard deviation as illustrated in Table 4.52. According to NCHRP 465, (2002) any R<sup>2</sup> value >60% is considered as 'fair' keeping this in mind all the models described here are acceptable and seem to be reasonable for predicting the fracture strength of the mixes.

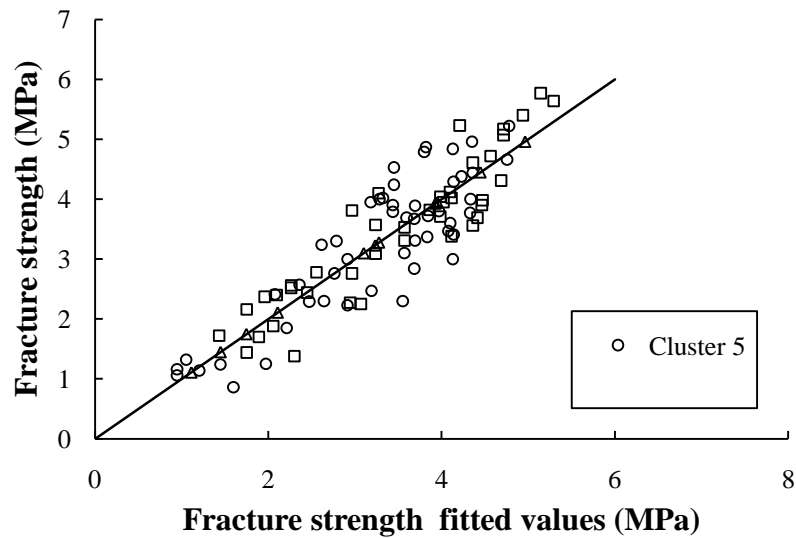


**Figure 4.2- Line of equality plot for fracture strength**

#### **4.7.2. Statistical model for fracture temperature**

The regression equations derived for the prediction of fracture temperature are given in Equations 4.6 thru 4.8. The criteria for the selection of the equations were the same as or the case of regression equations for fracture strength.

$$\begin{aligned}
 FT = & -15.6 - 0.836 \text{ size} * \text{modi} + 1.23 \text{ modi} - 1.35 \text{ aggr} + 0.813 \text{ acgr} + \\
 & 0.747 \text{ grde} * \text{acc\%} - 1.49 \text{ acc\%} * \text{cool} - 0.745 \text{ grde} + 0.996 \text{ aggr} * \text{cool} - 0.668 \\
 & \text{aggr} * \text{size} + 0.539 \text{ modi} * \text{acgr}
 \end{aligned} \tag{4.6}$$

$$\begin{aligned}
 FT = & -14.7 - 1.36 \text{ aggr} + 0.901 \text{ aggr} * \text{grde} - 0.667 \text{ grde} * \text{size} - 0.956 \\
 & \text{grde} * \text{cool} - 1.32 \text{ size} * \text{acgr} - 0.954 \text{ size} * \text{cool} - 0.910 \text{ acc\%} * \text{cool} + \\
 & 0.000002 \text{ aggr} / \text{acc\%} + 0.000001 \text{ aggr} / \text{cool}
 \end{aligned} \tag{4.7}$$

$$\begin{aligned}
 FT = & -14.9 - 2.27 \text{ acc\%} + 2.23 \text{ aggr} * \text{cool} + 1.55 \text{ modi} * \text{cool} + 0.000003 \\
 & \text{aggr} / \text{acc\%} - 0.867 \text{ size} * \text{modi} + 0.551 \text{ aggr} * \text{acgr} + 0.000000 \text{ aggr} / \text{cool} - \\
 & 0.181 \text{ acgr} * \text{cool} + 0.0987 \text{ aggr} * \text{modi}
 \end{aligned} \tag{4.8}$$

where

FT:fracture temperature; aggr:aggregate type; grde: gradation; size:specimen size; acgr:asphalt type; modi:modification; acc %:asphalt cement content; and cool: cooling rate.

Similar to the case of regression equations for fractured strength, the equations for fracture temperature as presented in Equations 4.6 thru 4.8 also explains that aggregate type, gradation, asphalt grade, asphalt content, and no modification, either independently or in combination, are important for determining the fracture temperature of asphalt concrete mixes. Further, it concludes that all the variables studied here are equally important to influence the low temperature cracking performance of mixes. None of the experimental variables can be singled out to produce this influence.

**Table 4.53- Statistical parameters for fracture temperature**

<b>Cluster</b>	<b>sd</b>	<b>R<sup>2</sup></b>	<b>R<sup>2</sup>adj</b>	<b>Equation</b>
5	2.029	71	63	4.6
6	1.800	75	67	4.7
7	0.007	100	100	4.8

The plots for fitted data are illustrated in the Figure 4.3 while the statistical parameters for the regression equations are presented in Table 4.53. In this plot, the best estimation is provided by cluster 7 having the least standard deviation while cluster 5 gives higher standard deviation but an acceptable coefficient of determination R<sup>2</sup> value.

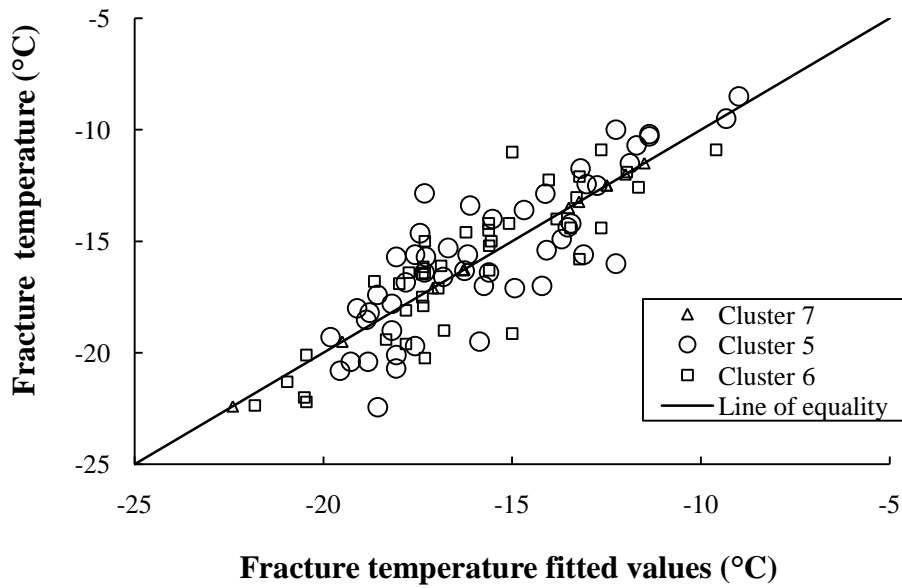


**Figure 4.3- Line of equality plot for fracture temperature**

#### **4.7.3. Statistical model for glass transition temperature**

The regression equations derived for the prediction of glass transition temperature is given in Equations 4.9 thru 4.11. The criteria for the selection of the equations were the same as for the regression equations for fracture strength and fracture temperature. The regression equations are given as follows:

$$GTT = -20.7 - 1.19 \text{ aggr} * \text{acc\%} - 0.844 \text{ modi} * \text{acgr} + 0.549 \text{ modi} * \text{acc\%} + 0.466 \text{ modi} \quad (4.9)$$

$$GTT = -26.5 - 0.702 \text{ acc\%} - 0.000000 \text{ grde} / \text{acc\%} + 0.291 \text{ aggr} * \text{acc\%} + 0.242 \text{ grde} * \text{acc\%} - 0.000000 \text{ acgr} / \text{acc\%} - 0.0784 \text{ aggr} * \text{modi} + 0.683 \text{ modi} * \text{acc\%} + 0.585 \text{ acgr} \quad (4.10)$$

$$GTT = -33.4 + 0.777 \text{ aggr} - 1.60 \text{ aggr} * \text{acc\%} + 0.744 \text{ aggr} * \text{grde} - 0.446 \text{ modi} * \text{acgr} - 0.000001 \text{ aggr} / \text{acc\%} \quad (4.11)$$

where

GTT:glass transition temperature; aggr:aggregate type; grde: gradation; size:specimen size; acgr:asphalt type; modi:modification; acc %:asphalt cement content; and cool: cooling rate.

The regression equations 4.9 thru 4.11 also shows that aggregate type, asphalt grade and modification are important parameters to influence the glass transition temperature of mixes. The fitted data to the regression models are illustrated in the Figure 4.4 and the statistical parameters for the regression equations are presented in Table 4.54. All clusters yield good models for the prediction of glass transition temperature as can be observed from the quality of fit to the line of equality in Figure 4.4 and from the corresponding  $R^2$  values in Table 4.54.

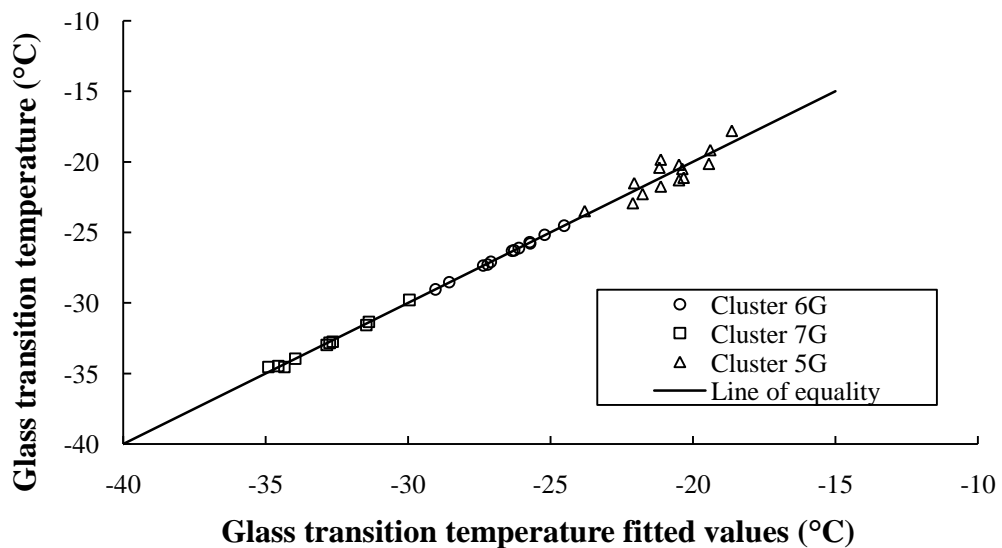


**Table 4.54- Statistical parameters for glass transition temperature**

<b>Cluster</b>	<b>sd</b>	<b>R<sup>2</sup></b>	<b>R<sup>2</sup>adj</b>	<b>Equation</b>
5G	0.860	77	67	4.9
6G	0.070	100	100	4.10
7G	0.250	99	98	4.11

**4.8. Parametric study of statistical models**

In the present study, because of the confounding technique used all possible combinations could not be tested, hence by using the mathematical models presented in Equations 4.3 thru 4.11, parametric studies of the model were carried out in order to find the values for fracture strength, fracture temperature and glass transition temperature. The analysis also helped to infer the behavior of mixes in response to changes in the variables that are studied. For this purpose, a total of  $2^5 \times 3^2 = 288$  combinations were examined and the values for fracture strength, fracture temperature and glass transition temperature were calculated. For identification purposes, a combination of seven digits variable was formulated Figure 4.5.

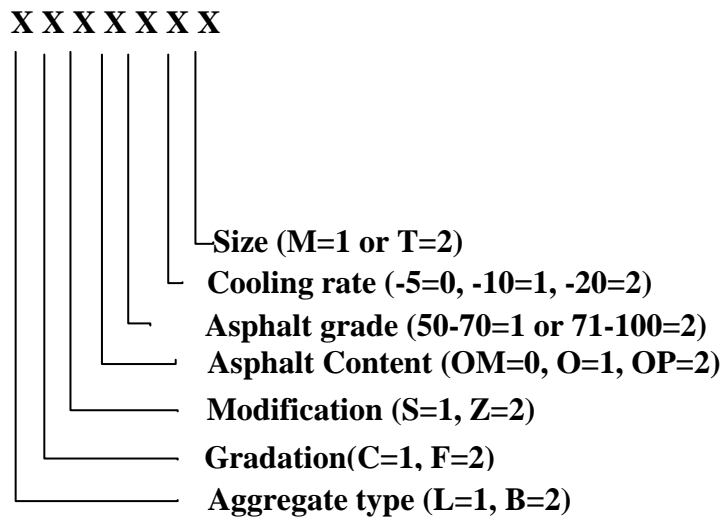


**Figure 4.5- Identification code for sample combination for parametric studies**

Hence all the possible mix combinations were coded in the form of seven digits as described in Figure 4.5. The equations derived from clusters having similar coding combinations were used to find the respective values of fracture strength, fracture temperature and glass transition temperature. These values are presented in the form of tables in Appendix G and in the form of plots in Figure 4.6 thru 4.8. These figures are plotted using line plots having two vertical axes the left axis for fracture strength and right axis either for fracture temperature or glass transition temperature. and one horizontal axis representing material combination responsible for producing the values for dependent variables. Each of the figures drawn separately shows how the change in material combination affects the dependent variables of the mix and if one of the dependent variables are chosen for one set of material combination what would be the predicted values of other dependent variables.

Figure 4.6 is a plot showing the variation of fracture strength against various untested material combinations and also it illustrates the corresponding values of fracture temperature and glass transition temperature of the mix. From Figure 4.6, it can be inferred that the maximum value of fracture strength can be obtained by using LCZ71OP20M (limestone aggregate having coarse gradation with no modification at asphalt content 0.5% more than the optimum), would result in fracture temperature of  $-16.164^{\circ}\text{C}$  and glass transition temperature  $-20.98^{\circ}\text{C}$  (see Figure 4.6). On the contrary, the smallest values of fracture strength and fracture temperature are obtained by using BFZ71O10T, even though it resulted in desirable glass transition temperature value (Table 4.55). These results substantiate the importance of aggregate type in the mix and a proper combination of material for better resistance to low temperature cracking. The figure also shows the trend in which fracture temperatures are always above the glass transition temperatures, which makes sense since the asphalt concrete always fail before the glass transition temperature is reached.

The Figure 4.7 illustrates the change in values of fracture temperature against material combination. By just looking at the labels in the figure, fracture temperature has a

maximum value of  $-24.11^{\circ}\text{C}$  for LCS71OP10M which also corresponds to fracture strength of 3.95 MPa and glass transition temperature of  $-25.44^{\circ}\text{C}$ . On the extreme right of the figure the corresponding values of fracture temperature, fracture strength and glass transition temperature are  $-10.43^{\circ}\text{C}$ , 1.76 MPa and  $-27.89^{\circ}\text{C}$  for material combination BFS71OM20M.

The value of glass transition temperature in ascending order is shown in Figure 4.8. The figure shows an optimum value of glass transition temperature as  $-41.37^{\circ}\text{C}$  with the corresponding fracture strength value of 2.00 MPa and fracture temperature value of  $-16.98^{\circ}\text{C}$  obtained from BCZ71O20T, while the lowest values are obtained from BFS71OP10M. Contrary to the previous findings, , now the basalt mixes will take more time to reach the fracture strength than the limestone mixes. But the values of fracture strength and fracture temperature are very less to show the validity of this inference.

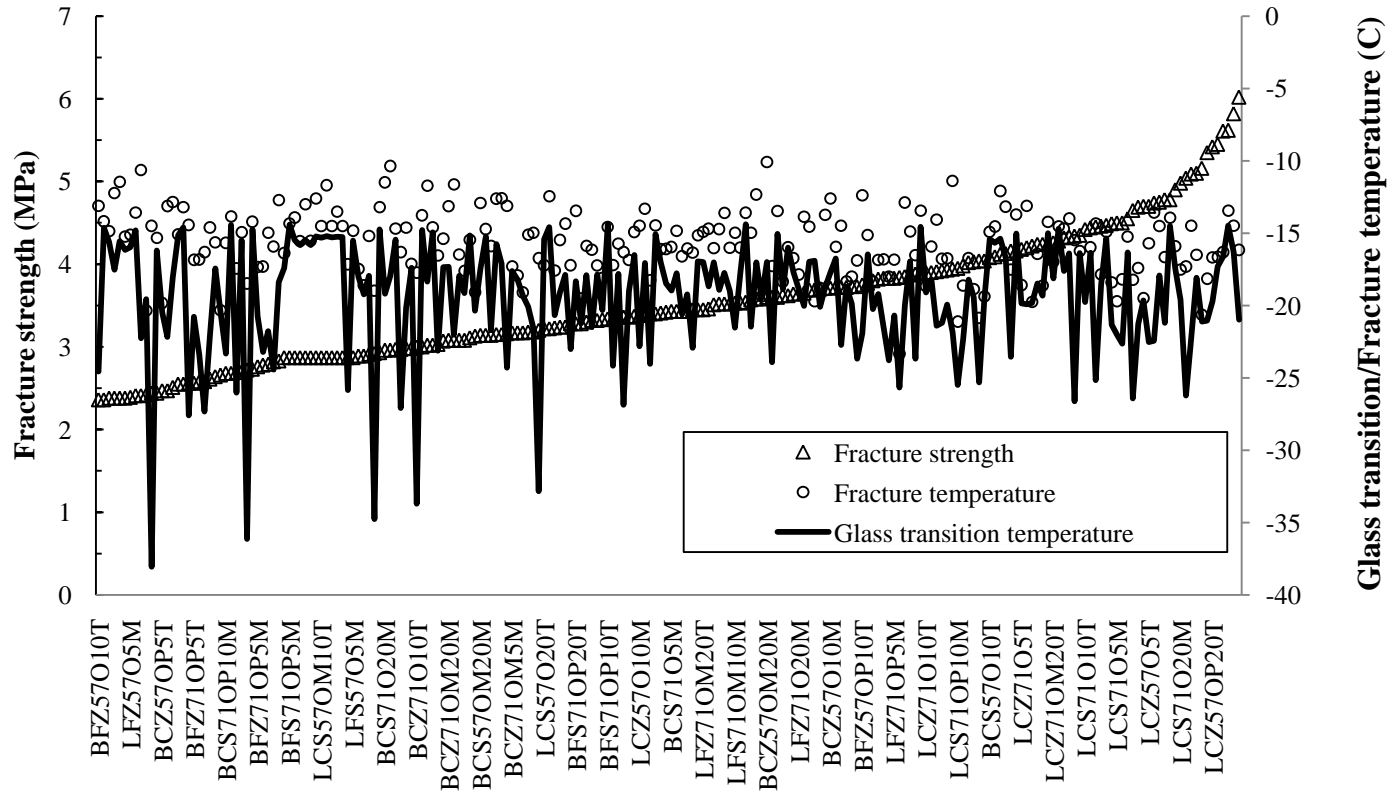


Figure 4.6- Fracture strength for samples not tested

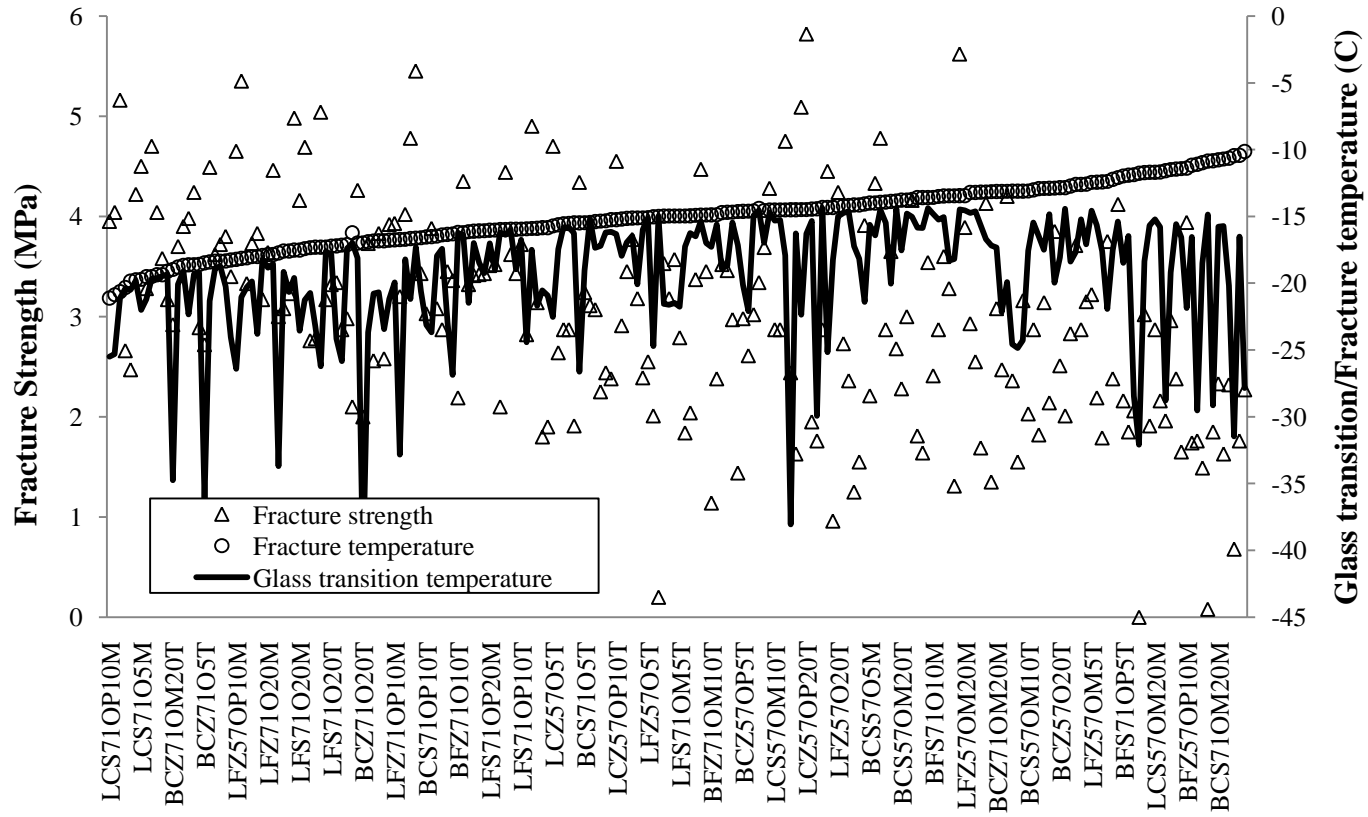


Figure 4.7- Fracture temperature for samples not tested

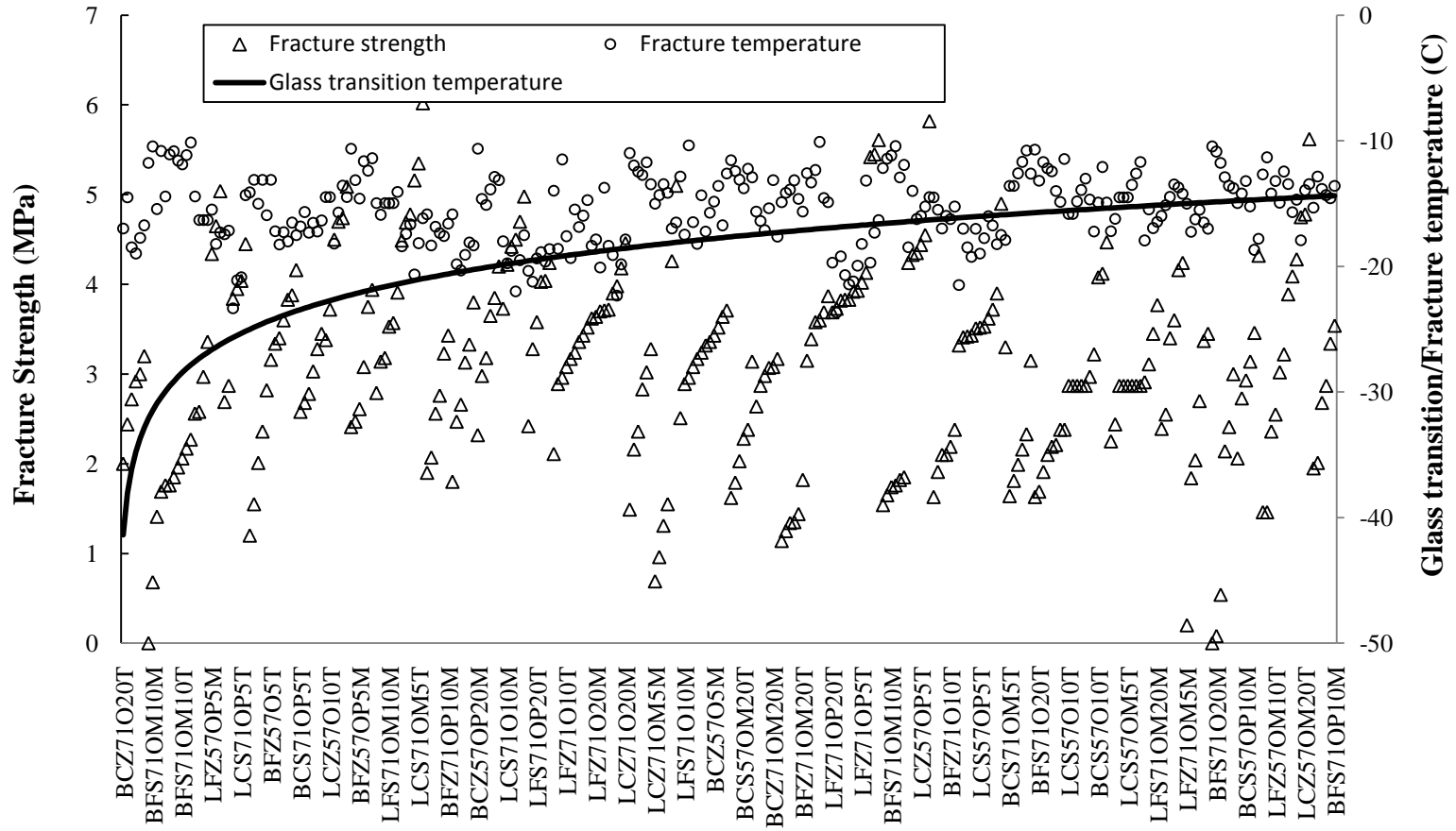


Figure 4.8- Glass transition temperature for samples not tested

## CHAPTER 5

### CONCLUSIONS AND RECOMMENDATIONS

#### 5.1. Introduction

This chapter summarizes the findings of this study and recommends steps to help the future researchers in pavement engineering for developing new research methodologies. It should be kept in mind that even though the technique adopted for testing statistical analysis was highly innovative and universal, the summarized results shown may vary depending on the experimental program used, materials selected for fabricating test specimens, and test procedures and conditions.

#### 5.2. Conclusions

In this experimental program, 144 prismatic beam specimens were tested for fracture strength using the TSRST equipment. All data about the experimental parameters were treated as independent variables while the data about the fracture strength, fracture temperature, transition temperature, relaxation stress, stress-temperature slope ( $\Delta S/\Delta T$ ), air voids and eccentric deviation were treated as dependent variables. The measured number of variables for glass transition temperature was smaller as compared to those for fracture strength tests studied in this research. The two independent variables that are not included in the glass transition temperature measurements were the specimen size and the cooling rate. The length of all the test specimen was selected 30 cm and a constant rate of cooling of  $-1^{\circ}\text{C}/\text{min}$  was maintained for all the 36 test specimens. The results were analysed by both ANOVA and cluster analysis techniques to identify which factors and design parameters are important in determining the fracture resistance of asphalt concrete at low temperatures. The findings of the study can be summarized as follow:

1. Aggregate type proved to be an important contributor in determining low temperature resistance of asphalt concrete mixtures in this study. Limestone mixes

showed higher fracture strength and lower fracture temperature as compared to mixes fabricated with basalt aggregate. The reason might be the difference between the two aggregates in terms of surface texture and aggregate shape that affect the bonding strength of binder. Since it is desirable for asphalt concrete mixes to sustain higher tensile stresses and lower climatic temperatures; therefore, the mixes having limestone seem to be preferable against the mixes with basalt aggregate.

2. The mixes having coarse gradation showed better performance in low temperature cracking as compared to mixes having fine gradation suggesting that the mixes should preferably be made with coarse gradation to resist low temperature cracking.
3. The asphalt content played an important role on the dependent variables and the outcomes of this study. The mixes having optimum asphalt content resulted in higher fracture strength and lower fracture temperature values as compared to mixes having less than or more than optimum asphalt content.
4. The ANOVA outcomes were highly significant for air void contents and it seemed to be correlated very well with all the dependent variables.
5. Even though smaller specimens resulted in higher fracture strengths and lower fracture temperatures in the TSRTS, analyses results were, however, not statistically significant ( $p > 0.05$ ). This may be because of the heterogeneity of asphalt mixes that caused large variability in the test results.
6. The cooling rate did not affect low temperature cracking of test mixtures.
7. The results of ANOVA analysis for eccentricity were insignificant and did not show any correlation with the dependent variables. This suggests that the tech-

nique used in centring and preparing test specimen before testing was achieved successfully.

8. The glass transition temperature of mixtures ranged -18 between -37° C showing variations for type of aggregates, gradation, asphalt content and type of modifier used. Based on these findings, it was assumed that mixtures with limestone aggregate could sustain lower pavement temperature without fracture and the development of thermal stress will be slower within the  $T < T_g$  range given with smaller thermal coefficient of 1.15. However, once the glass transition temperature exceeded, a more brittle behaviour was evidenced by a higher thermal coefficient of 7.03. The presented results can be used to compare thermal properties of two mixtures prepared by limestone and basalt aggregates; however, a detailed investigation is still recommended using a larger data set to reach concluding results.
9. The impact of asphalt type on glass transition temperature was found to be statistically insignificant in the ANOVA analyses. However, in the statistical modelling, asphalt type seemed to be one of the components contributing to glass transition temperature. This may suggest that there were some groups within the data that indicate the influence of asphalt type on glass transition temperature.
10. Statistical modeling technique adopted in this research was effective for analyzing the data and deriving a statistical model. The model was successfully calibrated to the test results to estimate fracture strength, fracture temperature and glass transition temperature. Based on the model results, some of the statistically insignificant factors, i.e., binder modification and asphalt type were found to be significant and contributing factors when subjected to cluster analysis. This highlights the importance of application of clustering technique to large set of experimental data.
11. The common factor identified in the derived models are aggregate type, mix gradation, asphalt type and asphalt cement content which are acting independ-

ently and in combination with other factors on the strength and fracture temperature of mixes. These findings support the results of multivariate ANOVA about the significance of these factors for different mix configurations.

### **5.3. Recommendations for future work**

The following recommendations for future studies can be made based on the outcomes of this study:

1. There is a need for using performance graded binders in place of penetration grading which seems to have deficiencies to determine low temperature potential of asphalt concrete. This conclusion is reached by the fact that the asphalt binders selected in the testing program according to penetration grading did not show any statistical significance in the test outcomes.
2. It should be emphasized that the cooling rate does not seem to be a significant factor low temperature cracking properties of asphalt concrete. Therefore, large number of specimens can be tested in a short time period by using cooling rate of  $-10^{\circ}\text{C/h}$  which will significantly save testing time. Alternatively, TSRST can be conducted at a slower cooling rate to utilize the cooling device instead of liquid nitrogen to reduce the testing cost.

## REFERENCES

American Association of State Highway and Transportation Officials(AASHTO), AASHTO R 35-‘Standard Test Method for Superpave Volumetric design for Hot Mix Asphalt’

American Association of State Highway and Transportation Officials (AASHTO), AASHTO T 166 ‘Standard Test Method for Bulk Specific Gravity Determination of Asphalt mixtures using Saturated Surface -Dry specimens’ -Method A.

American Association of State Highway and Transportation Officials (AASHTO), AASHTO T 209 -‘Standard Test Method for Theoretical Maximum Specific Gravity and Density of Bituminous Paving Mixtures’.

American Association of State Highway and Transportation Officials (AASHTO), AASHTO T 312-‘Standard Test Method for Preparing and Determining the Density of Hot Mix Asphalt by means of the Superpave Gyrotory Compactor’.

American Association of State Highway and Transportation Officials (AASHTO), AASHTO TP 10-07 ‘Standard Test Method for Thermal Stress Restrained Specimen Tensile Strength (TSRST) ’.

American Association of State Highway and Transportation Officials (AASHTO) AASHTO TP 63-03 ‘Standard Method of Test for determining Rutting Susceptibility of Asphalt Paving Mixtures Using the Asphalt Pavement Analyzer (APA)

Arand, W. (1987).’Influence of bitumen hardness on the fatigue behavior of asphalt pavements of different thickness due to bearing capacity of subbase, traffic loading, and temperature’, *Proceedings of Sixth International Conference on Structural Behavior of Asphalt Pavements*, University of Michigan, Pages. 65-71

ASTM D7405 - 10a Standard Test Method for Multiple Stress Creep and Recovery (MSCR) of Asphalt Binder Using a Dynamic Shear Rheometer

Bahia, H. U., & Anderson, D. A. (1993). ‘ Glass Transition Behavior and Physical Hardening of Asphalt Binders’, *Journal of the Association of Asphalt Paving Technologists*, V. 62-93, pp. 93–129.

Biran, A. & Breiner, M.(2002). ‘MATLAB 6 for Engineers’, *3<sup>rd</sup> Edition, Prentice hall publication*, Great Britain.

Bonnaure,F., Gravouts, A. & Udron, J.(1977). ‘A New Method of Predicting The Stiffness of Asphalt Paving Mixtures’, *Proceeding Association of Asphalt Paving Technologies*, Volume 46, pp 64-100.

Breen,J.J. & Stephens, J.E.,(1967). ‘The Glass Transition Temperature and Mechanical Properties of Asphalt’, *Annual Conference of Canadian Technical Asphalt Association*. Total pp 14.

Centria (2009), ‘Opening the door, walking outside, A 365 day blogging promise to spend time each day in the great outdoors’.

<http://centria.wordpress.com/2009/04/>

Last updated:January 2010

Chehab, G. R., and Y. R. Kim (2005), ‘Viscoelastoplastic Continuum Damage Model, a publication to Thermal Cracking of Asphalt Concrete’, *Journal of Materials in Civil Engineering, ASCE*, Volume 17, No. 4, pp. 384–392.

Dongré, R. (2007) ‘Low Temperature cracking’, *Norwegian Association of Asphalt*  
[http://www.norskasfaltforening.com/FaggruPageser/NABin/1836/LowTemperatureCracking\\_Norway.pdf](http://www.norskasfaltforening.com/FaggruPageser/NABin/1836/LowTemperatureCracking_Norway.pdf)

Last updated: 28 October 2010

Drüschner, L., Hagner, T., Harders, O., and Stephan, F. (2004). 'Contribution of aggregate quality on crack formation of wearing courses', *Proceedings of Fifth International RILEM Conference on Reflective Cracking in Pavements*, Limoges, France, pp. 257-264.

Epps, A. (1998). 'A Comparison of Measured and Predicted Low Temperature Cracking Conditions', *Association of Asphalt Paving Technologies*, Volume 67, pp. 277-310.

Fakhri, M . & Mahmood, N. (2006), 'Resistance of large stone asphalt mixes to rutting', *22<sup>nd</sup> ARRB Conference Research into Practice*, Canberra, Australia, pp 1-12.

Finn, F., C.L. Saraf, R. Kulkarni, K. Nair, W. Smith, and A. Abdullah. (1986). 'Development of pavement structural subsystems', NCHRP 291.

FHWA(1998). 'Accelerating Infrastructure Innovations'  
<http://www.fhwa.dot.gov/publications/focus/98dec/index.cfm>  
Site updated: 11 June 2010

Haas, R., Meyer, R. Assaf, G., Lee, H., (1987). 'A comprehensive study of cold climate Airport Pavement Cracking', *Journal of Association of Asphalt Paving Technologists*. Volume 56, Research Board, Washington, D.C.-USA, pp. 198-245.

Ho, S. & Zanzotto, L. (2005). 'The low temperature properties of conventional and Modified asphalt binders evaluated by failure energy and secant modulus from direct tension test', *Materials and Structures*, Volume 38 , pp. 137-143.

Jones, G.M., Darter, M.I., and Littlefield, G.( 1968). ' Thermal expansion–contraction of asphalt concrete', *Asphalt Paving Technology, Proceedings of the Association of Asphalt Paving Technologists*, 37 pp. 57–100.

Jongepier, R & Kuilman, B (1969). 'Characteristics of the rheology of bitumens', *Proceedings of the Association of Asphalt Paving Technologists*, Volume 38, pp. 98.

Jung, D.H. & Vinson, T.S. (1994). 'Low temperature cracking: Test selection' Report No SHRP-A-400, *Strategic Highway Research Programme*, National Research Council, Washington, D.C.

Kanerva, H., Vinson, T. S., & Zeng, H., (1994). 'Low-Temperature Cracking: Field Validation of Thermal Stress Restrained Specimen Test', SHRP-A-401, *Strategic Highway Research Program*, National Research Council, Washington, D.C.-USA.

King, G. N., King, H.W., Harders, O., Orand, W. & Planche, P. (1993) 'Influence of AC type and polymer concentration on the low temperature cracking performance of polymer modified asphalt', *Proceeding Association of Asphalt Paving technology* No.62, pp 1-22.

Kliwer, J. E. & Zeng, H. (1996. ). 'Aging and low temperature cracking of asphalt concrete mixtures,' *Journal of Cold Regions Engineering*, Volume 10, No. 3, pp. 134-148.

Lee, S.Q.S, Vanbarnveld, A. & Corbert, M.A.(2009). 'Low temperature cracking performance of Superpave and cold in-place recycled pavements in Ottawa-Carleton', *Environment and Transportation*, Department Regional Municipality of Ottawa-Carleton Ottawa, Ontario, pp. 21.

Lytton, R.L., Shanmugham, U. & Garrett, B. (1983). 'Design of flexible pavements for thermal fatigue cracking', *Research Report No. FHWA/TX-83/06+284-4*, Texas Trans. Inst., Texas A&M University

Marasteanu, M., (2004). 'Low temperature Fracture test for Asphalt mixtures', *Proceedings of Fifth International RILEM conference on cracking in Pavements held on 5-7 May 2004*, Limoges, France, pp 249-256

Meyer R. & Krueger D.(1998) ‘A Minitab guide to Statistics’, *Prentice Hall publishers*, Great Britain.

Mouillet, V., Molinengo, J. C. , Durrieu, F. & Planche, J.P. (2004). ‘Effect of aging on Low temperature cracking properties of bituminous binders: New insight from BBR measurements’, *Proceedings of Fifth International RILEM Conference on Reflective Cracking in Pavements*, Limoges, France, pp. 351-358

Nam, K.(2005) ‘Effects of Thermo volumetric properties of modified asphalt mixtures on low temperature cracking’, *Ph.D. Dissertation*, University of Wisconsin, pp.1-162.

Nam, K. & Bahia, H.U. (2005). ‘Measuring and predicting thermally induced stresses in modified asphalt mixtures’. Paper No: 05-2425, *Transportation Research Board, 84th Annual Meeting*, National Research Council, Washington, D.C.

Nam, K. & Bahia, H.U. (2009. ) ‘Effect of Modification on Fracture Failure and Thermal-Volumetric Properties of Asphalt Binders’, *Journal of Materials in Civil Engineering*, pp.198-209

National Cooperative Highway Research Program, NCHRP (2003) ‘Simple performance test for superpave mix design’, *NCHRP 9-19*, Interim Rep., National Research Council.

National Cooperative Highway Research Program, NCHRP (2002). ‘Simple Performance test for Superpave mix design’, *Report 465*.National Cooperative Highway Research Program, National Academic press-Washington DC -2002

NIST-Statistical Handbook

<http://www.itl.nist.gov/div898/handbook/pri/section3/pri3381.htm>

Site updated-23 June 2010

North Central Superpave Center Facilities

<https://engineering.purdue.edu/NCSC/about/facilities.htm>

Last visited: 01 December 2010

Papagiannakis, A.T. & Masad, E.A. (2007). 'Pavement Design and Materials', *Published by John Wiley & Sons*.

Pellinen, T. K., & Xiao S., (2006). 'Stiffness of Hot-Mix Asphalt', *Final Report*, Joint Transportation Research Program, pp 1-405.

Product data sheet, Sikadu-31, 2 part thixotropic adhesive

Qudais, S.A., & Shweily, H. A. (2007) 'Effect of aggregate properties on asphalt mixtures stripping and creep behavior', *Construction and Building Materials*, V.21, Issue 9, pp. 1886-1898.

Roberts, F., Kandhal, P.S., Brown, E.R., Lee, D.Y., & Kennedy, T.W. (1996). 'Hot Mix asphalt Materials, Mixture design and Construction', *Second Edition NAPA Research and Education Foundation*, Lanham, Maryland.

Ruth, B.E., Bloy, L.L. & Avital, A.A. (1982). 'Prediction of pavement cracking at low temperatures', *Proceeding of Asphalt Paving Technologies*, Volume 51, pp.53-103.

Schmidt, J. & Santucci, L. E. (1966) 'A practical method for determining the glass transition temperature of asphalts and calculation of their low temperature viscosities', *Proceedings of the Association of Asphalt Paving Technologists*, Volume 35, pp. 61.

Sebaaly, P.E. (2002). 'Evaluation of Low-Temperature Properties of HMA Mixtures', *Journal of Transportation Engineering*, pp. 578-586.

Sebaaly, P. E., Lake, A. & Epps, J.(2002) ‘Evaluation of Low-Temperature Properties of HMA Mixtures’, *Journal of Transportation Engineering*, Volume 128, Issue 6, pp. 578-586

Shah,A.(2004) ‘Influence of binders & Mixture properties on the performance of Asphalt Concrete pavements’, *PhD Dissertation*, Purdue University, pp.1-216

Shen W. & Kirkener D., (2001). ‘Thermal Cracking of Viscoelastic Concrete Pavement’, *Journal of Engineering Mechanics*. Volume 127 no.7, pp.700-709.

Stuart, K. D. & Youtchef, J.S. (2001). ‘Understanding the performance of modified asphalt binders in mixtures: low-temperature properties’ *Report: FHWA-RD-02-074*, Federal Highway Administration, Washington, D.C.

Tan, Y.Q., Xu, H. N. , Dong, Z. J. & Gong, W. Q., (2008). ‘Effect of aggregate grading on low temperature cracking resistance in asphalt mixtures based on mathematical statistics’, *Proceedings of Eighth International RILEM conference on cracking in Pavements held on 2008, Limoges, France*, pp. 387-394

Transport Pooled Fund Study 776 (2007). ‘Investigation of low temperature cracking in asphalt pavements’, *Final Report*, University of Minnesota, Minneapolis, Minn.

Turkish General Directorate of Highways, Yayin( Specifications) No: 267 (2006)

Van-der-Poel, C., (1954). ‘A general system describing the visco-elastic properties of bitumens and its relation to routine test data’, *Journal of Applied Chemistry*, Volume 4, pp. 221-236.

Vinson T.S. & Jung, D.H (1994). ‘Low temperature cracking and rutting in asphalt concrete pavement’, *Roads and Airfield in Cold regions*, Technical Councils on Cold Regions Engineering Monograph, ASCE. pp. 203-248.

Velásquez, R. A., Labuz, J. F., Marasteanu, M. O., & Zofka, A. M. (2009) 'Revising Thermal Stresses in the TSRST for Low-Temperature Cracking Prediction', *Journal of Materials in Civil Engineering*, pp. 680-687

Vinson, T. S., Janoo, V. C. & Haas, R. C. G. (1996). 'Low Temperature and Thermal Fatigue Cracking', *Summary Report for A-003A* of the Strategic Highway Research Program (SHRP), Washington, D.C.-USA.

Wada, Y. & Hirose, H. (1960) 'Glass Transition Phenomena and Rheological Properties of Petroleum Asphalt', *Journal of Physical Society of Japan*, Volume 15, No 10, pp. 1885-1894.

Wargo, A D. (2008) 'The Development of a Simple Test Method to Measure the Low Temperature Cracking Resistance of Hot Mix Asphalt', *Master thesis*, Ohio University, Civil Engineering (Engineering and Technology), USA. pp.1-151.

Williams, S. G. (2003). 'The Effects of HMA Mixture Characteristics on Rutting susceptibility', *22<sup>nd</sup> ARRB Conference*, Research into Practice, Canberra Australia, pp.1-17.

Xinjun L., Marasteanu, M. O., Kvasnak, A., Bausano J., Williams, R. C. & Worrel, B. (2010) 'Factor Study in Low Temperature Fracture Resistance of Asphalt Concrete', *Journal of Materials in Civil Engineering*, ASCE, pp.145-152.

Zhao, D., Lei, M., & Yao, Z. (2009). 'Evaluation of Polymer Modified Hot-Mix Asphalt: Laboratory Characterization', *Journal of Material in Civil Engineering* ASCE, April 2009, Vol.21. No.4 . pp163-169.

Zeng. H. & Isacsson, U (1998 ). 'Low temperature cracking of Polymer-modified asphalt', *Materials and structures*. Volume 31. pp. 58-63.

## A- FRACTURE PLOTS

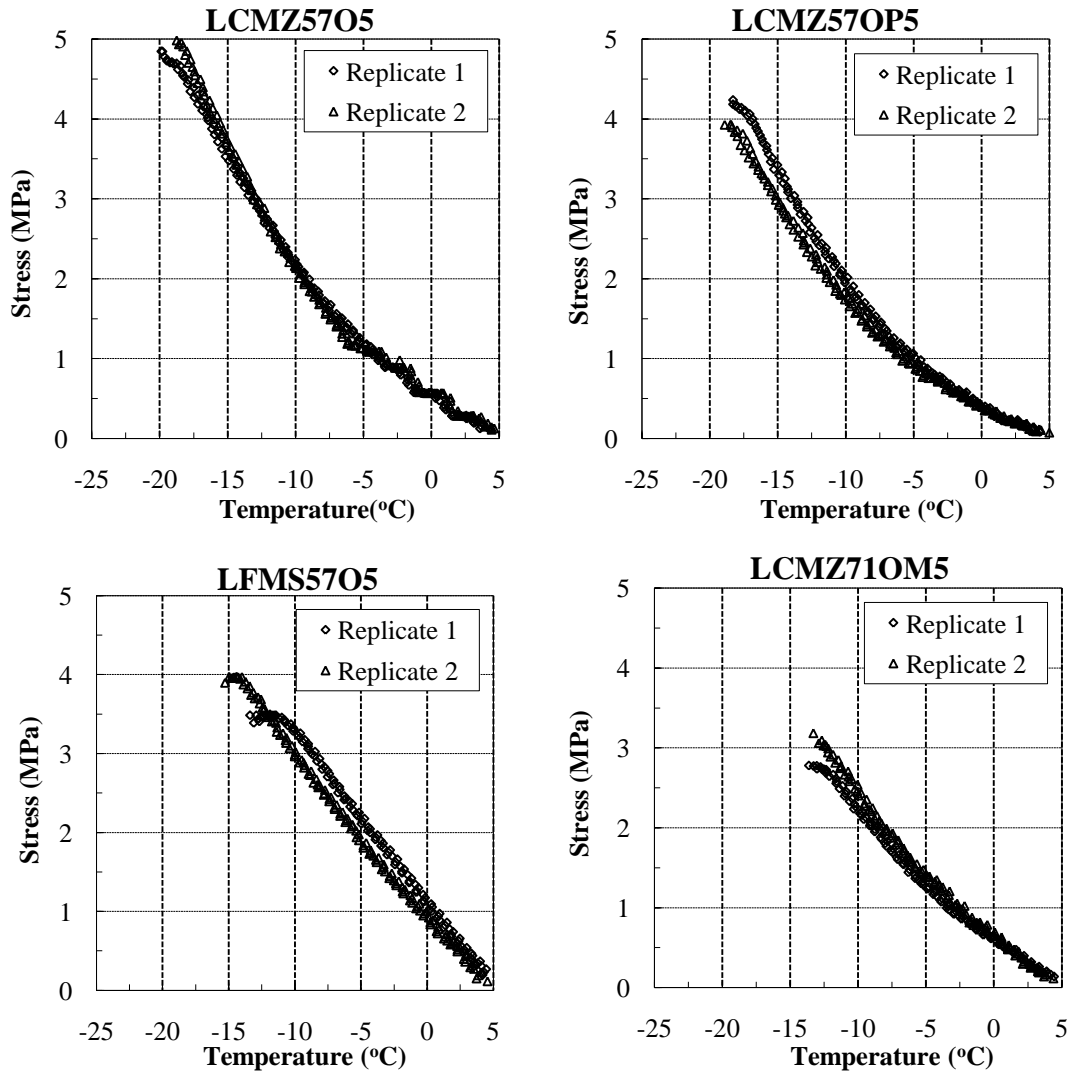


**Figure A1- Fracture plot of small samples tested at -5°C/h**

In the figure, LCMZ57O5 mean L- Limestone (aggregate) + C-Coarse (gradation) + Z (no modification) + M (small specimen, 20 cm)+50-70 (penetration graded asphalt) +Optimum (AC content) +5(-5°C/h cooling rate). Similar methodology shall be applied to understand the configuration of all the mix presented in figures.

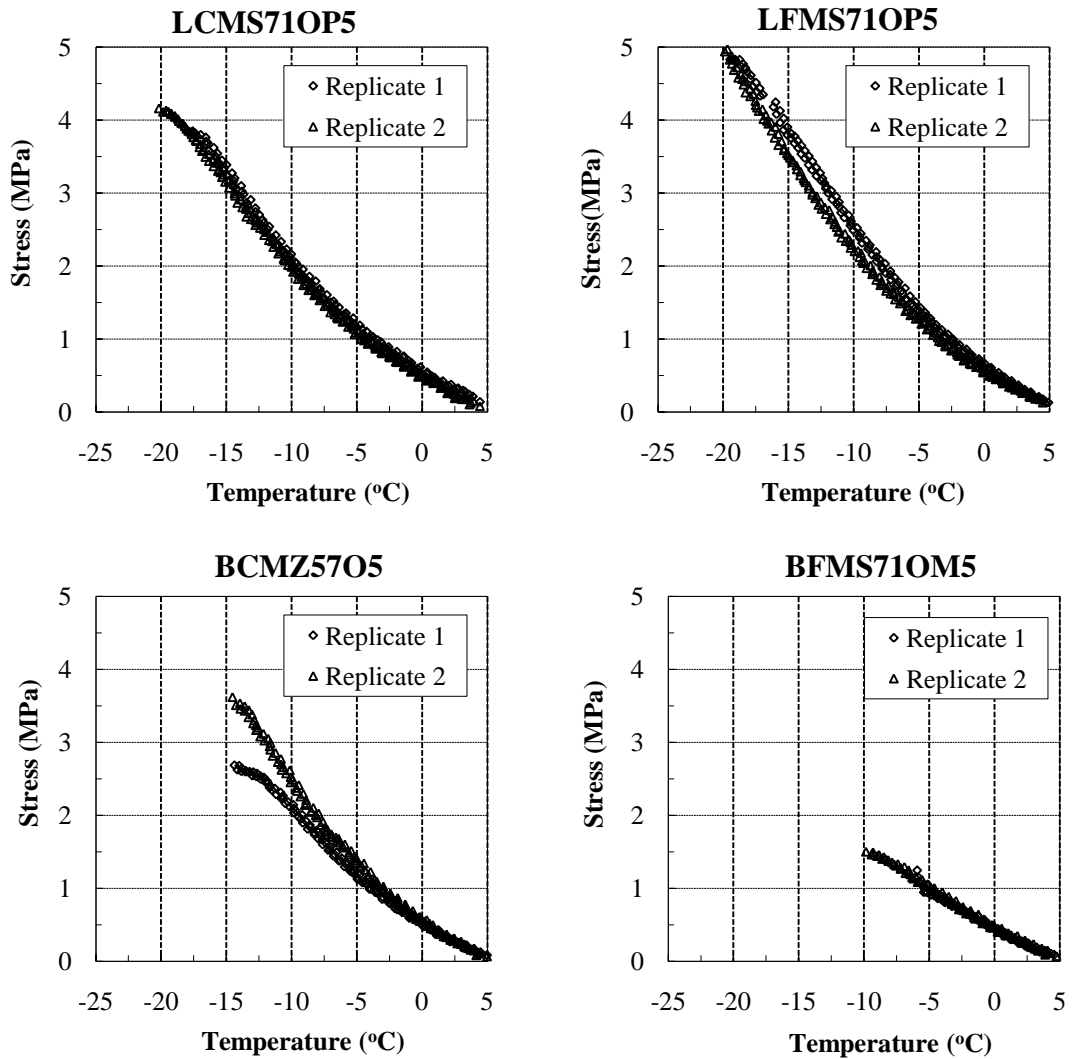


**Figure A1 (continued)**

**Symbols used:**

Aggregate : L-limestone, B-Basalt; Gradation: C-Coarse, F-Fine; Specimen length: T-Tall, M-Small; Polymer modification: Z-no Modification ,S-SBS Modification; AC type: 57-50 70, 71-71 100; AC content: O-optimum, OP optimum plus, OM optimum minus; Cooling rate: 5= -5°C/h, 10= -10°C/h, 20= -20°C/h

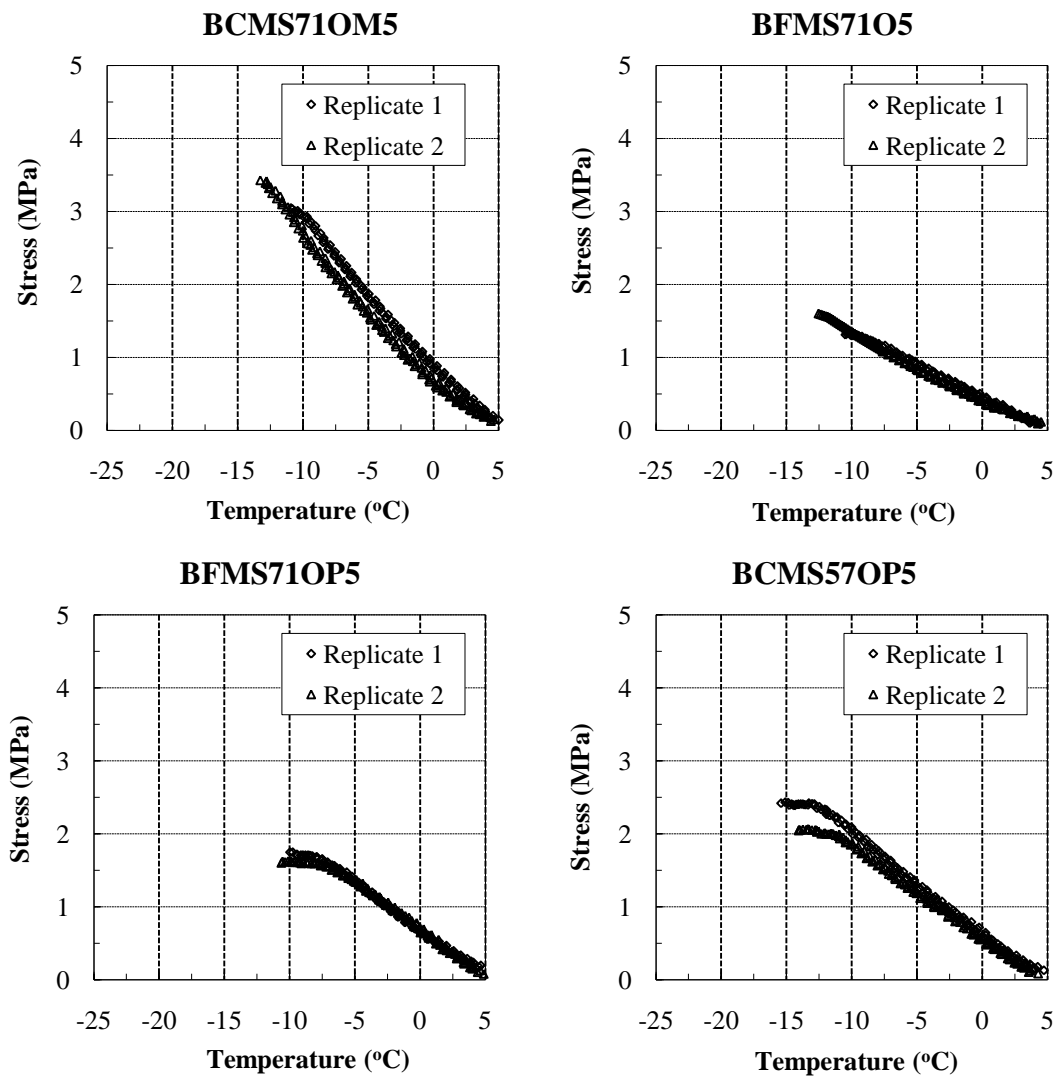


**Figure A1 (continued)**

**Symbols used:**

Aggregate : L-limestone, B-Basalt; Gradation: C-Coarse, F-Fine; Specimen length: T-Tall, M-Small; Polymer modification: Z-no Modification ,S-SBS Modification; AC type: 57-50 70, 71-71 100; AC content: O-optimum, OP optimum plus, OM optimum minus; Cooling rate: 5= -5°C/h, 10= -10°C/h, 20= -20°C/h

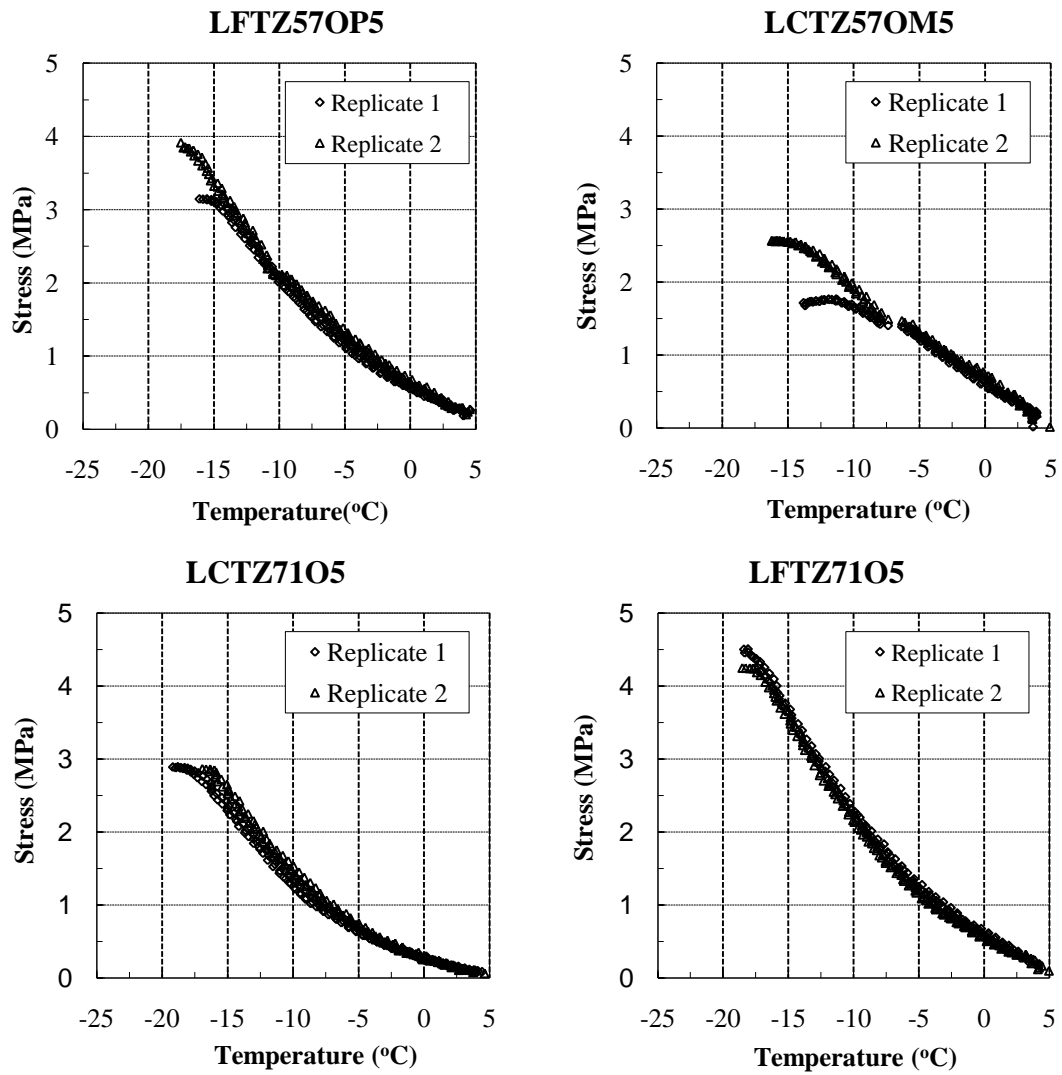


**Figure A2- Fracture plot of tall samples tested at -5°C/h**

**Symbols used:**

Aggregate : L-limestone, B-Basalt; Gradation: C-Coarse, F-Fine; Specimen length: T-Tall, M-Small; Polymer modification: Z-no Modification ,S-SBS Modification; AC type: 57-50 70, 71-71 100; AC content: O-optimum, OP optimum plus, OM optimum minus; Cooling rate: 5= -5°C/h, 10= -10°C/h, 20= -20°C/h

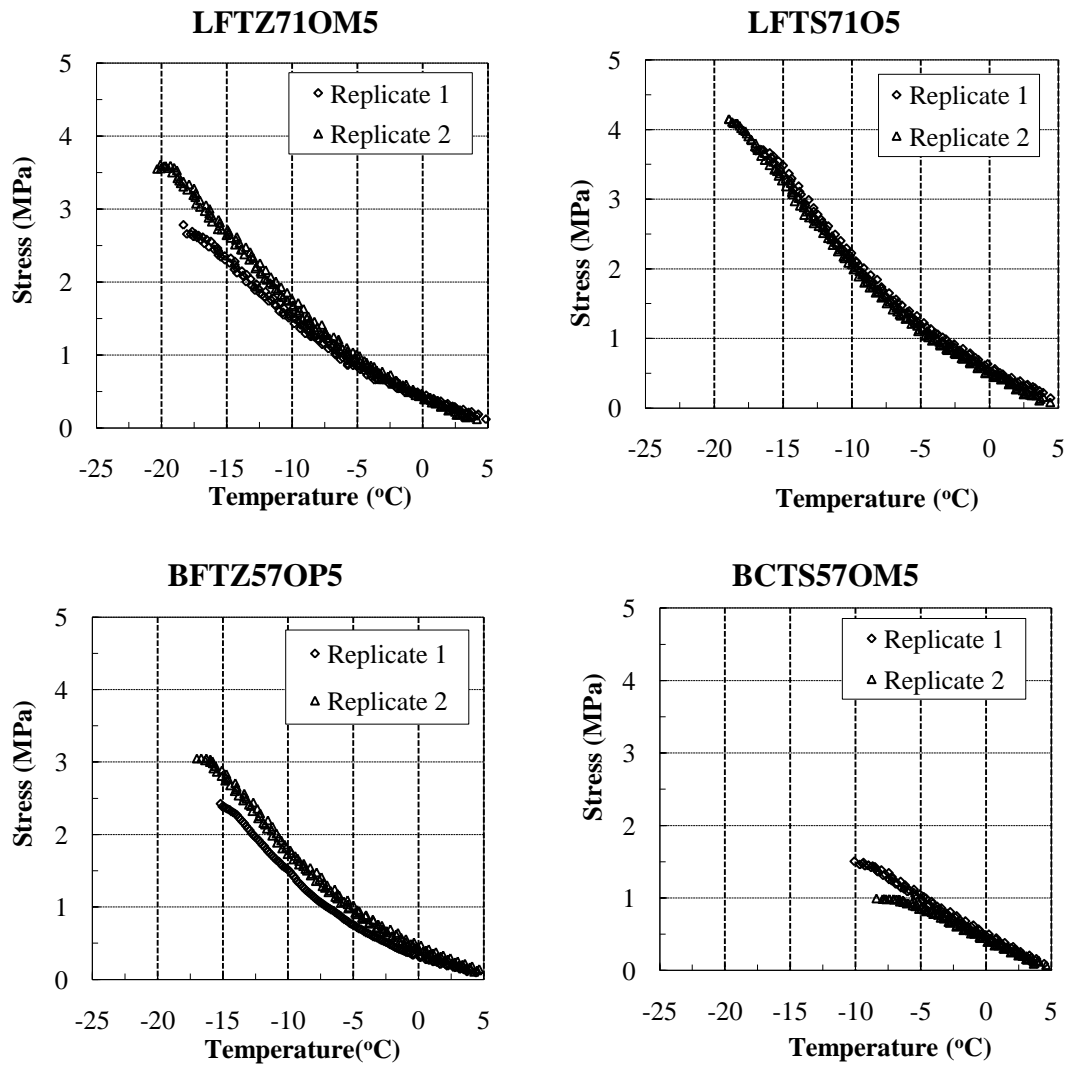
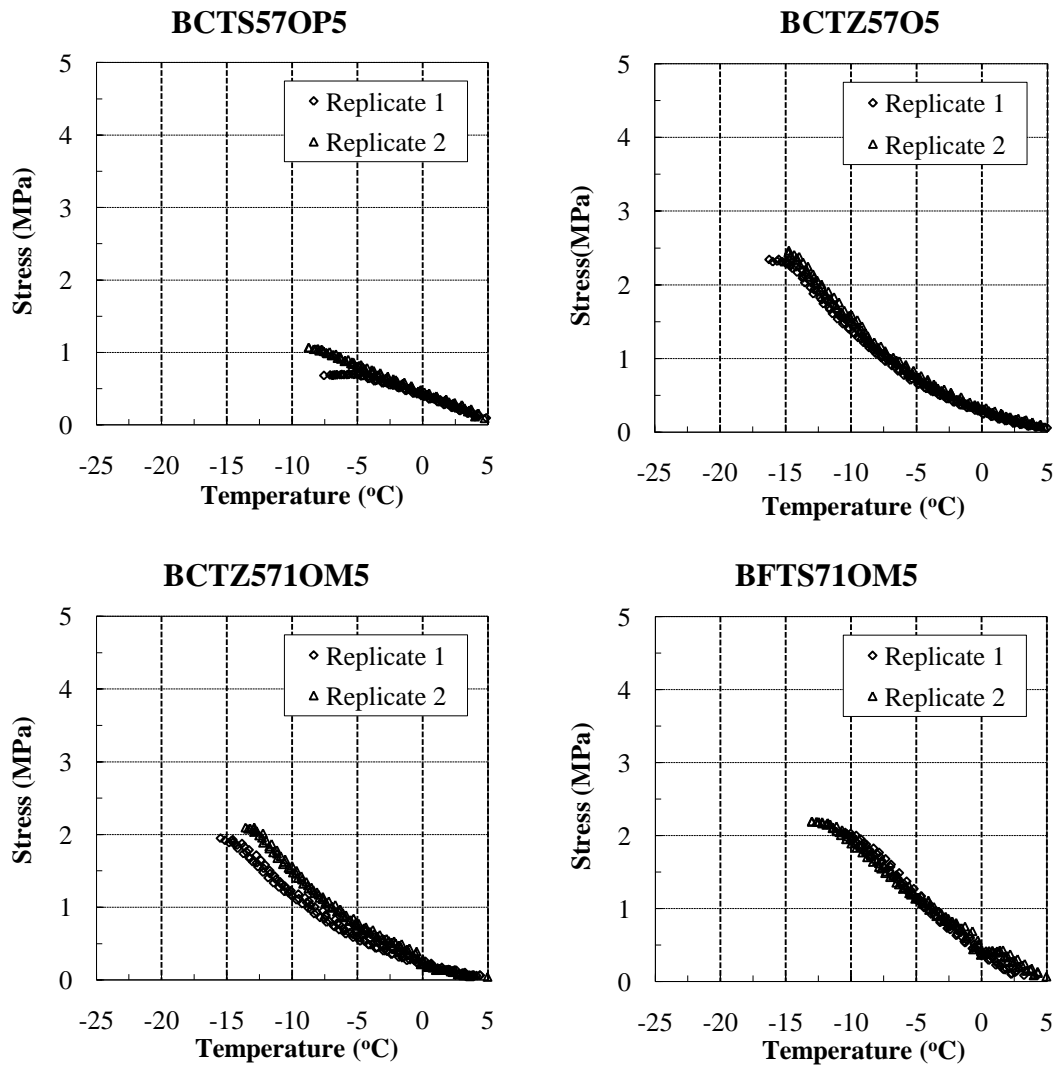


Figure A2 (continued)

**Symbols used:**

Aggregate : L-limestone, B-Basalt; Gradation: C-Coarse, F-Fine; Specimen length: T-Tall, M-Small; Polymer modification: Z-no Modification ,S-SBS Modification; AC type: 57-50 70, 71-71 100; AC content: O-optimum, OP optimum plus, OM optimum minus; Cooling rate: 5= -5°C/h, 10= -10°C/h, 20= -20°C/h



**Figure A2 (continued)**

**Symbols used:**

Aggregate : L-limestone, B-Basalt; Gradation: C-Coarse, F-Fine; Specimen length: T-Tall, M-Small; Polymer modification: Z-no Modification ,S-SBS Modification; AC type: 57-50 70, 71-71 100; AC content: O-optimum, OP optimum plus, OM optimum minus; Cooling rate: 5= -5°C/h, 10= -10°C/h, 20= -20°C/h

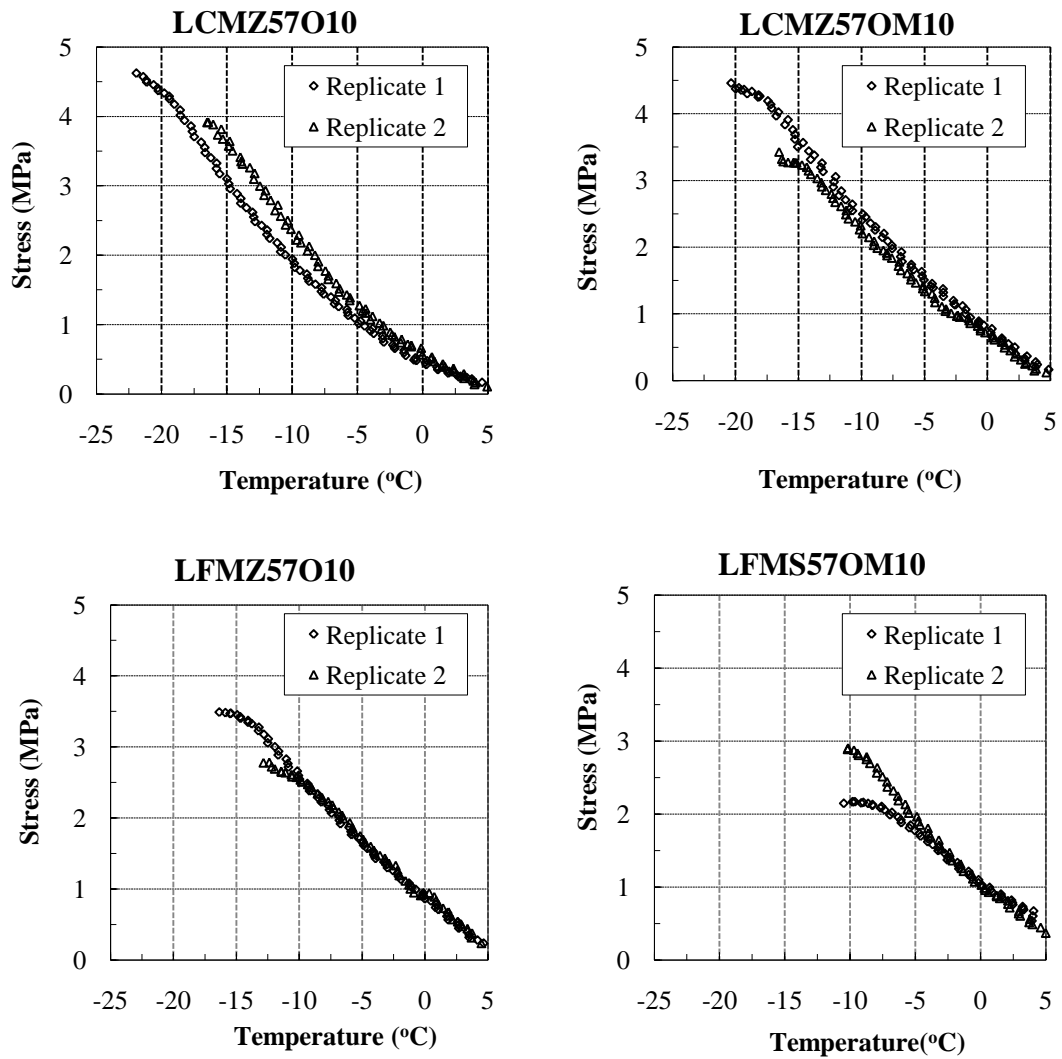


**Figure A3- Fracture plot of small samples tested at -10°C/h**

**Symbols used:**

Aggregate : L-limestone, B-Basalt; Gradation: C-Coarse, F-Fine; Specimen length: T-Tall, M-Small; Polymer modification: Z-no Modification ,S-SBS Modification; AC type: 57-50 70, 71-71 100; AC content: O-optimum, OP optimum plus, OM optimum minus; Cooling rate: 5= -5°C/h, 10= -10°C/h, 20= -20°C/h.

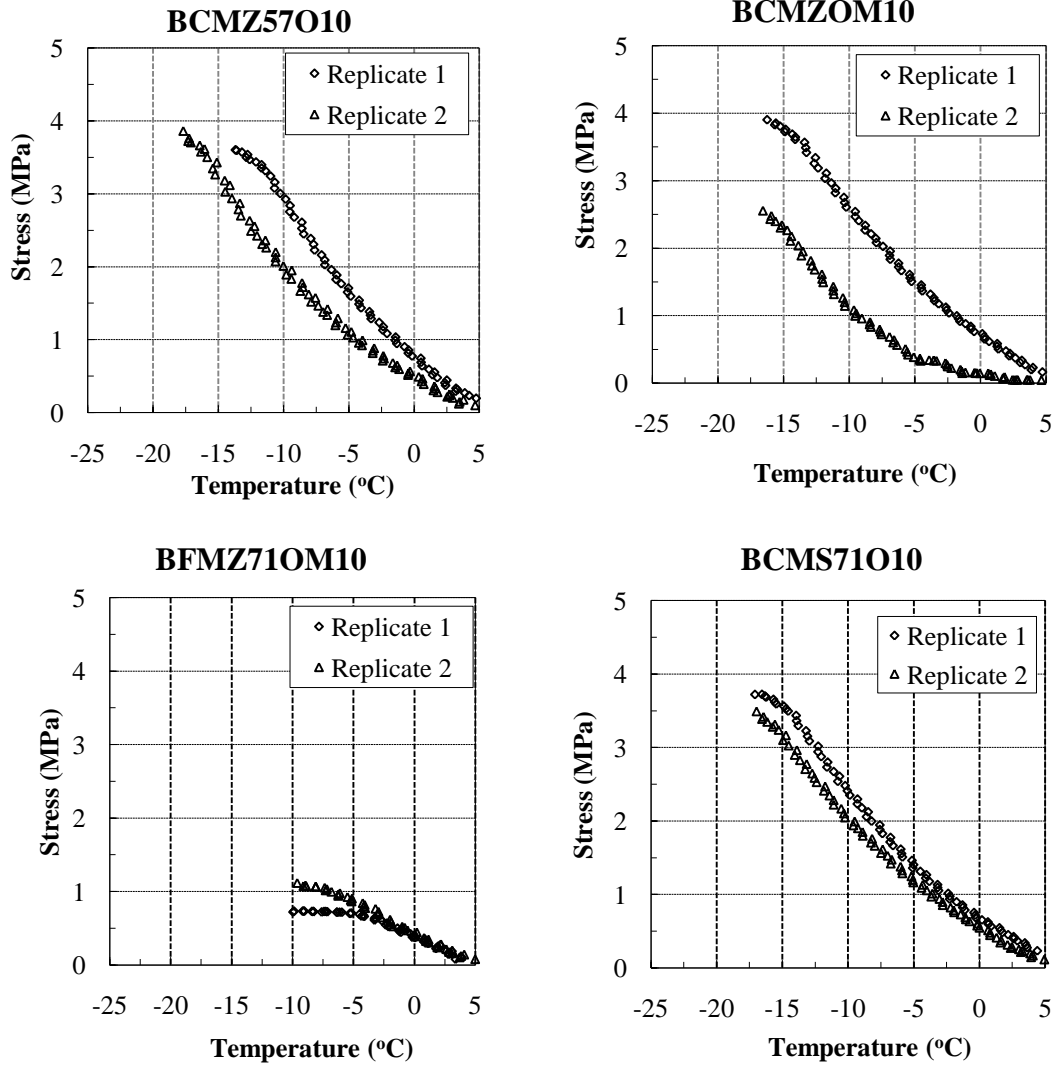


**Figure A3 (continued)**

**Symbols used:**

Aggregate : L-limestone, B-Basalt; Gradation: C-Coarse, F-Fine; Specimen length: T-Tall, M-Small; Polymer modification: Z-no Modification ,S-SBS Modification; AC type: 57-50 70, 71-71 100; AC content: O-optimum, OP optimum plus, OM optimum minus; Cooling rate: 5= -5°C/h, 10= -10°C/h, 20= -20°C/h.

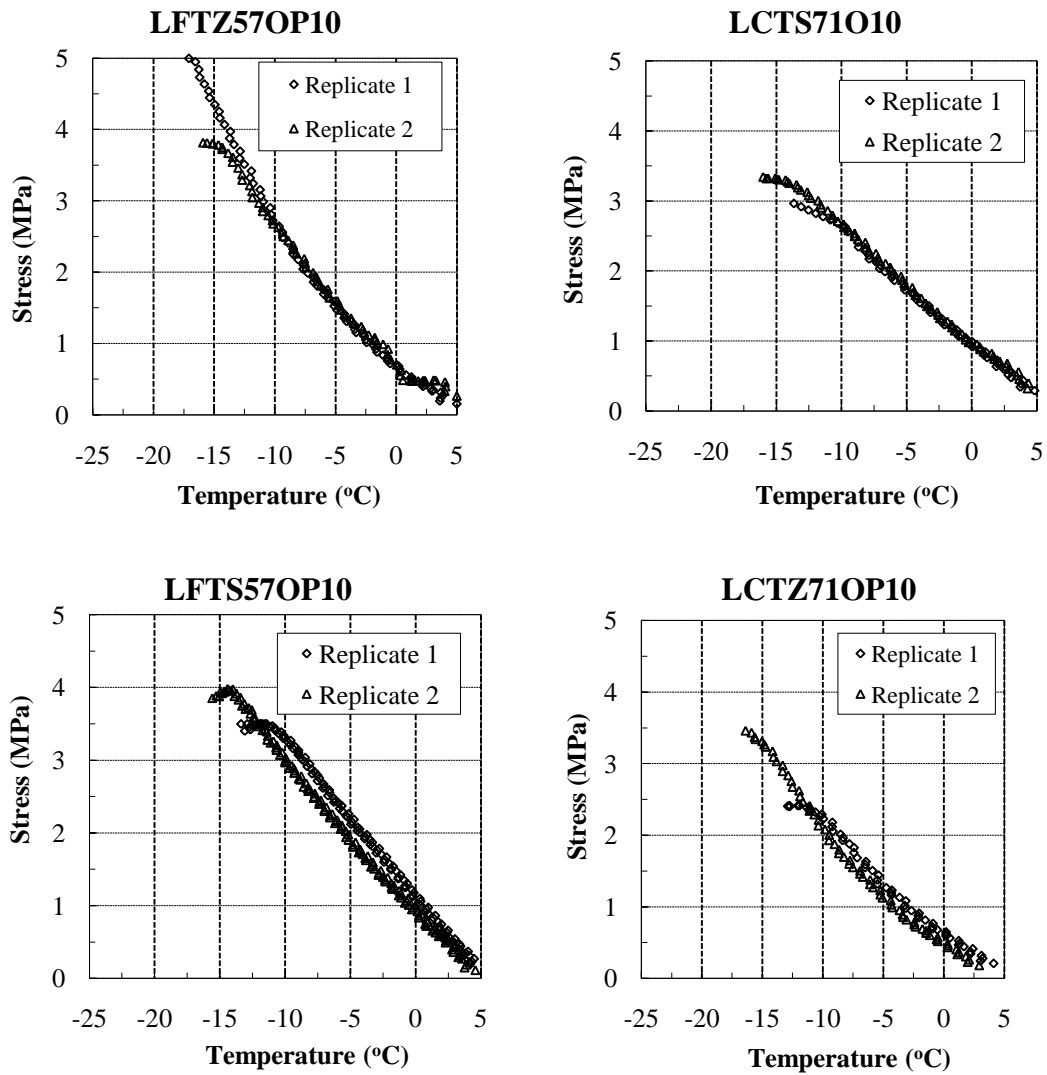


**Figure A4- Fracture plot of tall samples tested at -10°C/h**

**Symbols used:**

Aggregate : L-limestone, B-Basalt; Gradation: C-Coarse, F-Fine; Specimen length: T-Tall, M-Small; Polymer modification: Z-no Modification ,S-SBS Modification; AC type: 57-50 70, 71-71 100; AC content: O-optimum, OP optimum plus, OM optimum minus; Cooling rate: 5= -5°C/h, 10= -10°C/h, 20= -20°C/h.

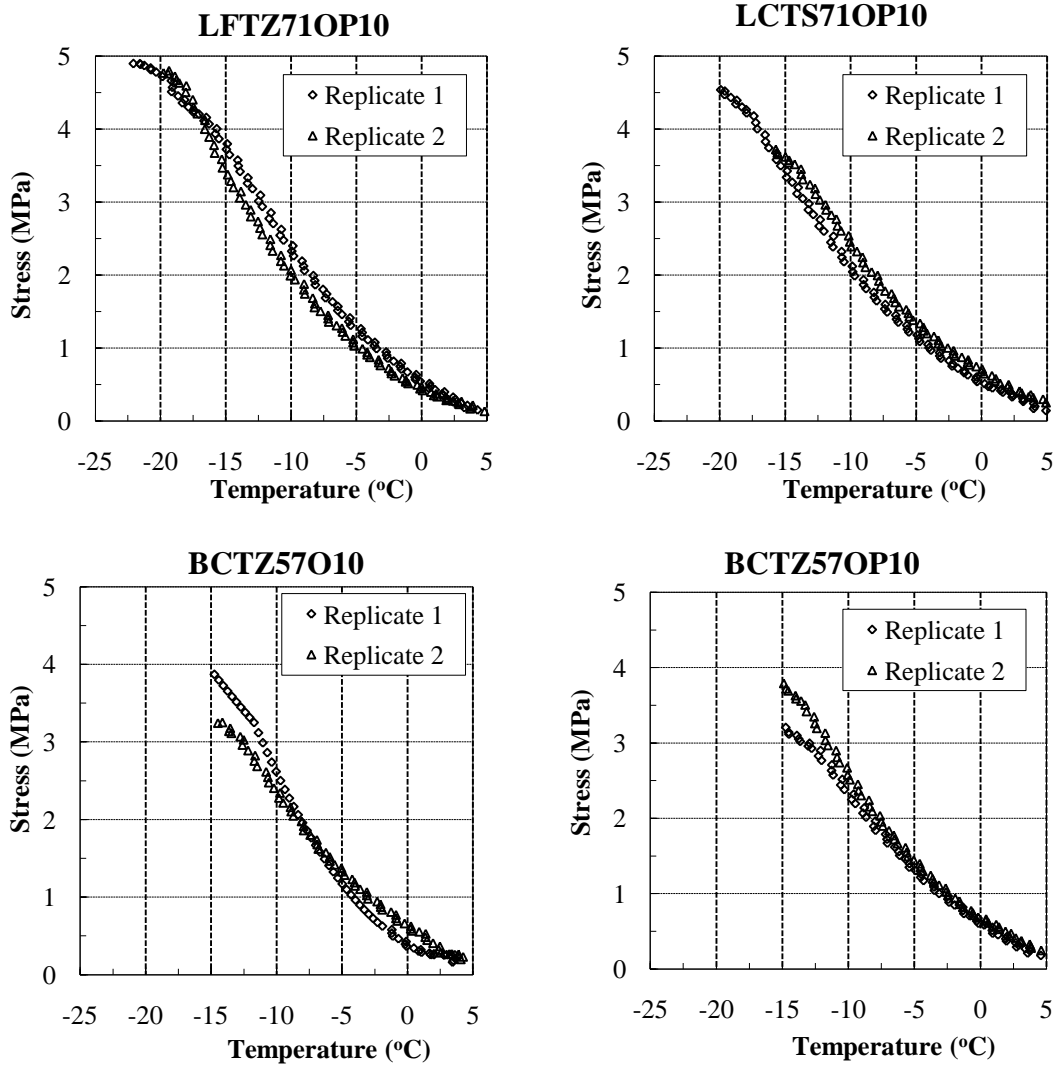


**Figure A4 (continued)**

**Symbols used:**

Aggregate : L-limestone, B-Basalt; Gradation: C-Coarse, F-Fine; Specimen length: T-Tall, M-Small; Polymer modification: Z-no Modification ,S-SBS Modification; AC type: 57-50 70, 71-71 100; AC content: O-optimum, OP optimum plus, OM optimum minus; Cooling rate: 5= -5°C/h, 10= -10°C/h, 20= -20°C/h.

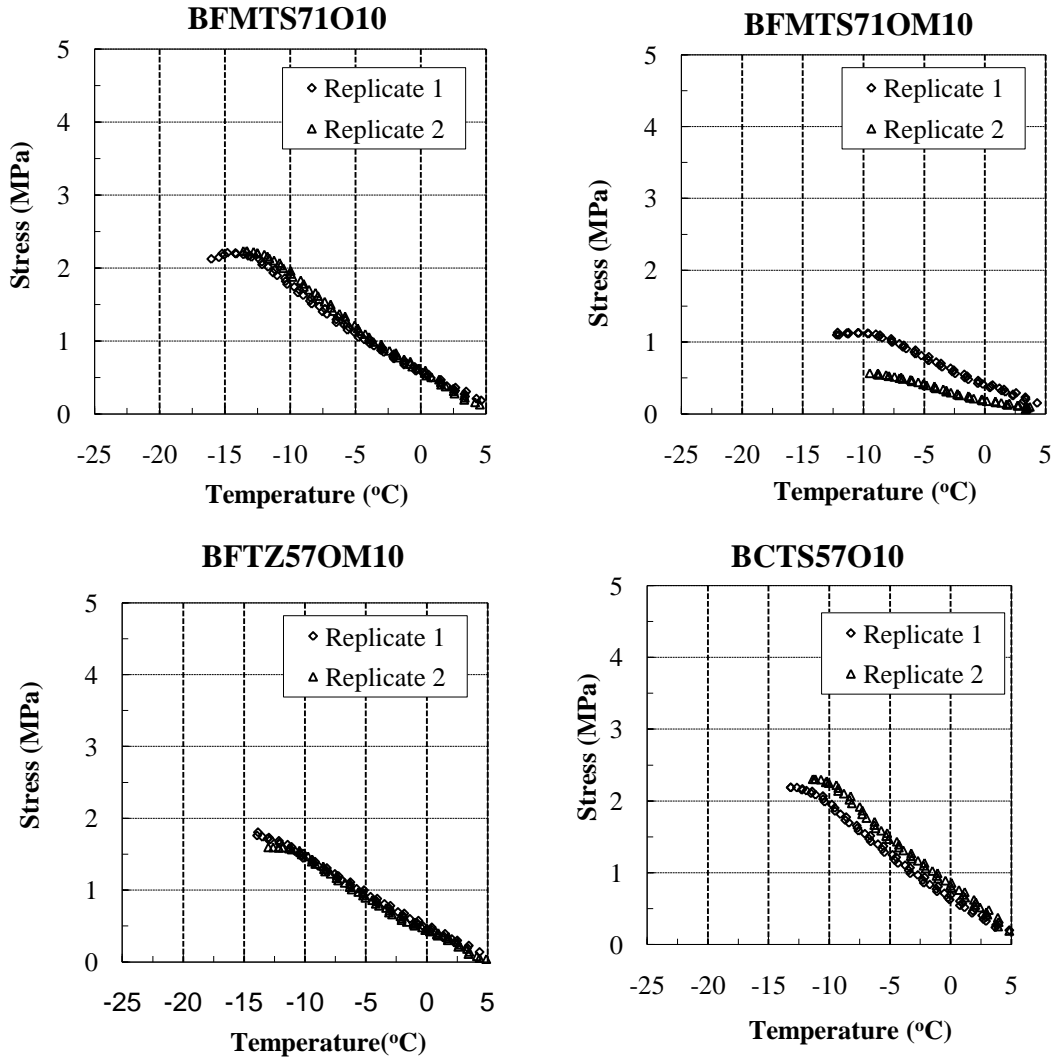


**Figure A4 (continued)**

**Symbols used:**

Aggregate : L-limestone, B-Basalt; Gradation: C-Coarse, F-Fine; Specimen length: T-Tall, M-Small; Polymer modification: Z-no Modification ,S-SBS Modification; AC type: 57-50 70, 71-71 100; AC content: O-optimum, OP optimum plus, OM optimum minus; Cooling rate: 5= -5°C/hr, 10= -10°C/hr, 20= -20°C/hr.

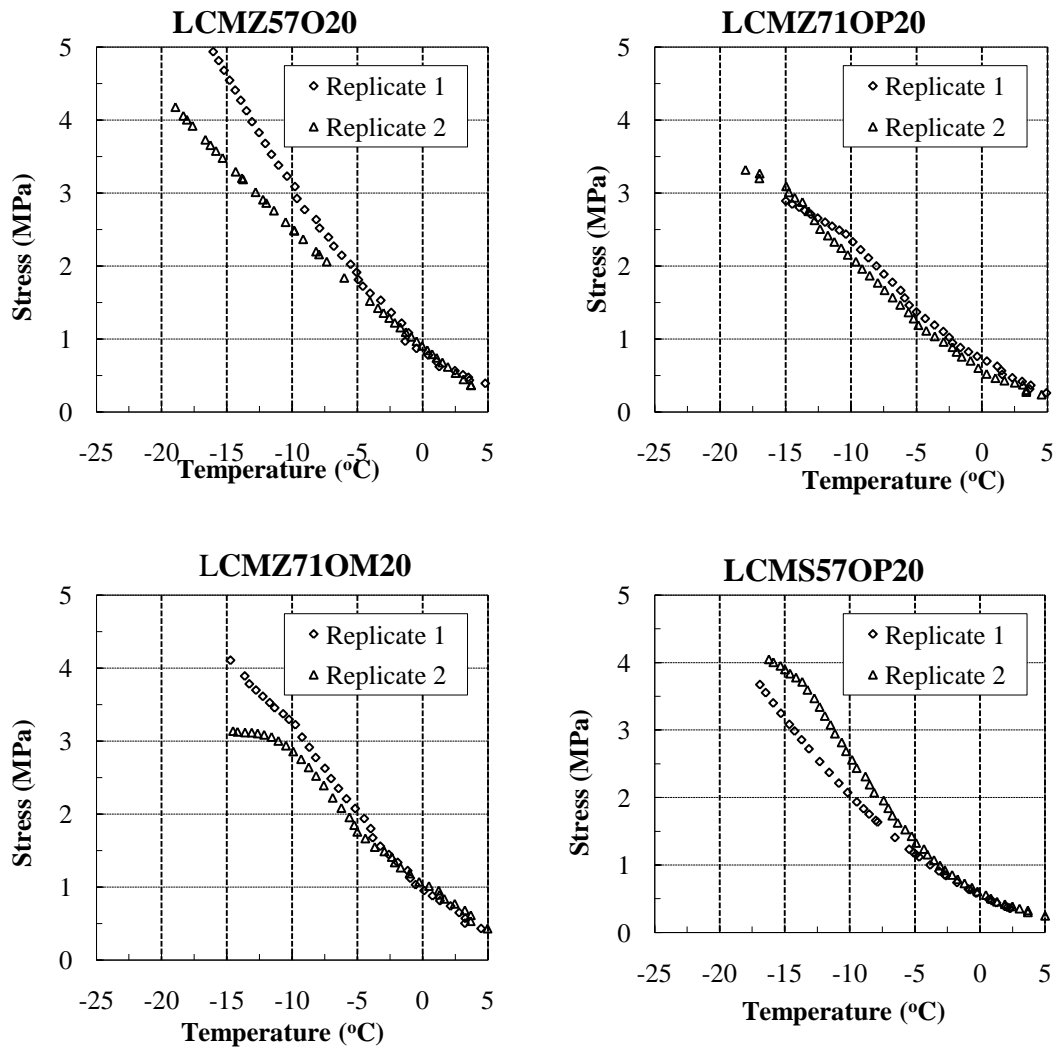


**Figure A5- Fracture plot of small samples tested at -20°C/h**

**Symbols used:**

Aggregate : L-limestone, B-Basalt; Gradation: C-Coarse, F-Fine; Specimen length: T-Tall, M-Small; Polymer modification: Z-no Modification ,S-SBS Modification; AC type: 57-50 70, 71-71 100; AC content: O-optimum, OP optimum plus, OM optimum minus; Cooling rate: 5= -5°C/h, 10= -10°C/h, 20= -20°C/h.

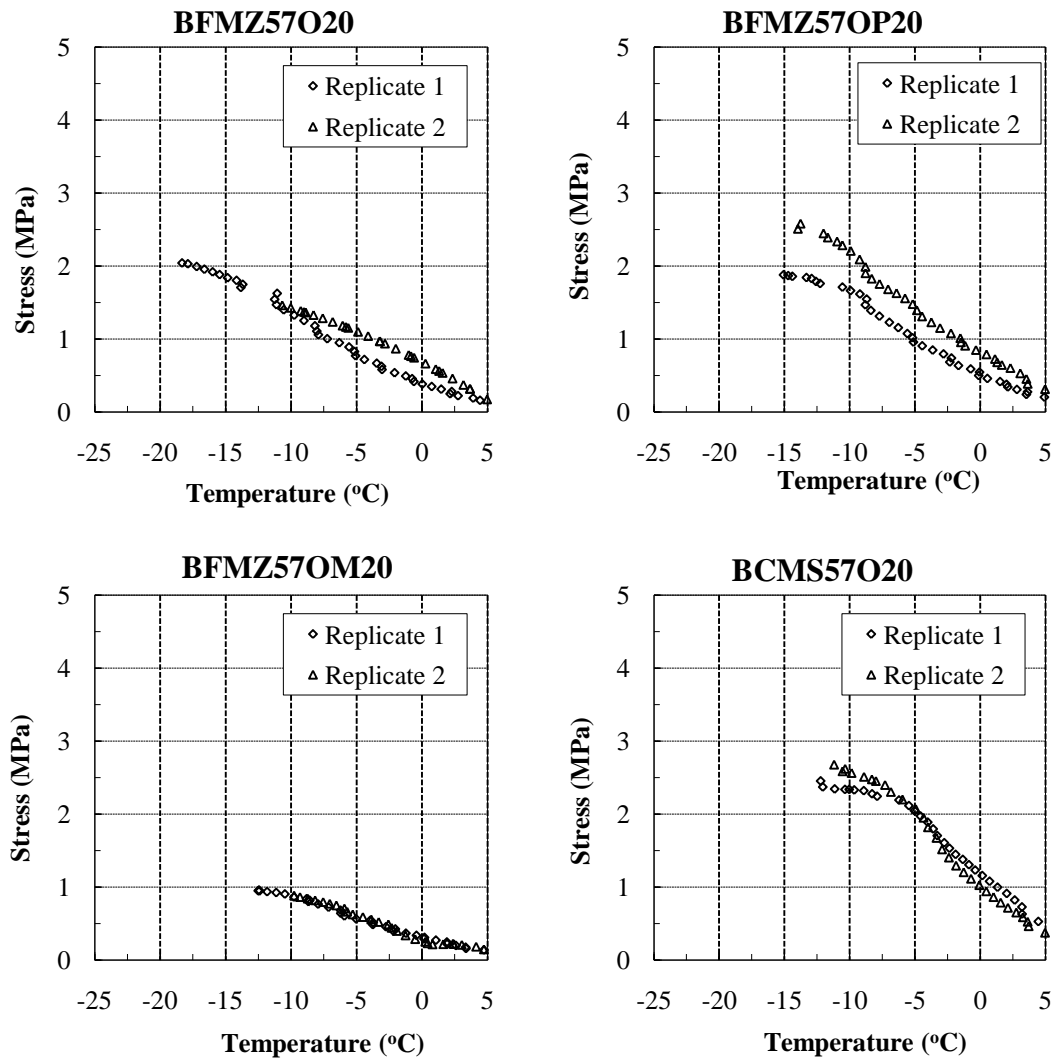


**Figure A5 (continued)**

**Symbols used:**

Aggregate : L-limestone, B-Basalt; Gradation: C-Coarse, F-Fine; Specimen length: T-Tall, M-Small; Polymer modification: Z-no Modification ,S-SBS Modification; AC type: 57-50 70, 71-71 100; AC content: O-optimum, OP optimum plus, OM optimum minus; Cooling rate: 5= -5°C/h, 10= -10°C/h, 20= -20°C/h.

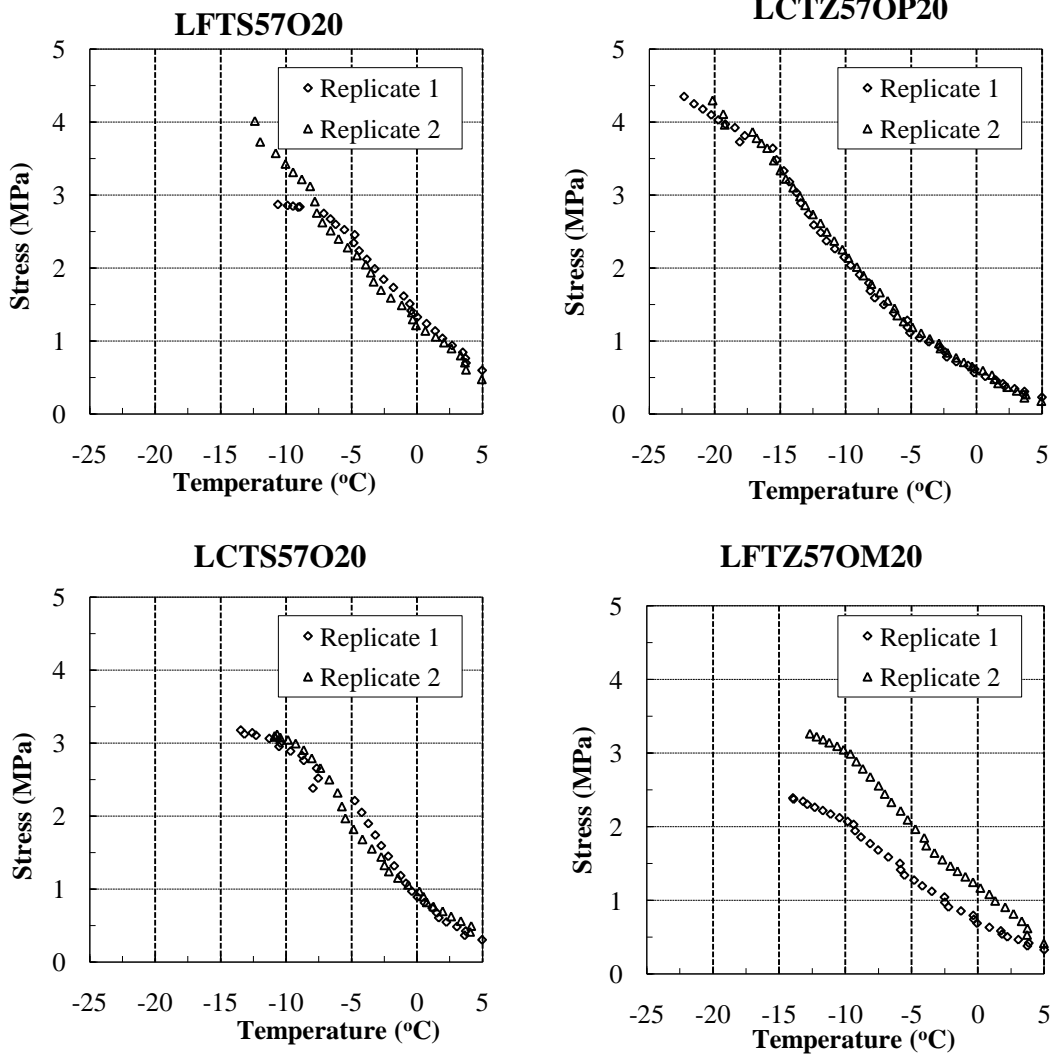


**Figure A6- Fracture plot of tall samples tested at -20°C/h**

**Symbols used:**

Aggregate : L-limestone, B-Basalt; Gradation: C-Coarse, F-Fine; Specimen length: T-Tall, M-Small; Polymer modification: Z-no Modification ,S-SBS Modification; AC type: 57-50 70, 71-71 100; AC content: O-optimum, OP optimum plus, OM optimum minus; Cooling rate: 5= -5°C/h, 10= -10°C/h, 20= -20°C/h.

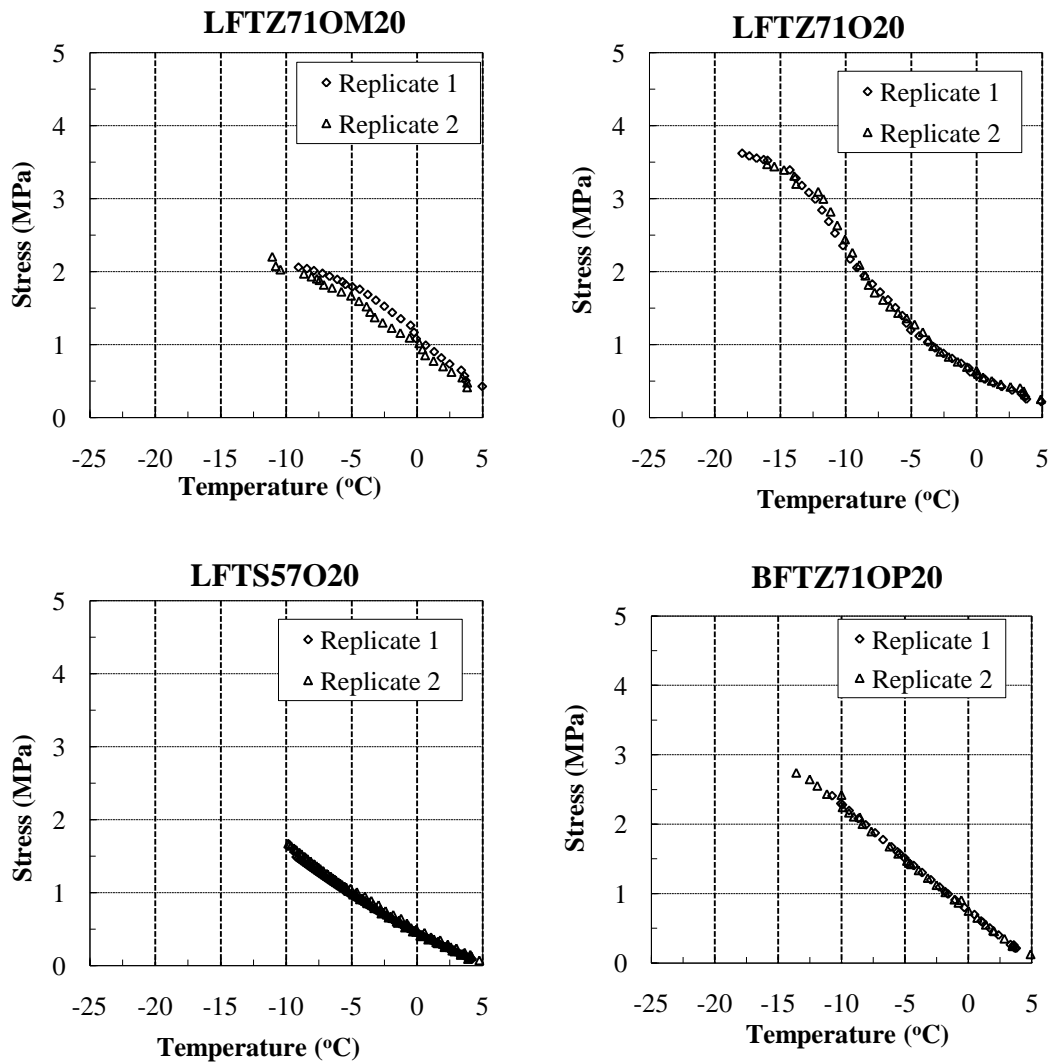


**Figure A6 (continued)**

**Symbols used:**

Aggregate : L-limestone, B-Basalt; Gradation: C-Coarse, F-Fine; Specimen length: T-Tall, M-Small; Polymer modification: Z-no Modification ,S-SBS Modification; AC type: 57-50 70, 71-71 100; AC content: O-optimum, OP optimum plus, OM optimum minus; Cooling rate: 5= -5°C/hr, 10= -10°C/hr, 20= -20°C/hr.

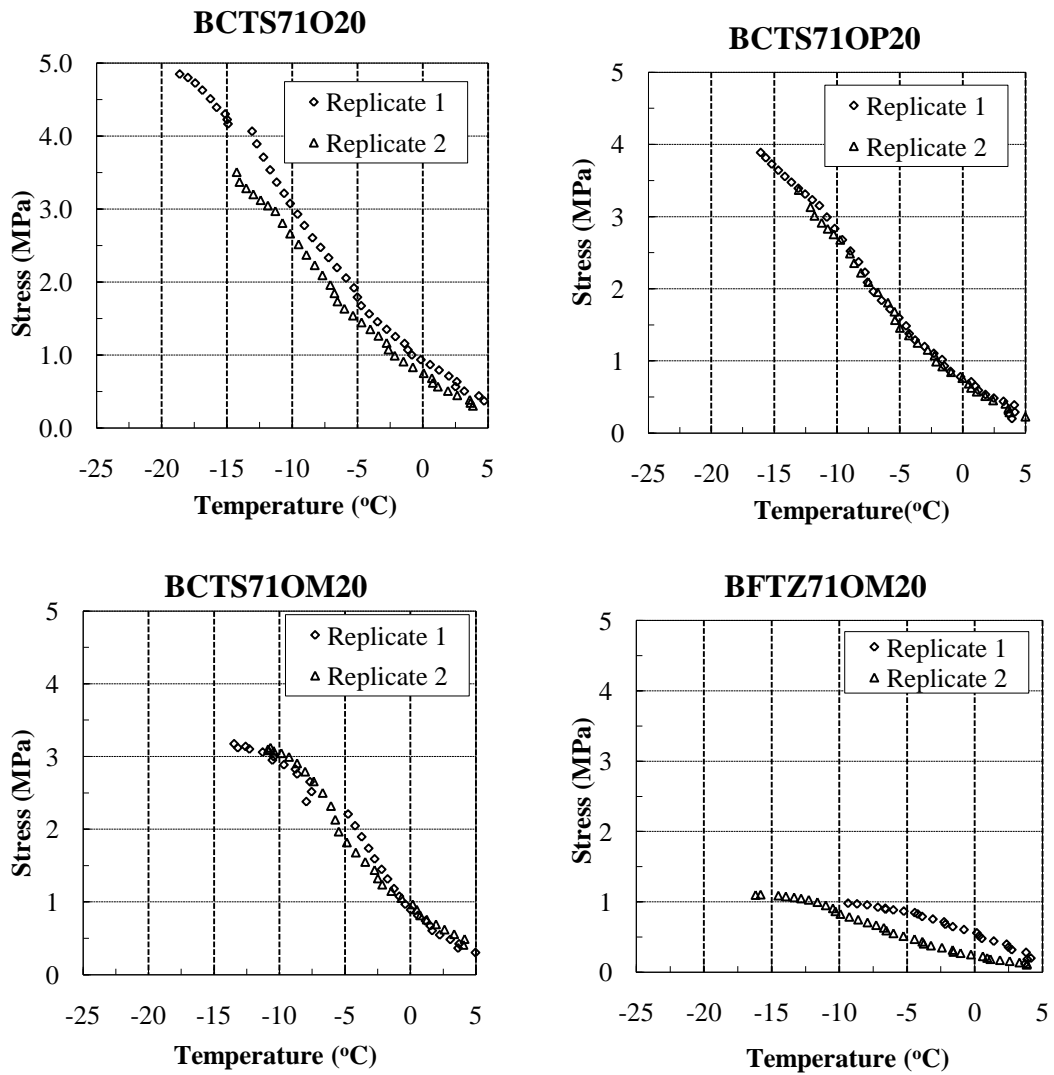


**Figure A6 (continued)**

**Symbols used:**

Aggregate : L-limestone, B-Basalt; Gradation: C-Coarse, F-Fine; Specimen length: T-Tall, M-Small; Polymer modification: Z-no Modification ,S-SBS Modification; AC type: 57-50 70, 71-71 100; AC content: O-optimum, OP optimum plus, OM optimum minus; Cooling rate: 5= -5°C/hr, 10= -10°C/hr, 20= -20°C/hr.

## B- GLASS TRANSITION PLOTS

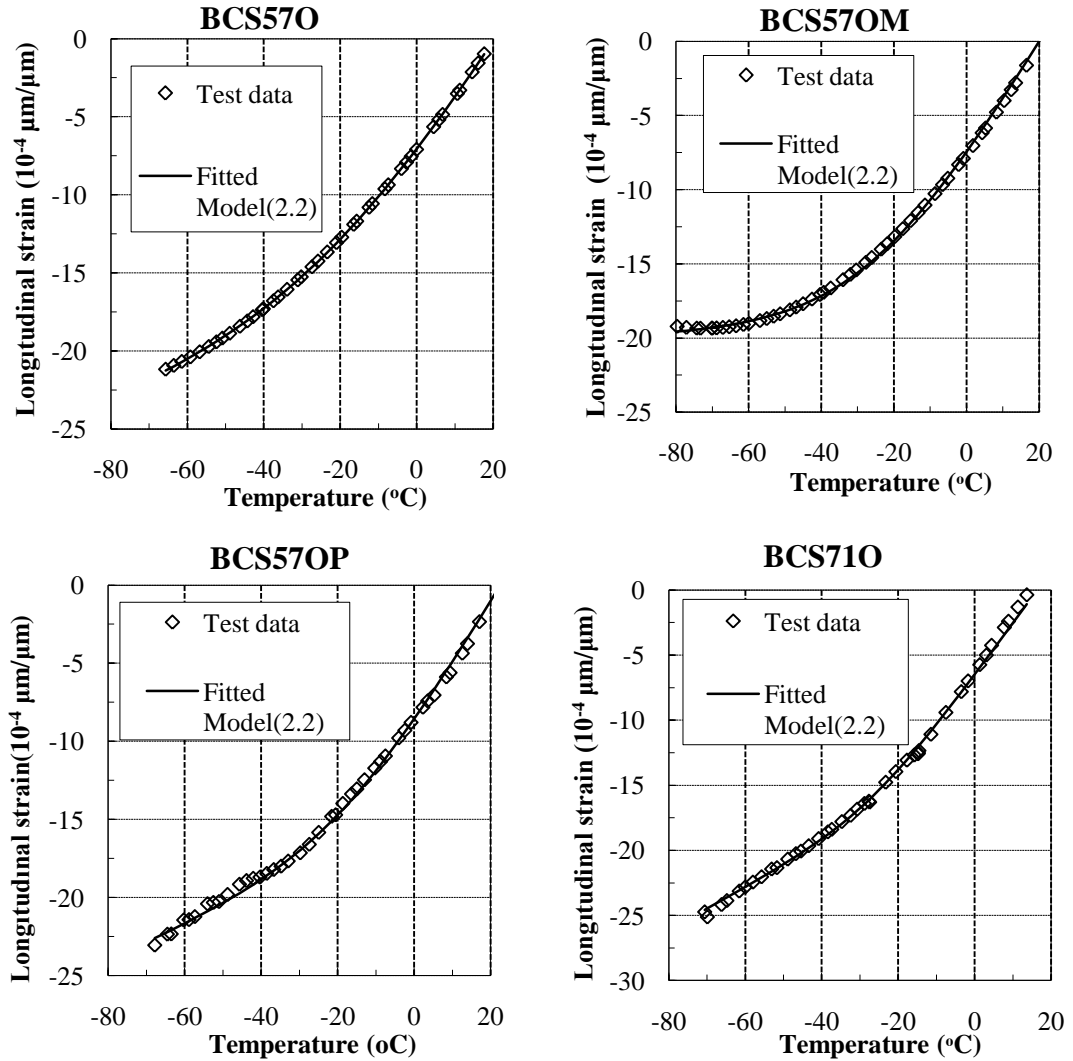


**Figure B1- Glass transition temperature plots**

**Symbols used:**

Aggregate : L-limestone, B-Basalt; Gradation: C-Coarse, F-Fine; Polymer modification: Z-no Modification ,S-SBS Modification; AC type: 57-50 70, 71-71 100;AC content: O-optimum, OP- Optimum plus, OM- Optimum minus.

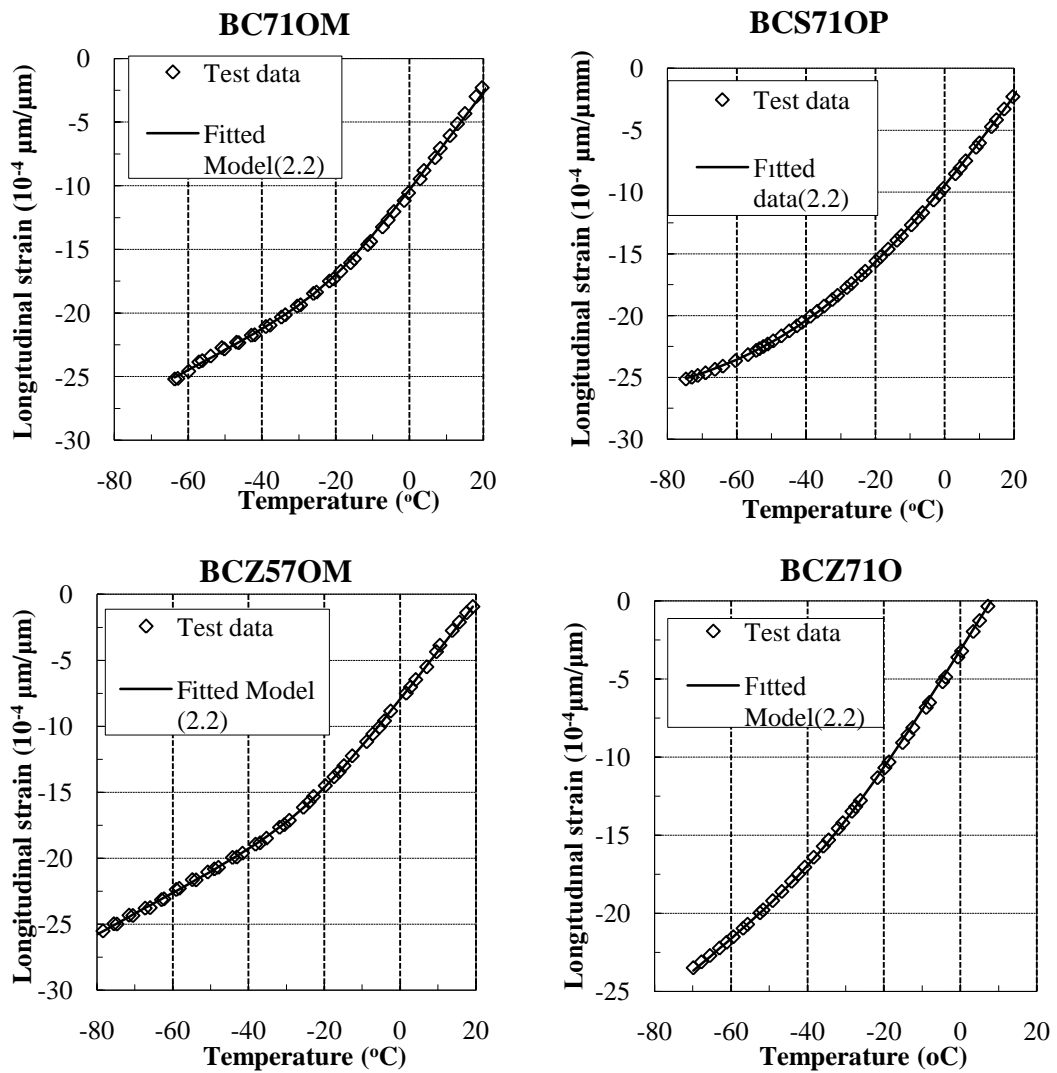
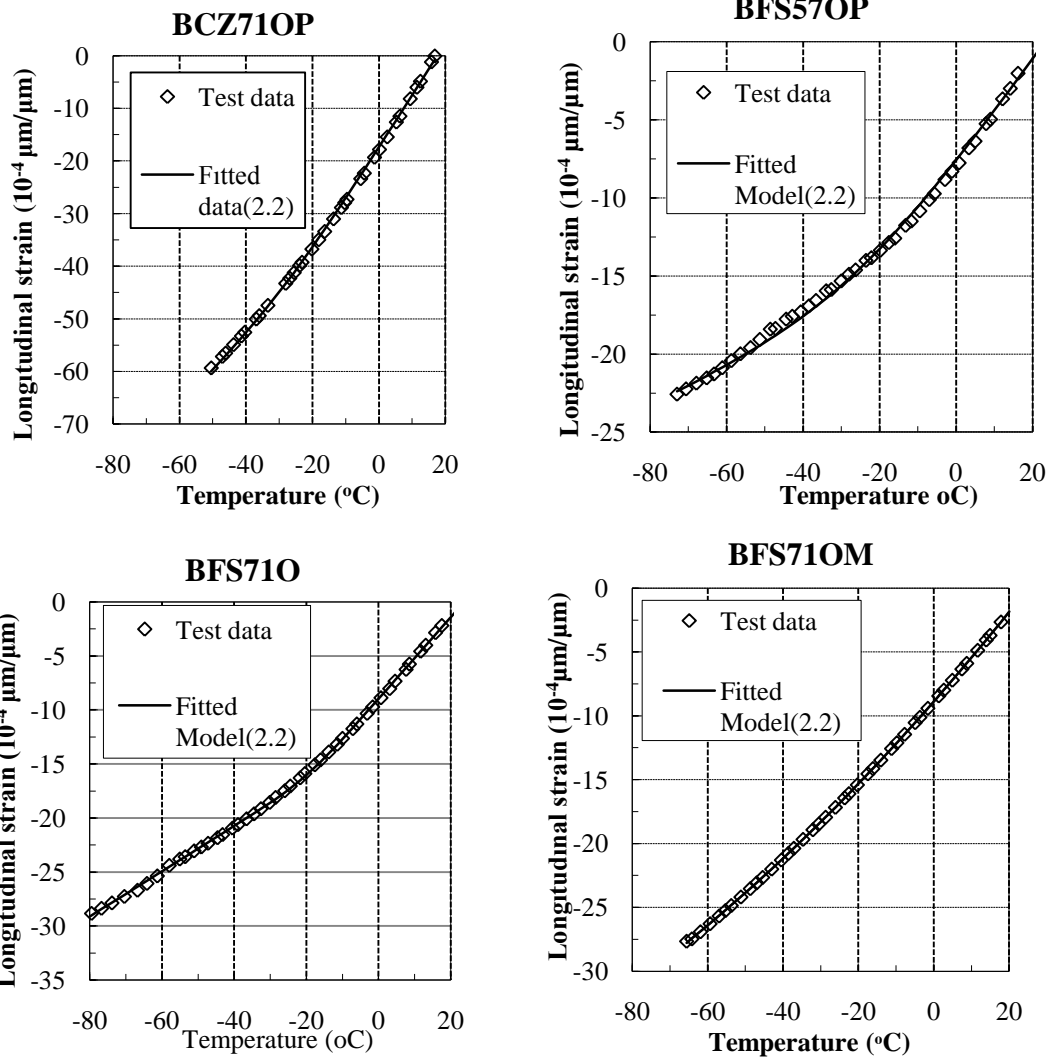


Figure B1 (continued)

**Symbols used:**

Aggregate : L-limestone, B-Basalt; Gradation: C-Coarse, F-Fine; Modification: Z-no Modification ,S-SBS Modification; AC type: 57-50 70, 71-71 100;AC content: O- optimum, OP- Optimum plus, OM- Optimum minus.



**Figure B1 (continued)**

**Symbols used:**

Aggregate : L-limestone, B-Basalt; Gradation: C-Coarse, F-Fine; Polymer modification: Z-no Modification ,S-SBS Modification; AC type: 57-50 70, 71-71 100;AC content: O-optimum, OP- Optimum plus, OM- Optimum minus.

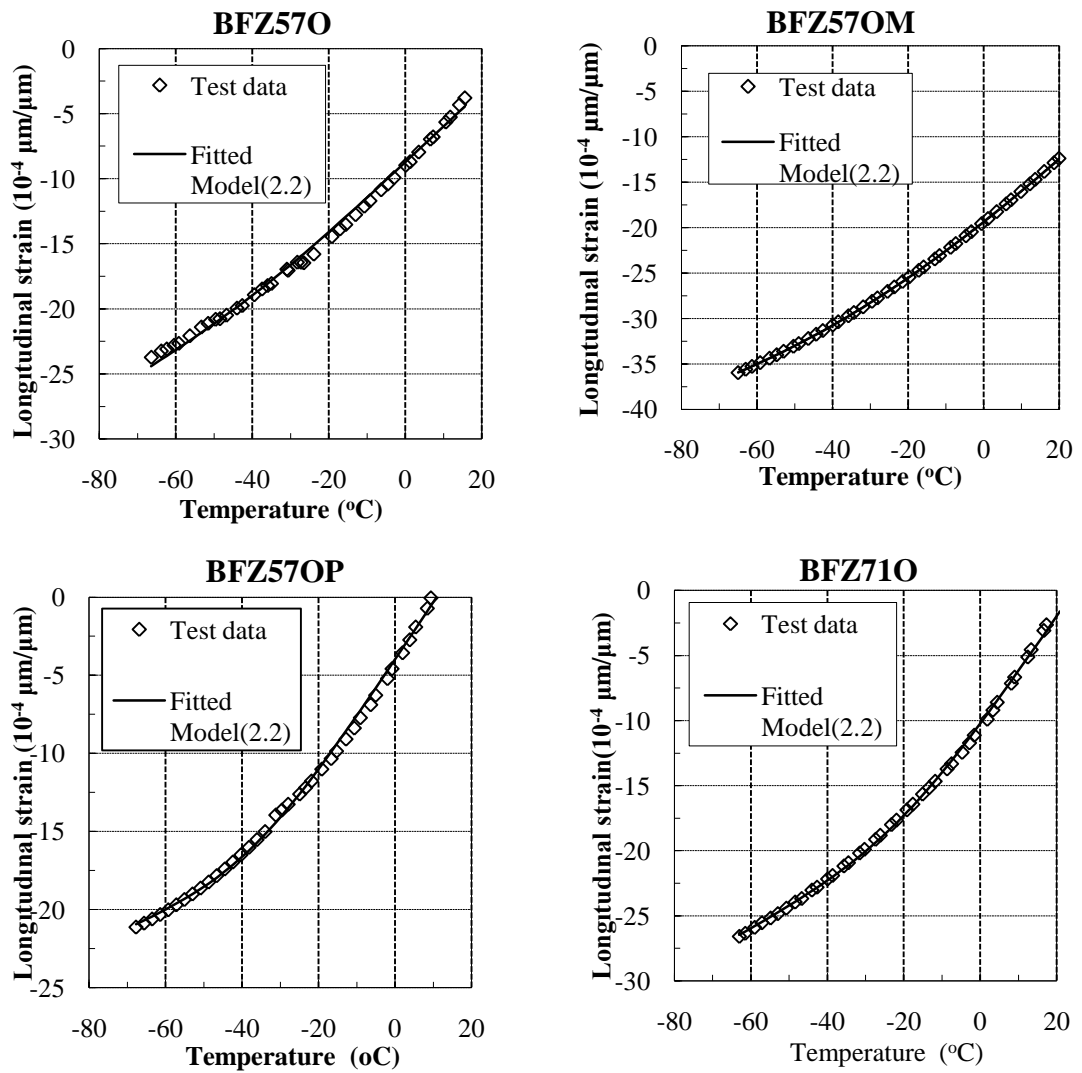


**Figure B1 (continued)**

**Symbols used:**

Aggregate : L-limestone, B-Basalt; Gradation: C-Coarse, F-Fine; Polymer modification: Z-no Modification ,S-SBS Modification; AC type: 57-50 70, 71-71 100;AC content: O-optimum, OP- Optimum plus, OM- Optimum minus.

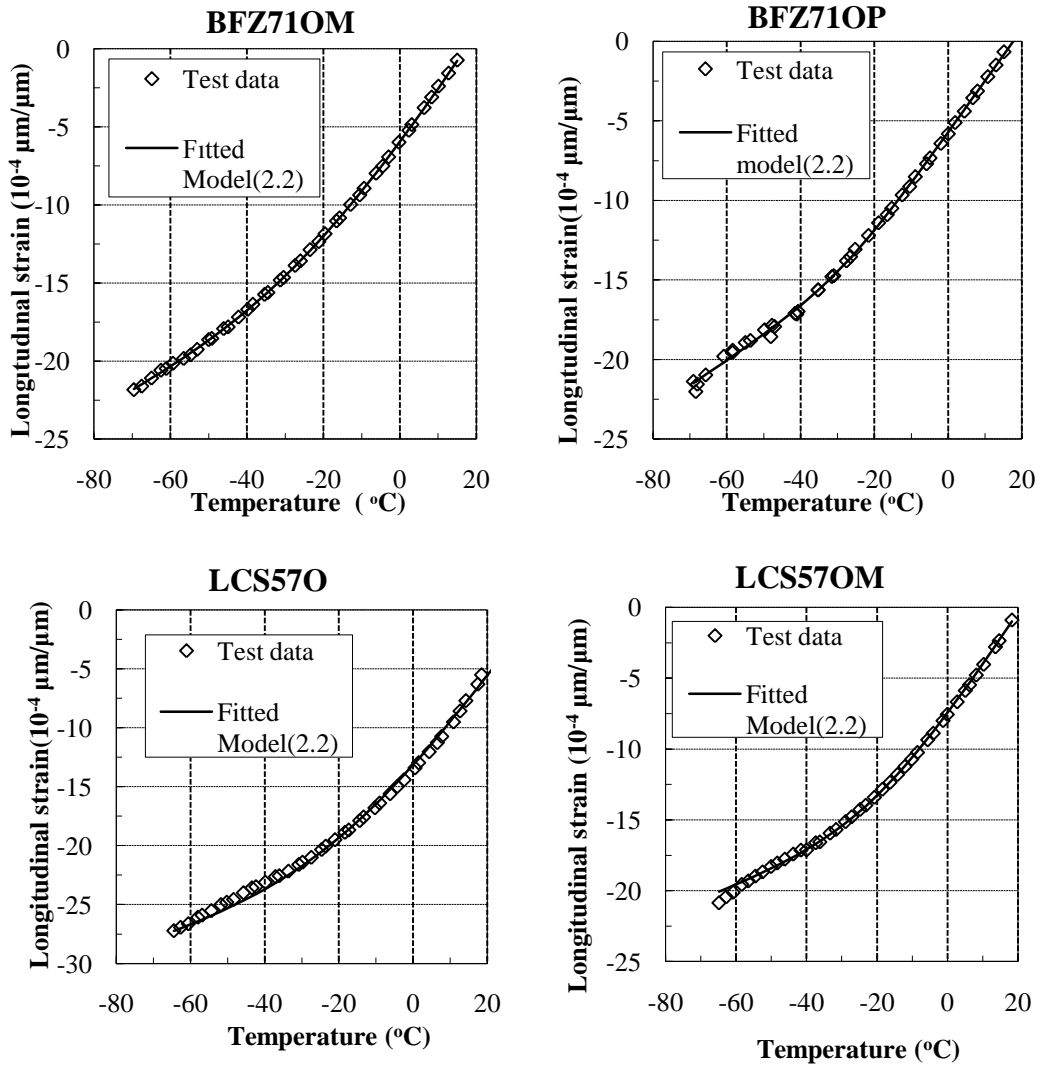


**Figure B1 (continued)**

**Symbols used:**

Aggregate : L-limestone, B-Basalt; Gradation: C-Coarse, F-Fine; Modification: Z-no Modification ,S-SBS Modification; AC type: 57-50 70, 71-71 100;AC content: O-optimum, OP optimum plus, OM optimum minus.

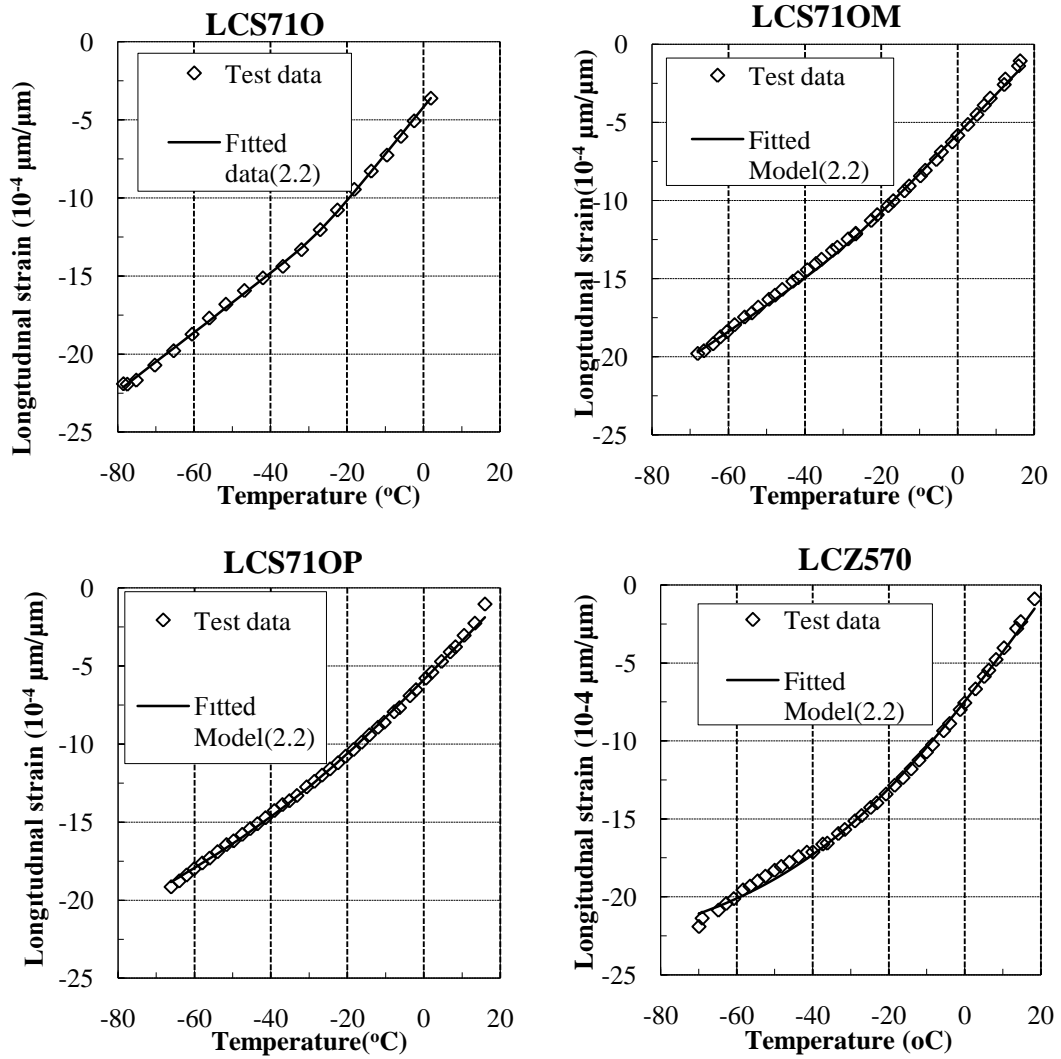


**Figure B1 (continued)**

**Symbols used:**

Aggregate : L-limestone, B-Basalt; Gradation: C-Coarse, F-Fine; Polymer modification: Z-no Modification ,S-SBS Modification; AC type: 57-50 70, 71-71 100;AC content: O-optimum, OP- Optimum plus, OM- Optimum minus.

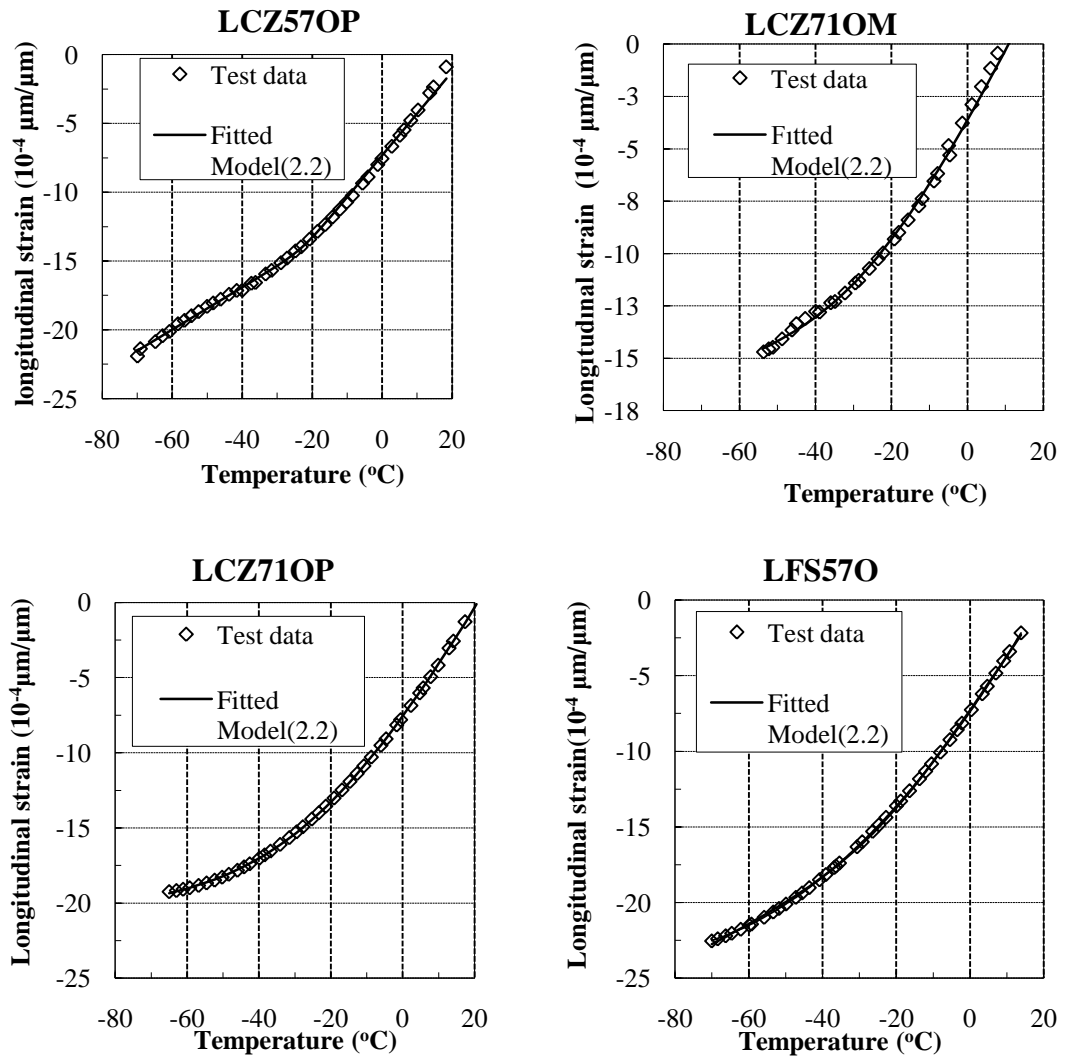


**Figure B1 (continued)**

**Symbols used:**

Aggregate : L-limestone, B-Basalt; Gradation: C-Coarse, F-Fine; Modification: Z-no Modification ,S-SBS Modification; AC type: 57-50 70, 71-71 100;AC content: O-optimum, OP optimum plus, OM optimum minus.

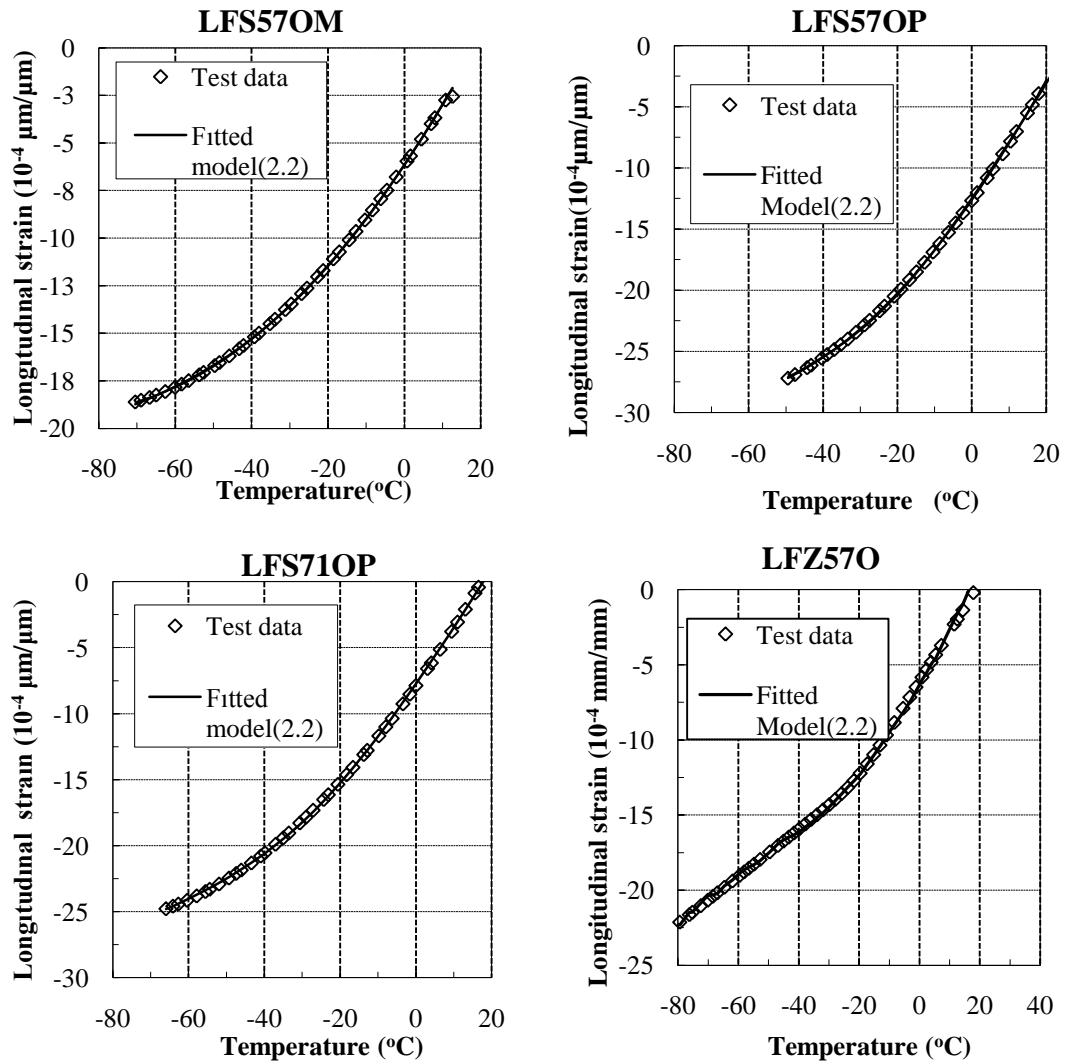


**Figure B1 (continued)**

**Symbols used:**

Aggregate : L-limestone, B-Basalt; Gradation: C-Coarse, F-Fine; Polymer modification: Z-no Modification ,S-SBS Modification; AC type: 57-50 70, 71-71 100;AC content: O-optimum, OP- Optimum plus, OM- Optimum minus.

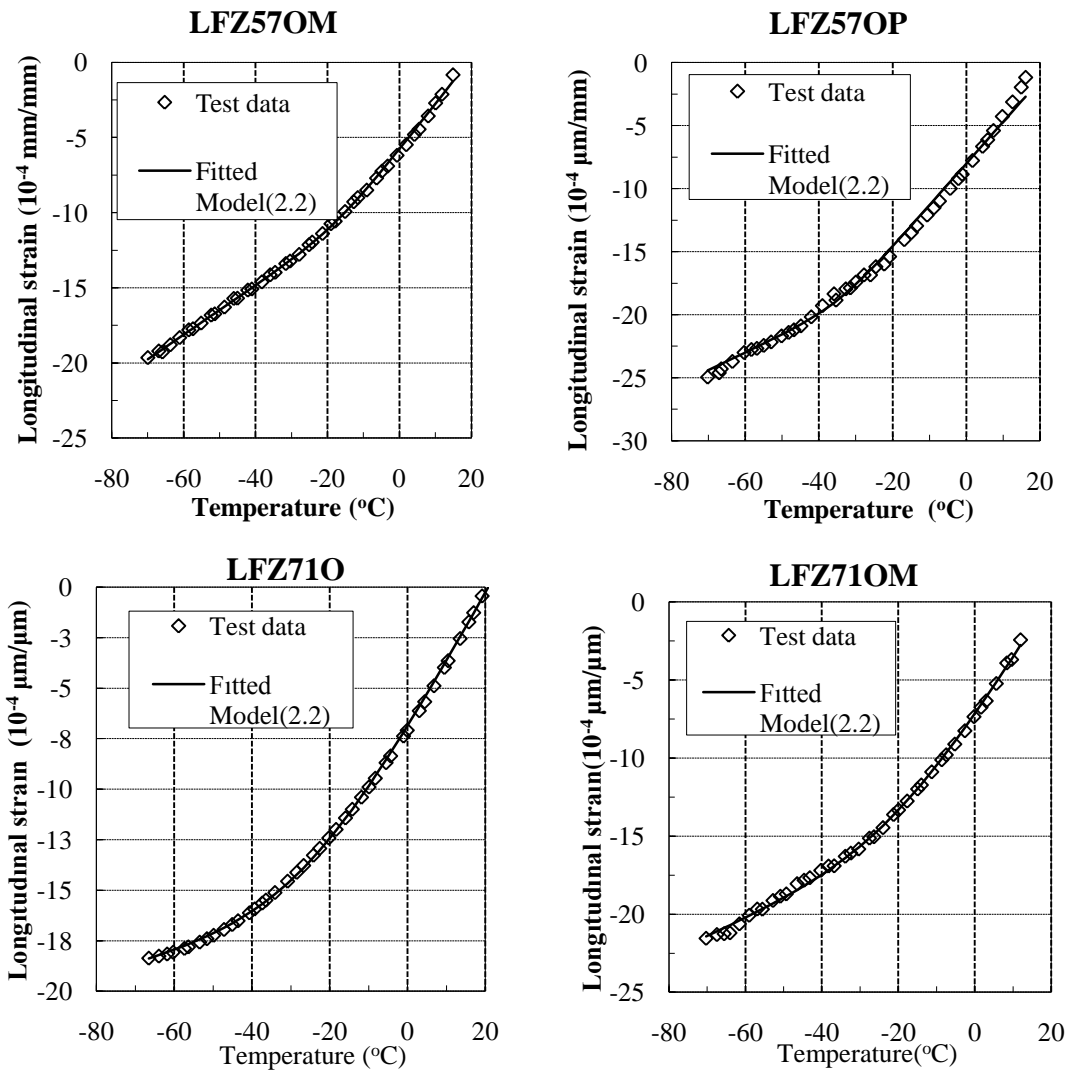


**Figure B1 (continued)**

**Symbols used:**

Aggregate : L-limestone, B-Basalt; Gradation: C-Coarse, F-Fine; Polymer modification: Z-no Modification ,S-SBS Modification; AC type: 57-50 70, 71-71 100;AC content: O-optimum, OP- Optimum plus, OM- Optimum minus.

## C- MATLAB CODES

### C1- For fracture analysis

```
K = menu('Low Temperature Cracking of Asphalt Concrete','Start Using the Programme','Calculation of Coefficient of linear expansion ','Calculation of Fracture Stress and Temperature','Exit')
if K==2;
    clc
    FileName=input('Enter File Name with txt extension: ','s')
    [A,LVD1,LVD2,D,E,T,Lo,CF ] = textread(FileName,'%f%f%f%f%f%f%f%f','headerlines',1);
    SampleId=input('Enter Sample Id= ','s');
    Samplename=input('Enter full description of Sample tested= ','s');
    Samplecode=input('Enter Sample Code= ','s');
    Length=input('Enter Length of Sample tested(millimeters),300 or 200= ');
    L=length(T);
    L1=sum(LVD1);
    L2=sum(LVD2);
    deltaL=(L1+L2)./2;
    DeltaT=T(L)-T(1);
    Alpha=(deltaL)/(L*1000000*DeltaT);
    disp([' Sample Id= ',SampleId])
    disp(['Description of Sample tested= ',Samplename])
    disp(['Sample Code= ',Samplecode])
    disp(['Coefficient of linear expansion for the sample=',num2str(Alpha)])
    break
elseif K==3
    clear all, close all hidden
    FileName=input('Enter File Name with txt extension: ','s')
```

```

[Time,LVD1,LVD2,D,E,T,Lo,CF ] = tex-
tread(FileName,'%f%f%f%f%f%f%f%f', 'headerlines',1);
SampleId=input('Enter Sample Id= ','s');
Samplename=input('Enter full description of Sample tested= ','s');
Samplecode=input('Enter Sample Code= ','s');
Area=input('Enter Area of Cross Section of Sample tested(square millimeters)= ');
P = polyfit(Lo, Time,2);
Y = polyval(P,Lo);
ypred = polyval(P,Lo);
dev = Time -mean(Time );
SST = sum(dev.^2);
resid = Time -ypred;
SSE = sum(resid.^2);
normr = sqrt(SSE); % residual norm
Rsqr = 1 -SSE/SST ; % R2 Error
timepredic=polyval(P,max(Lo));
AVERAGELVDT=0.5*(LVD1+LVD2);
P1 = polyfit(Time, AVERAGELVDT,1);
Y = polyval(P1,Time);
ypred1 = polyval(P1,Time);
dev1 = AVERAGELVDT -mean(AVERAGELVDT );
SST1 = sum(dev.^2);
resid1 = AVERAGELVDT -ypred;
SSE1 = sum(resid.^2);
normr1 = sqrt(SSE); % residual norm
Rsqr2 = 1 -SSE/SST ;% R2 Error
timebeforefracture=timepredic-60;
avglvdatfracture=polyval(P1,timebeforefracture);
P1 = polyfit(Time, AVERAGELVDT,1);
Y = polyval(P1,Time);
ypred1 = polyval(P1,Time);

```

```

dev1 = AVERAGELVDT -mean(AVERAGELVDT );
SST1 = sum(dev.^2);
resid1 = AVERAGELVDT -ypred;
SSE1 = sum(resid.^2);
normr1 = sqrt(SSE); % residual norm
Rsq2 = 1 -SSE/SST ;% R2 Error
timebeforefracture=timepredic-300;
avglvdatfracture=polyval(P1,timebeforefracture);
P2 = polyfit(Time, LVD1,1);
Y = polyval(P2,Time);
ypred2 = polyval(P2,Time);
dev2 = LVD1 -mean(LVD1 );
SST2 = sum(dev.^2);
resid2 = LVD1 -ypred;
SSE2 = sum(resid.^2);
normr2 = sqrt(SSE); % residual norm
Rsq3 = 1 -SSE/SST ;% R2 Error
LVDVALUEATFRACTURE=polyval(P2,timebeforefracture);
ECCENTRICITY=LVDVALUEATFRACTURE-avglvdatfracture;

x= min(T);
y=max(Lo);
L=length(T);
L1=length(Lo );
Temp=dot(T,CF,L);
Loads=dot(Lo,CF,L);
Temp=Temp(Temp~=0);
Loads=Loads(Loads~=0);
L=length(Temp);
L1=length(Loads );
Stress=Loads.*9.81/Area;

```

```

AA=smooth(Stress ,25);
BB=smooth(Temp,25);

%evaluating the data for Linear fit
    P = polyfit(BB, AA,1);
Y = polyval(P,Temp);
ypred = polyval(P,Temp);
dev = Stress -mean(Stress );
SST = sum(dev.^2);
resid = AA -ypred;
SSE = sum(resid.^2);
normr = sqrt(SSE); % residual norm
Rsq = 1 -SSE/SST ; % R2 Error
%evaluating the data for Quadratic fit
P1 = polyfit(BB, AA,2);
Y1 = polyval(P1,Temp);
ypred1 = polyval(P1,Temp);
dev1 = Stress -mean(Stress );
SST1 = sum(dev.^2);
resid1 = AA -ypred1;
SSE1 = sum(resid1.^2);
normr = sqrt(SSE1); % residual norm
Rsq1 = 1 -SSE1/SST1 ; % R2 Error
%evaluating the data for Cubic fit
P2 = polyfit(BB, AA,3);
Y2 = polyval(P2,Temp);
ypred2 = polyval(P2,Temp);
dev2 = Stress -mean(Stress );
SST2 = sum(dev.^2);
resid2= AA -ypred2;
SSE2 = sum(resid2.^2);

```

```

normr = sqrt(SSE2); % residual norm
Rsq2 = 1 -SSE2/SST2 ; % R2 Error
%evaluating the data for Fourth Order fit
P3 = polyfit(BB, AA,4);
Y3= polyval(P3,Temp);
ypred3 = polyval(P3,Temp);
dev3 = Stress -mean(Stress );
SST3 = sum(dev.^2);
resid3= AA -ypred3;
SSE3 = sum(resid3.^2);
normr = sqrt(SSE3); % residual norm
Rsq3 = 1 -SSE3/SST3 ; % R2 Error

% Estimating the best option
R1=Rsq;
R2=Rsq1;
R3=Rsq2;
R4=0;
R=[R1 R2 R3 R4];
Rmax=max(R);
% Plotting if linear fit is ok
if R1==Rmax
close all

scrsz = get(0,'ScreenSize');

figure(1) = figure('Position',[1 scrsz(2)/1.5 scrsz(2)/1.5 scrsz(2)/1.5], 'PaperSize',[41
41],...
'Name',SampleId,...
'Color',[0.9725 0.9725 0.9725]);
hold on

```

```

box('on');
hold('all')
% Create title
title({'Sample Description:',Samplename,Samplecode },...
      'FontSize',16,...
      'FontName','Times New Roman',...
      'HorizontalAlignment','center');
FS=polyval(P,x);
ylim([0 (round(FS)+1)]);xlim([roundn(min(T),1)-5 round(max(T))+2])
k=min(T):.05:roundn((max(Temp))+2);
kk=polyval(P,k);
plot(Temp,Stress ,'Marker','o','LineStyle','none','Color',[1 0 0],...
      'DisplayName','Original data')
plot(k,kk,'blue*-', 'DisplayName','Best Fit')
% Create xlabel
xlabel({'Temperature C'});
% Create ylabel
ylabel('Stress MPa');

hold on
legend('show');
% Create xlabel
xlabel({'Temperature C'});

% Create ylabel
ylabel('Stress MPa');
hold on
% Plotting if quadratic fit is ok
elseif R2==Rmax
Y=Y1;
close all

```

```

scrsz = get(0,'ScreenSize');

figure(1) = figure('Position',[1 scrsz(2)/1.5 scrsz(2)/1.5 scrsz(2)/1.5], 'PaperSize',[41
41],...
    'Name',SampleId,...
    'Color',[0.9725 0.9725 0.9725]);
hold on
box('on');
hold('all')
% Create title
title({'Sample Description:',Samplename,Samplecode },...
    'FontSize',16,...
    'FontName','Times New Roman',...
    'HorizontalAlignment','center');

FS=polyval(P1,x);
ylim([0 (round(FS)+1)]);xlim([roundn(min(T),1)-5 round(max(T))+2])
k=min(T):.05:roundn((max(Temp))+2);
kk=polyval(P1,k);
plot(Temp,Stress,'Marker','o','LineStyle','none','Color',[1 0 0],...
    'DisplayName','Original data')
plot(k,kk,'yellow*-', 'DisplayName','Best Fit')
% Create xlabel
xlabel({'Temperature C'});

% Create ylabel
ylabel('Stress MPa');

hold on
% Plotting if cubic fit is ok
elseif R3==Rmax

```

```

close all
scrsz = get(0,'ScreenSize');

figure(1) = figure('Position',[1 scrsz(2)/1.5 scrsz(2)/1.5 scrsz(2)/1.5], 'PaperSize',[41
41],...
    'Name',SampleId,...
    'Color',[0.9725 0.9725 0.9725]);
hold on
box('on');
hold('all')
% Create title
title({'Sample Description:',Samplename,Samplecode },...
    'FontSize',16,...
    'FontName','Times New Roman',...
    'HorizontalAlignment','center');
FS=polyval(P2,x);
ylim([0 (round(FS)+1)]);xlim([roundn(min(T),1)-5 round(max(T))+2])
k=min(T):.05:roundn((max(Temp))+2);
kk=polyval(P2,k);
plot(Temp,Stress , 'Marker','o','LineStyle','none','Color',[1 0 0],...
    'DisplayName','Original data')
plot(k,kk,'black*-', 'linewidth',6,'DisplayName','Best Fit')
% Create xlabel
xlabel({'Temperature C'});

% Create ylabel
ylabel('Stress MPa');

hold on
% Plotting if fourth order fit is ok
else

```

```

close all

scrsz = get(0,'ScreenSize');

figure(1) = figure('Position',[1 scrsz(2)/1.5 scrsz(2)/1.5 scrsz(2)/1.5], 'PaperSize',[41
41],...
    'Name',Samplename,...
    'Color',[0.9725 0.9725 0.9725]);
hold on
box('on');
hold('all')
% Create title
title({'Sample Description:',Samplename,Samplecode },...
    'FontSize',16,...
    'FontName','Times New Roman',...
    'HorizontalAlignment','center');
FS=polyval(P3,x);
k=min(T):min(Temp);
kk=polyval(P3,k);
ylim([0 (round(FS)+1)]);
xlim([-25 round(max(T))+1])
plot(Temp,Stress , 'Marker','o','LineStyle','none','Color',[1 0 0],...
    'DisplayName','Original data')
plot(Temp,Y3,'black','linewidth',6,'DisplayName','Best Fit')
plot(k,kk,'black','linewidth',6,'DisplayName','Best Fit')
% Create xlabel
xlabel({'Temperature C'});

% Create ylabel
ylabel('Stress MPa');
hold on

```

```

end
N1=3*L/4;
N1=round(N1);
N1=L-N1;
    TL1=smooth(Temp(N1:L),25);
        LL1=smooth(Stress (N1:L),25);
    ST1 = polyfit(TL1, LL1,1);
        ypredicted1=polyval(ST1,TL1);
d1= LL1-mean(LL1);
sst1 = sum(d1.^2);
residue1= LL1 -ypredicted1;
sse1 = sum(residue1.^2);
norresidue1 = sqrt(sse1); % residual norm
r1 = 1 -sse1/sst1;
Ak1=(min(T)):(min(Temp)+1);
Akk1=polyval(ST1,Ak1);

N2=L/4;
N2=round(N2);
N2=L-N2;

    TL2=smooth(Temp(N2:L),25);
        LL2=smooth(Stress (N2:L),25);
    ST2 = polyfit(TL2, LL2,1);
        ypredicted2=polyval(ST2,TL2);
d2 = LL2 -mean(LL2);
sst2 = sum(d2.^2);
residue2= LL2 -ypredicted2;
sse2 = sum(residue2.^2);
norresidue1 = sqrt(sse2); % residual norm
r2 = 1 -sse2/sst2;

```

```

Ak2=(min(T)):(min(Temp)+1);
Akk2=polyval(ST2,Ak2);

N3=L/2;
N3=round(N3);
N3=L-N3;

    TL3=smooth(Temp(N3:L),25);
        LL3=smooth(Stress (N3:L),25);
    ST3 = polyfit(TL3, LL3,1);
        ypredicted3=polyval(ST3,TL3);
d3 = LL3 -mean(LL3);
sst3 = sum(d3.^2);
residue3= LL3 -ypredicted3;
sse3 = sum(residue3.^2);
norresidue3 = sqrt(sse3); % residual norm
r3 = 1 -sse3/sst3;
Ak3=(min(T)):(min(Temp)+1);
Akk3=polyval(ST3,Ak3);

% checking at L/3

N4=L/3;
N4=round(N4);
N4=L-N4;

    TL4=smooth(Temp(N4:L),25);
        LL4=smooth(Stress (N4:L),25);
    ST4 = polyfit(TL4, LL4,1);
        ypredicted4=polyval(ST4,TL4);
d4 = LL4 -mean(LL4);

```

```

sst4 = sum(d4.^2);
residue4= LL4 -ypredicted4;
sse4 = sum(residue4.^2);
norresidue4 = sqrt(sse4); % residual norm
r4 = 1 -sse4/sst4;
Ak4=(min(T)):(min(Temp)+1);
Akk4=polyval(ST4,Ak4);

r=[r1,r2,r3,r4];
rmax=max(r);
if r1==rmax
plot(TL1,ypredicted1,'green','linewidth',6,'DisplayName','Linear Portion of curve')
hold on
plot(Ak1 ,Akk1,'green','linewidth',6,'LineStyle','-','DisplayName','Linear Portion of
curve')
hold on
xx1=-ST1(2)/ST1(1)
plot([xx1 TL1(1)],[0 ypredicted1(1)],'blue','linewidth',8,'LineStyle','--
','DisplayName','Extension of linear plot')
hold on
u=plot([TL1(1) TL1(1)],[0 ypredicted1(1)],'DisplayName','Start of Transition Tem-
perature');
    set(u,'Color',[1,0,0],'linewidth',2,'LineStyle','--')
    hold on
    uu=plot([TL1(1) max(xlim) ],[ypredicted1(1) ypre-
dicted1(1)],'DisplayName','Start of Relaxation Stress');
    set(uu,'Color',[1,0,0],'linewidth',2,'LineStyle','--')
    set(uu,'Color',[0,1,1],'linewidth',2,'LineStyle','--')
    annotation('textbox',[0.5953 0.3041 0.2119 0.04375],...
'String',{'Stress Relaxation(MPa)=' ,ypredicted1(1)},...
'FontSize',10,...

```

```

    'FontName','Times New Roman',...
    'HorizontalAlignment','center',...
    'FitBoxToText','on',...
    'LineStyle','none');

% Create textbox
annotation('textbox',[0.4102 0.1178 0.2109 0.04375],...
    'String',{'Transition Temperature(C)='},TL1(1)},...
    'FontSize',10,...
    'FontName','Times New Roman',...
    'HorizontalAlignment','center',...
    'FitBoxToText','on',...
    'LineStyle','none');

uuu=plot([x x],[0 FS],'DisplayName','Fracture Temperature');
    set(uuu,'Color',[1,0,1],'linewidth',2,'LineStyle','--')
    hold on
    gh=plot([x min(xlim) ],[FS FS],'DisplayName','Fracture Stress');
    set(gh,'Color',[1,0,0],'linewidth',2,'LineStyle','--')
    set(gh,'Color',[0,1,1],'linewidth',2,'LineStyle','--')
    annotation('textbox',[0.1647 0.521 0.1752 0.108],...
    'String',{'Fracture Stress(MPa='},FS)},...
    'FontSize',10,...
    'FontName','Times New Roman',...
    'HorizontalAlignment','center',...
    'FitBoxToText','on',...
    'LineStyle','none');

% Create textbox
annotation('textbox',[0.1977 0.1536 0.2197 0.04375],...
    'String',{'Fracture Temperature(C)='},x)},...

```

```

    'FontSize',10,...
    'FontName','Times New Roman',...
    'HorizontalAlignment','center',...
    'FitBoxToText','on',...
    'LineStyle','none');

    hold off
    % Create legend
        legend('show');

disp(['Description of Sample tested= ',Samplename]);
disp(['Sample Code= ',Samplecode]);
disp(['Transition Temperature(C)=' ,num2str(TL1(1))])
    disp(['Stress Relaxation(MPa)=' ,num2str(ypredicted1(1))])
    disp(['Rate of Change of Stress,"1 MPa per degree C Fall in Temperature"
=' ,num2str(1/ST1(1))])
        disp(['Fracture Temperature(C)=' ,num2str(min(T))])
        disp(['Fracture Stress(MPa)=' ,num2str(FS)])
        disp(['Eccentricity(micron)=' ,num2str(ECCENTRICITY)])
elseif r2==rmax
plot(TL2,ypredicted2,'green','linewidth',6,'DisplayName','Linear Portion of curve')
hold on
plot(Ak2,Akk2,'green','linewidth',6,'LineStyle','-','DisplayName','Linear Portion of
curve')
hold on
xx2=-ST2(2)/ST2(1)
plot([xx2 TL2(1)],[0 ypredicted2(1)],'blue','linewidth',8,'LineStyle','--
','DisplayName','Extension of linear plot')
hold on
v=plot([TL2(1) TL2(1)],[0 ypredicted2(1)],'DisplayName','Start of Transition Tem-
perature');

```

```

set(v,'Color',[1,0,0],'linewidth',2,'LineStyle','--')
hold on
vv=plot([TL2(1) max(xlim)],[ypredicted2(1) ypre-
dicted2(1)'],'DisplayName','Start of Relaxation Stress');
set(vv,'Color',[1,0,0],'linewidth',2,'LineStyle','--')
set(vv,'Color',[0,1,1],'linewidth',2,'LineStyle','--')
annotation('textbox',[0.5953 0.3041 0.2119 0.04375],...
'String',{'Stress Relaxation(MPa)='},ypredicted2(1)},...
'FontSize',10,...
'FontName','Times New Roman',...
'HorizontalAlignment','center',...
'FitBoxToText','on',...
'LineStyle','none');
% Create textbox
annotation('textbox',[0.4102 0.1178 0.2109 0.04375],...
'String',{'Transition Temperature(C)='},TL2(1)},...
'FontSize',10,...
'FontName','Times New Roman',...
'HorizontalAlignment','center',...
'FitBoxToText','on',...
'LineStyle','none');

vvv=plot([x x],[0 FS'],'DisplayName','Fracture Temperature');
set(vvv,'Color',[1,0,1],'linewidth',2,'LineStyle','--')
hold on
vh=plot([x min(xlim) ],[FS FS'],'DisplayName','Fracture Stress');
set(vh,'Color',[1,0,0],'linewidth',2,'LineStyle','--')
set(vh,'Color',[0,1,1],'linewidth',2,'LineStyle','--')
annotation('textbox',[0.1647 0.521 0.1752 0.108],...
'String',{'Fracture Stress(MPa)='},FS)},...
'FontSize',10,...

```

```

'FontName','Times New Roman',...
'HorizontalAlignment','center',...
'FitBoxToText','on',...
'LineStyle','none');

% Create textbox
annotation('textbox',[0.1977 0.1536 0.2197 0.04375],...
'String',{'Fracture Temperature(C)=',x},...
'FontSize',10,...
'FontName','Times New Roman',...
'HorizontalAlignment','center',...
'FitBoxToText','on',...
'LineStyle','none');

hold off
% Create legend
legend('show');

disp(['Description of Sample tested= ',Samplename]);
disp(['Sample Code= ',Samplecode]);
disp(['Transition Temperature(C)=',num2str(TL2(1))])
disp(['Stress Relaxation(MPa)=',num2str(ypredicted2(1))])
disp(['Rate of Change of Stress,"1 MPa per degree C Fall in Temperature"
=',num2str(1/ST2(1))])
disp(['Fracture Temperature(C)=',num2str(min(T))])
disp(['Fracture Stress(MPa)=',num2str(FS)])
disp(['Eccentricity(micron)=',num2str(ECCENTRICITY)])

% IF L/2 IS THE BEST FIT
elseif r3==rmax
plot(TL3,ypredicted3,'green','linewidth',6,'DisplayName','Linear Portion of curve')
hold on

```

```

plot(Ak3,Akk3,'green','linewidth',6,'LineStyle','-','DisplayName','Linear Portion of
curve')
hold on
xx3=-ST3(2)/ST3(1);
plot([xx3 TL3(1)],[0 ypredicted3(1)],'blue','linewidth',8,'LineStyle','--
','DisplayName','Extension of linear plot')
hold on
w=plot([TL3(1) TL3(1)],[0 ypredicted3(1)],'DisplayName','Start of Transition Tem-
perature');
    set(w,'Color',[1,0,0],'linewidth',2,'LineStyle','--')
    hold on
    ww=plot([TL3(1) max(xlim)],[ypredicted3(1) ypre-
dicted3(1)],'DisplayName','Start of Relaxation Stress');
    set(ww,'Color',[1,0,0],'linewidth',2,'LineStyle','--')
    set(ww,'Color',[0,1,1],'linewidth',2,'LineStyle','--')
    annotation('textbox',[0.5953 0.3041 0.2119 0.04375],...
'String',{'Stress Relaxation(MPa)=' ,ypredicted3(1)},...
'FontSize',10,...
'FontName','Times New Roman',...
'HorizontalAlignment','center',...
'FitBoxToText','on',...
'LineStyle','none');

% Create textbox
annotation('textbox',[0.4102 0.1178 0.2109 0.04375],...
'String',{'Transition Temperature(C)=' ,TL3(1)},...
'FontSize',10,...
'FontName','Times New Roman',...
'HorizontalAlignment','center',...
'FitBoxToText','on',...
'LineStyle','none');

```

```

www=plot([x x],[0 FS],'DisplayName','Fracture Temperature');
    set(www,'Color',[1,0,1],'linewidth',2,'LineStyle','--')
    hold on
    wh=plot([x min(xlim) ],[FS FS],'DisplayName','Fracture Stress');
    set(wh,'Color',[1,0,0],'linewidth',2,'LineStyle','--')
    set(wh,'Color',[0,1,1],'linewidth',2,'LineStyle','--')
    annotation('textbox',[0.1647 0.521 0.1752 0.108],...
'String',{'Fracture Stress(MPa=','FS')},...
'FontSize',10,...
'FontName','Times New Roman',...
'HorizontalAlignment','center',...
'FitBoxToText','on',...
'LineStyle','none');

% Create textbox
annotation('textbox',[0.1977 0.1536 0.2197 0.04375],...
'String',{'Fracture Temperature(C)=','x'},...
'FontSize',10,...
'FontName','Times New Roman',...
'HorizontalAlignment','left',...
'FitBoxToText','on',...
'LineStyle','none');

    hold off
    % Create legend
        legend('show');

        disp(['Description of Sample tested= ',Samplename]);
disp(['Sample Code= ',Samplecode]);
disp(['Transition Temperature(C)=',num2str(TL3(1))])

```

```

disp(['Stress Relaxation(MPa)=' num2str(ypredicted3(1))])
disp(['Rate of Change of Stress," 1 MPa per degree C Fall in Temperature"
=' num2str(1/ST3(1))])
disp(['Fracture Temperature(C)=' num2str(min(T))])
disp(['Fracture Stress(MPa)=' num2str(FS)])
disp(['Eccentricity(micron)=' num2str(ECCENTRICITY)])

else r4==rmax
plot(TL4,ypredicted4,'green','linewidth',6,'DisplayName','Linear Portion of curve')
hold on
plot(Ak4,Akk4,'green','linewidth',6,'LineStyle','-','DisplayName','Linear Portion of
curve')
hold on
xx4=-ST4(2)/ST4(1);
plot([xx4 TL4(1)],[0 ypredicted4(1)'],'blue','linewidth',8,'LineStyle','--
','DisplayName','Extension of linear plot')
hold on
w=plot([TL4(1) TL4(1)],[0 ypredicted4(1)'],'DisplayName','Start of Transition Tem-
perature');
set(w,'Color',[1,0,0],'linewidth',2,'LineStyle','--')
hold on
ww=plot([TL4(1) max(xlim)],[ypredicted4(1) ypre-
dicted4(1)'],'DisplayName','Start of Relaxation Stress');
set(ww,'Color',[1,0,0],'linewidth',2,'LineStyle','--')
set(ww,'Color',[0,1,1],'linewidth',2,'LineStyle','--')
annotation('textbox',[0.5953 0.3041 0.2119 0.04375],...
'String',{'Stress Relaxation(MPa)=' ypredicted4(1)'},...
'FontSize',10,...
'FontName','Times New Roman',...
'HorizontalAlignment','center',...

```

```

    'FitBoxToText','on',...
    'LineStyle','none');

% Create textbox
annotation('textbox',[0.4102 0.1178 0.2109 0.04375],...
    'String',{'Transition Temperature(C)='},TL4(1)},...
    'FontSize',10,...
    'FontName','Times New Roman',...
    'HorizontalAlignment','center',...
    'FitBoxToText','on',...
    'LineStyle','none');

www=plot([x x],[0 FS],'DisplayName','Fracture Temperature');
set(www,'Color',[1,0,1],'linewidth',2,'LineStyle','--')
hold on
wh=plot([x min(xlim) ],[FS FS],'DisplayName','Fracture Stress');
set(wh,'Color',[1,0,0],'linewidth',2,'LineStyle','--')
set(wh,'Color',[0,1,1],'linewidth',2,'LineStyle','--')
annotation('textbox',[0.1647 0.521 0.1752 0.108],...
    'String',{'Fracture Stress(MPa='},FS)},...
    'FontSize',10,...
    'FontName','Times New Roman',...
    'HorizontalAlignment','center',...
    'FitBoxToText','on',...
    'LineStyle','none');

% Create textbox
annotation('textbox',[0.1977 0.1536 0.2197 0.04375],...
    'String',{'Fracture Temperature(C)='},x)},...
    'FontSize',10,...
    'FontName','Times New Roman',...

```

```

    'HorizontalAlignment','center',...
    'FitBoxToText','on',...
    'LineStyle','none');

disp(['Description of Sample tested= ',Samplename]);
disp(['Sample Code= ',Samplecode]);
disp(['Transition Temperature(C)=',num2str(TL4(1))])
    disp(['Stress Relaxation(MPa)=',num2str(ypredicted4(1))])
    disp(['Rate of Change of Stress,"1 MPa per degree C Fall in Temperature"
= ',num2str(1/ST4(1))])
        disp(['Fracture Temperature(C)=',num2str(min(T))])
    disp(['Fracture Stress(MPa)=',num2str(FS)])
    disp(['Eccentricity(micron)=',num2str(ECCENTRICITY)])
end
end

```

## C2- For ANOVA of fracture data

```
clear all;close all hidden

fid = fopen('ALLDATA.txt'); % open the data file datamatrix.txt
% read the data file content to array r
r = textscan(fid,'%s %s %s %s %s %s %s %f %f %f %f %f %f');
fclose(fid); % close the data file publicationdata.txt

factors = {[r{1}] [r{2}] [r{3}] [r{4}] [r{5}] [r{6}] [r{7}]};

% caculate 2-way anova
VNames = {'Aggregate' 'Gradation' 'SIZE' 'Modification' 'AC type' 'AC content'
'Cooling rate' };
anovan([r{8}],{[r{1}],[r{2}],[r{3}],[r{4}],[r{5}], [r{6}], [r{7}]},2,2,VNames)
anovan([r{9}],{[r{1}],[r{2}],[r{3}],[r{4}],[r{5}], [r{6}], [r{7}]},2,2,VNames)
anovan([r{10}],{[r{1}],[r{2}],[r{3}],[r{4}],[r{5}], [r{6}], [r{7}]},2,2,VNames)
anovan([r{11}],{[r{1}],[r{2}],[r{3}],[r{4}],[r{5}], [r{6}], [r{7}]},2,2,VNames)
anovan([r{12}],{[r{1}],[r{2}],[r{3}],[r{4}],[r{5}], [r{6}], [r{7}]},2,2,VNames)
anovan([r{13}],{[r{1}],[r{2}],[r{3}],[r{4}],[r{5}], [r{6}], [r{7}]},2,2,VNames)
anovan([r{14}],{[r{1}],[r{2}],[r{3}],[r{4}],[r{5}], [r{6}], [r{7}]},2,2,VNames)
```

### C3- For ANOVA of glass transition temperature data

```
clear all;close all hidden
clc
fid = fopen('GLASSANOVA.txt'); % open the data file datamatrix.txt
% read the data file content to array r
r = textscan(fid,['%s %s %s %s %s %f %f %f %f %f %f %f']);
fclose(fid); % close the data file publicationdata.txt

factors = {[r{1}] [r{2}] [r{3}] [r{4}] [r{5}] [r{6}] [r{7}]};

% caculate 2-way anova for gradation, ac content and manuf. sand content
VNames = {'Aggregate ' 'Gradation' 'Modification' 'AC type' 'AC content' };
anovan([r{6}],{[r{1}],[r{2}],[r{3}],[r{4}],[r{5}] },2,2,VNames);
anovan([r{7}],{[r{1}],[r{2}],[r{3}],[r{4}],[r{5}] },2,2,VNames);
anovan([r{8}],{[r{1}],[r{2}],[r{3}],[r{4}],[r{5}] },2,2,VNames);
anovan([r{9}],{[r{1}],[r{2}],[r{3}],[r{4}],[r{5}] },2,2,VNames);
anovan([r{10}],{[r{1}],[r{2}],[r{3}],[r{4}],[r{5}] },2,2,VNames);
anovan([r{11}],{[r{1}],[r{2}],[r{3}],[r{4}],[r{5}] },2,2,VNames);
anovan([r{12}],{[r{1}],[r{2}],[r{3}],[r{4}],[r{5}] },2,2,VNames)
```

## D-ANOVA TABLES

**Table D1- For fracture strength response**

Source	Sum Sq.	d.f.	Prob>F
Aggregate type	29.91	1	0.00
Gradation	1.69	1	0.04
Specimen length	0.39	1	0.32
Polymer modification	1.06	1	0.10
AC type	1.03	1	0.11
AC content	10.13	2	0.00
Cooling rate	1.32	2	0.19
Aggregate type*Gradation	4.85	1	0.00
Aggregate type *Specimen length	1.60	1	0.04
Aggregate type * Polymer modification	0.09	1	0.63
Aggregate type *AC type	0.45	1	0.28
Aggregate type *AC content	0.35	2	0.64
Aggregate type *cooling rate	1.28	2	0.20
Gradation*Specimen length	3.76	1	0.00
Gradation* Polymer modification	0.02	1	0.84
Gradation*AC type	0.31	1	0.37
Gradation*AC content	2.66	2	0.04
Gradation*Cooling rate	3.58	2	0.01
Specimen length * Polymer modification	0.16	1	0.52
Specimen length *AC type	0.75	1	0.17
Specimen length *AC content	0.61	2	0.46
Specimen length *Cooling rate	3.55	2	0.01
Polymer modification *AC type	7.05	1	0.00
Polymer modification *AC content	0.58	2	0.47
Polymer modification *Cooling rate	0.15	2	0.82
AC type*AC content	2.55	2	0.04
AC type*Cooling rate	0.12	2	0.86
AC content*Cooling rate	7.32	4	0.00
Error	38.78	100	
Total	191.35	143	

**Table D2- For fracture temperature response**

<b>Source</b>	<b>Sum Sq.</b>	<b>d.f.</b>	<b>Prob&gt;F</b>
Aggregate type	167.76	1	0.00
Gradation	0.38	1	0.80
Specimen length	2.81	1	0.49
Polymer modification	28.13	1	0.03
AC type	5.93	1	0.31
AC content	49.33	2	0.02
cooling rate	6.57	2	0.57
Aggregate type *Gradation	3.32	1	0.45
Aggregate type *Specimen length	1.34	1	0.63
Aggregate type *Polymer modification	4.65	1	0.37
Aggregate type *AC type	20.52	1	0.06
Aggregate type *AC content	35.43	2	0.05
Aggregate type *cooling rate	31.90	2	0.07
Gradation*Specimen length	7.98	1	0.24
Gradation*Polymer modification	6.74	1	0.28
Gradation*AC type	5.30	1	0.34
Gradation*AC content	12.42	2	0.35
Gradation*cooling rate	39.57	2	0.04
Specimen length*Polymer modification	0.69	1	0.73
Specimen length*AC type	6.49	1	0.29
Specimen length*AC content	0.24	2	0.98
Specimen length*cooling rate	32.79	2	0.06
Polymer modification *AC type	31.63	1	0.02
Polymer modification *AC content	42.25	2	0.03
Polymer modification *cooling rate	1.46	2	0.88
AC type*AC content	67.44	2	0.00
AC type*cooling rate	6.05	2	0.59
AC content*cooling rate	61.03	4	0.04
Error	577.51	100	
Total	1,416.73	143	

**Table D3- For response of relaxation stress**

Analysis of Variance	Relaxation stress		
	Sum Sq.	d.f.	Prob>F
Aggregate type	10.26	1	0.00
Gradation	1.92	1	0.03
Specimen length	0.03	1	0.79
Polymer modification	0.35	1	0.34
AC type	0.20	1	0.48
AC content	5.64	2	0.00
Cooling rate	0.28	2	0.70
Aggregate type *Gradation	1.21	1	0.08
Aggregate type *Specimen length	1.02	1	0.11
Aggregate type *Polymer modification	0.69	1	0.19
Aggregate type *AC type	0.06	1	0.69
Aggregate type *AC content	1.51	2	0.15
Aggregate type * Cooling rate	0.17	2	0.81
Gradation* Specimen length	3.05	1	0.01
Gradation*Polymer modification	0.10	1	0.61
Gradation*AC type	0.90	1	0.13
Gradation*AC content	0.89	2	0.32
Gradation* Cooling rate	0.29	2	0.69
Specimen length *Polymer modification	0.03	1	0.79
Specimen length *AC type	0.00	1	1.00
Specimen length *AC content	0.77	2	0.38
Specimen length * Cooling rate	0.76	2	0.38
Polymer modification*AC type	6.47	1	0.00
Polymer modification*AC content	1.48	2	0.16
Polymer modification* Cooling rate	0.16	2	0.82
AC type*AC content	0.69	2	0.41
AC type* Cooling rate	0.89	2	0.32
AC content* Cooling rate	3.75	4	0.05
Error	38.84	100	
Total	112.52	143	

**Table D4- For response of transition temperature**

Analysis of Variance	Transition temperature		
	Sum Sq.	d.f.	Prob>F
Aggregate type	120.03	1	0.00
Gradation	13.33	1	0.25
Specimen length	2.17	1	0.64
Polymer modification	142.26	1	0.00
AC type	5.75	1	0.45
AC content	171.28	2	0.00
Cooling rate	6.06	2	0.74
Aggregate type *Gradation	13.22	1	0.26
Aggregate type *Specimen length	69.92	1	0.01
Aggregate type *Polymer modification	12.95	1	0.26
Aggregate type *AC type	0.47	1	0.83
Aggregate type *AC content	193.23	2	0.00
Aggregate type * Cooling rate	0.67	2	0.97
Gradation*Specimen length	13.02	1	0.26
Gradation*Polymer modification	1.48	1	0.70
Gradation*AC type	12.13	1	0.28
Gradation*AC content	17.50	2	0.42
Gradation*Cooling rate	79.11	2	0.02
Specimen length*Polymer modification	0.62	1	0.81
Specimen length*AC type	1.02	1	0.75
Specimen length*AC content	2.82	2	0.87
Specimen length*cooling rate	22.92	2	0.33
Polymer modification*AC type	80.93	1	0.01
Polymer modification*AC content	126.70	2	0.00
Polymer modification*Cooling rate	10.65	2	0.59
AC type*AC content	22.45	2	0.33
AC type*Cooling rate	23.58	2	0.32
AC content*Cooling rate	98.43	4	0.05
Error	1,010.46	100	
Total	2,718.79	143	

**Table D5- For response of slope ( $\Delta S/\Delta T$ )**

Source	Sum Sq.	d.f.	Prob>F
Aggregate type	0.06	1	0.00
Gradation	0.01	1	0.15
Specimen length	0.00	1	0.68
Polymer modification	0.05	1	0.00
AC type	0.03	1	0.01
AC content	0.05	2	0.00
Cooling rate	0.02	2	0.08
Aggregate type *Gradation	0.06	1	0.00
Aggregate type *Specimen length	0.02	1	0.02
Aggregate type *Polymer modification	0.00	1	0.41
Aggregate type *AC type	0.01	1	0.18
Aggregate type *AC content	0.02	2	0.10
Aggregate type *Cooling rate	0.01	2	0.39
Gradation*Specimen length	0.01	1	0.18
Gradation*Polymer modification	0.00	1	0.36
Gradation*AC type	0.01	1	0.26
Gradation*AC content	0.00	2	0.85
Gradation* Cooling rate	0.03	2	0.04
Specimen length*Polymer modification	0.00	1	0.47
Specimen length*AC type	0.00	1	0.40
Specimen length*AC content	0.01	2	0.18
Specimen length*Cooling rate	0.01	2	0.31
Polymer modification*AC type	0.01	1	0.07
Polymer modification*AC content	0.01	2	0.31
Polymer modification*Cooling rate	0.00	2	0.71
AC type*AC content	0.01	2	0.18
AC type*Cooling rate	0.00	2	0.79
AC content*Cooling rate	0.02	4	0.34
Error	0.39	100	
Total	1.09	143	

**Table D6- For response of air voids**

Source	Sum Sq.	d.f.	Prob>F
Aggregate type	245.30	1	-
Gradation	29.47	1	0.00
Specimen length	0.12	1	0.72
Polymer modification	0.01	1	0.92
AC type	21.83	1	0.00
AC content	83.59	2	0.00
Cooling rate	7.14	2	0.02
Aggregate type *Gradation	39.19	1	0.00
Aggregate type *Specimen length	1.10	1	0.27
Aggregate type *Polymer modification	0.46	1	0.48
Aggregate type *AC type	3.81	1	0.04
Aggregate type *AC content	1.08	2	0.55
Aggregate type *Cooling rate	1.38	2	0.46
Gradation *Specimen length	3.43	1	0.05
Gradation *Polymer modification	2.87	1	0.08
Gradation *AC type	0.48	1	0.47
Gradation *AC content	7.80	2	0.02
Gradation *Cooling rate	6.19	2	0.03
Specimlength *Polymer modification	0.13	1	0.71
Specimen length *AC type	0.83	1	0.34
Specimen length *AC content	5.17	2	0.06
Specimen length *Cooling rate	5.53	2	0.05
Polymer modification *AC type	8.89	1	0.00
Polymer modification *AC content	5.36	2	0.05
Polymer modification *Cooling rate	1.17	2	0.52
AC type *AC content	2.60	2	0.24
AC type *Cooling rate	1.53	2	0.43
AC content *Cooling rate	9.16	4	0.04
Error	89.22	100	
Total	1149.25	143	

**Table D7- For response of tensile load eccentricity**

Source	Sum Sq.	d.f.	Prob>F
Aggregate type	3222.00	1	0.17
Gradation	321.96	1	0.66
Specimen length	496.09	1	0.59
Polymer modification	1965.28	1	0.28
AC type	5011.62	1	0.09
AC content	458.06	2	0.87
Cooling rate	10945.79	2	0.04
Aggregate type *Gradation	5977.26	1	0.06
Aggregate type *Specimen length	1.83	1	0.97
Aggregate type *Polymer modification	19527.48	1	0.00
Aggregate type *AC type	7472.61	1	0.04
Aggregate type *AC content	11585.18	2	0.04
Aggregate type *Cooling rate	2417.82	2	0.49
Gradation*Specimen length	228.93	1	0.71
Gradation*Polymer modification	1193.91	1	0.40
Gradation*AC type	1931.39	1	0.29
Gradation*AC content	7231.91	2	0.12
Gradation*Cooling rate	1484.75	2	0.65
Specimen length*Polymer modification	2073.25	1	0.27
Specimen length*AC type	590.49	1	0.56
Specimen length*AC content	8617.67	2	0.08
Specimen length*Cooling rate	1678.74	2	0.61
Polymer modification*AC type	64.84	1	0.84
Polymer modification*AC content	2600.49	2	0.47
Polymer modification*Cooling rate	6734.26	2	0.14
AC type*AC content	9302.17	2	0.07
AC type*Cooling rate	1130.06	2	0.72
AC content*Cooling rate	7338.26	4	0.37
Error	168627.04	100	
Total	275004.16	143	

**Table D8- For response of glass transition temperatures**

Source	Sum Sq.	d.f.	Prob>F
Aggregate type	133.65	1	0.04
Gradation	0.07	1	0.96
Polymer modification	57.00	2	0.34
AC type	9.83	1	0.53
AC content	33.52	2	0.52
Aggregate type*Gradation	2.29	1	0.76
Aggregate type*Polymer modification	9.31	1	0.55
Aggregate type*AC type	16.84	1	0.42
Aggregate type*AC content	29.35	2	0.56
Gradation*Polymer modification	0.32	1	0.91
Gradation*AC type	99.65	1	0.06
Gradation*AC content	64.27	2	0.30
Polymer modification*AC type	145.17	2	0.09
Polymer modification*AC content	133.15	3	0.19
AC type*AC content	40.88	2	0.45
Error	288.79	12	
Total	1110.94	35	

**Table D9- For response of thermal coefficients before glass transition temperature,  $\alpha_h$**

Source	Sum Sq.	d.f.	Prob>F
Aggregate type	2.68E-10	1	0.20
Gradation	5.98E-11	1	0.53
Polymer modification	2.44E-10	2	0.46
AC type	8.64E-11	1	0.46
AC content	8.76E-11	2	0.75
Aggregate type*Gradation	2.40E-10	1	0.22
Aggregate type*Polymer modification	5.54E-10	1	0.07
Aggregate type*AC type	6.63E-11	1	0.51
Aggregate type*AC content	1.99E-10	2	0.52
Gradation*Polymer modification	8.06E-11	1	0.47
Gradation*AC type	1.46E-12	1	0.92
Gradation*AC content	1.78E-10	2	0.56
Polymer modification*AC type	1.39E-10	2	0.63
Polymer modification*AC content	2.62E-10	3	0.63
AC type*AC content	7.60E-11	2	0.77
Error	1.74E-09	12	
Total	3.90E-09	35	

**Table D10- For response of thermal coefficients after glass transition temperature,  $\alpha_g$**

<b>Source</b>	<b>Sum Sq.</b>	<b>d.f.</b>	<b>Prob&gt;F</b>
Aggregate type	2.92E-10	1	0.22
Gradation	2.48E-11	1	0.71
Polymer modification	6.51E-11	2	0.83
AC type	1.10E-10	1	0.44
AC content	1.48E-10	2	0.66
Aggregate type*Gradation	4.08E-10	1	0.15
Aggregate type*Polymer modification	1.32E-10	1	0.40
Aggregate type*AC type	3.01E-11	1	0.68
Aggregate type*AC content	1.07E-10	2	0.74
Gradation*Polymer modification	4.37E-10	1	0.14
Gradation*AC type	3.32E-12	1	0.89
Gradation*AC content	1.49E-10	2	0.66
Polymer modification*AC type	1.45E-10	2	0.67
Polymer modification*AC content	1.61E-10	3	0.82
AC type*AC content	6.42E-11	2	0.83
Error	2.07E-09	12	
Total	4.93E-09	35	

## E- CLUSTERS DETAILS FROM FRACTURE TEST

**Table E1- Cluster (15 samples)**

<b>Aggre- gate type</b>	<b>Grada- tion</b>	<b>Speci- men length</b>	<b>Polymer modifica- tion</b>	<b>AC type</b>	<b>AC con- tent</b>	<b>Cooling rate</b>
L	F	M	S	71-100	OP	-5
L	C	M	S	71-100	OP	-5
L	F	M	S	50-70	O	-5
L	C	M	Z	50-70	OP	-5
L	C	M	Z	50-70	O	-5
L	F	T	Z	71-100	OM	-5
L	F	M	S	71-100	O	-10
B	C	M	S	71-100	O	-10
L	C	M	Z	50-70	OM	-10
L	F	M	Z	50-70	O	-10
B	C	T	Z	50-70	OP	-10
L	F	T	Z	71-100	OP	-20
L	C	M	Z	71-100	OP	-20
L	C	M	Z	71-100	OM	-20
L	F	T	S	50-70	OM	-20

**Table E2- Cluster (30 samples)**

<b>Aggre- gate type</b>	<b>Grada- tion</b>	<b>Speci- men length</b>	<b>Polymer modifica- tion</b>	<b>AC type</b>	<b>AC con- tent</b>	<b>Cooling rate</b>
B	C	M	Z	50-70	O	-5
B	C	M	S	50-70	OP	-5
B	C	M	S	71-100	OM	-5
B	C	M	S	71-100	OM	-5
B	F	M	S	71-100	OP	-5
L	F	T	Z	50-70	OP	-5
L	F	T	Z	50-70	OP	-5
B	F	T	Z	50-70	O	-5
B	F	T	Z	50-70	O	-5
B	C	T	Z	50-70	OM	-5
L	F	M	S	71-100	O	-10
B	C	M	S	71-100	O	-10
B	F	T	S	71-100	O	-10
B	C	T	Z	50-70	O	-10
L	C	M	Z	50-70	OM	-10

**Table E2 (continued)**

B	C	M	Z	50-70	OM	-10
L	F	T	S	50-70	OP	-10
L	F	T	Z	71-100	OP	-10
B	C	T	S	50-70	O	-10
B	F	T	Z	50-70	OM	-10
L	C	T	Z	71-100	OP	-10
L	C	T	Z	71-100	OP	-10
L	F	T	Z	71-100	OP	-20
L	C	M	Z	71-100	OM	-20
B	F	M	Z	50-70	O	-20
B	C	T	S	71-100	O	-20
B	C	T	S	71-100	OM	-20
L	F	M	S	71-100	O	-20
L	C	T	S	50-70	O	-20
L	C	M	S	71-100	OP	-20

**Table E3- Cluster from PC covariance (44 samples)**

<b>Aggregate type</b>	<b>Gradation</b>	<b>Specimen length</b>	<b>Polymer modification</b>	<b>AC type</b>	<b>AC content</b>	<b>Cooling rate</b>
B	C	M	Z	50-70	O	-5
B	C	M	S	50-70	OP	-5
B	C	M	S	71-100	OM	-5
B	C	M	S	71-100	OM	-5
B	F	M	S	71-100	O	-5
B	F	M	S	71-100	OP	-5
L	F	T	Z	50-70	OP	-5
L	F	T	Z	50-70	OP	-5
B	F	T	Z	50-70	O	-5
B	F	T	Z	50-70	O	-5
L	F	T	Z	71-100	OM	-5
L	C	T	Z	50-70	OM	-5
B	C	T	Z	50-70	OM	-5
L	F	M	S	71-100	O	-10
B	C	M	S	71-100	O	-10
B	F	T	S	71-100	O	-10

**Table E3 (continued)**

L	C	M	Z	50-70	O	-10
L	C	M	Z	50-70	O	-10
B	C	T	Z	50-70	O	-10
L	C	M	Z	50-70	OM	-10
B	C	M	Z	50-70	OM	-10
B	C	M	S	71-100	OP	-10
L	F	T	S	50-70	OP	-10
L	F	T	Z	71-100	OP	-10
L	F	T	Z	71-100	OP	-10
B	C	T	S	50-70	O	-10
B	F	T	Z	50-70	OM	-10
L	F	T	Z	50-70	OP	-10
L	C	T	Z	71-100	OP	-10
L	C	T	Z	71-100	OP	-10
L	C	T	S	71-100	OP	-10
L	F	T	Z	71-100	OP	-20
L	C	M	Z	71-100	OM	-20
B	F	M	Z	50-70	O	-20
B	F	M	Z	50-70	O	-20
B	F	T	S	71-100	OM	-20
L	C	M	Z	50-70	O	-20
L	C	M	Z	50-70	O	-20
B	C	T	S	71-100	O	-20
B	C	T	S	71-100	OM	-20
L	F	M	S	71-100	O	-20
L	C	T	S	50-70	O	-20
L	C	M	S	71-100	OP	-20
L	C	M	S	71-100	OP	-20

**Table E4- Cluster from PC covariance (40 samples)**

<b>Aggregate type</b>	<b>Gradation</b>	<b>Specimen length</b>	<b>Polymer modification</b>	<b>AC type</b>	<b>AC content</b>	<b>Cooling rate</b>
L	F	M	S	71-100	OP	-5
L	C	M	S	71-100	OP	-5
B	C	M	Z	50-70	O	-5
L	F	M	S	50-70	O	-5
L	F	M	S	50-70	O	-5
L	C	M	Z	50-70	OP	-5
B	F	T	Z	50-70	OP	-5
B	F	M	S	71-100	OP	-5
L	C	M	Z	50-70	O	-5
B	C	T	S	50-70	OP	-5
B	F	T	S	71-100	OM	-5
B	F	T	S	71-100	OM	-5
L	F	T	Z	71-100	OM	-5
L	F	M	S	71-100	O	-10
L	F	M	S	50-70	OM	-10
L	F	M	S	50-70	OM	-10
B	C	M	S	71-100	O	-10
B	C	T	Z	50-70	O	-10
L	C	M	Z	50-70	OM	-10
B	C	M	Z	50-70	OM	-10
L	F	M	Z	50-70	O	-10
L	F	M	Z	50-70	O	-10
B	F	M	Z	71-100	OM	-10
B	F	M	Z	71-100	OM	-10
B	C	T	Z	50-70	OP	-10
B	C	T	Z	50-70	OP	-10
B	F	T	S	71-100	OM	-10
L	F	T	Z	50-70	OM	-20
L	F	T	Z	71-100	OP	-20
L	C	M	Z	71-100	OP	-20
L	C	M	Z	71-100	OM	-20
B	F	M	Z	50-70	OP	-20
B	F	T	Z	71-100	OM	-20
B	F	T	Z	71-100	OM	-20
L	F	T	S	50-70	OM	-20
B	C	T	S	71-100	O	-20

**Table E4 (continued)**

B	C	T	S	71-100	OM	-20
L	F	M	S	71-100	O	-20
L	C	T	S	50-70	O	-20
B	C	M	Z	50-70	OM	-20

**Table E5- Cluster from PC correlation (50 samples)**

<b>Aggre- gate type</b>	<b>Grada- tion</b>	<b>Speci- men length</b>	<b>Polymer modifica- tion</b>	<b>AC type</b>	<b>AC con- tent</b>	<b>Cooling rate</b>
L	F	M	S	71-100	OP	-5
L	C	M	S	71-100	OP	-5
L	C	M	S	71-100	OP	-5
B	C	M	Z	50-70	O	-5
L	F	M	S	50-70	O	-5
L	F	M	S	50-70	O	-5
L	C	M	Z	50-70	OP	-5
L	C	M	Z	50-70	OP	-5
B	F	T	Z	50-70	OP	-5
B	F	M	S	71-100	OP	-5
L	C	M	Z	50-70	O	-5
B	C	T	S	50-70	OP	-5
B	C	T	S	50-70	OP	-5
B	F	T	S	71-100	OM	-5
B	F	T	S	71-100	OM	-5
L	F	T	S	71-100	O	-5
L	F	T	Z	71-100	OM	-5
L	F	T	Z	71-100	O	-5
L	F	M	S	71-100	O	-10
L	F	M	S	71-100	OP	-10
L	F	M	S	50-70	OM	-10
L	F	M	S	50-70	OM	-10
B	C	M	S	71-100	O	-10
B	C	M	Z	50-70	OM	-10
B	C	T	Z	50-70	O	-10
L	C	M	Z	50-70	OM	-10

**Table E5 (continued)**

B	C	M	Z	50-70	OM	-10
L	F	M	Z	50-70	O	-10
L	F	M	Z	50-70	O	-10
B	F	M	Z	71-100	OM	-10
B	F	M	Z	71-100	OM	-10
L	F	T	S	50-70	OP	-10
B	C	T	Z	50-70	OP	-10
B	C	T	Z	50-70	OP	-10
B	F	T	S	71-100	OM	-10
L	C	T	Z	50-70	OP	-20
L	F	T	Z	50-70	OM	-20
L	F	T	Z	71-100	OP	-20
L	C	M	Z	71-100	OP	-20
L	C	M	Z	71-100	OM	-20
B	F	M	Z	50-70	OP	-20
B	F	T	Z	71-100	OM	-20
B	F	T	Z	71-100	OM	-20
L	F	T	S	50-70	O	-20
L	F	T	S	50-70	OM	-20
B	C	T	S	71-100	O	-20
B	C	T	S	71-100	OM	-20
L	F	M	S	71-100	O	-20
L	C	T	S	50-70	O	-20
B	C	M	Z	50-70	OM	-20

**Table E6- Cluster from PC correlation (44 samples)**

<b>Aggregate type</b>	<b>Grada-tion</b>	<b>Speci-men length</b>	<b>Polymer modifica-tion</b>	<b>AC type</b>	<b>AC con-tent</b>	<b>Cooling rate</b>
B	C	M	Z	50-70	O	-5
B	C	M	S	50-70	OP	-5
B	C	M	S	71-100	OM	-5
B	C	M	S	71-100	OM	-5
B	F	M	S	71-100	OP	-5
L	F	T	Z	50-70	OP	-5
L	F	T	Z	50-70	OP	-5
B	C	T	S	50-70	OM	-5
B	F	T	Z	50-70	O	-5

**Table E6 (continued)**

B	F	T	Z	50-70	O	-5
L	F	T	Z	71-100	OM	-5
B	C	T	Z	50-70	OM	-5
L	F	M	S	71-100	O	-10
B	C	M	S	71-100	O	-10
B	F	T	S	71-100	O	-10
B	F	M	S	71-100	OM	-10
L	C	M	Z	50-70	O	-10
B	C	T	Z	50-70	O	-10
L	C	M	Z	50-70	OM	-10
B	C	M	Z	50-70	OM	-10
L	F	T	S	50-70	OP	-10
L	F	T	Z	71-100	OP	-10
L	F	T	Z	71-100	OP	-10
B	C	T	S	50-70	O	-10
B	F	T	Z	50-70	OM	-10
L	F	T	Z	50-70	OP	-10
L	C	T	Z	71-100	OP	-10
L	C	T	Z	71-100	OP	-10
L	C	T	S	71-100	OP	-10
L	F	T	Z	71-100	OP	-20
L	C	M	Z	71-100	OM	-20
B	F	M	Z	50-70	O	-20
B	F	M	Z	50-70	O	-20
B	F	T	S	71-100	OM	-20
L	C	M	Z	50-70	O	-20
B	C	T	S	71-100	O	-20
B	C	T	S	71-100	OM	-20
L	F	M	S	71-100	O	-20
L	C	T	S	50-70	O	-20
L	C	M	S	71-100	OP	-20
L	C	M	S	71-100	OP	-20
L	F	M	S	71-100	OP	-5
L	C	M	Z	71-100	OM	-5
B	F	M	S	71-100	O	-5
B	F	M	S	71-100	OM	-5
B	C	T	S	50-70	OM	-5
L	C	T	Z	50-70	OM	-5

**Table E6 (continued)**

B	C	M	S	71-100	OP	-10
L	C	T	S	71-100	OP	-10
L	F	T	Z	50-70	OM	-20
B	C	M	S	50-70	OP	-20
B	C	T	S	71-100	OP	-20

**Table E7- Cluster from PC correlation (11 samples)**

Agg	Gradation	Specimen length	Polymer modification	AC type	AC content	Cooling rate
L	F	M	S	71-100	OP	-5
L	C	M	Z	71-100	OM	-5
B	F	M	S	71-100	O	-5
B	F	M	S	71-100	OM	-5
B	C	T	S	50-70	OM	-5
L	C	T	Z	50-70	OM	-5
B	C	M	S	71-100	OP	-10
L	C	T	S	71-100	OP	-10
L	F	T	Z	50-70	OM	-20
B	C	M	S	50-70	OP	-20
B	C	T	S	71-100	OP	-20

**Symbol used:**

Aggregate type : L-limestone, B-Basalt; Gradation: C-Coarse, F-Fine; Specimen length: T-Tall, M-Small; Polymer modification: Z-no Modification ,S-SBS Modification; AC type: 57-50 70, 71-71 100;AC content: O-optimum, OP-optimum plus, OM -optimum minus; Cooling rate: 5= -5°C/hr, 10= -10°C/hr, 20= -20°C/hr

## F- CLUSTERS DETAILS FROM GLASS TEST

**Table F1- Glass transition temperature cluster (10 samples)**

<b>Aggregate type</b>	<b>Gradation</b>	<b>Polymer modification</b>	<b>AC type</b>	<b>AC content</b>
B	C	S	50-70	OM
B	C	S	71-100	O
B	C	Z	50-70	OM
B	F	S	50-70	OP
B	F	Z	71-100	OM
L	C	S	71-100	O
L	C	Z	71-100	OM
L	F	S	50-70	O
L	F	S	71-100	OP
L	F	Z	71-100	O

**Table F2- Glass transition temperature cluster (13 samples)**

<b>Aggregate type</b>	<b>Gradation</b>	<b>Polymer modification</b>	<b>AC type</b>	<b>AC content</b>
B	C	S	50-70	O
B	C	S	50-70	OP
B	C	S	71-100	OM
B	F	S	71-100	O
B	F	Z	71-100	O
L	C	S	50-70	O
L	C	S	50-70	OM
L	C	Z	50-70	OP
L	C	Z	71-100	OP
L	F	S	50-70	OP
L	F	S	50-70	OM
L	F	Z	50-70	O
L	F	Z	71-100	OM

**Table F3- Glass transition temperature cluster from PC covariance (10 samples)**

Aggregate type	Gradation	Polymer modification	AC type	AC content
B	C	S	50-70	O
B	C	S	50-70	OP
B	C	Z	71-100	O
B	C	Z	71-100	OP
B	F	S	71-100	O
B	F	Z	50-70	OM
B	F	Z	71-100	OM
B	F	Z	50-70	OP
B	F	Z	50-70	O
B	F	Z	71-100	OP

**Table F4- Glass transition temperature cluster from PC covariance (13 samples)**

Aggregate type	Gradation	Polymer modification	AC type	AC content
B	C	S	71-100	OM
B	C	Z	50-70	OM
B	F	S	50-70	OP
L	C	S	71-100	OP
L	C	S	50-70	O
L	C	S	50-70	OM
L	C	S	71-100	O
L	C	S	71-100	OM
L	C	Z	71-100	OP
L	F	S	50-70	O
L	F	S	71-100	OP
L	F	Z	50-70	OP
L	F	Z	50-70	OM

**Table F5- Glass transition temperature cluster from PC correlation**

**(10 samples)**

Aggregate type	Gradation	Polymer modification	AC type	AC content
B	C	S	50-70	O
B	C	S	50-70	OP
B	C	Z	71-100	O
B	C	Z	71-100	OP

**Table F5 (continued)**

B	F	S	71-100	O
B	F	Z	50-70	OM
B	F	Z	71-100	OM
B	F	Z	50-70	OP
B	F	Z	50-70	O
B	F	Z	71-100	OP

**Table F6- Glass transition cluster from PC correlation (13 samples)**

<b>Aggregate type</b>	<b>Gradation</b>	<b>Polymer modification</b>	<b>AC type</b>	<b>AC content</b>
B	C	S	71-100	OM
B	C	Z	50-70	OM
B	F	S	50-70	OP
L	C	S	71-100	OP
L	C	S	50-70	O
L	C	S	50-70	OM
L	C	S	71-100	O
L	C	S	71-100	OM
L	C	Z	71-100	OP
L	F	S	50-70	O
L	F	S	71-100	OP
L	F	Z	50-70	OP
L	F	Z	50-70	OM

**Table F7- Glass transition temperature cluster from discriminant analysis****(10 samples)**

<b>Aggregate type</b>	<b>Gradation</b>	<b>Polymer modification</b>	<b>AC type</b>	<b>AC content</b>
L	C	T	Z	50-70
L	F	T	Z	50-70
L	C	T	S	71-100
L	C	T	S	71-100
B	F	T	Z	50-70
B	F	T	Z	50-70
B	F	T	Z	50-70

**Table F7 (continued)**

B	C	T	Z	71-100
B	C	T	S	71-100
B	F	T	S	71-100

**Table F8- Glass transition temperature cluster from discriminant analysis****(12 samples)**

<b>Aggregate</b>	<b>Gradation</b>	<b>Polymer modification</b>	<b>AC type</b>	<b>AC content</b>
L	F	T	S	50-70
L	C	T	Z	71-100
L	F	T	Z	71-100
L	F	T	S	71-100
L	C	T	S	71-100
B	C	T	Z	50-70
B	F	T	S	50-70
B	C	T	Z	71-100
B	F	T	Z	71-100
B	C	T	s	50-70
B	C	T	s	71-100
B	F	T	Z	71-100

**Table F9- Glass transition temperature cluster from discriminant analysis****(14 samples)**

<b>Aggregate</b>	<b>Gradation</b>	<b>Polymer modification</b>	<b>AC type</b>	<b>AC content</b>
L	C	T	Z	50-70
L	F	T	Z	50-70
L	F	T	Z	50-70
L	C	T	S	50-70
L	C	T	Z	71-100
L	C	T	S	50-70
L	F	T	S	50-70
L	F	T	S	50-70
L	F	T	Z	71-100

**Table F9 (continued)**

B	C	T	S	50-70
B	C	T	S	50-70
B	F	T	S	71-100
B	F	T	Z	71-100
B	C	T	S	71-100

**Symbol used:**

Aggregate : L-limestone, B-Basalt; Gradation: C-Coarse, F-Fine; Specimen length: T-Tall, M-Small; Polymer modification: Z-no Modification ,S-SBS Modification; AC type: 57-50 70, 71-71 100;AC content: O-optimum, OP-optimum plus, OM - optimum minus.

## G- PREDICTED VALUES FROM STATISTICAL MODELS

**Table G1- FS, FT and GTT values for various material configurations**

MATERIALS	FS	FT	GTT
	MPa	°C	°C
BFS71OM20T	0.00	-10.45	-14.88
BFS71O20T	0.00	-11.77	-32.09
BFS71O20M	0.08	-10.86	-14.86
LFZ71OM5M	0.20	-15.01	-14.99
BFS71O10T	0.54	-11.77	-14.85
BFS71OM10M	0.68	-10.45	-31.46
LCZ71OM5M	0.69	-15.01	-18.28
LCZ71OM10M	0.96	-14.33	-18.24
BFZ71OM10T	1.14	-14.89	-17.27
BFZ57O20M	1.20	-14.11	-25.00
BFZ71OM5T	1.25	-14.14	-17.24
LCZ71OM10T	1.31	-13.46	-18.20
BFZ71OM10M	1.34	-13.89	-17.21
BFZ71OM20M	1.35	-13.15	-17.18
BFZ57OM20M	1.41	-15.43	-30.89
BFZ71OM5M	1.44	-14.63	-17.15
LCZ57OM5T	1.46	-12.68	-14.67
LFZ57OM20T	1.46	-11.32	-14.65
BFS71OP20M	1.49	-10.98	-18.51
BFS71OM10T	1.54	-12.17	-16.59
BFZ57O20T	1.55	-13.11	-24.85
LCZ71OM5T	1.55	-14.14	-18.17
BCS57OM5M	1.62	-11.55	-17.65
BFS71O20M	1.63	-10.70	-15.73
BFZ71O20M	1.63	-14.50	-16.28
BCS71OM5T	1.64	-13.59	-15.86
BFS71OM5T	1.65	-11.42	-16.56
BFS71OM5M	1.69	-10.81	-30.39
BFS71O20T	1.69	-13.19	-15.70
BFS71OM10M	1.74	-11.17	-16.54
BFZ57OM20T	1.76	-14.43	-29.94
BFS71OM20M	1.76	-10.43	-16.51

**FS=fracture strength, FT=fracture temperature, GTT=glass transition**

**Table G1 (continued)**

BFZ57OM5T	1.76	-11.09	-29.52
BCS57OM5T	1.79	-12.42	-17.61
BCZ71OP20M	1.80	-15.85	-20.54
BCS71OM10T	1.81	-13.59	-15.84
BFS71OM20T	1.82	-12.92	-16.49
BFZ71OM20T	1.82	-15.63	-17.12
LFZ71OM10M	1.84	-17.25	-14.97
BFS71OM5M	1.85	-11.92	-16.46
BFZ57OM10M	1.85	-10.84	-29.14
BFZ71OP20M	1.90	-15.85	-20.92
BFS71O5T	1.91	-11.70	-15.68
BFZ71O5T	1.91	-15.49	-16.26
BFS71OP20T	1.95	-15.33	-14.46
BFZ57OM5M	1.96	-11.58	-28.79
BCS71OM5M	1.99	-12.59	-15.81
BCZ71O20T	2.00	-16.98	-41.37
BFS71OP20M	2.01	-12.84	-14.44
BFZ57O10M	2.01	-15.02	-24.70
BCS57OM10T	2.03	-13.10	-17.58
LFZ71OM10T	2.04	-16.25	-14.96
BFS71OM10T	2.06	-11.88	-28.46
BCS57OP5T	2.06	-14.95	-14.77
BFZ71OP20T	2.07	-18.34	-20.85
BFZ71O20T	2.10	-16.99	-16.23
BFS71O5M	2.10	-12.19	-15.66
BFZ71OM20T	2.10	-15.99	-16.21
BCS71O20T	2.11	-13.97	-19.28
BFS71O5M	2.14	-12.90	-14.83
BCS71OM10M	2.16	-11.68	-15.79
BFS71OP5T	2.16	-11.97	-18.47
BFS71OM5T	2.17	-11.13	-28.15
BFS71O10T	2.19	-12.44	-15.64
BFZ71O10T	2.19	-16.24	-16.19
BCS57O5M	2.21	-14.00	-15.62

**FS=fracture strength, FT=fracture temperature, GTT=glass transition**

**Table G1 (continued)**

BFS71OM20M	2.27	-10.14	-27.86
LFS71OM10M	2.25	-17.20	-15.35
BCS57OM20T	2.28	-13.78	-17.55
BCZ57OP20M	2.32	-10.64	-20.19
BCS71OM20M	2.33	-10.77	-15.77
BFS71OP5M	2.36	-12.46	-18.43
BFZ57O10T	2.36	-13.11	-24.56
LFZ57OM10M	2.36	-14.19	-14.63
BCS57O5T	2.38	-14.87	-15.60
BCS57OM10M	2.38	-12.23	-17.52
BFS71O10M	2.38	-11.45	-15.57
BFZ71O10M	2.38	-15.24	-16.16
LFZ57O5M	2.39	-15.99	-15.11
BFS71O10M	2.41	-13.58	-14.81
BFZ57OP20M	2.41	-10.64	-22.27
LFS71OP5M	2.42	-20.35	-19.56
BCZ71O20M	2.44	-14.50	-38.06
LFS71OM10T	2.44	-16.21	-15.33
BCZ57OP5T	2.47	-19.83	-20.48
BFZ57OP20T	2.47	-13.13	-22.18
BCZ57O20T	2.51	-12.85	-18.06
LFZ57O5T	2.55	-15.13	-15.09
LFZ57OM10T	2.55	-13.20	-14.61
BFZ57OM10T	2.56	-14.43	-27.59
BFZ71OP5T	2.56	-16.84	-20.79
BCS71OP5T	2.58	-16.82	-23.44
LFZ57OP5T	2.58	-16.31	-27.33
BFZ57OP5M	2.61	-14.61	-22.10
BCZ71OM20T	2.64	-15.63	-17.45
BCZ71OP5M	2.66	-20.32	-20.42
BFS71OP5T	2.68	-13.84	-14.43
BCS71OP10M	2.68	-15.67	-23.33
LCS71OP10T	2.69	-17.44	-26.03
LFZ71OM5T	2.70	-15.50	-14.94
BCZ71O5T	2.72	-18.48	-36.13
BCS57OP10T	2.73	-14.21	-14.75

**FS=fracture strength, FT=fracture temperature, GTT=glass transition**

**Table G1 (continued)**

BFZ71OP5M	2.76	-17.34	-20.73
BCS71OP5M	2.78	-17.31	-23.22
LFS71OM5T	2.79	-14.97	-21.77
BFZ57O5M	2.82	-15.93	-24.42
BFS71OP10T	2.83	-12.72	-18.39
BCZ71OM10T	2.87	-16.38	-17.42
LCS57O10M	2.87	-13.92	-15.49
LCS57O10T	2.87	-15.83	-15.55
LCS57O20M	2.87	-13.01	-15.47
LCS57O5M	2.87	-14.83	-15.51
LCS57O5T	2.87	-15.83	-15.53
LCS57OM10M	2.87	-12.60	-15.23
LCS57OM10T	2.87	-14.51	-15.31
LCS57OM20M	2.87	-11.69	-15.21
LCS57OM20T	2.87	-14.51	-15.29
LCS57OM5M	2.87	-13.51	-15.25
LCS57OM5T	2.87	-14.51	-15.27
LCS71OP20T	2.87	-17.15	-25.84
BFS71OP5M	2.87	-14.33	-14.41
LFS71O10M	2.89	-17.48	-18.02
LFZ71O10M	2.89	-18.60	-19.23
LFS71OM5M	2.91	-17.94	-15.19
BCZ71OM20T	2.92	-18.97	-34.76
BCS57OP10M	2.93	-13.21	-14.74
BCS71O20M	2.96	-11.49	-19.19
BCZ57O20M	2.96	-10.36	-17.99
BCS57O10M	2.97	-14.68	-15.45
LFZ57OP10T	2.97	-16.31	-27.09
BCZ71OM5T	2.98	-17.12	-17.39
BCZ57OP5T	2.98	-14.62	-20.14
BCZ71O10T	3.00	-17.73	-33.70
BFS71O5T	3.00	-13.77	-14.79
BFS71OP10M	3.02	-11.72	-18.35
LFZ57OM5M	3.02	-14.94	-14.60
BCS71OP10T	3.03	-16.54	-23.12
BCZ71OM10M	3.07	-15.38	-17.36

**FS=fracture strength, FT=fracture temperature, GTT=glass transition**

**Table G1 (continued)**

BFZ57OP5T	3.08	-11.63	-22.01
BCZ71OM20M	3.08	-13.14	-17.33
LFS71O10T	3.08	-16.48	-17.95
LFZ71O10T	3.08	-17.60	-19.14
LFS71OM5T	3.11	-15.46	-15.17
BCZ57OP10T	3.13	-19.08	-20.36
BCS57OP5M	3.14	-15.23	-14.72
LFS71OM5M	3.14	-15.89	-21.70
BCS57OM20M	3.14	-12.91	-17.49
BCS71OM20T	3.15	-12.62	-15.75
BCZ57OM20T	3.15	-12.58	-17.09
BFZ57O5T	3.16	-13.11	-24.29
LFS71O5M	3.17	-18.22	-17.92
LFZ71OM20T	3.17	-19.34	-19.10
BCZ71OM5M	3.17	-17.62	-17.30
LFS71OM10T	3.18	-14.97	-21.62
BCZ57OP5M	3.18	-15.11	-20.08
BCZ71O10M	3.20	-16.73	-32.83
LCS57O20T	3.22	-17.22	-15.43
LFZ57OM5T	3.22	-12.45	-14.58
BFZ71OP10T	3.23	-17.59	-20.66
BCS71O5T	3.24	-15.47	-19.05
BCZ57O5T	3.24	-14.34	-17.88
BCS71OP20T	3.28	-17.22	-23.02
LFS71OP5T	3.28	-21.22	-19.51
BFS71OP20T	3.28	-13.46	-18.32
LCS57OP20T	3.30	-17.90	-15.88
LFS71O20T	3.32	-17.23	-17.85
LCS57OP5M	3.32	-21.48	-16.14
BCZ71OP10M	3.33	-18.09	-20.31
LFS71O5M	3.34	-17.21	-24.16
BFS71OP10T	3.34	-14.58	-14.39
LFZ57OP20T	3.36	-16.31	-26.86
LFS71O5T	3.36	-15.73	-17.81
LFZ71O5T	3.36	-16.86	-19.01
LFZ71OM20M	3.37	-16.50	-14.92

**FS=fracture strength, FT=fracture temperature, GTT=glass transition**

**Table G1 (continued)**

LCZ57O10M	3.38	-14.49	-22.82
BCZ57OM10T	3.39	-13.32	-17.06
LFS71O10M	3.40	-18.26	-24.03
LFZ57O10M	3.40	-14.47	-15.07
LCS57OP20M	3.41	-17.00	-16.11
LFS71OP5M	3.42	-18.49	-16.09
BFZ71OP10M	3.43	-16.60	-20.60
LCS57OP10M	3.43	-19.24	-16.07
BCS71O5M	3.43	-15.96	-18.96
BCZ57O5M	3.43	-14.84	-17.78
BCS71OP20M	3.45	-16.35	-22.92
LFS71OM20T	3.45	-16.95	-15.15
LFZ71OM20T	3.45	-17.00	-14.90
BCS57OP20T	3.46	-18.68	-14.70
LFS71OP20M	3.51	-17.01	-16.04
BCS71O10T	3.52	-14.72	-18.92
BCZ57O10T	3.52	-13.60	-17.75
LCS57OP5T	3.52	-18.99	-16.02
LFS71OM10M	3.53	-14.98	-21.54
LFS71OP10M	3.53	-17.75	-16.00
BFS71OP10M	3.54	-13.59	-14.38
LFS71OM20T	3.57	-14.97	-21.47
LFS71OP20T	3.58	-19.37	-19.47
BCZ57OM10M	3.58	-12.33	-17.03
BCZ57OM20M	3.60	-10.09	-17.00
LFS71O10T	3.60	-17.27	-23.91
LFZ57O10T	3.60	-13.47	-15.05
LFS71OP5T	3.62	-16.01	-15.97
LCZ71O20T	3.62	-18.35	-18.88
LFS71O20M	3.64	-16.73	-17.71
LFZ71O20M	3.64	-17.86	-18.84
BCZ57OP10T	3.65	-13.87	-20.03
BCZ57OM5M	3.69	-14.56	-16.97
LFZ71OP20T	3.69	-19.70	-16.92
LCZ71O10M	3.70	-20.09	-18.79
BCS71O10M	3.71	-13.73	-18.75

**FS=fracture strength, FT=fracture temperature, GTT=glass transition**

**Table G1 (continued)**

BCZ57O10M	3.71	-12.60	-17.68
LFZ71O20T	3.72	-18.35	-18.71
LCZ57O10T	3.72	-14.49	-22.72
LFS71OP10T	3.72	-16.75	-15.95
LCZ71O5M	3.73	-23.68	-16.89
LCS71O20T	3.73	-18.01	-19.87
BFZ57OP10T	3.75	-12.38	-21.93
LFS71OM20M	3.77	-16.46	-15.13
BCZ57OP20T	3.80	-18.33	-20.25
LCS71OP20M	3.82	-19.20	-16.86
LFZ71OP5M	3.83	-20.69	-16.83
LFS71O20T	3.83	-18.01	-23.79
LCZ71OP10M	3.83	-21.44	-16.81
LCS71OP5M	3.84	-23.34	-25.66
BCZ57OP10M	3.85	-12.88	-19.97
BCZ57OM5T	3.87	-14.89	-16.95
LFS71O5T	3.88	-16.52	-23.67
LFZ57OM20M	3.89	-13.45	-14.56
LCS57OP10T	3.90	-18.24	-15.93
LCZ71O10T	3.90	-19.09	-18.67
LFS71OM20M	3.91	-14.07	-21.40
LCZ57OP5T	3.92	-21.19	-16.78
LFZ71OP10M	3.93	-19.95	-16.75
BFZ57OP10M	3.94	-11.39	-21.85
LCS71OP10M	3.95	-21.11	-25.49
LCZ71OM20T	3.98	-22.33	-18.63
LFZ71OP5T	4.02	-18.21	-16.72
LFS71OP20M	4.03	-18.87	-19.42
LCS71OP5T	4.04	-20.86	-25.32
LFS71OP10M	4.04	-19.62	-19.37
BCS57O10T	4.08	-14.91	-15.41
LCZ57OM10M	4.09	-15.68	-14.54
BCS57O20M	4.12	-12.09	-15.39
LCZ57OP10T	4.13	-13.17	-16.70
LFS71O20M	4.16	-17.52	-23.55
LFZ57O20M	4.16	-13.72	-15.03

**FS=fracture strength, FT=fracture temperature, GTT=glass transition**

**Table G1 (continued)**

LCZ71O5T	4.18	-19.84	-18.59
BCZ57OP20T	4.20	-13.12	-19.92
LCS71O10M	4.22	-19.75	-19.82
LFZ57O20T	4.24	-14.22	-15.01
LFS71OP10T	4.24	-18.62	-19.32
LCZ57OP5M	4.24	-18.47	-16.43
LCZ71OM20T	4.26	-16.99	-18.13
LCZ57OM10T	4.28	-14.69	-14.53
BCS57OP20M	4.32	-17.81	-14.68
LCZ57OP20M	4.33	-13.99	-16.41
LFZ57OP5M	4.34	-15.48	-26.63
LCZ57OP10M	4.35	-16.23	-16.38
LCS71O10T	4.42	-18.76	-19.76
LCZ57OP5T	4.44	-15.98	-16.36
LCS71OP20M	4.45	-14.33	-25.16
LCZ71O20M	4.46	-17.85	-18.55
BCS57O20T	4.47	-14.91	-15.37
LCS71OM10M	4.49	-18.40	-21.33
LCS71O5M	4.50	-21.99	-19.71
LCZ57O5M	4.50	-18.19	-22.63
LCZ57OP10T	4.55	-15.24	-16.33
LFZ57OP10M	4.65	-18.22	-26.42
LCS71OM10T	4.69	-17.41	-21.26
LCS71O5T	4.70	-19.50	-19.66
LCZ57O5T	4.70	-15.71	-22.53
LCZ57O20M	4.74	-13.58	-22.44
LCZ57OM5M	4.75	-17.92	-14.51
LCS71OM20T	4.78	-16.66	-21.19
LCZ57OM20T	4.78	-13.94	-14.49
LFS71OP20T	4.90	-17.50	-15.90
LCS71O20M	4.98	-17.52	-19.61
LFZ57OP20M	5.04	-17.31	-26.22
LCZ57O20T	5.09	-14.49	-22.35
LCZ71OM20M	5.10	-16.50	-18.09
LCS71OM5M	5.16	-20.64	-21.12
LCS71OM5T	5.35	-18.15	-21.05

**FS=fracture strength, FT=fracture temperature, GTT=glass transition**

**Table G1 (continued)**

LCZ57OP20T	5.42	-19.70	-16.67
LFZ71OP20M	5.45	-17.31	-16.64
LFZ71OP10T	5.61	-16.31	-16.62
LCZ57OM20M	5.62	-13.45	-14.48
LCZ57OP20T	5.82	-14.49	-16.31
LCZ71OP20M	6.02	-16.16	-20.98

**FS=fracture strength, FT=fracture temperature, GTT=glass transition**

**Symbol used:**

Aggregate : L-limestone, B-Basalt; Gradation: C-Coarse, F-Fine; Specimen length: T-Tall, M-Small; Polymer modification: Z-no Modification ,S-SBS Modification; AC type: 57-50 70, 71-71 100;AC content: O-optimum, OP-optimum plus, OM - optimum minus; Cooling rate: 5= -5°C/hr, 10= -10°C/hr, 20= -20°C/hr

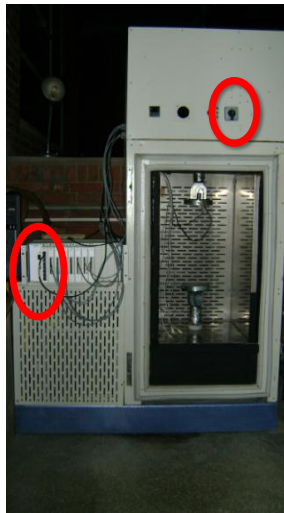
## H-SOFTWARE MANUALS

### Software for Fracture Test

Tutorial

Slide 2

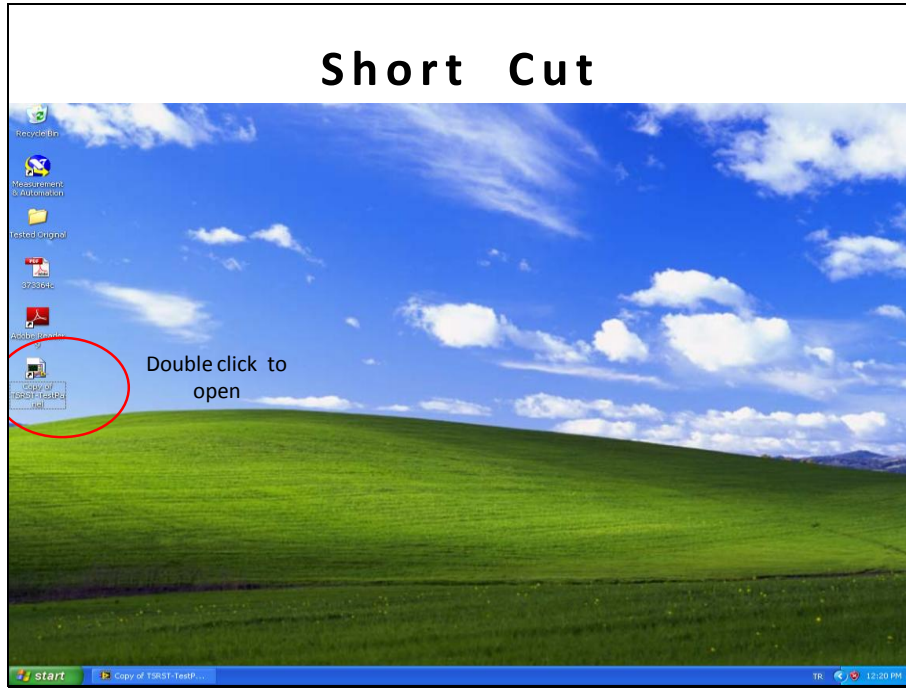
### Software for Fracture Test



Caution:  
Before Opening the Software First  
Open The Machine button as  
Circled

**Figure H1- Manual for fracture strength test**

Slide 3



Slide 4

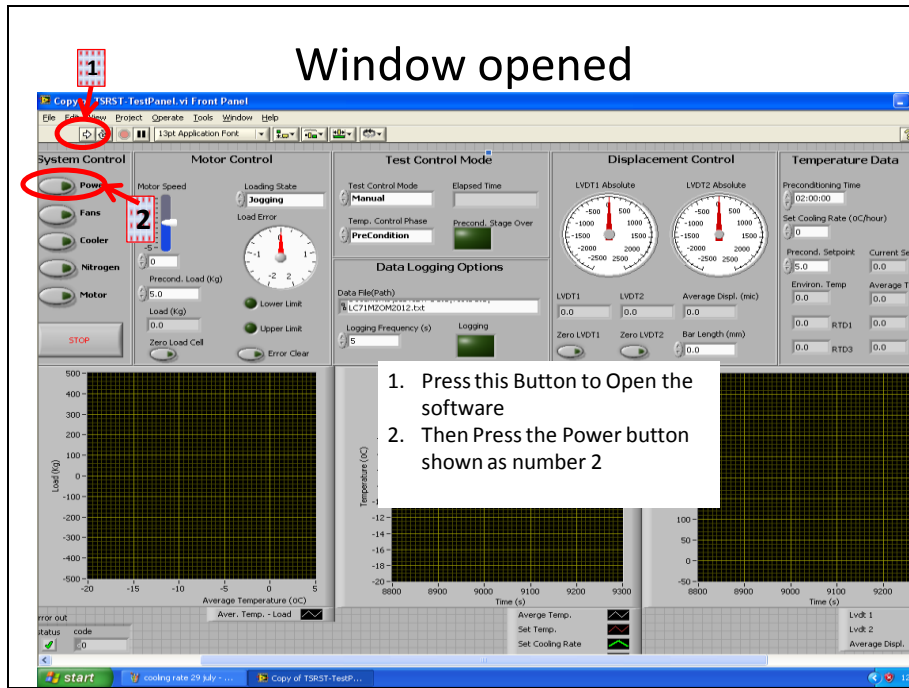
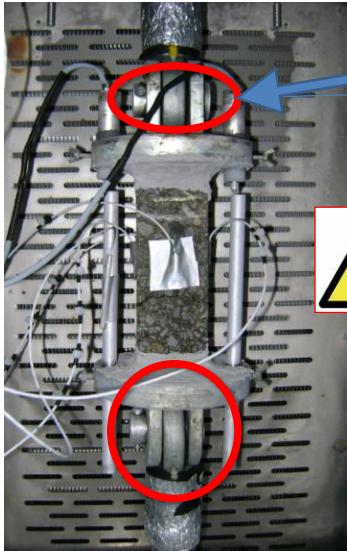


Figure H1 (continued)

Slide 5

## Mounting the Sample



First Hang the sample from the top then adjust the length at the bottom by following steps 3 , 4 and 5 shown in the next page

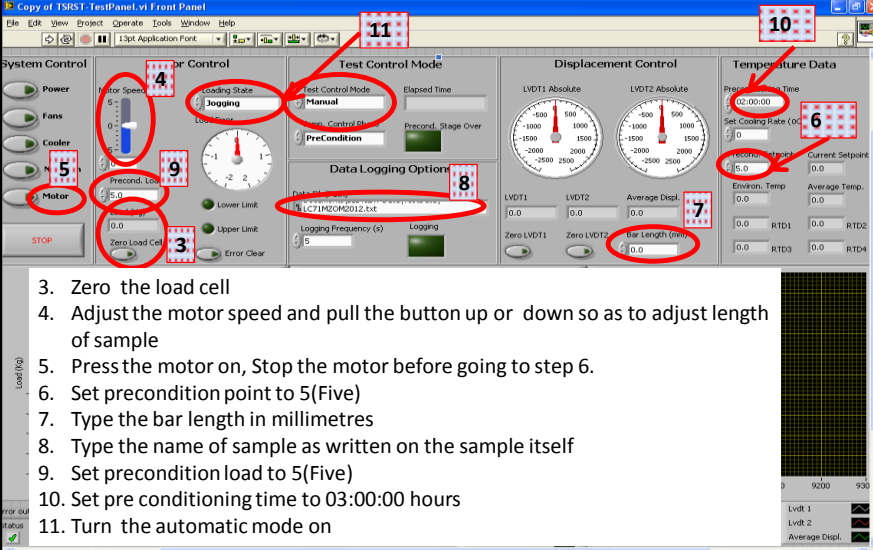


**Caution:**  
Make sure that the load is set to zero and immediately close the motor once the pin is passed to the other side of clamp

Mount the RTDS & LVDTs as shown on the sample and on the ROD, tighten the screws take the length of the Rod from bottom of the plate to the LVDT touching the surface of rods

Slide 6

## Window opened-Jogging Mode



3. Zero the load cell
4. Adjust the motor speed and pull the button up or down so as to adjust length of sample
5. Press the motor on, Stop the motor before going to step 6.
6. Set precondition point to 5(Five)
7. Type the bar length in millimetres
8. Type the name of sample as written on the sample itself
9. Set precondition load to 5(Five)
10. Set pre conditioning time to 03:00:00 hours
11. Turn the automatic mode on

Figure H1 (continued)

Slide 7

## Changing to Loading mode

10. Zero the LVDTs as indicated  
 11. Press ON Fans, Cooler and motor in a order as shown 11, 12 and 13.  
 14. Check that window show PreCondition Mode  
 15. Change the Loading state to Loading

Slide 8

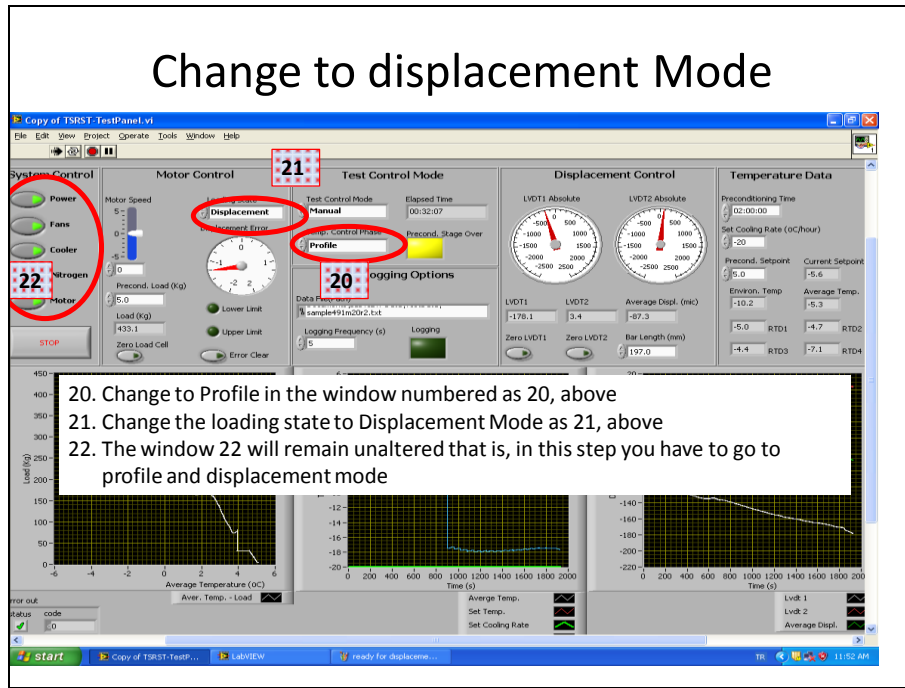
## Changing to Displacement mode

16. See that the window numbered as 16 have this state  
 17. Please also see that Enviro. Temp and Average temperature are approximately showing 5  
 18. Check that window elapsed time is more than 2 hours 30 minutes and the precondition stage light (change from green to yellow) is blinking  
 19. Now type the cooling rate in this window; it is -5 or -10 or -20.

Figure H1 (continued)

Slide 9

## Change to displacement Mode



Slide 10

## Switching to Nitrogen Mode

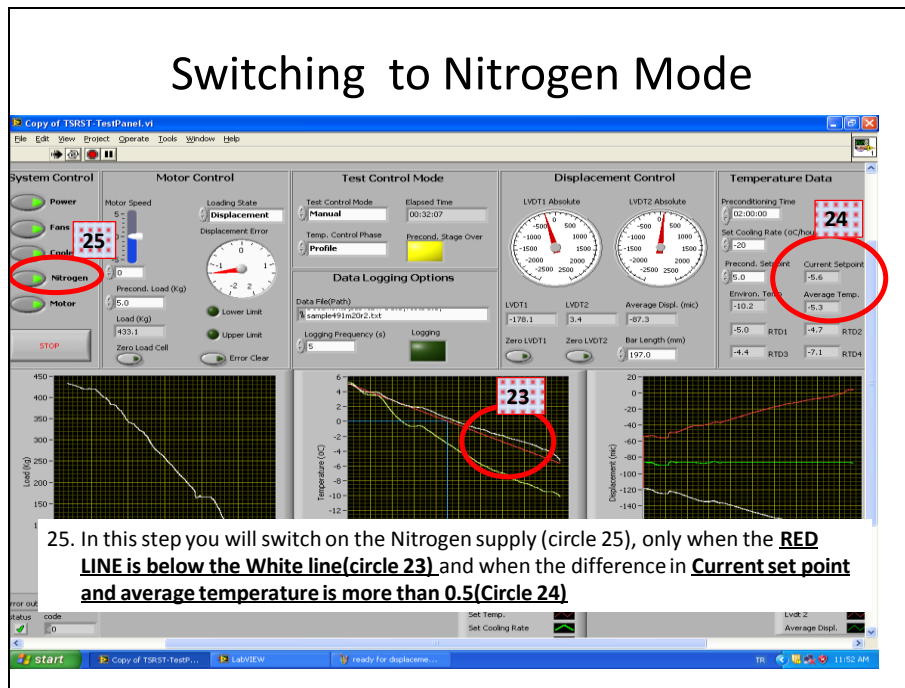


Figure H1 (continued)

## Stopping the Software

26. The experiment is now completed as the circle 26 shows that the load has fallen to Zero

27. Do not turn off the motor and **do not turn the power off at this stage**

28. **Follow the sequence 28 and 29 in switching off first the Cooler and then Fan**

## Stopping the Software

**FIRST REMOVE THE RTDS AND LVDT GENTLY, USING HAIR DRIER TO MELT THE ICE IF NECESSARY, REMOVE THE PIN AND IF REQUIRED CHANGE TO JOGGING MODE IN LOADING STATE TO MOVE THE SAMPLE UP AND FOR REMOVING THE PINS.**

30. ONCE SAMPLE IS REMOVED TURN OFF THE POWER AS CIRCLE 30

31. **Stop the Software circle 31**

32. **Exit the programme from 32**

Do not close the machine before exiting the software

Figure H1 (continued)

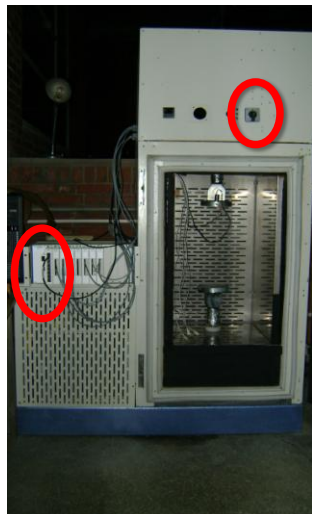
Slide 1

# Software for Glass Transition Test

Tutorial

Slide 2

# Software for Glass Transition Test

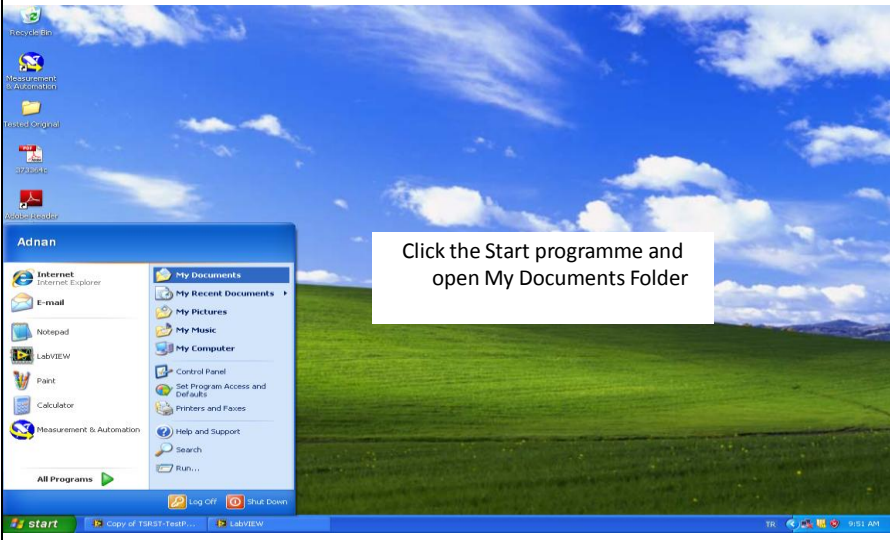


Caution:  
Before Opening the Software First  
Open The Machine button as  
Circled

**Figure H2- Manual for glass transition temperature test**

Slide 3

## Starting the Software

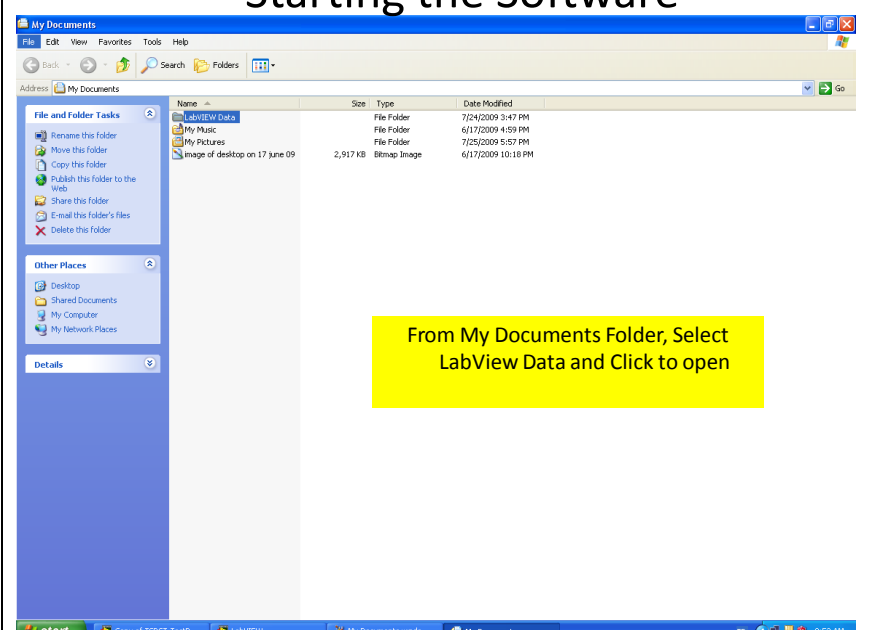


The screenshot shows a Windows XP desktop with a blue sky and green hills background. The Start menu is open, displaying the user's name 'Adnan' and a list of programs including Internet Explorer, E-mail, Notepad, LabVIEW, Paint, Calculator, and Measurement & Automation. The 'My Documents' folder is highlighted in the Start menu. A white text box with a black border is overlaid on the right side of the Start menu, containing the instruction: 'Click the Start programme and open My Documents Folder'. The taskbar at the bottom shows the Start button, a taskbar with 'Copy of TSPCT-Testp...' and 'LabVIEW', and the system tray with the time '9:51 AM'.

Click the Start programme and open My Documents Folder

Slide 4

## Starting the Software



The screenshot shows a Windows Explorer window titled 'My Documents'. The address bar shows 'My Documents'. The main pane displays a list of folders and files:

Name	Size	Type	Date Modified
LabVIEW Data		File Folder	7/24/2009 2:47 PM
My Music		File Folder	6/17/2009 4:59 PM
My Pictures		File Folder	7/25/2009 5:57 PM
image of desktop on 17 June 09	2,917 KB	Bitmap Image	6/17/2009 10:18 PM

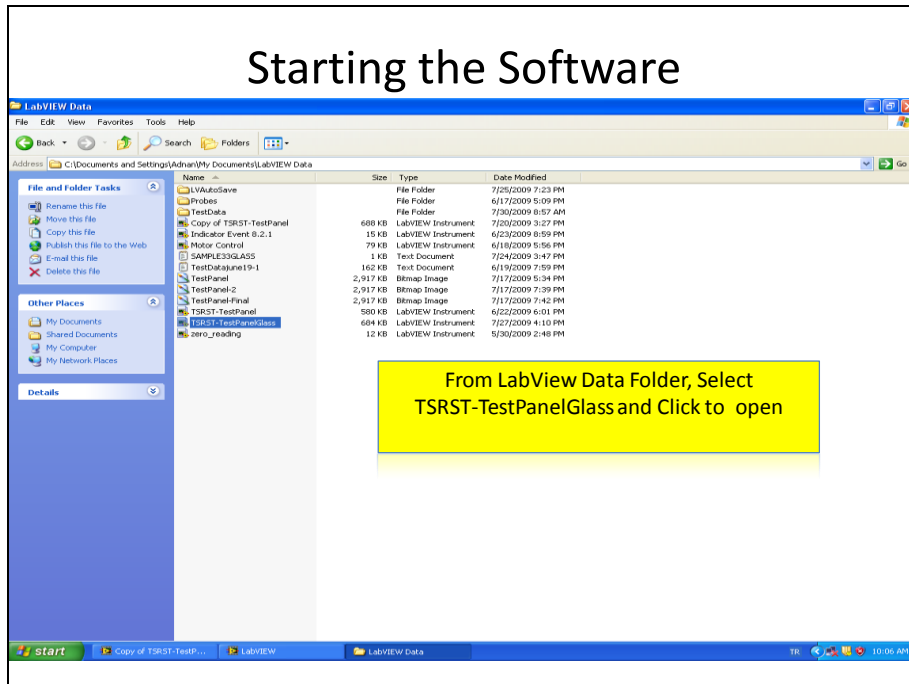
The 'LabVIEW Data' folder is selected. A yellow text box with a black border is overlaid on the right side of the Explorer window, containing the instruction: 'From My Documents Folder, Select LabVIEW Data and Click to open'. The taskbar at the bottom shows the Start button, a taskbar with 'Copy of TSPCT-Testp...', 'LabVIEW', 'My Documents window...', and 'My Documents', and the system tray with the time '9:53 AM'.

From My Documents Folder, Select LabVIEW Data and Click to open

**Figure H2 (continued)**

Slide 5

# Starting the Software



Slide 6

# Window opened

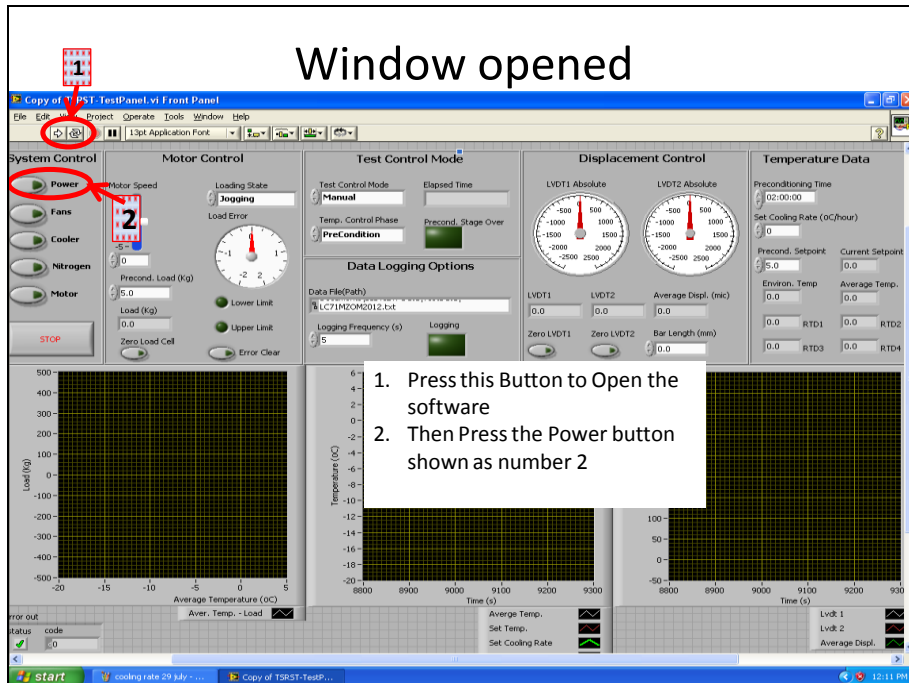
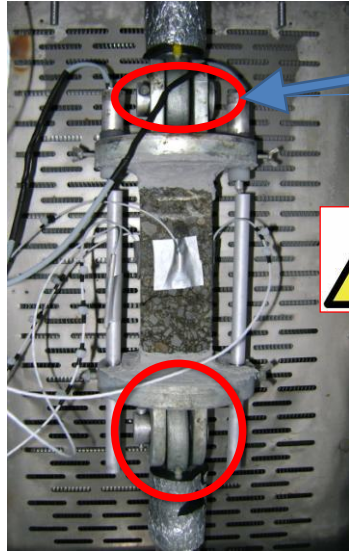


Figure H2 (continued)

## Mounting the Sample



First Hang the sample from the top then adjust the length at the bottom by following steps 3, 4 and 5 shown in the next page



**Caution:**  
Make sure that the load is set to zero and immediately close the motor once the pin is passed to the other side of clamp

Mount the RTDS & LVDTs as shown on the sample and on the ROD, tighten the screws take the length of the Rod from bottom of the plate to the LVDT touching the surface of rods

## Window opened-Jogging Mode

3. Zero the load cell

4. Adjust the motor speed and pull the button up or down so as to adjust length of sample

5. Press the motor on, Stop the motor before going to step 6.

6. Set precondition point to 25(Twenty Five)

7. Type the bar length in millimetres

8. Type any dummy name of sample.

9. Set precondition load to 5(Five)

Figure H2 (continued)

## Changing to Loading mode

10. Zero the LVDTs as indicated

11. Press ON Fans, Cooler and motor in a order as shown 11, 12 and 13.

14. Check that window show PreCondition Mode

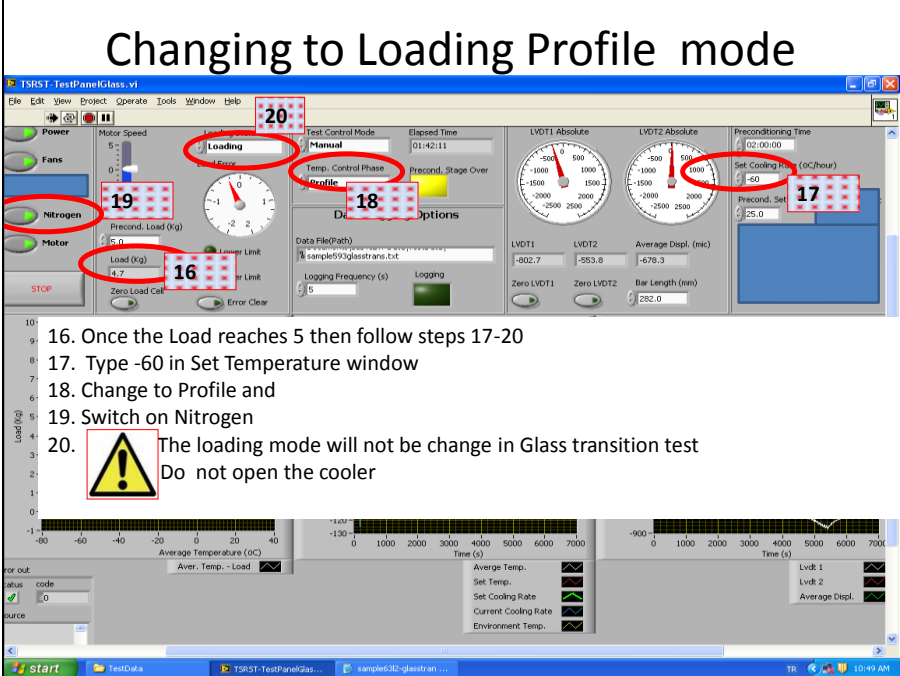
15. Change the Loading state to Loading

## Shifting to loading-Profile mode

- Once the sample reaches 25C(Average temperature, exit the software by first switching off motor, then cooler, Fan, Power and stop the software , after that exit.
- Reopen the glass transition software
- Click the Power
- Set the precondition temperature to 25 and precondition load to 5 as before.
- Write the actual file name now, type the bar length
- Now switch on Fan and Motor only
- Change to Loading Mode

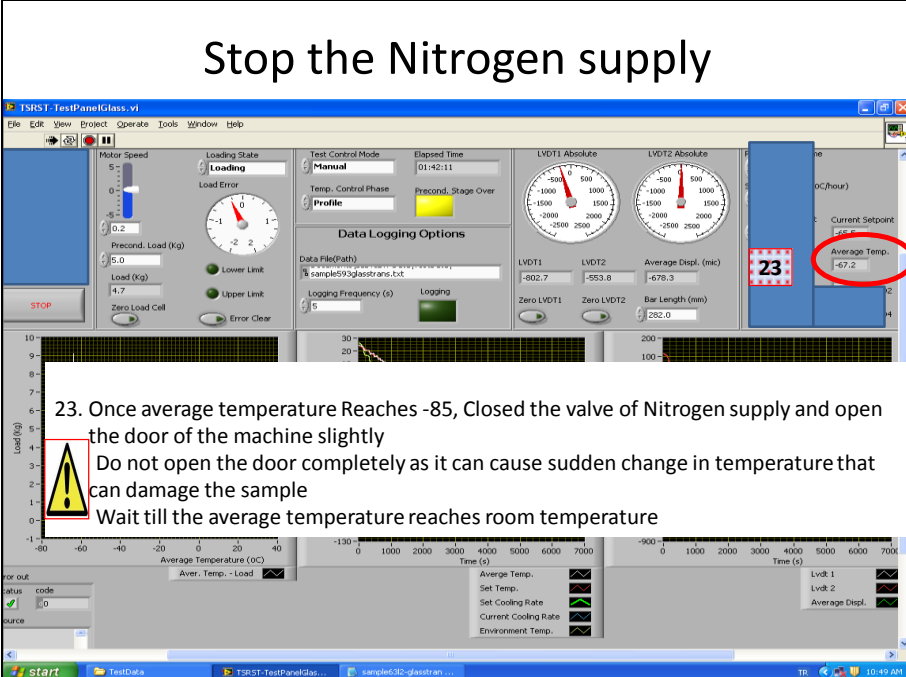
**Figure H2 (continued)**

## Changing to Loading Profile mode



16. Once the Load reaches 5 then follow steps 17-20
17. Type -60 in Set Temperature window
18. Change to Profile and
19. Switch on Nitrogen
20.  The loading mode will not change in Glass transition test  
Do not open the cooler

## Stop the Nitrogen supply



23.  Once average temperature Reaches -85, Closed the valve of Nitrogen supply and open the door of the machine slightly  
Do not open the door completely as it can cause sudden change in temperature that can damage the sample  
Wait till the average temperature reaches room temperature

Figure H2 (continued)

## Stopping the Software

**25** (Power button)

**26** (STOP button)

**27** (Close button)

**FIRST REMOVE THE RTDS AND LVDT GENTLY, USING HAIR DRIER TO MELT THE ICE IF NECESSARY, REMOVE THE PIN AND IF REQUIRED CHANGE TO JOGGING MODE IN LOADING STATE TO MOVE THE SAMPLE UP AND FOR REMOVING THE PINS.**

**24. Now turn off the Motor, Nitrogen, cooler and Fans**

**25. ONCE SAMPLE IS REMOVED TURN OFF THE POWER AS CIRCLE 25**

**26. Stop the Software circle 26**

**27. Exit the programme from 27**

**Do not close the machine before exiting the software**

Figure H2 (continued)

# CURRICULUM VITAE

## PERSONAL INFORMATION

Surname, Name: Qadir, Adnan

Nationality: Pakistani

Date and Place of Birth: 11 January 1968, Karachi, Pakistan

Marital Status: Married having two children

Phone: (+92-21) 99261903

Email: [qadiradnan@yahoo.com](mailto:qadiradnan@yahoo.com)

## EDUCATION

### Degree Institution Year of Graduation

**M.Sc.** N.E.D. University of Engineering 1998  
and Technology, Karachi, Pakistan

**B.E.** N.E.D. University of Engineering 1991  
and Technology, Karachi, Pakistan

## WORK EXPERIENCE

Year	Place	Enrolment
1997-Present		N.E.D. University of Engineering Assoc. Professor and Technology, Karachi, Pakistan

## FOREIGN LANGUAGE

English

## PUBLICATIONS

1. **Traffic Delays and Queue Build-Up Due To Damaged Roads of Karachi**, 23rd – 24th January 2001, First International Road Transport Conference, Lahore, Pakistan
2. **Post Disaster Mitigation – A Relief To Human Sufferings** 14th – 15th November, 2002, International Conference on Protection of Structures Against Hazards, Singapore

3. **Use of Recycled plastic waste as an aggregate in Pavement structure**,14-16 March, 2005, International Symposium on Pavement Recycling, SAO PAULO Brazil)
4. **Utilization of Plastic waste in Pavement Structure**, Journal of Solid waste and technology, Pages 185-194, volume 32, August 2006
5. **A paradigm for down grading the nuisance of Polyethylene bag pollution** Technology Updates Journal, Volume 3, Academic Year 2006-2008.Pages 1-12
6. **Experimental Testing of Hot Mix Asphalt Mixture made of Recycled Aggregates**, Journal of Waste Management Research -2010 (Paper accepted for publication-In Press)

#### CONFERENCE PRESENTATION

1. **Using Dynamic Modulus as an Indicator for Thermal Strength of Asphalt Concrete**, First Meeting and Technical Conference of the Middle East Society of Asphalt Technologist, MESAT-2010. July 5-8, Beirut, Lebanon.
2. **Effect of Aggregate and Rate of Temperature Change on Fracture Strength of Asphalt Concrete**, Abstract accepted for the 5th International Conference on 'Bituminous Mixtures and Pavements', (5th ICONFBMP), 1-3 June 2011, Thessaloniki , Greece .